Sleep, circadian and behavioural characterisation of two schizophrenia-relevant transgenic mouse models

David Pritchett

Wadham College, University of Oxford
Nuffield Department of Clinical Neurosciences
Nuffield Laboratory of Ophthalmology

A thesis submitted in fulfilment of the requirements for the degree of Doctor of Philosophy at the University of Oxford

January 2015

Abstract

The experiments described in this thesis involved the sleep, circadian and behavioural characterisation of two schizophrenia-relevant transgenic mouse models, both of which are models of altered glutamatergic function. Although schizophrenia cannot be recapitulated in rodents, the study of transgenic mouse models can yield insights into the roles of schizophrenia candidate genes in brain function and dysfunction.

D-amino acid oxidase knockout (*Dao*$^{-/-}$) mice do not express DAO, a glial peroxisomal enzyme that catalyses the degradation of D-amino acids including D-serine. In turn, D-serine is the primary endogenous co-agonist of the synaptic N-methyl-D-aspartate receptor, an ionotropic glutamate receptor that is strongly implicated in learning and memory, which may be hypoactive in schizophrenia. Given evidence of DAO overactivity in schizophrenia, DAO inhibiting drugs have been proposed as a potential treatment for the disorder.

To assess the behavioural consequences of *Dao* inactivation, *Dao*$^{-/-}$ mice were subjected to a range of psychiatrically-relevant behavioural tests. Anxiety-like behaviour was increased in *Dao*$^{-/-}$ mice, while short-term memory performance was enhanced. By contrast, long-term spatial memory acquisition was unaltered in *Dao*$^{-/-}$ mice. However, the Morris watermaze performance of *Dao*$^{-/-}$ mice was critically dependent on the radial distance of the hidden platform from the side-wall. Analyses of spatial swimming behaviour revealed that *Dao*$^{-/-}$ mice demonstrated an increased preference for the periphery of the watermaze arena, which may be another manifestation of heightened anxiety. Prepulse inhibition testing revealed a complex interplay between genotype, sex and stress levels. Likewise, genotype-by-sex interactions were evident in the Morris watermaze and the novelty-suppressed feeding test. *Dao*$^{-/-}$ mice showed no evidence of sleep or circadian rhythm disruption (SCRD). Taken together, these results

suggest that DAO inhibition might ameliorate the memory deficits of schizophrenia patients, although these effects may not extend to long-term associative memory. In addition, these benefits could come at the cost of heightened anxiety. Our data also imply that DAO inhibitors might have different effects in male and female patients.

Metabotropic glutamate receptor 2 & *3* double-knockout (*Grm2/3*$^{-/-}$) mice lack the inhibitory autoreceptors mGlu2 and mGlu3, which are encoded by the genes *Grm2* and *Grm3*, respectively. Based on the results of genome-wide association studies, *Grm3* is amongst the strongest schizophrenia candidate genes. The *Grm2/3*$^{-/-}$ mouse was used to assess the 'shared neuropathophysiology' hypothesis of SCRD in schizophrenia. This theory posits that the high co-morbidity of schizophrenia and SCRD stems from dysfunction in common brain mechanisms that underpin both pathologies. Consistent with this hypothesis, *Grm2/3*$^{-/-}$ mice displayed significant SCRD, characterised by reduced sleep duration and increased sleep fragmentation. They also demonstrated increased sensitivity to the circadian effects of light. These data are consistent with the 'shared neuropathophysiology' hypothesis, and tentatively suggest that mGlu3 dysfunction could contribute to SCRD in schizophrenia. Since memory performance is also impaired in *Grm2/3*$^{-/-}$ mice, this model could be an ideal tool with which to investigate the relationship between sleep disruption and cognitive performance. Finally, *Grm2/3*$^{-/-}$ mice displayed perturbed wheel-running rhythms under a standard light/dark cycle, despite the fact that their home-cage activity rhythms were unaltered in the absence of a running wheel. Although the basis of this phenotype is unclear, these data speak to the debate about the suitability of running-wheels as a circadian assay for psychiatrically-relevant mouse models.

Acknowledgements

First and foremost, I would like to express my gratitude to the ‘three wise men’: my principal supervisors Stuart Peirson, David Bannerman and Paul Harrison. I am particularly grateful to Stuart for taking me on at short notice when I switched departments in 2011, and for his constant help and support throughout my DPhil. David and Paul also deserve special mention for providing regular supervision despite not being my official supervisors.

I would also like to acknowledge the regular advice and assistance from my colleagues in the Foster/Peirson lab (Eric Tam, Sibah Hasan, Laurence Brown, Lindsay Benson, Tom Watson, Aarti Jagannath, Violetta Pilorz, Steven Hughes, Simona di Pretoro and Russell Foster), the Behavioural Neuroscience Unit (particularly Gauri Ang and Tomasz Schneider), the Harrison lab (especially Tracy Lane, Phil Burnet and Li Chen), and the Sharp lab (especially Judith Schweimer and Trevor Sharp).

Special mention is also reserved for Amy Taylor and Katie Hewitt from the Behavioural Neuroscience Unit. Together, they ‘showed me the ropes’ of rodent behavioural testing. Amy also made an invaluable contribution to my final data paper by performing two experiments while I was writing my thesis.

Next, I would like to thank all of the animal technicians (particularly Andrew Pinsent and Jonathon Merrill) for their tireless efforts in taking care of my animals throughout my DPhil. ‘Overworked and underpaid’ doesn’t do them justice!

I also wish to acknowledge the funding organisations that supported my research: the Wellcome Trust, Roche, and the University of Oxford Christopher Welch fund, which provided me with a student stipend and research allowance. I also thank Pfizer and GlaxoSmithKline for providing the transgenic mice studied in this thesis.

Last but not least, I would like to thank my wife, friends and family for their constant support, advice and encouragement during the past few years, not to mention the regular lifts to and from the lab at various times of the day and the night! This thesis is dedicated to each and every one of you!

Contents

7. General discussion

8. Appendices

Abbreviations

5-HT	5-hydroxytryptamine (serotonin)
AAS	Ascending arousal system
AKA	α-keto acid
AKT1	RAC-alpha serine/threonine-protein kinase
AMPAR	α-amino-3-hydroxy-5-methyl-4-isoxazolepropionic acid receptor
ANOVA	Analysis of variance
AP	Action potential
AR	Adenosine receptor
AU	Arbitrary units
AVP	Arginine vasopressin
Bdr	Blind-drunk
BF	Basal forebrain
BMAL1	Brain and Muscle ARNT-Like 1
BWA	Black and white alleys
cAMP	Cyclic adenosine monophosphate
CBT	Cognitive behavioural therapy
CCK	Cholecystokinin
CCK-AR	Cholecystokinin A receptor
CK1	Casein kinase 1
CLOCK	Circadian locomotor output cycles kaput
CNV	Copy number variation
COMT	Catechol-O-methyl transferase
cpd	Cycles per degree of visual angle
CREB	cAMP response element-binding protein
CRH	Corticotrophin-releasing hormone
CRY1 & 2	Cryptochrome 1 & 2
CSF	Cerebrospinal fluid
CT	Circadian time
DALYs	Disability adjusted life years
DAO	D-amino acid oxidase (also known as DAAO)
DAOA	D-amino acid oxidase activator (also known as G72)
DD	Constant dark
DISC1	Disrupted in schizophrenia 1
dKO	Double knockout
DMH	Dorsomedial hypothalamus
DRD2	Dopamine receptor D2
DRN	Dorsal raphe nucleus
Dtnbp1	Dystrobrevin binding protein 1
e-Box	Enhancer box
EDTA	Ethylenediamine tetraacetic acid
EEG	Electroencephalography
ELISA	Enzyme-linked immunosorbent assay
EMG	Electromyography
ENU	N-ethyl-N-nitrosourea
EPM	Elevated plus maze
EPSP	Excitatory postsynaptic potential
ERG	Electroretinography

GluN	Glutamate receptor ionotropic, NMDA 1 (also known as Grin1)
G_{olf}	Olfactory neuron specific-G protein
Grm2 & *3*	Metabotropic glutamate receptor 2 & 3 (genes)
GSK3	Glycogen synthase kinase 3
GWAS	Genome-wide association study
HPA	Hypothalamic-pituitary-adrenal
ID	Inhibitor of DNA-binding
ipRGC	Intrinsically photosensitive retinal ganglion cell
ITI	Inter-trial interval
LC	Locus coeruleus
LD	Light/dark
LDT	Laterodorsal tegmental nucleus
LE	Long Evans
LED	Light-emitting diode
LH	Lateral hypothalamus
LL	Constant light
LSD	Lysergic acid diethylamide
LTC	Light-tight chamber
LTD	Long-term depression
LTP	Long-term potentiation
LTSM	Long-term spatial memory
MAM	Methylazoxymethanol acetate
MCH	Melatonin-concentrating hormone
mGlu2 & 3	Metabotropic glutamate receptor 2 & 3 (proteins)
MIR137	microRNA-137
MK-801	Dizocilpine
MRN	Medial raphe nucleus
mRNA	Messenger ribonucleic acid
MWM	Morris watermaze
NAc	Nucleus accumbens
NAM	Negative allosteric modulator
NHP	Non-human primate
NIR	Near-infrared
NMDAR	N-methyl-D-aspartate receptor
NO	Nitric oxide
NOS	Nitric oxide synthase
NREM	Non rapid eye movement
NRG1	Neuregulin 1
NSB	Non-specific binding
NSF	Novelty-suppressed feeding
OD	Optical density
OFT	Open field test
OKN	Optokinetic nystagmus
PACAP	Pituitary adenylate cyclase-activating polypeptide
PAM	Positive allosteric modulator
PCP	Phencyclidine
PDE4	Phosphodiesterase-4 inhibitor
PER1 & 2	Period 1 & 2
PFC	Portsmouth football club/Prefrontal cortex
PIR	Passive-infrared

PKA	cAMP-dependent protein kinase A
pNpp	p-nitrophenyl phosphate
PPI	Prepulse inhibition
PPT	Pedunculopontine nucleus
PVN	Paraventricular nucleus
RCF	Relative centrifugal force
REM	Rapid eye movement
REV-ERB*a*	Nuclear receptor subfamily 1, group D, member 1 (also known as NR1D1)
RHT	Retinohypothalamic tract
RNAi	Ribonucleic acid interference
ROR*a*	Retinoic acid-related orphan receptors alpha
RORE	Retinoic acid-related orphan receptor response element
SCN	Suprachiasmatic nucleus
SCRD	Sleep and circadian rhythm disruption
SD	Sprague Dawley
SEM	Standard error of the mean
SNAP-25	Synaptosomal-associated protein, 25kDa
SNP	Single nucleotide polymorphism
SPZ	Subparaventricular zone
SRR	Serine racemase
STSM	Short-term spatial memory
SUN	4H-furo[3,2-b]pyrrole-5-carboxylic acid
TCF4	Transcription factor 4
TGFα	Transforming growth factor alpha
TMN	Tuberomammillary nucleus
TRN	Thalamic reticular nucleus
TTFL	Transcriptional-translational feedback loop
UHR	Ultra-high risk
VIP	Vasoactive intestinal peptide
Vipr2	Vasoactive intestinal peptide receptor 2 (gene)
VLPO	Ventrolateral preoptic nucleus
VPAC2	Vasoactive intestinal peptide receptor 2 (protein)
VPAG	Ventral periaqueductral gray
VTA	Ventral tegmental area
WT	Wildtype
ZNF804A	Zinc finger protein 804A
ZT	Zeitgeber time

1. Introduction

1.1. Introduction to schizophrenia

1.1.1. Epidemiology

Schizophrenia is a debilitating psychiatric disease that affects around 0.3-0.7% of individuals at some stage during their lifetime [1]. It is currently estimated that more than 21 million people are affected worldwide[1]. Schizophrenia exerts a massive social and economic burden on society; in the UK alone, approximately 87% of individuals with the disorder are unemployed [2]. And, according to a UK parliamentary report in 2012, 11.8 billion pounds is spent on the treatment of schizophrenia in the UK each year[2].

Schizophrenia accounts for approximately 1% of worldwide disability-adjusted life years (DALYs), a measure of disease burden that quantifies the number of years lost to ill health and early death [3]. Indeed, the mortality rate for schizophrenia patients is about double the population average [4], while average life expectancy is 12 - 15 years shorter than that for individuals without the disorder [5]. Suicide accounts for around a quarter of the premature deaths of schizophrenia patients [4], while heart disease and cancer account for the majority of natural premature deaths [5]. Accidental and homicidal deaths are also more frequent among schizophrenia patients than in the general population [6, 7]. Psychiatric comorbidities are common in schizophrenia patients, with an estimated prevalence of 15% for panic disorder, 29% for post-traumatic stress disorder, 23% for obsessive compulsive disorder, 50% for depression, and 47% for substance abuse [8].

[1] World Health Organisation estimate. Correct as of January 2015. (http://www.who.int/mental_health/management/schizophrenia/en/)

[2] UK Parliamentary report. Published November 2012. (http://www.lse.ac.uk/LSEHealthAndSocialCare/pdf/LSE-economic-report-FINAL-12-Nov.pdf)

Schizophrenia is diagnosed 1.4 times more frequently in men than in women [3, 9-11]. Age of onset also differs between the sexes; the peak ages of onset are 20-28 years for males, and 26-32 years for females [12]. Onset during childhood, middle-age or old-age is relatively rare [13, 14]. In the UK, there have been several reports that schizophrenia is more common in the Afro-Caribbean population than in the Caucasian population [15]. Finally, in contrast to the widely-held belief that schizophrenia is evenly distributed worldwide, there is good evidence that disease prevalence varies between countries, within countries, and even at a neighbourhood level [9-11, 16-18].

1.1.2. Symptoms

The symptoms of schizophrenia are categorised into three domains: positive, negative, and cognitive [19]. Positive symptoms include hallucinations (perceptions of sensory events that did not occur) and delusions (firmly-held beliefs that persist despite superior evidence to the contrary). Delusions can be further categorised into delusions of grandeur, delusions of reference, delusions of persecution, and delusions of control. Hallucinations can affect any sensory modality, although auditory hallucinations are the most common. The negative symptoms of schizophrenia include avolition (a general lack of motivation or drive to pursue meaningful goals), alogia (poverty of speech), anhedonia (inability to experience pleasure), apathy, flattened affect and social withdrawal. Finally, schizophrenia patients are afflicted by a variety of cognitive deficits, including impairments of memory, attention, response inhibition/impulsivity, cognitive flexibility/compulsivity, and processing speed [20, 21]. Of the three symptom groups, the cognitive symptoms may be the best predictor of functional outcomes for schizophrenia patients [22]. Memory is the cognitive domain which is worst affected, with working memory and episodic memory deficits the most prominent [23-25]. Crucially, these deficits are not a by-product of the positive or negative symptoms of the

disorder, nor a side effect of antipsychotic medication [26-29]. The exact combination of symptoms varies between patients, resulting in the classification of different subtypes of schizophrenia and schizophrenia-related disorders [1].

1.1.3. Treatment

Patients with schizophrenia are typically treated with antipsychotic medication. First generation (or typical) antipsychotic drugs were discovered in the 1950s, while second generation (or atypical) antipsychotic drugs emerged in the 1980s. Both classes of drug antagonise D_2 dopamine receptor binding in the brain, while atypical antipsychotics tend to antagonise 5-HT_{2A} serotonin receptors as well [30]. The use of antipsychotic medication can lead to a range of side effects, including movement disorders and weight gain [31]. Initially, it was thought that atypical antipsychotics were less likely to trigger movement disorders, but this is no longer a widely-held belief [32]. The efficacy of antipsychotic drugs is suboptimal; amongst patients that take antipsychotic medication for a period of 3 years, only 13% achieve remission, 33% report long-lasting symptom reduction, and 27% are satisfied with their quality of life [33]. Moreover, although antipsychotic medication is relatively effective at alleviating the positive symptoms of schizophrenia, it has little or no impact on the negative or cognitive symptoms [34]. In the words of Geyer and Tamminga [34]: *"Antipsychotic drugs have emptied out our mental institutions, but have delivered their residents to impoverished lives outside. Research has linked elements of this poor psychosocial function to persistent cognitive impairments."*

1.2. Aetiology of schizophrenia

1.2.1. Genetic contribution to schizophrenia

It is widely accepted that both environmental and heritable genetic factors contribute to the risk of schizophrenia. The strongest evidence that schizophrenia is a genetic disorder comes from twin studies, from which heritability of risk is estimated to be around 80% [35, 36]. To date, a number of genes have been linked with schizophrenia, through a combination of genetic linkage studies, genome-wide association studies (GWAS) and appraisals of biological plausibility. Those most established in the 'candidate gene' literature are *Nrg1* [37-39], *Akt1* [40], *Disc1* [41, 42], *Grm3* [43], *Dao* [44, 45], *Comt* [46], *Dtnbp1* [47] and *ErbB4* [38]. More recent additions to the literature include *Snap-25* [48], *Vipr2* [49], *Cckar* [50], *Gsk3b* [51], *Pde4d* [52-54], *Tcf4* [55], *MIR137* [56] and *ZNF804A* [57].

However, despite years of research, no gene has been unequivocally established as conferring increased susceptibility to schizophrenia [58]. The literature is littered with genes that have yielded positive results in one or two genetic association studies, only for several follow-up studies to draw a blank [58]. The likely explanation for these results is that schizophrenia results from the additive effect of variation in a large number of genes, with each gene having a very small effect [59]. In this context, extremely large samples are required to detect statistically significant associations. Hence, the recent paper by Ripke and colleagues represents a major breakthrough in the literature [60]. By assimilating data from multiple GWAS studies – encompassing 36,989 schizophrenia patients and 113,075 healthy controls – they identified 128 significant associations spanning 108 genetic loci. Of these associations, 83 were entirely novel [60].

In addition to common genetic variants with low penetrance, rare but highly penetrant genetic variants may also contribute to schizophrenia. Copy-number variations (CNVs) are alterations in the genome whereby there are too many or too few copies of a particular segment of DNA [61]. The most obvious example of a psychiatric disorder caused by a CNV is Down syndrome, which is due to the presence of an additional copy of chromosome 21. Most CNVs are much smaller segments of DNA however, ranging from 1,000 to 1,000,000 base pairs. Hence, a large CNV can encompass dozens of individual genes [61]. Although this is a relatively new field, there is already evidence of significant associations between specific CNVs and susceptibility to schizophrenia [62-65]. Although these CNVs occur in very few individuals, a high proportion of these individuals exhibit clinical symptoms. A deletion at the chromosomal location 22q11.2, for example, leads to the development of schizophrenia in around 30% of cases [66, 67].

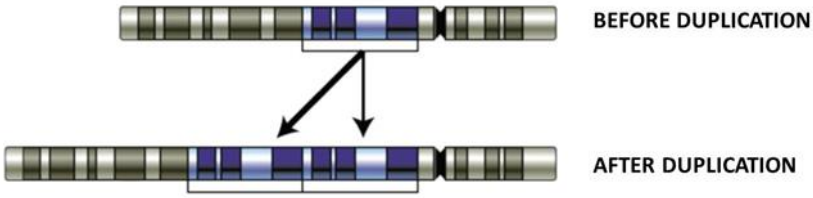

Figure 1.1. This gene duplication has created a copy number variation (CNV). The chromosome now has two copies of this section of DNA, rather than one. Figure adapted from wikipedia.org.

CNVs can either be inherited or *de novo* (i.e. not present in either parent). The latter may be more crucial than the former; as a result of the reduced fecundity associated with the disorder, highly-penetrant CNVs will rarely be transmitted from parent to child. Hence, CNVs are more likely to account for sporadic cases of schizophrenia than familial ones. In support of this hypothesis, *de novo* CNVs are significantly more frequent in sporadic cases of schizophrenia than in familial cases or unaffected individuals [68, 69].

1.2.2. Environmental contribution to schizophrenia

Epidemiological studies have provided evidence of an environmental contribution to schizophrenia. A wide range of perinatal risk factors have been associated with the incidence of schizophrenia, including viral infection, malnutrition, obstetrical complications (e.g. hypoxia), exposure to toxins, insufficient exposure to sunlight, and urban birth [70, 71]. Of these associations, malnutrition is among the strongest. It has been shown that the offspring of mothers exposed to famine during early gestation are twice as likely to develop schizophrenia in later life [72]. The risk of schizophrenia also increases with the number and severity of hypoxia-associated obstetric complications [73-75]. Environmental influences may also explain the 'seasonality effect' in schizophrenia; the phenomenon by which individuals born in winter and spring are more likely to develop schizophrenia than individuals born in summer or autumn [71]. This may reflect the fact that in these individuals, the critical third trimester of neurodevelopment will occur during the winter months, the same time at which several prenatal risk factors (e.g. viral infection, malnutrition and insufficient exposure to sunlight) typically peak [71].

1.2.3. Schizophrenia as a neurodevelopmental disorder

Based on the evidence described above, it has been suggested that environmental and genetic risk factors converge and interact during perinatal development to disrupt neurodevelopment and confer increased susceptibility to schizophrenia [76, 77]. In support of this hypothesis, many schizophrenia susceptibility genes are implicated in neurodevelopment [78]. Besides this observation, there is a growing body of evidence that schizophrenia is a developmental disorder [70, 71, 77-83]. Firstly, most environmental risk factors for schizophrenia are perinatal. Secondly, pre-schizophrenic children exhibit impaired motor, behavioural and intellectual functioning, suggesting that brain development is abnormal many years prior to onset of the

disease. Thirdly, there is a higher incidence of minor physical anomalies and abnormal dermatoglyphics in schizophrenia, which are known to reflect intrauterine growth disturbances. Fourthly, *in vivo* imaging studies show that brain changes are present in first-episode patients, and thereafter are essentially non-progressive, suggesting that the disease process occurs before the onset of symptoms. Next, there are no neurofibrillary tangles, amyloid plaques, or any other markers of known neurodegenerative processes in the schizophrenic brain. Nor is there any evidence of gliosis, a tell-tale sign of brain injury. Finally, cellular changes in the cortex (e.g. neurons with shortened dendrites and fewer dendritic spines) are supportive of a developmental disease process.

1.2.4. The 'two-hit' hypothesis

Despite plentiful evidence that schizophrenia is a neurodevelopmental disorder, the symptoms of schizophrenia rarely emerge prior to adolescence [12]. Moreover, in addition to the multiple perinatal environmental risk factors associated with the disorder, other environmental risk factors, such as stress and substance abuse, exert their influence later in life [70]. The neurodevelopmental hypothesis was therefore extended to account for these findings [84]. According to the new, 'two-hit' hypothesis, aberrant neurodevelopment renders certain individuals more susceptible to schizophrenia, but the disease is not triggered until these vulnerable individuals are exposed to further environmental risk factors in adulthood or early adolescence. A major challenge for future research is to identify the pathophysiological features which define the 'pre-schizophrenic brain', and the mechanisms by which environmental risk factors trigger disease onset in vulnerable individuals.

1.2.5. Neurotransmitter-based hypotheses

Dopamine hypothesis

The dopamine hypothesis is a model that attributes the positive symptoms of schizophrenia to dopaminergic overactivity in the mesolimbic dopaminergic pathway [85]. This hypothesis arose from observations that drugs which increase dopamine levels in the brain (e.g. cocaine and amphetamine) can trigger symptoms in healthy individuals that resemble the positive symptoms of schizophrenia, and can exacerbate the positive symptoms of schizophrenia patients themselves [86, 87]. Conversely, antipsychotic drugs – which ameliorate the positive symptoms of schizophrenia – antagonise dopamine receptor binding, particularly at D_2 dopamine receptors [88]. Indeed, there is an inverse relationship between the D_2 receptor binding affinity of antipsychotic drugs and their required therapeutic dosages [89, 90]. Numerous post-mortem studies have revealed increased striatal D_2 receptor binding in the brains of schizophrenia patients [91]. Likewise, *in vivo* imaging studies have yielded evidence of increased striatal dopamine release in schizophrenia patients relative to controls following acute amphetamine challenge [92]. Finally, many of the genes which are significantly associated with schizophrenia have an established role in the regulation of dopamine function, such as *Comt* [46] and *Akt1* [40].

Many years after the original dopamine hypothesis was formulated, functional neuroimaging data began to accrue implicating prefrontal cortex (PFC) dysfunction in the negative and cognitive symptoms of schizophrenia [93]. In addition, preclinical data revealed that PFC function was highly dependent on dopaminergic neurotransmission, particularly at D_1 dopamine receptors [94]. Based on these findings, the classical dopamine hypothesis was extended; the negative and cognitive symptoms of schizophrenia were attributed to dopaminergic *underactivity* in the mesocortical dopaminergic pathway [95, 96]. This did not

invalidate the original hypothesis, since prefrontal dopaminergic activity exerts inhibitory control over subcortical dopaminergic activity [96].

Glutamate hypothesis

According to the glutamate hypothesis of schizophrenia, dysfunctional glutamatergic neurotransmission via N-methyl-D-aspartate (NMDA) receptors is critically involved in the pathophysiology of schizophrenia [97-100]. NMDA receptors (NMDARs) are widely expressed ionotropic glutamate receptors that contribute to a number of important physiological processes, including synaptic plasticity, neurodevelopment, neuroprotection and neurotoxicity [101]. Convergent evidence suggests that NMDAR function is downregulated in schizophrenia. Firstly, the administration of NMDAR antagonists (e.g. PCP, MK-801 and ketamine) provokes schizophrenia-like symptoms in healthy individuals, and exacerbates the symptoms of schizophrenia patients [102-104]. Unlike cocaine and amphetamine, these include symptoms that resemble the positive, negative *and* cognitive symptoms of schizophrenia. Conversely, direct and indirect NMDAR agonists have shown some promise in the alleviation of patients' symptoms [105]. Post-mortem studies have revealed alterations in glutamate receptor binding and subunit protein expression in the brain; for example, expression of the NR1 subunit of the NMDAR is reduced in the hippocampus and PFC of schizophrenia patients [106]. Likewise, *in vivo* imaging studies have yielded evidence of reduced NMDAR binding in the hippocampus of medication-free schizophrenia patients [107]. Finally, many of the genes which are significantly associated with schizophrenia have an established role in the regulation of NMDAR function, such as *Dao* [45], *Grm3* [43] and *Nrg1* [39].

Serotonin hypothesis

A link between serotonin (5-HT) and schizophrenia was first suggested with the discovery that the drug lysergic acid diethylamide (LSD) triggers hallucinations in healthy individuals, and that its likely mechanism of action is its agonistic effect on serotonin receptors [108]. Consistent with this early observation, a number of direct and indirect 5-HT receptor agonists can exacerbate the positive symptoms of schizophrenia patients [109]. Conversely, most atypical antipsychotic drugs – which ameliorate the positive symptoms of schizophrenia – are 5-HT_{2A} receptor antagonists [109]. Post-mortem studies have revealed alterations in 5-HT receptor binding and expression in the brains of schizophrenia patients; for example, 5-HT_{2A} receptor binding and expression are reduced in the PFC of schizophrenia patients, whereas 5-HT_{1A} receptor binding is increased [110]. Finally, polymorphisms of the gene encoding the 5-HT_{2A} receptor have been significantly associated with schizophrenia [111-113].

Interaction between the hypotheses

It should be noted that the three neurotransmitter-based hypotheses described above are not mutually exclusive; instead, it is possible that all three neurotransmitter systems contribute to the symptoms of schizophrenia. Moreover, the three neurotransmitter systems are highly interactive, so dysfunction in one may lead to dysfunction in the others [114].

1.2.6. Brain morphology, cellular morphology and synaptic connectivity

In vivo imaging studies and post-mortem histological studies have revealed robust morphological changes in the brains of schizophrenic patients. The 'schizophrenic brain' is characterised by enlarged lateral ventricles and reduced cortical thickness, particularly in the frontal and temporal lobes [115-117]. In general, hippocampal volume is reduced [118, 119], as is the volume of the cerebellar vermis [120, 121]. Cellular changes have also been reported

in the cortex; pyramidal neurons, for example, have shortened dendrites and fewer dendritic spines [79, 81]. Lastly, it has been argued that schizophrenia may be a disorder of synaptic connectivity. This is based on observations from post-mortem and neuroimaging studies which show that the gross morphological changes in the brains of schizophrenia patients are the result of a reduction in the number of dendrites and synapses, rather than a loss of neuronal or glial cell bodies [122]. These changes are likely the result of aberrant neurodevelopment [122]. Synaptic dysconnectivity may not have obvious functional consequences prior to a wave of synaptic pruning in early adulthood [123], an idea which is consistent with the 'two-hit' hypothesis (see Section 1.2.4.)

1.3. Behavioural screening of schizophrenia-relevant transgenic mouse models

Animal studies afford a level of control that is simply not possible in human studies [124, 125]. Human participants differ from each other in all manner of dimensions, including their age, education, medication history, genetic makeup and life experiences. In this context, it is difficult to attribute a specific behavioural parameter (e.g. impaired memory) to a specific underlying trait (e.g. possession of a risk-conferring genetic variant). In animal studies, there are relatively fewer confounds, so making such attributions is more straightforward. Genetic manipulation is also possible in rodents, enabling the investigator to move beyond correlation and infer causality.

Positive symptoms

In rodents, some schizophrenia-relevant behaviours are harder to model than others. The positive symptoms of schizophrenia present a particular challenge; hallucinations and delusions are only revealed through patients' verbal reports, so these symptoms are difficult to investigate in rodents. Nonetheless, NMDAR antagonist-induced hyperlocomotion, ataxia and stereotypy are considered by many to reflect the positive symptoms of schizophrenia [126, 127].

Negative symptoms

In terms of the negative symptoms of schizophrenia, reduced social interaction in rodents is often presented as a direct analogue of reduced social interaction in schizophrenia [127, 128]. Behavioural despair – quantified as immobility in the Porsolt forced swim test and tail suspension test – is another frequently cited 'analogue' of human depression [129]. Anhedonia

can also be estimated in rodents, by means of the sucrose preference test or intracranial self-stimulation [130].

Cognitive symptoms

There is a considerable battery of behavioural tests that can be used to test schizophrenia-relevant rodent cognition. Short- and long-term memory are routinely tested in rodents, and tend to involve the spatial exploration of large mazes, such as the T-maze, Y-maze, Morris watermaze or radial arm maze [131]. Non-spatial memory tasks also exist, such as the spontaneous object recognition memory task [132]. This is a valuable assay given that object recognition memory is impaired in schizophrenia patients [133]. Besides memory, several other aspects of cognition can be assessed in rodents. The attentional set-shifting task, for example, is a test of cognitive flexibility, which is based directly on its human counterpart, the Wisconsin Card Sorting Test [134, 135]. Attention, impulsivity and compulsivity (i.e. perseveration) can also be evaluated with tests such as the 5-choice serial reaction time task [136]. Finally, prepulse inhibition (PPI) is a measure of sensorimotor gating that can be tested almost identically in humans and rodents [137]. Reduced PPI is regularly reported in schizophrenia patients [137-141], although it is unclear if this deficit is relevant to the positive, negative or cognitive symptoms of schizophrenia (see Section 4.1.).

Limitations associated with the behavioural screening of schizophrenia-relevant transgenic mouse models

Modelling schizophrenia in animals raises a number of complex theoretical and experimental design issues for the investigator [124, 125, 142-144]. The first and perhaps biggest challenge is the process of selecting which gene to manipulate. The schizophrenia candidate gene literature is littered with failed attempts to replicate statistically significant associations [58];

hence, the validity of almost any model can be questioned. Moreover, since no single gene is either necessary or sufficient to cause the disorder, the validity of single gene models can be questioned. Double- or triple-gene models may be more realistic, but are more complex and costly to produce. A further limitation is that some schizophrenia risk genes (e.g. *Daoa*/*G72*) have no known orthologue in rodents [44].

Besides choosing which gene to manipulate, the investigator must decide how to manipulate it. Knockout models are the simplest and therefore the most common, but again, are unlikely to represent schizophrenia that faithfully. There is no evidence for null mutations in schizophrenia, but there is evidence for the altered expression of many genes [78]. From this perspective, transgenic over-expression or heterozygous knockout may be more suitable strategies. The investigator must also decide whether the genetic manipulation is constitutive or conditional. Most models are constitutive; that is, the manipulation is present throughout the brain and throughout the animal's lifetime. Given evidence that brain abnormalities in schizophrenia are more pronounced in some brain areas than others, and that they can develop over time [145], the constitutive approach may not be the most appropriate. Conditional models, in which the timing and location of the manipulation are more tightly regulated, provide a more flexible alternative.

Schizophrenia-relevant models

To summarise, it would be a significant overstatement to suggest that schizophrenia can be recapitulated in rodents. Since schizophrenia is a complex multi-gene disorder, it seems improbable that a single-, double- or even triple-gene model could ever demonstrate the full range of symptoms observed in a patient. Hence, these models should be described as 'schizophrenia-relevant' models rather than models *of* schizophrenia. Having said this,

transgenic models are still a valuable tool for elucidating the roles of specific genes in specific behaviours or aspects of brain function. A related issue is that the exact subset of symptoms presented in schizophrenia often varies from patient to patient [146]. Likewise, some of the symptoms of schizophrenia are also seen in other psychiatric disorders, such as depression. Moreover, there is a significant amount of overlap in the susceptibility genes and environmental risk factors that are associated with different psychiatric disorders. From this perspective, it may be advantageous to investigate the contribution of specific genes to specific behaviours in isolation [147].

Established schizophrenia-relevant rodent models

Established schizophrenia-relevant models include lesion-based models (e.g. the neonatal ventral hippocampal lesion model [148]), pharmacological models (e.g. the PCP model [102]), and transgenic models [149]. There are also a number of neurodevelopmental models, including perinatal protein deficiency [150, 151], neonatal hypoxia [152, 153] and prenatal immune challenge [154, 155]. A relatively recent addition to the literature are 'gene-by-environment' models, which combine a developmental insult with a subsequent environmental challenge during puberty [156]. Such models may better reflect the 'two-hit' aetiology of schizophrenia, as described in Section 1.2.4.

1.4. Introduction to circadian rhythms

1.4.1. What are circadian rhythms?

Circadian rhythms are endogenous 24 h oscillations in physiology and behaviour that enable an organism to anticipate and adapt to the changing temporal demands of the environment [157]. The term *circadian* is derived from the Latin words *circa*, meaning 'approximately', and *diem*, meaning 'day'. The sleep/wake cycle is perhaps the most obvious example of a circadian rhythm (see Section 1.5). Other examples include daily fluctuations in locomotor activity, core body temperature, heart-rate, blood pressure, renal activity, liver metabolism, and the secretion of glucocorticoids, melatonin and testosterone [158-162]. Circadian rhythms in physiological parameters are not unique to man; they are observed in organisms as diverse as cyanobacteria, fungi, algae, plants, drosophila and rodents [163]. Circadian rhythms are thought to have evolved because they confer a survival advantage to organisms that possess them, increasing their reproductive fitness [164-169]. For example, ground squirrels lacking endogenous rhythms are more vulnerable to predation and show a 20% reduction in lifespan [165].

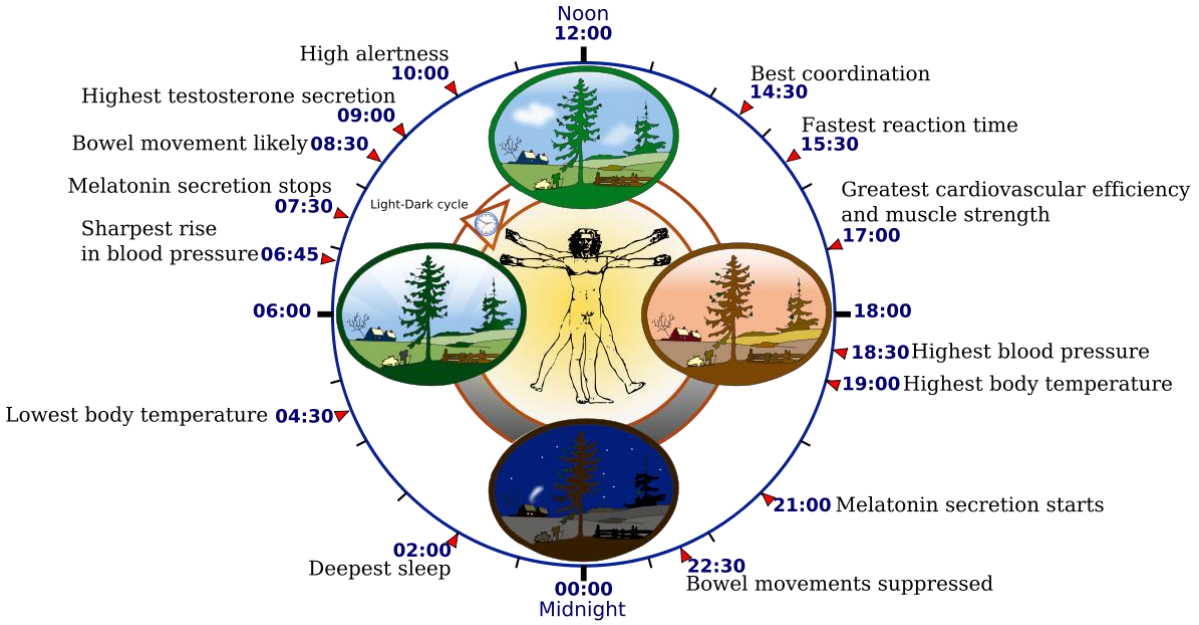

Figure 1.2. Examples of physiological and biological parameters that show circadian variation in humans, including the timing of their peak and nadir. Figure reproduced from wikipedia.org.

A genuine circadian rhythm must meet three criteria [157]. Firstly, it must *persist under constant conditions* (i.e. in the absence of changes in temperature or light) with an endogenous (or 'free running') period of approximately 24 h. This criterion is required to distinguish internally-driven rhythms from straightforward responses to external daily cues. Secondly, it must be *entrainable*. For a rhythm to enable an organism to anticipate daily environmental events (e.g. sunrise), it must be able to adjust to changes in the timing of these events (e.g. the timing of sunrise varies between geographical locations and changes across the seasons). This process of synchronisation is known as *entrainment*, and an external stimulus that can synchronise a circadian rhythm is called a *zeitgeber*, which is German for 'time-giver'. Finally, circadian rhythms must be *temperature-compensated*. Put simply, its periodicity should remain constant over a range of physiological temperatures.

1.4.2. Mechanistic basis of circadian rhythms

The suprachiasmatic nucleus

The mechanistic basis of circadian rhythmicity is now fairly well understood. Mammals possess a circadian 'master-clock' which resides in the suprachiasmatic nucleus (SCN), a small brain structure composed of approximately 50,000 neurons in humans (10-20,000 in rodents), which is located in the anterior hypothalamus, just above the optic chiasm [170]. The role of the SCN was first revealed by rodent lesion studies; in rats, circadian rhythms in water consumption, locomotor activity and corticosterone secretion were all abolished by SCN ablation [171, 172]. It was later demonstrated that, following SCN ablation in hamsters, circadian rhythms could be restored by the transplantation of neonatal hypothalamic tissue containing the SCN [173]. Moreover, when SCN tissue was taken from *tau* mutant hamsters, which have a 20 h circadian period, the recipients of the transplants displayed this same, shortened period [174]. The first evidence that the SCN plays an analogous role in humans was

the observation that compression of the SCN by expanding pituitary tumours causes progressive circadian disintegration [175].

In the 1970s and 1980s, *in vivo* oscillations in glucose uptake and electrical activity were first reported in the rat SCN; both were upregulated in the day relative to the night [176, 177]. Analogous observations were subsequently reported with *in vitro* slice preparations [178]. In 1995, it was demonstrated that circadian oscillations result from sub-cellular mechanisms rather than cell-cell interactions [170]. In this seminal experiment, individual neurons were isolated from neonatal rat SCN and cultured on fixed microelectrode arrays, enabling the recording of spontaneous action potentials from isolated SCN neurons. Around 50% of these cultured cells demonstrated circadian rhythms in neural firing rate, suggesting that the SCN contains a large population of autonomous, single-cell circadian oscillators.

The transcriptional-translational feedback loop

Today, following several decades of research, the molecular basis of circadian oscillations is well characterised in a number of model organisms, including both eukaryotic and prokaryotic species [179]. In each case, the basic mechanism takes the form of an autoregulatory transcriptional-translation feedback loop (TTFL), although the identity of the genes involved varies between species [179]. In mammals, the TTFL involves four 'core clock genes': *Period* (*Per1* and *Per2*), *Cryptochrome* (*Cry1* and *Cry2*), *Brain and Muscle ARNT-Like* (*Bmal1*), and *Circadian Locomotor Output Cycles Kaput* (*Clock*) [180]. These genes encode the proteins PER (1 & 2), CRY (1 & 2), BMAL1, and CLOCK, respectively [180]. The mechanistic basis of the TTFL is outlined in Figure 1.3.

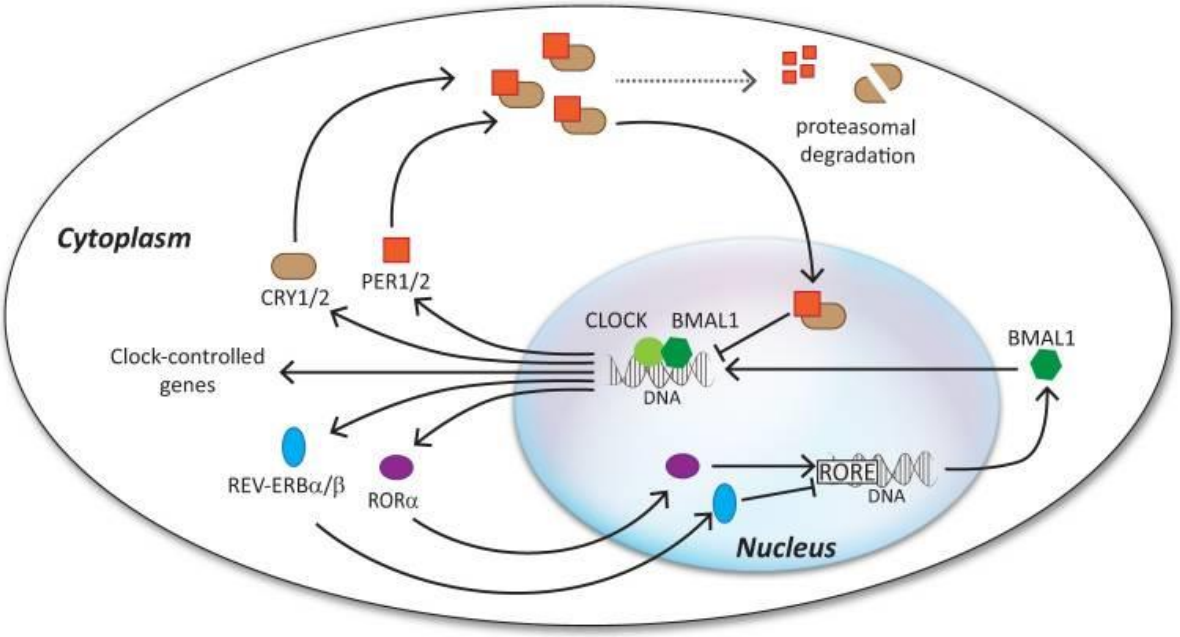

Figure 1.3. Schematic illustration of the mammalian transcriptional-translational feedback loop (TTFL). To begin the cycle, CLOCK and BMAL1 proteins heterodimerise. The resulting CLOCK-BMAL1 heterodimers bind to regulatory DNA sequences called E-boxes, which activates the transcription of *Per* and *Cry*. As a consequence, PER and CRY proteins accumulate in the cytoplasm, and then translocate to the nucleus following their own heterodimerisation. Inside the nucleus, PER-CRY heterodimers suppress the transcription of their own genes, *Per* and *Cry*, by interfering with the activity of the CLOCK-BMAL1 heterodimers. This halts the accumulation of PER and CRY in the cytoplasm. Over time, the remaining PER and CRY proteins are degraded, releasing *Per* and Cry from their auto-inhibition, and the cycle can begin again. The entire sequence takes approximately 24 hours to complete, and is entirely self-sustaining. CLOCK-BMAL1 heterodimers also activate the transcription of *Rorα*, and *Rev-erbα*/β. These rhythmically-expressed genes form an accessory loop, which enhances the amplitude, precision and stability of the TTFL. REV-ERB*α* suppresses *Bmal1* transcription, while ROR*α* promotes it. Figure provided by Akhliesh Reddy [181].

Besides the four core clock genes, several other genes are known to regulate the mammalian TTFL. Casein kinase 1 (*Ck1*), for example, plays an important role in setting core clock speed by phosphorylating PER proteins, which targets them for ubiquitination followed by proteasomal degradation (Eide et al., 2005). The more efficient the CK1 enzyme, the faster PER proteins are degraded, and the shorter the period of the clock. Indeed, the shortened circadian period of the *tau* mutant hamster [182] is a direct consequence of genetic variation in *Ck1* [183]. In addition, the amplitude, precision and stability of the TTFL are enhanced by an accessory loop involving two more rhythmically-expressed genes, *Rev-Erba* and *Rora* [184]. Like *Per* and *Cry*, these genes possess E-box sequences, so their expression is driven by

CLOCK and BMAL1. REV-ERB*a* and ROR*a* proteins modulate *Bmal1* transcription by binding to retinoic acid-related orphan receptor response elements (ROREs) in the *Bmal1* promoter; REV-ERB*a* suppresses *Bmal1* transcription, while ROR*a* promotes it. Together, they ensure that BMAL1 levels increase at the same time that the negative feedback from *Per* and *Cry* is diminishing. Unlike *Bmal1*, *Per* and *Cry*, *Clock* is the only one of the four core clock genes that does not exhibit rhythmic expression [157].

Input to the SCN

The TTFL in the SCN is synchronised with the environmental light/dark cycle via light input to the retina. This process is known as photic entrainment. Light information is transmitted directly from the eye to the SCN, via a subset of retinal ganglion cells, called intrinsically photosensitive retinal ganglion cells (ipRGCs) [185]. Although they also receive input from rod and cone photoreceptors (via bipolar cells), ipRGCs are intrinsically photosensitive because they contain the photopigment melanopsin [185]. The contribution of ipRGCs to photic entrainment is clear from the fact that their selective ablation impairs photic entrainment in mice [185]. In contrast, pattern-forming visual function remains intact [185]. The axons of ipRGCs, which form the retinohypothalamic tract (RHT), synapse directly with the SCN [186, 187]. Glutamate and pituitary adenylate cyclase-activating polypeptide (PACAP) are the principal neurotransmitters at these synapses [188-193]. The effect of manipulations on RHT-SCN synapses is described in Section 5.1. Although light information is the primary *zeitgeber* for the entrainment of the circadian clock, the timing of other events such as feeding and exercise can also be considered *zeitgebers*, which affect the SCN via non-photic pathways [157].

Outputs from the SCN

How does the action of the TTFL translate into circadian rhythms in physiology and behaviour? The immediate output of the TTFL is the rhythmic expression of 'clock-controlled genes' within the SCN itself [175, 194]. These are genes which are not part of the TTFL, but nonetheless show rhythmic expression because they possess E-box or RORE sequences. In turn, these clock-controlled genes regulate the expression of their own downstream target genes. The net result is that roughly 10% of the SCN transcriptome is rhythmically expressed, although it is not known how this leads to the rhythmic patterns of electrical activity observed in the SCN [195]. Circadian signals are conveyed from the SCN to other brain regions by way of monosynaptic or multisynaptic neurotransmission, or via the rhythmic synthesis and secretion of peptide hormones such as vasoactive intestinal peptide (VIP) [175, 194]. It is the SCN's target regions that are ultimately responsible for the coordination of circadian physiology and behaviour. Examples include the rhythmic secretion of the hormone melatonin from the pineal gland, and the rhythmic secretion of corticotrophin-releasing hormone (CRH) from the hypothalamus, which ultimately leads to the release of glucocorticoids from the adrenal glands [175, 194].

Tract tracing shows that the SCN innervates few target regions directly; most are innervated via relays in the thalamus and hypothalamus. Hence, lesions of specific relays impair distinct circadian functions; ablation of the paraventricular nucleus of the hypothalamus, for example, produces a selective impairment in pineal gland rhythms [175, 194]. In contrast, communication from the SCN to brain regions that govern locomotor activity is thought to be chemical, since rest-activity rhythms persist when the SCN is surgically isolated from the rest of the brain [175, 194]. Rest-activity rhythms are also seen in animals that have received SCN transplants, even though there is little innervation of the host brain from the SCN [196]. Both

procedures result in the eradication of non-locomotor rhythms, which suggests that the control of locomotor rhythms is a special case [175, 194]. Transforming growth factor alpha (TGFα) may be the chemical signal responsible [197].

.

Circadian rhythms outside the SCN

By isolating tissue from different parts of the brain and body of mammals and drosophila, and maintaining them *in vitro*, self-sustained rhythmic clock gene expression has been observed in a variety of brain regions beside the SCN, as well as a host of peripheral organs [194, 198]. The first such observation was made in fibroblasts isolated from the rat [199], while one of the best characterised peripheral organs is the liver [200]. It has been demonstrated that, just as in the SCN, around 10% of the transcriptome in most peripheral organs is rhythmically expressed [201]. In the brain, rhythmic electrical activity, clock gene expression and/or hormone output has been reported in the olfactory bulb, amygdala, lateral habenula, hippocampus, motor cortex, and cerebellum, together with a variety of nuclei in the hypothalamus [194, 198]. Taken together, it appears that the brain and body are full of localised, autonomous circadian clocks. Hence, the ultimate role of the SCN may be to direct signals that synchronise these 'peripheral clocks' with each other and the external environment [175, 194] (see Fig. 1.4). Glucocorticoids may be one such signal; the administration of the glucocorticoid dexamethasone is known to synchronise 60% of the liver's circadian transcriptome [175, 194].

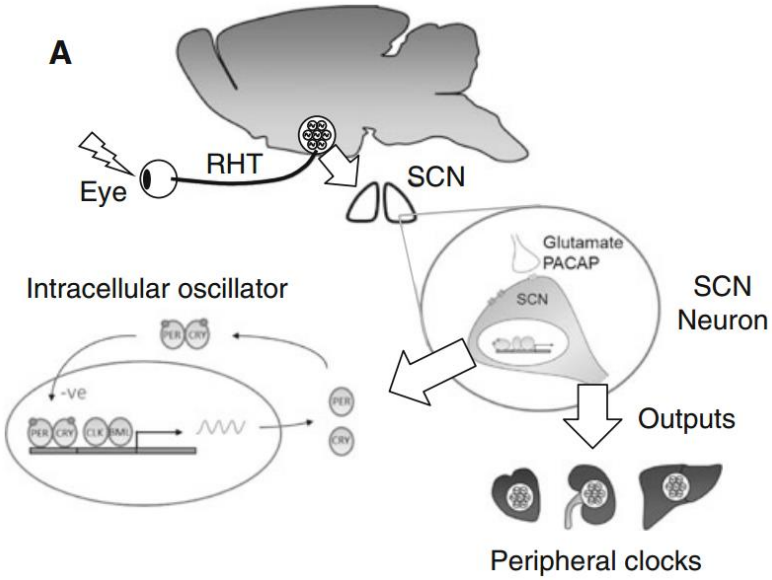

Figure 1.4. Schematic illustration of the mechanisms underlying circadian rhythm generation. Light detected by the eye is relayed to the suprachiasmatic nuclei (SCN) in the hypothalamus via the retinohypothalamic tract (RHT), which uses the neurotransmitters glutamate and PACAP. Circadian rhythms are generated by a cell autonomous transcriptional–translational feedback loop (TTFL) involving a set of core clock genes. The molecular clock in the SCN synchronises circadian clocks found in tissues throughout the body, which regulate local physiology.

Non-transcriptional circadian clocks

Very recently, evidence was unearthed indicating that the TTFL is not the only mechanisms by which circadian rhythms can be generated. O'Neill, Reddy and colleagues observed circadian oscillations in the redox state of oxygen-scavenging peroxiredoxin proteins in human erythrocytes (red blood cells) [202]. These oscillations met the three criteria of circadian rhythms outlined above. This discovery was striking, since erythrocytes lack a nucleus, and are therefore incapable of transcription. Similar rhythms were subsequently demonstrated in plants kept in constant darkness; conditions in which transcription is arrested [203]. These phenomena provide strong evidence for the existence of an alternative, non-transcriptional mechanism that can generate circadian rhythms. The exact nature of this mechanism remains to be elucidated, but it is believed to be evolutionarily ancient, given that peroxiredoxin redox rhythms are present in both eukaryotic and prokaryotic organisms, and the proteins themselves are highly conserved across multiple species [179].

1.5. Introduction to sleep

1.5.1. What is sleep?

Sleep is a recurring physiological state characterised by altered consciousness, reduced perception of environmental stimuli and the inhibition of most voluntary muscles [204]. Although we spend around a third of our lives asleep, the exact functions of sleep are not well understood. Popular theories include the rejuvenation of the immune system [205], cellular detoxification [206], and the repair and regeneration of nervous tissue, bone and muscle [204]. From a cognitive perspective, sleep may be important for memory consolidation [207], while, according to the synaptic homeostasis hypothesis, sleep is required to reverse the net increase in synaptic strength which occurs in many brain circuits during wakefulness [208]. Whatever the functional roles of sleep, its importance is underscored by the myriad health problems that are associated with sleep disruption (see Table 1.1).

Emotional effects	Cognitive effects	Somatic effects
Fluctuations in mood [209-212]	Impaired cognitive performance and ability to multi-task [229-231]	Drowsiness, micro-sleeps and unintended sleep [246-250]
Depression and psychosis [213-216]	Impaired memory, attention and concentration [232-235]	Bodily sensations of pain and cold [251-253]
Increased irritability, impulsivity and frustration [217-219]	Impaired communication and decision-making skills [236-240]	Increased risk of cancer [254, 255]
Increased risk-taking [220-223]	Reduced creativity and productivity [241-244]	Metabolic abnormalities, cardiovascular disease and diabetes [256-261]
Increased stimulant, sedative and alcohol abuse [224-228]	Dissociation/detachment from reality [245]	Reduced immunity to disease and viral infection [262, 263]
		Impaired motor performance [231, 264]
		Altered regulation of the HPA axis [265]

Table 1.1. The primary emotional, cognitive and somatic effects of sleep disruption in humans.

1.5.2. Sleep stages

In humans, sleep consists of both rapid eye movement (REM) sleep and non-rapid eye movement (NREM) sleep, which itself can be subdivided into three stages [266-268]. During sleep, the body repeatedly cycles through these stages in a predictable and sequential manner. The first cycle begins with NREM stage 1 sleep, progresses through NREM stages 2 and 3, and ends with a period of REM sleep. Typically, this first cycle lasts 70 to 100 minutes, while subsequent cycles can last 90 to 120 minutes. Around four or five cycles are completed each night. REM sleep accounts for 20-25% of total sleep time. However, the proportion of REM in is not static; instead, it tends to increase across cycles. By contrast, the proportion of NREM stage 3 sleep (also known as slow-wave sleep) tends to decrease across cycles (see Fig. 1.5)

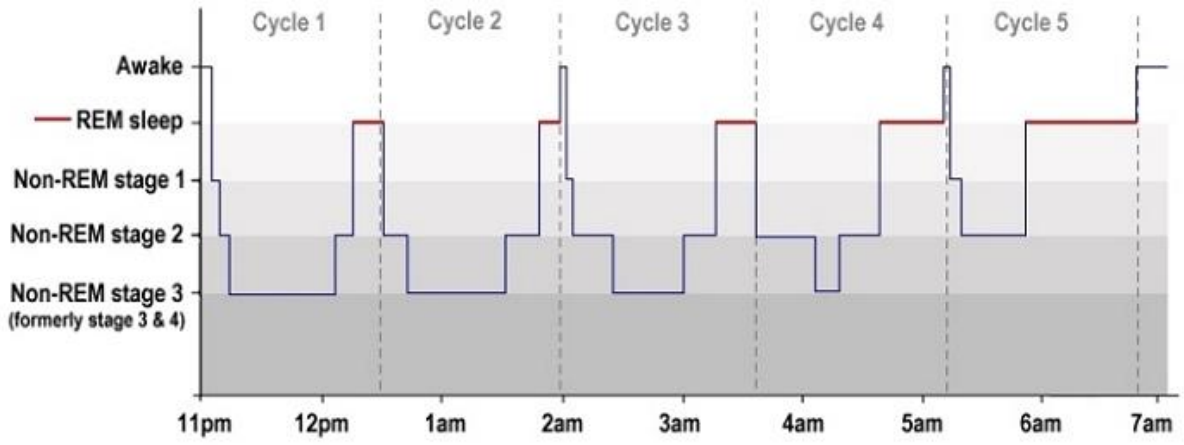

Figure 1.5. A representative human hypnogram, showing the amount of time spent in each sleep stage during a single night's sleep. Note that the proportion of REM sleep increases across successive cycles, whereas the proportion of NREM stage 3 sleep decreases. Figure reproduced from www.howsleepworks.com

As an individual descends through the three stages of NREM sleep, they become progressively harder to awaken, while muscle activity and eye movements decrease [266-268]. The three stages of NREM sleep are characterised by oscillatory brain activity of different frequencies, as described in Table 1.2. In addition, short bursts of oscillatory activity occur at the onset of stage 2 sleep; these are known as sleep spindles and K-complexes. During REM sleep, there is

vigorous eye movement, but most voluntary muscles are temporarily paralysed. Brain activity in REM sleep closely resembles that observed during wakefulness. REM sleep is also associated with dreaming, an association first noted in the early 1950s [269].

(A) Human				
Band/wave		**Frequency (Hz)**	**Vigilance state**	**Associated attributes**
δ	Delta	0.5 – 4	NREM sleep stages 3-4	Deep sleep
θ	Theta	4.5 – 8	NREM sleep stage 1	Transition sleep
α	Alpha	8 – 12	Pre-sleep	Relaxed/quiet state
σ	Sigma	11 – 15	NREM sleep stage 2	Light sleep (with spindles)
β	Beta	15 – 40	Wake	Full consciousness
β	Beta	15 – 30	REM	Desynchronised EEG
γ	Gamma	>35	Wake	Cognitive performance

(B) Rodent				
Band/wave		**Frequency (Hz)**	**Vigilance state**	**Associated attributes**
δ	Delta	0.5 – 4	NREM sleep	Deep sleep
θ	Theta	5 – 9	REM sleep	Hippocampal activity
θ	Theta	4.5 – 11	Wake	Arousal level
σ	Sigma	10 – 15	NREM sleep	Light sleep
β	Beta	15 – 35	Wake	Desynchronised EEG
β	Beta	15 – 35	REM sleep	Desynchronised EEG
γ	Gamma	>35	Wake	Attentive waking

Table 1.2. Categorisation of oscillatory brain activity during sleep in humans (A) and rodents (B). This table outlines the standard nomenclature for the different electroencephalography (EEG)-determined sleep stages, and the behavioural states to which they correspond. Table provided by Sibah Hasan.

1.5.3. Mechanistic basis of sleep and wakefulness

The ascending arousal system and wakefulness

Wakefulness is a state of alertness characterised by high forebrain and cortical activity, which is promoted by the 'ascending arousal system' or AAS [270]. The AAS originates in the upper brainstem (see Fig. 1.6A), near the junction of the pons and midbrain [271], and divides into two separate pathways at the diencephalon [272, 273]. Each branch innervates distinct brain regions and involves different neurotransmitters [274]. The first pathway consists of cholinergic projections from the pedunculopontine (PPT) and laterodorsal tegmental (LDT) nuclei of the brainstem to specific targets in the thalamus [275]. PPT and LDT neurons are more active during wakefulness and REM sleep, and less active during NREM sleep [276]. One of their key targets is the thalamic reticular nucleus (TRN), which inhibits thalamocortical rhythms to promote wakefulness [277].

The second pathway innervates multiple targets in the hypothalamus, forebrain and cerebral cortex [274, 278, 279]. It consists of noradrenergic projections from the locus coeruleus (LC) of the brainstem, serotonergic projections from the dorsal and medial raphe nuclei (DRN and MRN) of the brainstem, dopaminergic projections from the ventral periaqueductal gray (VPAG) of the midbrain, and histaminergic projections from the tuberomammillary nucleus (TMN) of the hypothalamus [270]. It also includes cholinergic and GABAergic projections from basal forebrain (BF) nuclei, and peptidergic projections from lateral hypothalamic (LH) nuclei [270]. These peptidergic neurons can be subdivided into those that release orexin (also known as hypocretin), and those that release melatonin-concentrating hormone (MCH).

The monoamingergic and orexinergic neurons in this pathway are most active during wakefulness, less active during NREM sleep, and least active during REM sleep [271, 280-

283]. In contrast, the MCH-releasing neurons are most active during REM sleep [284], and the cholinergic neurons are most active during REM sleep and wakefulness [285]. In rodents, lesions to this pathway result in narcolepsy and other sleep disturbances [282, 286].

The ventrolateral preoptic nucleus and sleep

The AAS can be inhibited by the ventrolateral preoptic nucleus, or VLPO (see Fig. 1.6B), a small cluster of neurons in the anterior hypothalamus [270]. During sleep, a subpopulation of VLPO neurons are highly active [287], and suppress the aforementioned components of the AAS, through the release of the inhibitory neurotransmitters GABA and galanin [288, 289]. Central VLPO lesions are known to reduce NREM sleep, while lesions to the extended VLPO decrease REM sleep [290]. This dissociation makes sense anatomically, since the VLPO cluster projects to the TMN, which is involved in NREM sleep regulation, while the extended VLPO innervates the LDT, DRN and LC; nuclei implicated in REM sleep gating [270].

Sleep/wake transitions: the hypothetical 'flip-flop' switch model

In addition to the suppression of the AAS by the VLPO, neurons in the VLPO can be inhibited by the AAS. This inhibition is driven by noradrenergic projections to the VLPO from the LC, serotonergic projections from the MRN, and GABAergic and galinergic projections from the TMN [291-294]. Hence, there is reciprocal inhibition between the AAS and the VLPO; the AAS inhibits the VLPO during wake, and the VLPO inhibits the AAS during sleep. It has been proposed that this reciprocal inhibition creates a bistable, on/off feedback loop – or 'flip-flop' circuit – whereby sleep and wake cannot be promoted at the same time. This putative mechanism, also known as the 'sleep switch', may explain why sleep-wake transitions are so swift [274, 276]. Sleep disorders characterised by excessive sleep-wake cycling may reflect dysfunction of the sleep switch [270].

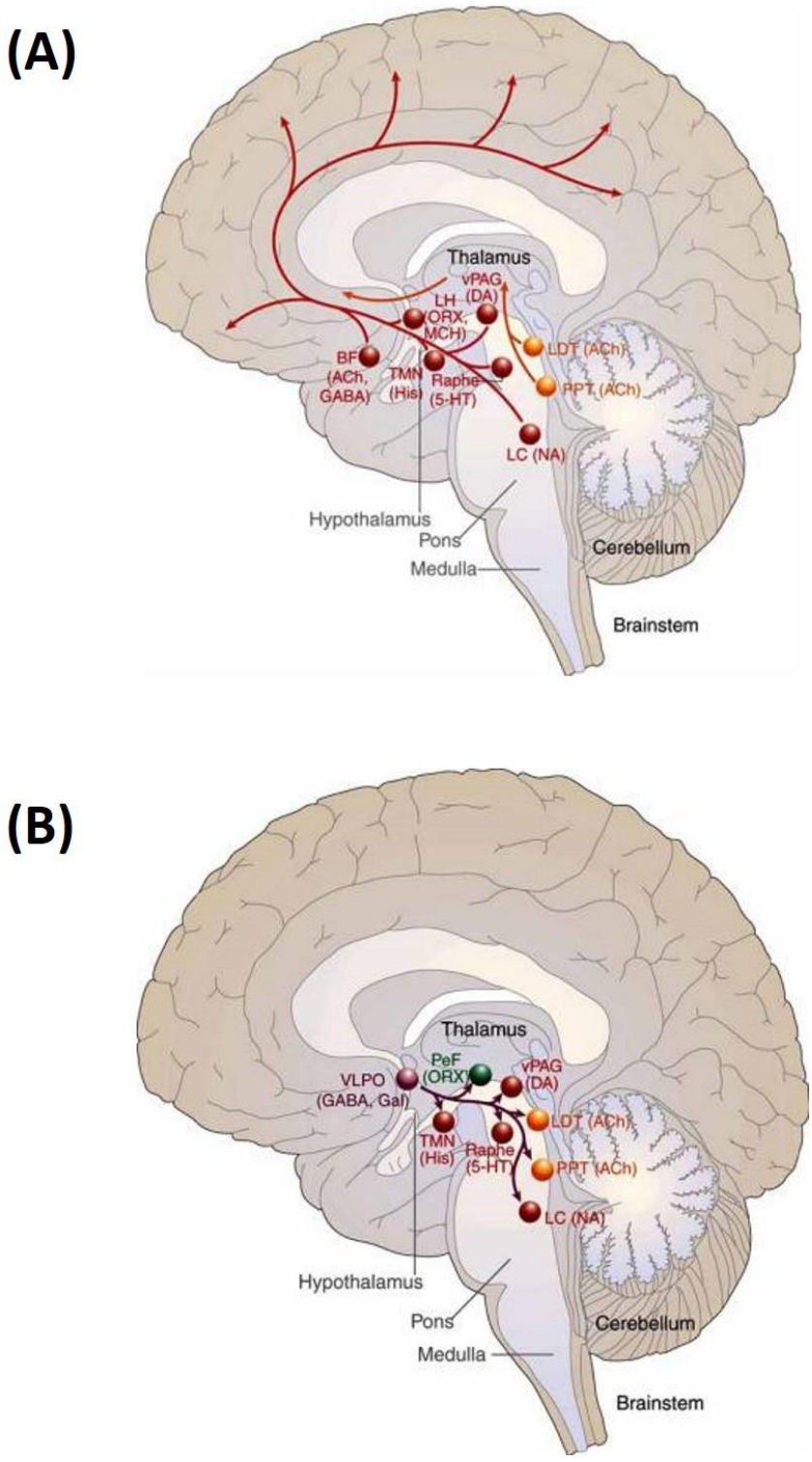

Figure 1.6. Schematic drawings showing key components of the ascending arousal system (A) and the primary projections of the VLPO to the main components of the ascending arousal system (B). Reproduced from Schwartz & Roth [295]. 5-HT = serotonin. ACh = acetylcholine. BF = basal forebrain. DA = dopamine. GABA = gamma-aminobutyric acid. Gal = Galanin. His = histamine. LC = locus coeruleus. LDT = laterodorsal tegmental nucleus. LH = lateral hypothalamus. MCH = melatonin-concentrating hormone. NA = noradrenaline (norepinephrine). ORX = orexin (hypocretin). PeF = perifornical area. PPT = pedunculopontine nucleus. TMN = tuberomammillary nucleus. VLPO = ventrolateral preoptic nucleus. vPAG = ventral periaqueductal gray.

Sleep timing: the two-process model of sleep

According to the two-process model of sleep regulation [296, 297], sleep timing is dependent on two mechanisms (see Fig. 1.7). The first, known as 'Process S', describes a homeostatic drive for sleep, which increases progressively during wakefulness and dissipates during sleep. The biological substrate of this mechanism is unproven, although adenosine is a likely candidate. Adenosine accumulates in the brain during wakefulness [298], while the administration of adenosine or adenosine receptor agonists promotes sleep in rats and cats [299, 300]. These pharmacological effects are likely mediated by the excitation of sleep-promoting brain regions *and* the inhibition of wake-promoting regions (see Schwartz & Roth, 2008). Recent evidence suggests that adenosine accumulation is also responsible for the antidepressant effect of sleep deprivation [301].

The second component of the two-process model, 'Process C', describes the contribution of the circadian clock to sleep regulation [296, 297]. More specifically, it describes a circadian drive for wakefulness, which rises during the day and falls during the evening and night. According to the two-process model, Process C counteracts Process S to keep us awake during the daytime when homeostatic sleep pressure is steadily increasing. In the evening, sleep onset coincides with the opening of the 'sleep gate'; the point at which the discrepancy between Processes S and C reaches a critical threshold (see Fig. 1.7).

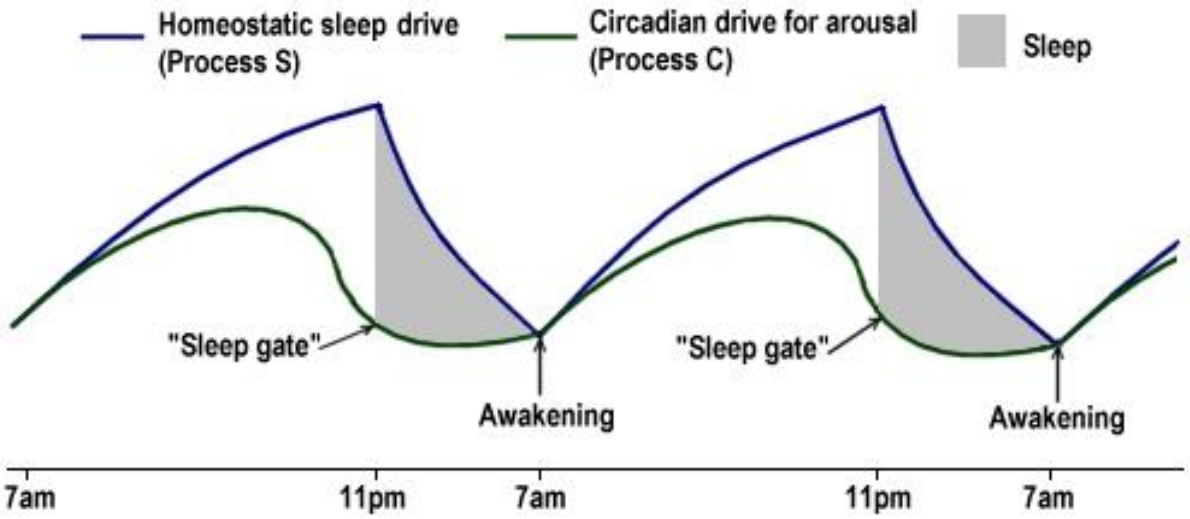

Figure 1.7. Sleep regulation by homeostatic and circadian mechanisms. The homeostatic drive for sleep (Process S) increases during wakefulness. During the day, this is counteracted by the circadian drive for arousal/wakefulness (Process C). Process C subsides during the evening, and sleep onset coincides with the opening of the 'sleep gate', when the discrepancy between Processes S and C reaches a critical threshold. Figure reproduced from www.howsleepworks.com

SCN lesions in primates result in increased sleep time as well as arrhythmia [302]. This suggests that under normal conditions, signals from the SCN oppose the homeostatic drive for sleep, providing a plausible biological substrate for Process C. These signals may be carried by projections from the SCN to the ventral subparaventricular zone (SPZ) and the dorsomedial nucleus of the hypothalamus (DMH). In rats, lesions of both structures impair the circadian rhythmicity of the sleep/wake cycle [290, 303]. The DMH may be a critical relay between Processes C and S, as it receives inputs from the SCN and SPZ, and innervates both the VLPO and the LH nuclei of the AAS [303]. Further evidence of a circadian contribution to sleep was provided by a study in which 8 men were observed for over a month in the absence of any time cues. A 28 h rest-activity cycle was imposed so that sleep episodes occurred at all phases of the endogenous circadian cycle. (This is known as a 'forced desynchrony' protocol). Despite the enforced sleep schedule, circadian rhythms were observed in a number of sleep parameters, such as REM sleep timing, slow wave sleep timing and sleep spindle activity [304].

1.6. Sleep and circadian screening of transgenic mouse models

Circadian and sleep screening

The most commonly used method to assess circadian function in transgenic mice is to characterise their most obvious behavioural rhythm: the rest-activity rhythm. Since mice are nocturnal, activity levels are typically higher in the dark phase than the light phase of a standard 12:12 h light/dark (12:12 LD) cycle. Rest-activity rhythms can be assessed simply by monitoring an animal's activity within their homecage, using a near-infrared (NIR) video camera, an infrared photobeam frame, piezoelectric sensors, or passive-infrared (PIR) motion detectors [305-308]. Alternatively, a mouse can be given free access to a running wheel, and its wheel-running activity can be recorded continuously. A range of circadian parameters can be extracted from the raw activity data that is generated, as described in Section 5.2. These include measures of absolute activity levels, together with indices of the consistency and fragmentation of the rest-activity rhythm [309, 310]. In addition, the timing and intensity of light exposure can be manipulated, yielding insights into the sensitivity of the circadian system to light [309].

When circadian disruption is observed in a transgenic mouse, it is important to identify the level of the circadian system at which this disturbance arises. Does the deficit affect inputs to the SCN, the function of the SCN itself, or the physiological outputs of the SCN? Such knowledge is vital to understand the contribution of the manipulated gene to circadian function, and to inform the selection and/or development of the most appropriate therapeutic intervention. How can one determine the level at which circadian disturbances arise? Light input to the SCN can be evaluated by measuring behavioural and molecular responses to light (e.g. phase shifting, negative masking, and light-induced gene expression in the SCN) [309, 311], whilst core oscillator function can be assessed at a behavioural level via rest-activity

rhythms under constant conditions, and at a molecular level from SCN clock gene expression and clock gene reporter assays (e.g. Per2::Luc) [312]. Clock outputs can be determined from hormonal rhythms, and from gene expression and reporter assays in peripheral tissues. Hormones such as corticosterone can be measured from faeces [313] or in real-time with *in vivo* microdialysis [314].

Sleep can also be assessed in transgenic mice, using both invasive and non-invasive methods. Non-invasive methods involve the estimation of sleep based on the quantification of immobility, a parameter closely associated with sleep [307]. Again, immobility data can be gathered with NIR cameras, an infrared photobeam frame, piezoelectric sensors or PIR motion detectors [305-308]. As an invasive method, sleep electroencephalography (EEG) is more time-consuming, expensive, technically demanding and potentially harmful to the mice involved, but yields more qualitative data, such as the frequency and timing of REM and NREM sleep bouts [315]. There is also some suggestion that REM and NREM sleep can be estimated from video data, but this approach is still in its infancy [316].

Limitations associated with the sleep and circadian screening of transgenic mouse models

As with behavioural screening, there are several limitations associated with the sleep and circadian screening of transgenic mouse models. Sleep and circadian rhythms in humans and rodents are not identical, not least as rodents are nocturnal and humans diurnal. In addition, humans typically sleep once every 24 hours, whereas rodents tend to alternate between short bouts of sleep and wakefulness [307]. As a result, the sleep and circadian phenotype of a rodent model may not translate directly to humans. In addition, environmental light intensity varies continuously in the natural world, whereas most experimental paradigms employ a discrete transition from light to dark and vice versa [309]. Likewise, humans have voluntary control

over their light environment through the use of electric lights. Moreover, most sleep and circadian screening protocols require mice to be singly-housed. This reduces the ecological validity of the approach, has deleterious effects on physical health, and significantly affects performance in a range of behavioural tests [317, 318].

The way we assess the sleep and circadian phenotypes of mice might also cause problems. Crucially, wheel-running activity is the assay of choice in many circadian laboratories, but wheel-running is a measure of voluntary exercise rather than general homecage activity. Indeed, wheel-running is a complex behaviour that may be subject to multiple influences including arousal, motivation, anxiety, motor coordination, and sensitivity to reward [319-321]. Hence, wheel-running might not be the most appropriate circadian assay for constitutive transgenic disease models, which typically display a range of behavioural alterations [322]. This topic is engaged more thoroughly in Chapters 6 and 7.

Strain differences should also be taken into consideration. For example, C57Bl/6 mice are more sensitive to the circadian effects of light than C3H mice, and are able to entrain to light/dark cycles at much lower irradiances [323]. Moreover, 129 substrains are extremely photosensitive, and display almost complete activity suppression in constant light [324]. There is also evidence that pineal melatonin content varies between strains; in contrast to wild mice, melatonin is lacking from the pineal glands of several inbred strains, including C57Bl/6 mice [325, 326].

1.7. Sleep and circadian rhythm disruption (SCRD) in schizophrenia

1.7.1. Introduction

The relationship between schizophrenia and abnormal sleep was first described in the late nineteenth century by the German psychiatrist Emil Kraepelin [327]. Today, sleep and circadian rhythm disruption (SCRD) is reported in 30–80% of patients with schizophrenia, and is increasingly recognised as one of the most common features of the disorder [328]. Moreover, recent evidence suggests that the degree of SCRD is correlated with the severity of positive, negative, and cognitive symptoms [329-332].

Sleep disturbances in schizophrenia include increases in sleep latency, and reductions in total sleep time, sleep efficiency, REM sleep latency, REM sleep density and slow-wave sleep duration [327, 328, 333-335]. Schizophrenia is also associated with significant circadian disruption, including the abnormal phasing, inconsistency and fragmentation of rest-activity rhythms [336-339]. Crucially, schizophrenia patients with SCRD score badly on many quality-of-life clinical subscales, highlighting the human cost of SCRD in schizophrenia [328, 340, 341]. To reinforce this, schizophrenia patients often comment that an improvement in sleep is one of their highest priorities during treatment [342].

1.7.2. Explanations for the co-morbidity of schizophrenia and SCRD

Antipsychotic medication

SCRD in schizophrenia could be viewed as a side effect of antipsychotic medication. Although intuitively plausible, antipsychotic medication cannot be the only cause of SCRD in schizophrenia, since SCRD affects both medication-naïve [343] and medicated patients [344].

Indeed, the emergence of sleep disruption often precedes the diagnosis of schizophrenia, occurring before any drugs have been prescribed [343, 345]. Recent data would suggest that, if anything, antipsychotic medication actually *improves* sleep quality in schizophrenia [328, 344, 346], presumably due to the strong sedative effects of these compounds [347]. Schizophrenia patients treated with typical antipsychotics show an increase in their sleep efficiency and total sleep time [328], while atypical antipsychotics are even more effective than typical antipsychotics at improving sleep quality in schizophrenia [348].

Social isolation

Social isolation, and the resulting absence of social constraints, is also routinely suggested as a cause of SCRD in schizophrenia. This hypothesis was recently addressed by comparing the sleep patterns of schizophrenia patients with those of unemployed healthy volunteers [349]. Major sleep disruption was observed in all schizophrenia patients, including those that followed a rigid daily routine. Conversely, undisturbed sleep was seen in a number of control participants that did not follow a fixed routine. Hence, although social isolation may contribute to some degree, it cannot be the primary cause of SCRD in schizophrenia.

Shared neuropathophysiology

If SCRD in schizophrenia is more than a side effect of antipsychotic medication or a by-product of social isolation, how can it be explained? One possibility is that SCRD and schizophrenia stem from dysfunction in common brain mechanisms (e.g. specific enzymes, neuroreceptors or neurotransmitter pathways) that contribute to both pathologies [125]. According to this hypothesis, SCRD should not be seen as a consequence of schizophrenia's onset; instead it could be conceptualised as a core symptom of the disorder that is intrinsically rooted in its underlying neuropathophysiology.

This account seems eminently plausible given that schizophrenia is a disorder of distributed brain circuits, affecting a range of neurotransmitter systems [350], many of which overlap with those involved in sleep regulation [343]. As explained in Section 1.2.5., dopamine, glutamate and serotonin are all implicated in schizophrenia, while all three neurotransmitters are involved in sleep and circadian function (see Fig. 1.6 and Section 5.1). Moreover, multiple schizophrenia candidate genes have a credible biological connection with sleep and circadian function within the brain (see Section 1.7.3. and 7.3).

If these genes (together with other, as-yet-unidentified genes) are the substrates which underpin the co-morbidity of SCRD and schizophrenia, one would expect their manipulation to result in both SCRD and schizophrenia-relevant behavioural abnormalities (e.g. impaired memory or reduced prepulse inhibition). Although this prediction is impossible to test in humans, it can be falsified relatively easily using animal models. Indeed, there is a new but rapidly-growing literature which speaks to this question, as described in the following paragraphs.

1.7.3. Existing evidence of simultaneous SCRD and schizophrenia-relevant behavioural abnormalities in schizophrenia-relevant genetic mouse models

Snap-25 (*blind-drunk*) mutant mouse

Previous work has shown that the *blind-drunk* (*Bdr*) mouse, a model of SNAP-25 exocytotic disruption, displays schizophrenia-related behaviours such as reduced PPI, that are modulated by environmental stress [351, 352]. Furthermore, their PPI deficits are alleviated with the atypical antipsychotic clozapine [352], just like the PPI deficits of schizophrenia patients [353, 354]. *Bdr* mutants also show disturbances in circadian organisation that appear to specifically

affect outputs of the SCN. The rest/activity rhythms of *Bdr* mice are phase-advanced and fragmented under a standard light/dark cycle. Retinal inputs appear normal in *Bdr* mice, as light-induced phase shifts, negative masking, pupil constriction and retinal histology are all unaffected. Similarly, clock gene rhythms within the SCN are normally phased both *in vitro* and *in vivo*. However, the 24 h rhythms of arginine vasopressin within the SCN and plasma corticosterone are both markedly phase-advanced in *Bdr* mice. These data suggest that the circadian phenotype of the *Bdr* mouse arises from a disruption of synaptic connectivity within the SCN that alters critical output signals [355].

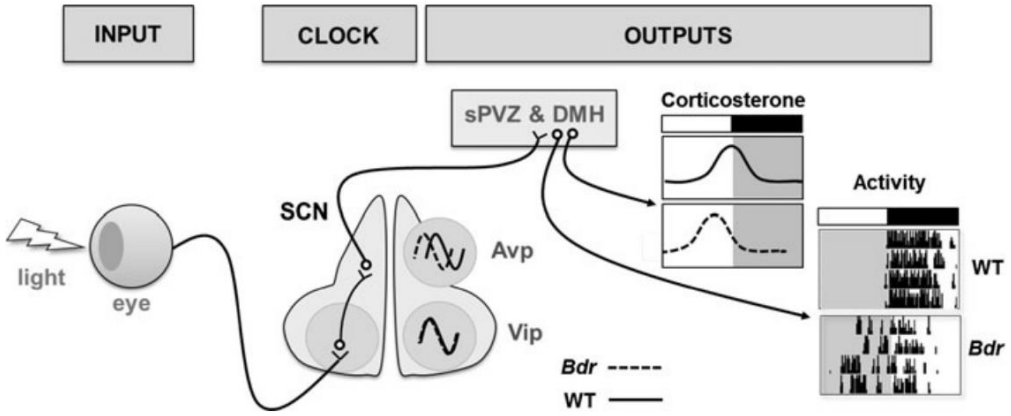

Figure 1.8. Summary of findings in the *blind-drunk* (*Bdr*) mouse model. The rest/activity rhythms of *Bdr* mice are phase-advanced and fragmented under a light/dark cycle. Retinal inputs appear normal in *Bdr* mice, and clock gene rhythms within the suprachiasmatic nucleus (SCN) (e.g. *Per2*) are normally phased both *in vitro* and *in vivo*. Likewise, circadian oscillations in vasoactive intestinal peptide (Vip) are normally phased within the SCN. However, the 24 h rhythms of arginine vasopressin (Avp) within the SCN and plasma corticosterone are both markedly phase advanced in *Bdr* mice. DMH = dorsomedial hypothalamus. sPVZ = subparaventricular zone.

Vipr2 knockout mouse

Recent studies have shown that *Vipr2* microduplication confers a significant risk for schizophrenia [49]. Vasoactive intestinal polypeptide (VIP) and its receptor, VPAC2, encoded by the gene *Vipr2*, play a critical role within the SCN [356]. VPAC2 is required for the maintenance of circadian oscillations within SCN neurons, the synchronisation of oscillations between subregions of the SCN, and the coupling of the SCN with other brain regions [357-

359]. Under 12:12 LD, the activity rhythms of *Vipr2*$^{-/-}$ mice do not differ from wildtype controls, but under DD, some *Vipr2*$^{-/-}$ mice display fragmented activity rhythms and a shorter circadian period, while others become completely arrhythmic [360, 361]. Unlike *Bdr* mice, the circadian abnormalities of *Vipr2*$^{-/-}$ mice appear to result from a dysfunctional core clock. In *Vipr2*$^{-/-}$ mice, neuronal activation within the SCN remains unchanged across the circadian cycle, whereas wildtype mice show greater activation during the subjective day [360]. Although schizophrenia-relevant behaviours have yet to be tested in *Vipr2*$^{-/-}$ mice, VIP-deficient mice exhibit an impairment of hippocampus-dependent associative memory [362], a cognitive deficit often seen in schizophrenia [133, 363, 364]. This phenotype may stem from the fact that VPAC2 is involved in cyclic adenosine monophosphate (cAMP) signalling, which is known to modulate NMDAR-mediated synaptic transmission in the hippocampus [365].

Nrg1 mutant mouse

Neuregulin 1 (NRG1) is a growth factor involved in neurodevelopment and plasticity [37, 38], which has been associated with both schizophrenia [39, 366] and schizotypal personality disorder [367]. There is some evidence that its expression is increased in the brains of schizophrenia patients [37, 368]. Relative to wildtypes, *Nrg1*-deficient mice have fewer functional NMDARs in the forebrain, and exhibit reduced PPI [39] and impaired object recognition memory performance [369, 370]. *Nrg1*$^{type\ 1\text{-}tg}$ mice, which overexpress *Nrg1*, also display reduced PPI [371], together with impaired hippocampus-dependent spatial working memory [372]. From a circadian perspective, mice heterozygous for a disruption in the *Nrg1* gene show disturbed rest/activity rhythms [373], whilst wheel-running activity is inhibited by the long-term infusion of NRG1 into the third ventricle of hamsters [374]. *Nrg1* is expressed in the SCN and in retinal ganglion cells [375, 376], consistent with its proposed involvement in circadian function.

Cckar knockout mouse

The Cholecystokinin A receptor (CCK-AR) is a G-protein coupled receptor that binds the neuropeptide cholecystokinin (CCK) [377]. Abnormal levels of CCK mRNA have been observed in the brains of schizophrenia patients [378, 379], while several studies have reported an association between the *Cckar* gene and schizophrenia [50, 380-383]. Dopamine may mediate the relationship between CCK and schizophrenia, as CCK-ARs modulate CCK-stimulated dopamine release in the mesolimbic system [384]. There is also evidence that CCK plays a role in sleep regulation. The intraperitoneal administration of CCK promotes slow-wave sleep and inhibits locomotor activity in rats [385]. CCK may exert its effects through orexin, a neurotransmitter known to influence wakefulness, as CCK activates orexinergic neurons by binding to CCK-ARs [386]. CCK-ARs are also involved in photoentrainment; light-induced phase shifts are significantly attenuated in *Cckar* knockout mice, as is light-induced clock gene expression in the SCN [387]. Schizophrenia-relevant behaviours have yet to be tested in these mice.

Mouse Model	Description	Neuropsychiatric relevance	Sleep and circadian relevance
Snap-25 or *Blind-drunk* (*Bdr*) mutant	SNAP-25 is a membrane-bound protein involved in exocytosis and exocytotic vesicle recycling.	The *Bdr* mouse displays schizophrenia-related behaviours that are modulated by environmental stress. There are no definitive links between *Snap-25* mutations and schizophrenia, but synaptic dysfunction and abnormal neurotransmitter release underpin the disorder.	The rest/activity rhythms of *Bdr* mice are phase advanced and fragmented under a light/dark cycle. The 24 h rhythms of arginine vasopressin within the SCN and plasma corticosterone are both markedly phase-advanced in *Bdr* mice. SNAP-25 mRNA is present in the SCN and the retina.
Vipr2$^{-/-}$	VPAC2 is a G-protein coupled receptor that binds the peptide hormone vasoactive intestinal peptide (VIP).	*Vipr2* duplications confer a significant risk for schizophrenia.	VPAC2 is required for the maintenance of circadian oscillations within SCN neurons, and for the synchronisation of oscillations between these neurons. *Vipr2*$^{-/-}$ mice demonstrate circadian abnormalities, including a shortened circadian period of approximately 22 h.
Nrg1 mutant	NRG1 is a growth factor involved in neurodevelopment and plasticity.	*Nrg1* is associated with both schizophrenia and schizotypal personality disorder. *Nrg1* expression may be increased in the brains of schizophrenia patients.	Mice heterozygous for a disruption in the *Nrg1* gene show disrupted rest/activity rhythms. Wheel-running activity is inhibited by the long-term infusion of NRG1 into the third ventricle of hamsters. *Nrg1* is expressed in the SCN and retinal ganglion cells.
Cckar$^{-/-}$	CCKAR is a G-protein coupled receptor that binds the peptide hormone cholecystokinin (CCK).	*Cckar* is associated with schizophrenia. The level of CCK mRNA is altered in the brains of schizophrenia patients. Dopamine may mediate the relationship between CCK and schizophrenia, as CCKARs modulate CCK-stimulated dopamine release in the mesolimbic system.	The intraperitoneal administration of CCK promotes slow-wave sleep and inhibits locomotor activity in rats. CCK may exert its effects through orexin, a neurotransmitter known to influence wakefulness, as CCK activates orexinergic neurons by binding to CCKARs. Light-induced phase shifts are significantly attenuated in *Cckar* knockout mice, as is light-induced clock gene expression in the SCN.

Table 1.3. Existing evidence of sleep and circadian rhythm disruption (SCRD) in schizophrenia-relevant genetic mouse models.

1.7.4. SCRD in schizophrenia-relevant genetic mouse models: future directions

The preceding paragraphs describe four schizophrenia-relevant transgenic mouse models with significant circadian abnormalities. The *Bdr* mutant [351, 352] also shares behavioural features in common with schizophrenia patients, which is consistent with the claim that the *Snap-25* gene contributes to the co-morbidity of SCRD and schizophrenia. By contrast, schizophrenia-relevant behaviours have yet to be tested in *Vipr2*$^{-/-}$ or *Cckar*$^{-/-}$ mice. In future, both models should be subjected to tests that assess behaviours relevant to the positive, negative and cognitive symptoms of schizophrenia. Circadian rhythm disruption and schizophrenia-relevant behaviours have both been observed in *Nrg1* transgenic mice, although it should be noted that several different models have been used and simultaneous deficits have yet to be reported in any of these models. Chapter 7 includes a brief introduction to eight more schizophrenia-associated genes that might contribute to the co-morbidity of SCRD and schizophrenia. Future studies could characterise sleep, circadian rhythms and schizophrenia-relevant behaviours in mice in which these genes have been manipulated (see Section 7.3).

1.8. A causal relationship between SCRD and the behavioural symptoms of schizophrenia?

1.8.1. Introduction

Another unresolved issue in the field concerns the relationship between SCRD and the three behavioural symptom groups (positive, negative and cognitive) which characterise schizophrenia. Do these symptoms arise independently of SCRD, or does SCRD make a causal contribution to them? The answer to this question could have significant implications for the treatment of schizophrenia; if SCRD does make a causal contribution, then the targeted treatment of SCRD should benefit the overall health and social functioning of schizophrenia patients [125]. The potential value of this approach is amplified by the fact that existing treatments (i.e. antipsychotic medication) have little impact on the negative and cognitive symptoms of schizophrenia (see Section 1.1.3.). Nonetheless, solid evidence of a causal relationship between SCRD and the behavioural symptoms of schizophrenia is needed before this putative treatment strategy can become part of clinical practice. As the following paragraphs demonstrate, the majority of the current evidence is correlational rather than causal.

1.8.2. Evidence from schizophrenia patients and healthy human subjects

Cognitive symptoms

Behavioural alterations reminiscent of those seen in schizophrenia can be triggered in healthy individuals by sleep deprivation or transitory circadian de-synchronisation. For example, sleep deprivation [232, 388-392] and circadian de-synchronisation [393] are both known to impair cognitive performance in healthy individuals. On this basis, it is conceivable that SCRD might exacerbate – or even contribute to – the cognitive impairments of schizophrenia patients.

Consistent with this argument, associations have been reported between cognitive performance and specific sleep or circadian parameters in medication-naïve [394], medicated [330, 395-400], and unmedicated schizophrenia patients [260]. In one study, the severity of patients' cognitive symptoms was inversely related with slow-wave sleep duration and REM sleep density [260]. In another, the amplitude of rest-activity rhythms was strongly associated with performance in cognitive tasks that assess distractibility, reaction time, and verbal fluency [330]. A correlation has also been observed between attentional set-shifting performance and REM sleep latency [401]. Similar associations are evident in healthy individuals; for example, performance in the go/no-go task (a test of response inhibition) is associated with multiple slow-wave sleep parameters [402].

Memory consolidation is just one cognitive function that warrants further investigation in relation to SCRD, as it has been suggested that sleep makes a crucial contribution to this process [207]. Reduced overnight consolidation of procedural learning has been demonstrated in schizophrenia patients [403], and more recently, these deficits were shown to be accompanied by a reduction in slow-wave sleep duration [397]. Another study with schizophrenia patients unearthed an association between sleep spindle activity during NREM stage 2 sleep and overnight improvements in a finger-tapping, sequence learning task [398, 399]. Sleep spindle activity is significantly reduced in schizophrenia patients [404].

Positive symptoms

The positive symptoms of schizophrenia could also be aggravated – or even triggered – by SCRD. In healthy human subjects, sleep deprivation results in increased perceptual distortions [405, 406], increased paranoia [407], and reduced prepulse inhibition [406]. From a clinical perspective, sleep disturbance is recognised as a significant risk factor for the first episode of

psychosis [345], as well as a risk factor for relapse in recovering patients [408]. Severe sleep disturbance often precedes the onset of psychotic episodes in schizophrenia patients [332, 346, 409], while it is also predictive of the maintenance of these symptoms [409]. In addition, the severity of sleep disturbance is positively correlated with the severity of psychotic symptoms [346]. Finally, the positive symptoms of schizophrenia have been shown to be associated with the incidence of sleep spindles [410].

Negative symptoms

The negative symptoms of schizophrenia might also be related to SCRD, since circadian de-synchronisation increases negative mood, irritability and affective volatility in healthy volunteers [393, 411]. 24 hours of sleep deprivation in healthy human subjects also leads to increased anhedonia [406], one of the core negative symptoms of schizophrenia. Consistent with these observations, improvements in sleep quality are frequently correlated with the amelioration of negative symptoms in schizophrenia patients [341, 348]. Moreover, the negative symptoms of schizophrenia are associated with reduced REM sleep latency and various slow-wave sleep deficits [401, 412-414]. Likewise, in adolescents at ultra-high risk for psychosis, sleep disruption is associated with greater negative symptom severity [415].

However, somewhat counterintuitively, a single night of sleep deprivation has a powerful antidepressant effect in roughly 60% of patients with major depression [416-419]. The mechanistic basis of this effect is largely unknown, but may be linked to an upregulation of adenosine signalling [301] and/or the disinhibition of mesolimbic dopaminergic reward networks [420]. The therapeutic potential of this phenomenon is limited by the fact that it is temporary; the effect disappears immediately after recovery sleep [418, 419]. Short-term sleep

deprivation is also known to trigger episodes of inappropriate euphoria in healthy adults [389, 421, 422].

1.8.3. Evidence from wildtype rodents

Sleep deprivation

Just as sleep deprivation can trigger schizophrenia-like behavioural alterations in healthy humans, the same can be said of healthy wildtype rodents. For example, NMDAR antagonist-induced hyperlocomotion, which may be relevant to the positive symptoms of schizophrenia, is heightened by sleep deprivation in male Wistar rats [423]. There are also numerous reports of impaired cognition in rodents following sleep deprivation; these include object recognition memory deficits [424, 425], spatial recognition memory deficits [426, 427], long-term spatial memory deficits in the Morris water maze [428-432] and radial arm maze [433], and attentional impairments in the 5-choice serial reaction time task [434]. The findings appear to reflect genuine memory deficits, as partial sleep deprivation (by gentle handling) has little effect on exploratory locomotor activity or on indices of stress such as plasma corticosterone or adrenocorticotropic hormone levels [425]. In rats, sleep deprivation reduces prepulse inhibition [435-437], which may be relevant to the cognitive symptoms of schizophrenia (see Section 4.1.). As in the human literature, there is a more complex relationship between sleep deprivation and behaviours related to the negative symptoms of schizophrenia; rodents demonstrate reduced behavioural despair in the Porsolt forced swim test [301, 438, 439] and tail-suspension test [301] after 12 but not 72 h of partial sleep deprivation. Performance in these tasks has yet to be tested after chronic partial sleep deprivation.

Abnormal photic input

Another way to investigate the impact of SCRD on cognitive performance is to induce SCRD in wildtype rodents with abnormal photic input. For example, arrhythmia can be induced in healthy hamsters by a single light treatment; a combination of a nocturnal light pulse and a phase delay in LD (Note that this effect seems to be species-specific). Following this treatment, object recognition memory performance is impaired in arrhythmic animals, but not in those that remain rhythmic [440, 441]. There is no difference in total object exploration between arrhythmic and rhythmic animals, so this deficit is not an artefact of altered locomotor activity. Similar results have been reported in mice. LeGates and colleagues disrupted the circadian rhythms of mice by keeping them under a T7 cycle; an ultradian LD cycle consisting of a 3.5 h light phase followed by a 3.5 h dark phase [442]. This led to period lengthening of both body temperature and rest-activity rhythms, but no change in total sleep time, REM sleep time, or the rhythmic expression of *Per2* in the SCN [443]. Relative to mice kept under a standard 12:12 LD cycle, animals kept under a T7 cycle exhibited impaired object recognition memory performance. However, it is unclear whether this impairment reflects a genuine memory deficit or a reduction in object exploration, as locomotor activity data were not reported [442].

1.8.4. Evidence from clock gene transgenic mice

SCRD can also be induced in rodents through the genetic manipulation of core clock genes, such as *Cryptochrome* (*Cry1* and *2*). Under 12:12 LD, circadian rhythmicity is unaffected in *Cry* single-knockout (*Cry1*$^{-/-}$ and *Cry2*$^{-/-}$) and *Cry* double-knockout (*Cry1/2*$^{-/-}$) mice [444, 445]. Under DD, the single-knockout models maintain behavioural rhythmicity, although free-running period length is shortened relative to wildtypes in *Cry1*$^{-/-}$ mice, and lengthened relative to wildtypes in *Cry2*$^{-/-}$ mice. By contrast, *Cry1/2*$^{-/-}$ mice become immediately arrhythmic upon release into DD [444, 445], underscoring the importance of *Cry1* and *Cry2* to the generation

and maintenance of behavioural rhythmicity. Significantly, object recognition memory performance is impaired in *Cry1*$^{-/-}$ mice, *Cry2*$^{-/-}$ mice, and *Cry1/2*$^{-/-}$ mice [446]. These deficits cannot be explained in terms of altered activity, since total object exploration in the sample phase does not differ between knockouts and wildtypes [446]. They may be related to altered anxiety, however, as all three models exhibit heightened anxiety in the elevated plus-maze [446].

1.8.5. Moving from correlation to causality

The targeted treatment of SCRD in schizophrenia patients

SCRD is rarely targeted for treatment in schizophrenia, but when it is, patients report improvements in both their sleep quality and psychiatric symptoms. In a recent study, the treatment of insomnia with the $GABA_B$ receptor agonist sodium oxybate led to an improvement in both the sleep quality and negative symptoms of a group of schizophrenia patients [447]. In another study, insomnia was treated in 15 patients with persistent persecutory delusions and schizophrenia [331]. Following a cognitive behavioural therapy (CBT) intervention aimed at improving sleep quality, there were significant reductions in both insomnia and persecutory delusions. At least two-thirds of participants showed a substantial (>25 %) reduction in insomnia, whilst approximately half showed a substantial (>25 %) reduction in persecutory delusions. There were also reductions in levels of hallucinations, anxiety and depression. These two studies represent an important advance in the literature; they are the first to demonstrate that the targeted treatment of sleep disruption in schizophrenia patients can yield improvements in their 'classical' behavioural symptoms. These observations provide a strong hint that SCRD can make a causal contribution to the behavioural symptoms of schizophrenia. Having said this, the results of both studies should be interpreted with caution, due to a number of methodological limitations; the sample sizes were small, they did not include control groups,

and patients received antipsychotic medication throughout both studies. However, plans have been published to repeat the CBT experiment as a randomised control trial with 30 patients in the treatment group and 30 patients in the control group [448].

SCRD-targeting interventions in schizophrenia-relevant rodent models

Therapeutic interventions designed to improve SCRD can also be applied to rodent models that demonstrate simultaneous SCRD and schizophrenia-relevant behavioural abnormalities. If SCRD makes a causal contribution to the behavioural symptoms of schizophrenia, then these interventions would be expected to benefit both the animals' SCRD *and* their behavioural impairments. Proof-of-principle for this approach is provided by the targeted 'treatment' of SCRD in the R6/2 transgenic mouse model of Huntington's disease, a model which displays a progressive disintegration of sleep and circadian rhythmicity across its lifespan [449]. To date, interventions employed in this model include bright light therapy [450], temporally scheduled feeding [451, 452], temporally scheduled exercise [450], and the pharmacological imposition of a daily sleep/wake cycle with the sedative drug Alprazolam [453, 454] and/or the vigilance-promoting drug Modafinil [454].

Bright light therapy and scheduled exercise delayed the disintegration of rest-activity rhythms in the R6/2 model, but cognitive measures were not included in this study [450]. Scheduled feeding also had a restorative effect on behavioural rhythmicity [451, 452], but had no impact on cognitive performance [452]. Strikingly, however, Alprazolam administration had the dual effect of improving behavioural rhythmicity and slowing cognitive decline in the R6/2 model [453, 454]. This work tentatively suggests that SCRD makes a causal contribution to cognitive dysfunction in Huntington's disease. The same experimental approach could easily be applied to a schizophrenia-relevant mouse model, or indeed any neuropsychiatrically-relevant animal

model. Temporally scheduled exercise has already been shown to improve behavioural rhythmicity in the schizophrenia-relevant *Vipr2*$^{-/-}$ mouse model (Power et al., 2010), although measures of cognitive performance were not included in this study.

1.9. Introduction to D-amino acid oxidase (DAO)

1.9.1. The NMDA receptor

As outlined in Section 1.2.5., the NMDAR is an ionotropic glutamate receptor that is widely expressed in the brain [101]. Although there are exceptions, its localisation is predominantly neuronal, and primarily postsynaptic [101]. There is good evidence for the involvement of the NMDAR in learning and memory processes, while it is also implicated in neurodevelopment, neuroprotection and neurotoxicity [101]. The functional heterogeneity of the NMDAR is explained by its physical heterogeneity. The NMDAR is a heterotetamer consisting of at least one GluN1 subunit together with various combinations of GluN2 (of which there are 4 genetic variants) and/or GluN3 subunits (of which there are 2 genetic variants) [455]. There are 8 splice variants of the ubiquitously expressed GluN1 subunit, adding to the variety conferred by the multiple possible subunit combinations [456, 457]. Further variation stems from post-translational modifications that influence both the function and sub-cellular localisation of the receptor [458, 459].

The NMDAR has two distinctive properties. Firstly, it is both ligand-gated and voltage-dependent [101]; for its transmembrane ion channel to open, glutamate (or a similar substance such as NMDA) must bind to its glutamate binding site, and the membrane in which it resides must be depolarised. Ordinarily, the ion channel is blocked by extracellular Mg^{2+} ions, due to the resting membrane potential of -70mV (see Fig. 1.9A). This Mg^{2+} block is relieved by α-amino-3-hydroxy-5-methyl-4-isoxazolepropionic acid (AMPA) receptor-mediated membrane depolarisation (see Fig. 1.9B). Due to its dual requirement for glutamate binding and membrane depolarisation, the NMDAR acts as a detector of coincident pre- and post-synaptic activity. Hence, the NMDAR is a plausible biological substrate of Hebbian associative learning.

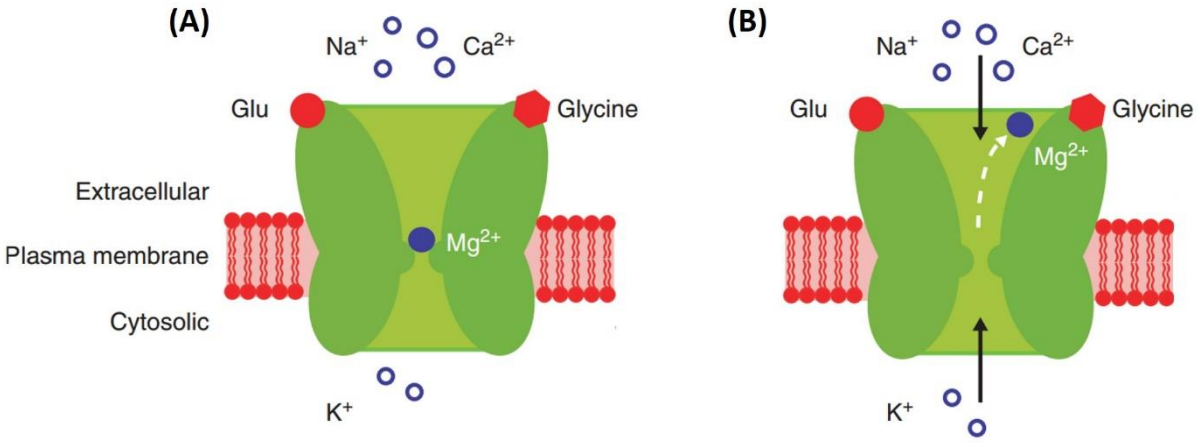

Figure 1.9. Schematic depicting the mechanism of the magnesium block on the N-Methyl-D-aspartate receptor (NMDAR). (A) At resting membrane potential, the pore of the NMDA receptor channel is blocked by magnesium ions. (B) Upon depolarization, the magnesium block is relieved. Na^+ and Ca^{2+} ions enter the cell and K^+ ions leave the cell. Figure reproduced from Zito & Schuess [101].

The opening of the NMDAR's transmembrane ion channel results in the influx of Na^+ and Ca^{2+} ions and the efflux of K^+ ions. It is the influx of Ca^{2+} ions which explains the involvement of the NMDAR in learning and memory, since Ca^{2+} influx can lead to the strengthening or the weakening of the synapse (i.e. long-term potentiation (LTP) and long-term depression (LTD), respectively). Whether the synapse is strengthened or weakened is dependent on the amount of Ca^{2+} that enters the postsynaptic neuron, which in turn is dependent on the relative timing of pre- and post-synaptic activity. This phenomenon is known as 'spike-timing dependent plasticity' (see Fig. 1.10). If the presynaptic action potential (AP) precedes the postsynaptic AP by less than 50 ms, there is dramatic Ca^{2+} influx. This activates protein kinases directly, and triggers second messenger cascades that lead to the increased expression of protein kinases within dendritic spines. In turn, protein kinases strengthen the synapse through at least 2 mechanisms: (1) the phosphorylation of existing postsynaptic ionotropic excitatory receptors (primarily AMPA receptors), which increases their ionic permeability; and (2) the recruitment of additional ionotropic excitatory receptors to the postsynaptic membrane. Protein kinases also promote the growth of dendritic spine volume. However, if the postsynaptic AP precedes the

presynaptic AP, Ca^{2+} influx is relatively weak. This activates protein phosphatases, which have the opposite effect to protein kinases.

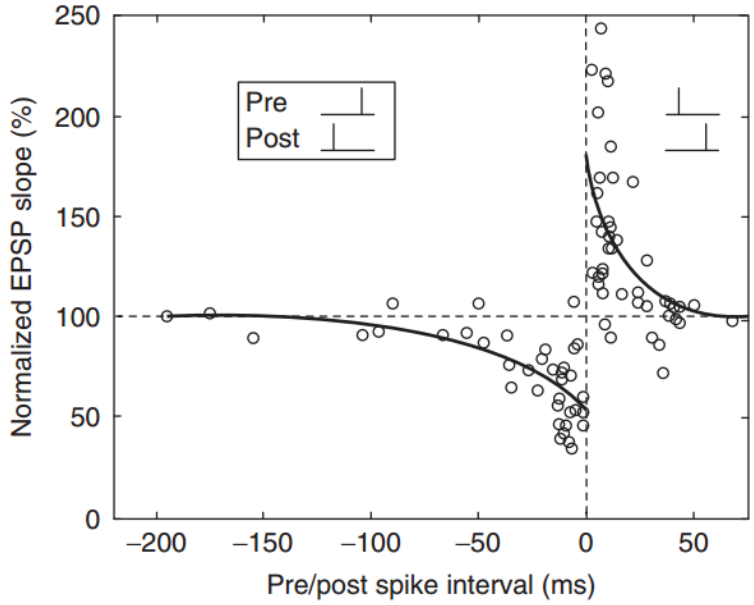

Figure 1.10. Spike-timing-dependent synaptic plasticity. Change in excitatory postsynaptic potential (EPSP) slope induced by repetitively paired pre- and postsynaptic spikes in layer 2/3 of rat visual cortex. Insets depict the sequence of spiking. Pre before postsynaptic spiking leads to potentiation while post before presynaptic spiking leads to depression. Figure reproduced from Zito & Schuess [101].

It is widely (although not universally) accepted that NMDAR-dependent synaptic plasticity is necessary for the encoding of long-term associative spatial memories in the hippocampus, a belief which is based on two lines of evidence [460, 461]. Firstly, NMDAR antagonists such as AP5 block the induction of hippocampal LTP and impair spatial learning in rodents. Secondly, transgenic mice lacking hippocampal NMDARs display reduced LTP and impaired long-term spatial memory performance. By contrast, there is relatively less evidence for the involvement of LTD in long-term associative spatial memory formation. Instead, LTD may be involved in short-term habituation processes [462-465], and reversal learning and extinction in long-term memory tasks [466].

The second distinctive property of the NMDAR is that it can only be activated when its co-agonist site is occupied. This site is commonly referred to as the glycine site, since glycine was originally believed to be the primary endogenous co-agonist of the NMDAR [101]. Subsequently, evidence emerged that D-serine was also a potent co-agonist of the NMDAR [101]. Today, D-serine is recognised as the primary endogenous co-agonist of *synaptic* NMDARs, while glycine is the primary endogenous co-agonist of *extrasynaptic* NMDARs [467-470].

1.9.2. The D-serine pathway and schizophrenia

D-serine is a neutral D-amino acid that is widely expressed in the brain; it is present in the cortex, hippocampus, anterior olfactory nucleus, amygdala, striatum, diencephalon and midbrain in rodents [471, 472]. Appropriately, its regional and temporal distribution is closely correlated with that of the NMDAR [471, 473]. Its action at the synapse is depicted in Figure 1.11. Since D-serine is also found in the human brain [474], abnormalities in the D-serine pathway could contribute to NMDAR dysfunction in schizophrenia. More specifically, a reduction in the availability of D-serine would be consistent with the downregulation of NMDAR function that characterises the disorder. In support of this hypothesis, a significant reduction in D-serine has been reported in the serum and cerebrospinal fluid (CSF) of schizophrenia patients; a finding that has been replicated in a number of studies [475-479].

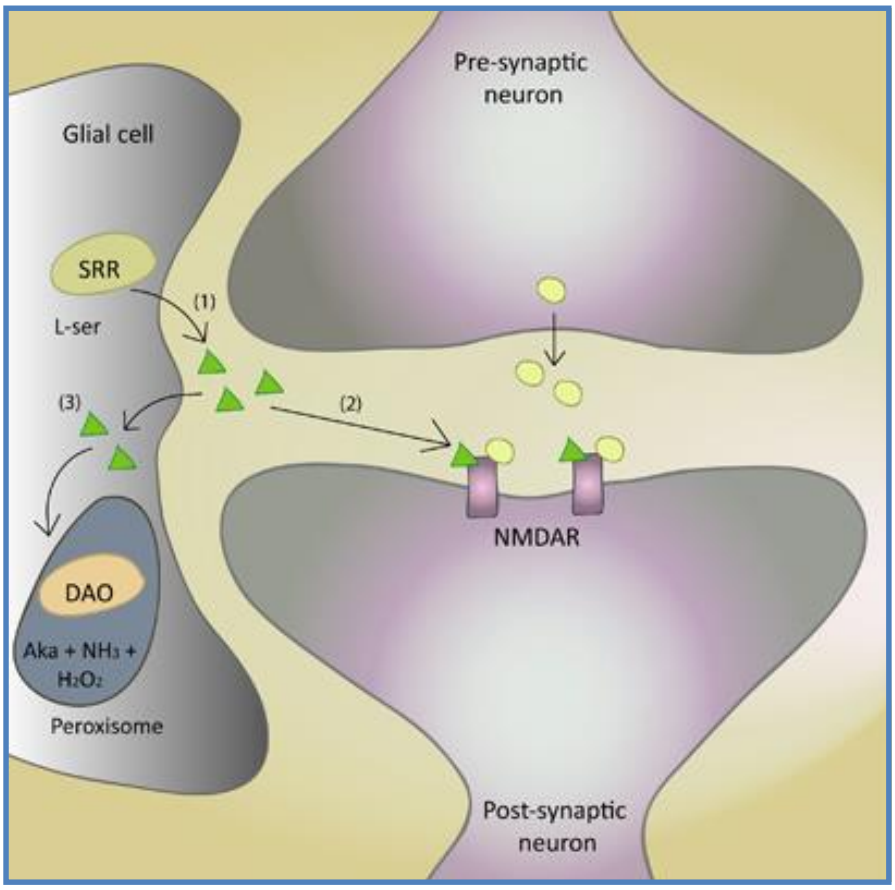

Figure 1.11. Schematic depicting the role of synaptic D-serine and its breakdown by DAO. Figure provided by Louise Verrall [45].

(1) Glial serine racemase (SRR) synthesizes D-serine (green triangles) from L-serine.
(2) D-serine is released at synapses to facilitate the action of synaptic glutamate (yellow circles) at NMDARs.
(3) Synaptic D-serine is taken up into glia and broken down by peroxisomal DAO, forming α-keto acid (Aka), ammonia and hydrogen peroxide.

Further support for the involvement of the D-serine pathway in schizophrenia comes from the results of genetic association studies; no less than three genes in the D-serine pathway have been associated with an increased risk of schizophrenia [44, 45]. Each of these genes encodes a protein that is thought to modulate the availability of D-serine within the brain (see Fig. 1.11. and 1.12.). Of these genes, *serine racemase* (*Srr*) is the most strongly associated with schizophrenia [45]. This gene encodes an enzyme that catalyses the synthesis of D-serine from L-serine [45]. There is also evidence for an association between *D-amino acid oxidase* (abbreviated to *Dao* or *Daao*) and schizophrenia [45]. Genetic association studies of *Dao* single nucleotide polymorphisms (SNPs) in schizophrenia patients have yielded inconsistent results,

although three meta-analyses provide moderate support for an association between *Dao* and schizophrenia [480-482]. The rs4623951 SNP, a non-coding SNP, is the most robustly associated with schizophrenia [480]. It is also associated with PPI and working memory deficits in healthy adult males [483], which is significant, since both are impaired in schizophrenia.

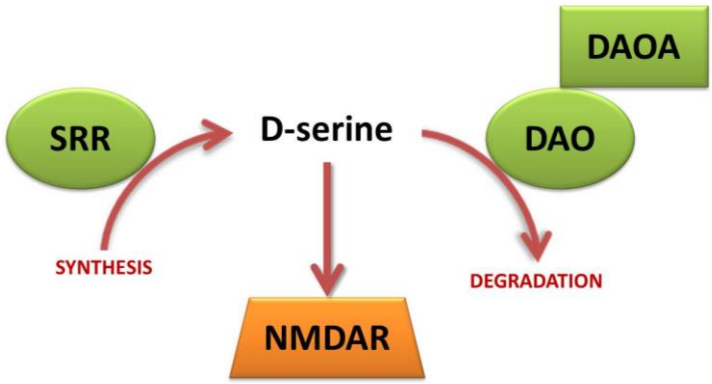

Figure 1.12. Schematic illustration of the D-serine pathway in humans. Each protein (depicted in green) modulates the availability of D-serine within the brain: D-amino acid oxidase (DAO) is an enzyme which catalyses the breakdown of D-serine into α-keto acid (Aka), ammonia and hydrogen peroxide. D-amino acid oxidase activator (DAOA) is a protein which regulates DAO activity; and serine racemase (SRR) is an enzyme which catalyses the synthesis of D-serine from L-serine. D-serine is the primary endogenous co-agonist of the synaptic N-methyl-D-aspartate receptor (NMDAR).

DAO is a glial peroxisomal enzyme that catalyses the breakdown of D-serine into α-keto acid, ammonia and hydrogen peroxide [484]. It is present in the kidney and liver in mammals (with the exception of the mouse liver) [472], and widely expressed in the human and rodent brain, especially in the cerebellum and other hindbrain structures, but also in the hippocampus and cortex [45, 485]. The spatial distribution of *Dao* expression and DAO activity is broadly similar in the brains of humans and rodents [486]. However, although DAO activity is seen frontal brain regions in humans, it is almost undetectable in these areas in mice [486]. This is despite the fact that DAO mRNA is found in the forebrain of both rodents and humans [45]. Recently, DAO activity has also been detected in the mouse retina [487]. In most brain regions, DAO and D-serine levels are inversely distributed [470], consistent with the involvement of DAO in

D-serine degradation. By contrast, DAO activity appears to have little impact on D-serine levels in the frontal cortex in humans, leading to speculation that D-serine concentration is regulated by an alternative mechanism in this region [45]. It should also be noted that although D-serine is the most abundant substrate of DAO in the mammalian brain, DAO also metabolises D-alanine, another potent NMDAR co-agonist [488-490]. Thus far, DAO has been implicated in a wide range of brain processes, including NMDAR modulation, cerebellar neurodevelopment, neurodegeneration (particularly in relation to amyotrophic lateral scleroris), and pain perception [45, 472].

A third gene in the D-serine pathway, *D-amino acid oxidase activator* (*Daoa*; also known as *G72*), has also been associated with schizophrenia [44]. *Daoa* encodes a protein believed to interact with DAO, although little is known about its function, given that the *Daoa* gene has no known orthologue in rodents [44]. It has been argued that DAOA facilitates DAO activity [44], inhibits DAO activity [491], and/or promotes mitochondrial fragmentation and dendritic arborisation [492]. Inhibition of DAO activity by DAOA in frontal cortex may explain why D-serine levels remain high in this region despite the presence of DAO [493].

1.9.3. D-amino acid oxidase (DAO) as a therapeutic target in schizophrenia

Crucially, *Dao* expression and DAO activity are significantly elevated in the cerebellum, hippocampus and cortex of schizophrenia patients, according to the results of post-mortem studies [485, 494-498]. It is therefore possible that the overactivity of DAO contributes to the reduction in D-serine levels and the downregulation of NMDAR function believed to exist in schizophrenia [45, 97-100, 493]. Consistent with this hypothesis, there is evidence that DAO modulates NMDAR function in rats and mice, both *in vivo* and *in vitro*, by regulating the availability of D-serine within synapses [467, 473, 499-501].

Based on the evidence outlined above, the administration of D-serine and DAO inhibiting drugs have both been suggested as putative treatments for schizophrenia [645,646,647]. Given the involvement of the NMDAR in learning and memory, these strategies may be a particularly effective treatment for the cognitive symptoms of schizophrenia, which, as explained in Section 1.1.3., represent a large, unmet clinical need [34]. Indeed, there is already some evidence that testifies to the efficacy of DAO inhibition and D-serine administration in a clinical setting. In schizophrenia patients, adjunctive treatment with the DAO inhibitor sodium benzoate was effective against a range of symptom domains, including cognition, in a small 6 week randomised clinical trial [502]. Pro-cognitive effects of sodium benzoate were also witnessed in a preliminary clinical trial involving dementia patients [503].

Likewise, D-serine has been administered to schizophrenia patients in conjunction with their antipsychotic medication, with moderate success [504-507]. Another possible approach is the combined administration of D-serine and a DAO inhibitor; there is evidence from mice that this strategy may be more effective than the administration of either compound alone [508]. At present, DAO inhibition is deemed safer than D-serine administration, due to concerns about the possible side effects of D-serine. In rats, D-serine administration causes nephrotoxicity (kidney toxicity) [509, 510], although this effect is absent in other species such as mice and hamsters [511]. It is currently unclear whether D-serine administration increases the risk of nephrotoxicity in humans, although there is some evidence that it does [505]. In another recent study, D-serine administration led to multiple cases of proteinuria (increased protein in the urine) [Scott Woods, *unpublished data*], which is an indicator of kidney damage.

1.9.4. Genetic mouse models of altered D-serine pathway function

One way to assess the potential therapeutic value of DAO inhibition is through the genetic ablation or inactivation of DAO. To date, two such models have been evaluated behaviourally (see Table 1.4). The ddY/*Dao*$^{-}$ mouse is a naturally-occurring mutant mouse that lacks DAO activity due to a point mutation in the gene [512, 513], while the *Dao1*^{G181R} mouse was created by transferring the same mutation from a ddY to a C57Bl/6J background [514]. ddY/*Dao*$^{-}$ mice (and presumably *Dao1*^{G181R} mice) show normal expression of a DAO enzyme rendered inactive by the point mutation [499, 512, 513]. Consistent with the role of DAO in D-serine catabolism, levels of D-serine are increased in the brains of both ddY/*Dao*$^{-}$ mice [472, 515-518] and *Dao1*^{G181R} mice [466]. And, consistent with the role of D-serine as an NMDAR co-agonist, there are several lines of evidence that NMDAR-mediated neurotransmission is upregulated in ddY/*Dao*$^{-}$ mice. Firstly, the behavioural effects of the NMDAR antagonists PCP and MK-801 (i.e. stereoptypy, ataxia and hyperlocomotion) are attenutated in the mutant mice [499, 519]. Secondly, NMDAR-mediated excitatory postsynaptic currents are enhanced in the dorsal horn of the spinal cord in mutant mice [501]. Formalin-induced licking behaviour, which is mediated by NMDARs in the spinal cord, is also increased [501].

Cognitive phenotyping of these models has focused predominantly on tests of long-term spatial memory. ddY/*Dao*$^{-}$ mice show enhanced performance in the Barnes maze [520] and improved acquisition in the Morris watermaze (MWM) [521]. Consistent with the proposed contribution of the NMDAR to LTP, enhanced hippocampal long-term potentiation (LTP) has been reported in ddY/*Dao*$^{-}$ mice, which may explain these behavioural observations. By contrast, *Dao1*^{G181R} mice display *unaltered* MWM acquisition, but enhanced MWM reversal learning and extinction, together with more rapid extinction in a contextual fear conditioning task [466]. Possible reasons for these inconsistent MWM findings are discussed in Chapter 3. Prepulse

inhibition has also been tested in *Dao* mutants, again with mixed results. An initial report of unaltered PPI in ddY/*Dao*$^{-}$ mice [499] is contradicted by a later study which found that PPI was significantly higher in ddY/*Dao*$^{-}$ mice than in wildtypes [520]. A possible explanation for these discrepant results is explored in Chapter 4. Next, both ddY/*Dao*$^{-}$ mice and *Dao1*^{G181R} mice demonstrate heightened anxiety-like behaviour in the elevated plus maze and open field test [514]. In both mutant models, this anxiety phenotype is more pronounced in females than males [514]. Another study failed to observe elevated anxiety in ddY/*Dao*$^{-}$ mice, but female mice were not tested in these experiments [520]. Finally, the ddY/*Dao*$^{-}$ mouse displays profoundly disrupted circadian rest-activity rhythms, as established with running wheels [Melanie Sobczyk, *unpublished data*]. By contrast, it demonstrates no obvious sleep disturbance [Melanie Sobczyk, *unpublished data*].

Mouse model	Test/parameter	Direction of observed effect
ddY/*Dao*$^{-}$	PCP-induced hyperlocomotion [499]	↓
	MK-801-induced stereotypy & ataxia [519]	↓
	NMDAR-mediated neurotransmission in spinal cord [501]	↑
	Hippocampal long-term potentiation [521]	↑
	Formalin-induced licking behaviour [501]	↑
	Barnes maze acquisition [520]	↑
	Morris watermaze acquisition [521]	↑
	Prepulse inhibition [499]	↔
	Prepulse inhibition [520]	↑
	Acoustic startle amplitude [499, 520]	↑*
	Anxiety-like behaviour in the elevated plus maze [514]	↑
	Anxiety-like behaviour in the elevated plus maze [520]	↔
	Anxiety-like behaviour in the open field test [514]	↑ in females only
	Anxiety-like behaviour in novelty-suppressed feeding [520]	↔
	Baseline locomotor activity [514]	↔
	Baseline locomotor activity [499, 520]	↓
	24 h inhibitory avoidance test [520]	↔
	Disruption of rest-activity rhythms [Melanie Sobczyk, *unpublished data*]	↑
	Sleep disturbance [Melanie Sobczyk, *unpublished data*]	↔
Dao1^{G181R}	Morris watermaze acquisition [466]	↔
	Morris watermaze reversal learning & extinction [466]	↑
	Acquisition of cued & contextual fear conditioning [466]	↔
	Extinction of conditioned contextual fear response [466]	↑
	Anxiety-like behaviour in the elevated plus maze [514]	↑ in females only
	Anxiety-like behaviour in the open field test [514]	↑ in females only
	Anxiety-like behaviour in the object neophobia test [514]	↔
	Baseline locomotor activity [514]	↔

Table 1.4. Summary of published studies characterising the behaviour of the ddY/*Dao*$^{-}$ mouse and the *Dao1*^{G181R} mouse, two related *Dao* mutants that lack *Dao* activity. The ddY/*Dao*$^{-}$ mouse is on a ddY background, while the *Dao1*^{G181R} mouse is on a C57Bl/6J background. ↔ denotes no difference between mutants and wildtypes; ↑ indicates a significant increase in mutants relative to widltypes; ↓ denotes a significant decrease in mutants relative to wildtypes. The asterisk highlights a study in which acoustic startle amplitude was numerically increased in mutants relative to wildtypes, but no p-value was reported [520].

1.9.5. Pharmacological rodent models of altered D-serine pathway function

Another way to assess the potential therapeutic value of DAO inhibition is to administer DAO inhibitors and/or D-serine to wildtype rodents. The effects of these interventions on several schizophrenia-relevant behaviours have already been characterised (see Table 1.5). In terms of cognitive performance, exogenous D-serine enhances rewarded alternation in the T-maze [522], reversal learning in the MWM [523] and performance in a social memory task [524]. Likewise, both D-serine and the DAO inhibitor 4H-furo[3,2-b]pyrrole-5-carboxylic acid (SUN) improve object recognition memory performance [522, 525, 526]. D-serine is also able to reverse deficits in object recognition memory performance induced by the administration of NMDAR antagonists [527, 528]. Note that all object recognition memory tests employed a retention interval of 2 h [528] or 24 h [522, 525-527], so they should be considered tests of long-term memory. Likewise, the social memory task performed by Shimazaki and colleagues involved a 90 min retention interval, so can also be considered a long-term memory test [524]. To date, Vardigan and colleagues are the only group to have assessed the effects D-serine in a behavioural test relevant to the negative symptoms of schizophrenia. In this experiment, D-serine reversed an NMDAR antagonist-induced reduction in sucrose preference [529]. Two studies have addressed the effects of D-serine and DAO inhibitors on NMDAR antagonist-induced hyperlocomotion, a behavioural test that may be relevant to the positive symptoms of schizophrenia. One reported that D-serine was able to reverse MK-801-induced hyperlocomotion [126], while the other found that the DAO inhibitor AS057278 was able to reverse PCP-induced hyperlocomotion [530]. Next, PPI has been shown to be increased after exogenous D-serine administration [531]. Likewise, NMDAR-antagonist induced PPI deficits can be reversed by D-serine [532] and the DAO inhibitor AS057278 [530]. Finally, wildtype mice display increased anxiety-like behaviour in the elevated plus maze following D-serine administration [514].

Compound administered	Test/parameter	Direction of observed effect
D-serine	T-maze rewarded alternation [522]	↑
	Morris watermaze reversal learning [523]	↑
	Hippocampal long-term depression [523, 533]	↑
	Social memory performance [524]	↑
	Object recognition memory [522, 526]	↑
	Reversal of PCP-induced object recognition memory deficit [527]	↑
	Reversal of MK-801-induced object recognition memory deficit [528]	↑
	Reversal of MK-801-induced hyperlocomotion [126]	↑
	Baseline locomotor activity [522]	↔
	Anxiety-like behaviour in the elevated plus maze [514]	↑
	Prepulse inhibition [531]	↑
	Reversal of MK-801-induced prepulse inhibition deficit [532]	↑
	Reversal of MK-801-induced prepulse inhibition deficit [531]	↔
	Acoustic startle amplitude [531]	↔
	Reversal of MK-801-induced reduction in sucrose preference [529]	↑
SUN (DAO inhibitor)	Contextual fear conditioning [525]	↑
	Object recognition memory [525]	↑
	Reversal of MK-801-induced object recognition memory deficit [526]	↔
	Hippocampal long-term potentiation [525]	↑
	Reversal of MK-801-induced prepulse inhibition deficit [532]	↑
AS057278 (DAO inhibitor)	Reversal of PCP-induced hyperlocomotion [530]	↑
	Reversal of PCP-induced prepulse inhibition deficit [530]	↑

Table 1.5. Summary of published studies characterising the behavioural effects of the administration of D-serine and DAO inhibiting drugs in wildtype rodents. ↔ denotes no difference between D-serine/DAO inhibitor-treated rodents and vehicle-treated rodents; ↑ indicates a significant increase in D-serine/DAO inhibitor-treated rodents relative to vehicle-treated rodents; ↓ denotes a significant decrease in D-serine/DAO inhibitor-treated rodents relative to vehicle-treated rodents.

1.9.6. Behavioural, sleep and circadian characterisation of the Dao$^{-/-}$ mouse

In the experiments described in this thesis, the behaviour of the first genetically engineered *Dao* knockout (*Dao*$^{-/-}$) mouse was characterised, with the aim of confirming and expanding upon the behavioural data gathered from the aforementioned genetic and pharmacological models. Importantly, the *Dao*$^{-/-}$ mouse has two key advantages over the previously characterised *Dao* mutants. Firstly, the *Dao*$^{-/-}$ mouse is on a 129Sv/Ev genetic background, which renders it more suitable for longitudinal sleep and circadian screening than the ddY/*Dao*$^{-}$ mutant, which is on the albino ddY genetic background. Secondly, while a catalytically inactive form of the DAO enzyme is widely expressed in the brains of ddY/*Dao*$^{-}$ mice (and presumably *Dao1*^{G181R} mice) [499, 512, 513], *Dao*$^{-/-}$ mice show no detectable expression of DAO mRNA or protein [534]. The use of a constitutive knockout thereby precludes the potential influence of a widely expressed – albeit catalytically inactive – DAO enzyme. In addition, we were hopeful that with careful experimental design, our results might shed light on some of the inconsistencies in the *Dao* mutant literature (c.f. the Morris water maze and prepulse inhibition). With these thoughts in mind, my primary research aims were to assess the behaviour of *Dao*$^{-/-}$ mice, in order to establish whether:

1) **Anxiety** is heightened, as it was in ddY/*Dao*$^{-}$ mice, *Dao1*^{G181R} mice, and wildtype mice after D-serine administration [514]. This question is addressed in **Chapter 2**.

2) **Short-term memory** performance is enhanced, as it was in wildtype mice after D-serine administration [522]. This question is addressed in **Chapter 2**. (Note that short-term memory performance has not been assessed in *Dao* mutant mice).

3) **Long-term spatial memory acquisition** is enhanced, as it was in ddY/*Dao*$^{-}$ mice [521] but not *Dao1*^{G181R} mice [466]. This question is addressed in **Chapter 3**.

4) **Prepulse inhibition** is increased, as it was in wildtype mice after D-serine administration [531], and as it was in ddY/*Dao*$^{-}$ mice in one study [520] but not another [499]. This question is addressed in **Chapter 4**.

5) **Sleep or circadian rhythms** are disrupted, as they were in ddY/*Dao*$^{-}$ mice [Melanie Sobczyk, *unpublished data*]. This question is addressed in **Chapter 5**.

A more comprehensive discussion of the relevant literature is provided in the introduction to each chapter. Existing evidence for the involvement of glutamate and the NMDAR in sleep and circadian function is detailed in Section 5.1.

1.10. Introduction to metabotropic glutamate receptors 2 and 3 (mGlu2 and mGlu3)

1.10.1. Group II metabotropic glutamate receptors

Unlike ionotropic glutamate receptors such as the NMDAR, metabotropic glutamate receptors (mGlu) does not contain a transmembrane ion channel. Instead, they exert their effects over neurotransmission indirectly, via G-protein-mediated intracellular signalling cascades [535]. There are 8 different types of mGlu, which can be subdivided into three groups, based on their structure and function. Group II includes mGlu2 and mGlu3, encoded by the genes *Grm2* and *Grm3*, respectively. They are best known as presynaptic autoreceptors, which regulate glutamatergic neurotransmission through the inhibition of glutamate release from presynaptic neurons [536, 537] and from glia [538]. The mechanism by which they achieve this is already well described [535]. Binding of glutamate to mGlu2 or mGlu3 activates a G-protein which inhibits adenylate cyclase, the enzyme that synthesises cyclic adenosine monophosphate (cAMP). Reduced cAMP synthesis results in reduced activation of cAMP-dependent protein kinase A (PKA). This leads to reduced phosphorylation of PKA's various cellular targets, and in turn, reduced presynaptic glutamate release. Since group II mGlus affect the probability of glutamate reaching ionotropic glutamate receptors at the postsynaptic membrane, they exert an influence over LTP and LTD [539].

Group II mGlus are widely distributed in the rodent brain, being prominent in the cerebral cortex, dentate gyrus of the hippocampus, olfactory nucleus, thalamic reticular nucleus, and some hypothalamic nuclei (including the SCN), brainstem nuclei and white matter tracts [540]. There is moderate expression in the basal ganglia and cerebellum, but little or no expression in the hippocampus proper [540]. *Grm2* is expressed in cholinergic amacrine cells in the retina

[541-543], but *Grm3* is not expressed in the mammalian retina [541-543]. *Grm2* expression is predominantly neuronal, whereas *Grm3* expression is primarily glial [540]. Expression in humans is broadly consistent with expression in rodents [544, 545].

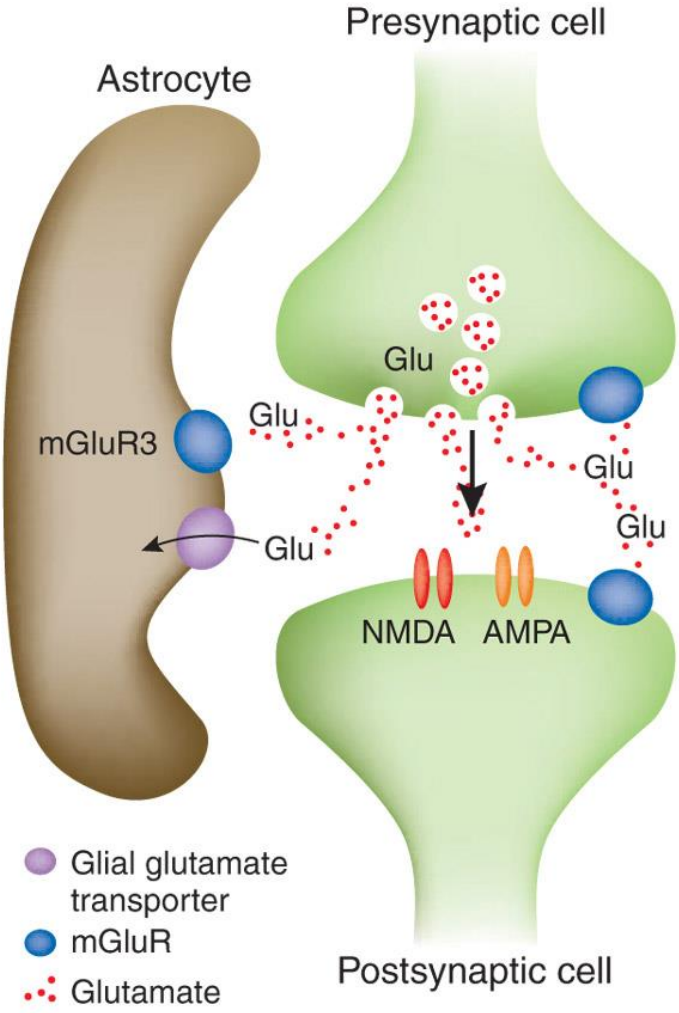

Figure 1.13. Schematic depicting the role of the group II metabotropic glutamate receptors mGlu2 and mGlu3 at the synapse. These receptors are predominantly located in the presynaptic membrane, where they act as inhibitory autoreceptors. Their activation by glutamate triggers an intracellular signalling cascade which inhibits further presynaptic glutamate release. Hence, they influence the activation of NMDAR and AMPA receptors, which are postsynaptic ionotropic glutamate receptors. mGlu3 is also expressed in glia, where its activation upregulates the expression of the glial glutamate transporter. Again, this serves to reduce glutamate levels within the synapse.

1.10.2. Metabotropic glutamate receptor 3 and schizophrenia

A relationship between Group II mGlus and schizophrenia was first suggested by the results of a study by Moghaddam and Adams in the late 1990s [546]. In this experiment, the administration of an mGlu2/3 agonist rescued the schizophrenia-like working memory deficits induced by the NMDAR antagonist PCP in rats. These results were replicated in a number of subsequent studies [43]. Importantly, an analogous effect was also observed in an experiment involving healthy human subjects; administration of an mGlu2/3 agonist evoked a dose-dependent improvement in the schizophrenia-like working memory deficits evoked by the NMDAR antagonist ketamine [547].

In the decade that followed the original work of Moghaddam and Adams, moderate evidence accrued for an association between the *Grm3* locus and schizophrenia; significant associations were revealed in six separate studies, although no association was found in another six [43]. The six positive results did not centre on a single polymorphism, but each highlighted distinct, non-coding single-nucleotide polymorphisms [43]. Nonetheless, these SNPs have functional consequences; they are associated with cognitive impairment, altered prefrontal glutamatergic neurotransmission and hippocampal pathophysiology [548, 549], all of which are relevant to schizophrenia. The inconsistent nature of the *Grm3* association literature speaks to the challenge described in Section 1.2.1., regarding the need for an extremely large sample to detect statistically significant associations. This challenge has been met in recent months, with the publication of a meta-analysis of GWAS studies encompassing 36,989 schizophrenia patients and 113,075 healthy controls [60]. A highly significant association was discovered between schizophrenia and a non-coding SNP in *Grm3*, establishing *Grm3* as one of the strongest schizophrenia candidate genes. Interestingly, there have also been reports of an association between *Grm3* and bipolar disorder [550, 551].

There is also preliminary evidence that *Grm3* expression is altered in the brains of schizophrenia patients. Early attempts to quantify *Grm3* expression in post-mortem brain tissue were confounded by the lack of antibodies selective for mGlu3 [43]. However, the first study to use mGlu3 specific antibodies revealed reduced expression of dimeric mGlu3, but unaltered expression of monomeric mGlu3 in the brains of schizophrenia patients [552]. Given evidence that the dimerization of metabotropic receptors is vital for their cell surface expression, G protein coupling and binding partner coupling [553-556], this tentatively suggests that mGlu3 function is downregulated in schizophrenia.

Clinical trials involving mGlu2/3 agonists have yielded mixed results. In the first such trial, the mGlu2/3 agonist LY2140023 was administered to 100 schizophrenia patients over a 4 week period. These patients were compared to 30 patients given the antipsychotic olanzapine, and 60 patients given placebo [557]. The drug was well tolerated and ameliorated patients' symptoms to a similar degree as olanzapine, making it the first drug that does not target the dopamine D_2 receptor to demonstrate antipsychotic efficacy [558, 559]. However, two subsequent attempts to replicate these results have failed. The failure of these clinical trials may have been due to the heterogeneity of the patient samples; a recent re-analysis of the data revealed that LY2140023 was actually effective in patients that had taken antipsychotic drugs for fewer than 3 years, but ineffective in the remainder of the sample [Nicholas Brandon, *personal communication*]. It therefore appears that in the first few years following diagnosis (and the prescription of antipsychotic medication), the brain changes in such a way that it become less responsive to treatment with mGlu2/3 agonists. It is unclear if these changes represent the natural course of the disorder, the effects of antipsychotic medication, or some combination of the two.

1.10.3. Behavioural characterisation of Grm2 and Grm3 knockout mice

Grm2 knockout (*Grm2*$^{-/-}$) and *Grm3* knockout (*Grm3*$^{-/-}$) mice have been studied extensively to gain insights into the functional role of each receptor. Given how widely *Grm2* and *Grm3* are expressed, the two models have surprisingly mild behavioural phenotypes (see Table 1.6). This may be due to the fact that the deletion of *Grm3* results in a compensatory upregulation in the expression of *Grm2*, and vice versa [560]. Consistent with this account, the *Grm2/3* double knockout (Grm2*/3*$^{-/-}$) mouse, which was created by crossing two single knockout lines, has a more obvious behavioural phenotype (see Table 1.6). In a recent study, *Grm2/3*$^{-/-}$ mice were impaired in an appetitively-motivated long-term spatial memory (Y-maze) task and an appetitively-motivated short-term spatial memory (T-maze rewarded alternation) task. They were also impaired in a spatial novelty preference (Y-maze) task, in which performance is influenced by animals' exploratory drive. By contrast, *Grm2/3*$^{-/-}$ mice were unimpaired in two aversively-motivated long-term spatial memory tasks: the Morris watermaze and the Y-maze swim escape task. This pattern of performance suggests that their memory function is unimpaired, but they are insufficiently aroused to perform optimally in appetitive tasks [561]. Consistent with this account, their performance in an appetitively-motivated short-term spatial memory (T-maze rewarded alternation) task improved following injection stress [561]. These findings reveals a role for group II metabotropic glutamate receptors at the interface between arousal and cognition. Note that reduced arousal should not be mistaken for reduced anxiety, as the behaviour of *Grm2/3*$^{-/-}$ mice was unaltered in several standard tests of anxiety [562].

Mouse model	Test/parameter	Direction of observed effect
Grm2$^{-/-}$	Appetitively-motivated LTSM (Y-maze) [562]	↔
	Spatial novelty preference (Y-maze) [562]	↔
	Aversively-motivated LTSM (Y-maze) [562]	↔
	Appetitively-motivated STSM (T-maze rewarded alternation) [562]	↓
	Anxiety-like behaviour in the EPM, OFT, BWA and NSF [562]	↔
	Motor coordination in the accelerating rotarod task [562]	↔
	Motor coordination in the accelerating rotarod task [563]	↓
	Motor coordination in the multiple static rods task [562]	↔
	Baseline locomotor activity [562]	↓↑
	Hippocampal long-term potentiation [564]	↔
	Aversively-motivated LTSM (Morris watermaze) [564]	↔
	Hippocampal long-term depression [564]	↓
	Prepulse inhibition [563]	↔
Grm3$^{-/-}$	Appetitively-motivated LTSM (Y-maze) [562]	↔
	Spatial novelty preference (Y-maze) [562]	↔
	Aversively-motivated LTSM (Y-maze) [562]	↔
	Appetitively-motivated STSM (T-maze rewarded alternation) [562]	↓↑
	Anxiety-like behaviour in the EPM, OFT, BWA and NSF [562]	↔
	Anxiety-like behaviour in the elevated plus maze [565]	↔
	Motor coordination in the accelerating rotarod task [562]	↔
	Motor coordination in the multiple static rods task [562]	↔
	Baseline locomotor activity [562]	↔
Grm2/3$^{-/-}$	Appetitively-motivated LTSM (Y-maze) [561]	↓
	Appetitively-motivated STSM (T-maze rewarded alternation) [561]	↓
	Spatial novelty preference (Y-maze) [561, 562]	↓
	Aversively-motivated LTSM (Y-maze) [561]	↔
	Aversively-motivated LTSM (Morris watermaze) [561]	↔
	Effect of injection stress on appetitively-motivated STSM (T-maze) [561]	↑
	Appetitively motivated, non-spatial, visual discrimination task [561]	↔
	Anxiety-like behaviour in the EPM, OFT, BWA and NSF [562]	↔
	Motor coordination in the accelerating rotarod task [562]	↓
	Motor coordination in the multiple static rods task [562]	↓
	Baseline locomotor activity [561]	↓
	Hippocampal long-term depression [566]	↔

Table 1.6. Summary of published studies characterising the behaviour of *Grm2*$^{-/-}$, *Grm3*$^{-/-}$ and *Grm2/3*$^{-/-}$ mice. ↔ denotes no difference between knockouts and wildtypes; ↑ indicates a significant increase in knockouts relative to widltypes; ↓ denotes a significant decrease in knockouts relative to wildtypes; ↑↓ and ↓↑ indicates bilateral effects that switched direction between the start and end of the test session. BWA = black and white alleys task. EPM = elevated plus maze. NSF = novelty-suppressed feeding. OFT = open field test. LTSM = long-term spatial memory. STSM = short-term spatial memory.

1.10.4. Administration of mGlu2/3 modulating drugs in wildtype rodents

As described above, mGlu2/3 agonists can reverse NMDAR antagonist-induced working memory deficits in wildtype rodents. But how do mGlu2/3 agonists achieve this effect? Intuitively, one might expect them to impair memory performance, given that mGlu2/3 agonists are likely to reduce presynaptic glutamate release, which should decrease NMDAR activation. In accordance with this logic, mGlu2/3 agonists can impair working memory performance when administered to wildtype rodents [567-569]. To understand the effects of mGlu2/3 agonists in the 'schizophrenic brain', one has to look beyond a single, prototypical synapse, and consider the brain as a complex, interconnected whole. One also has to extend the simple glutamate hypothesis of schizophrenia to consider that glutamatergic function may be differentially affected in distinct brain regions. As depicted in Figure 1.14, NMDAR hypofunction in regions such as the thalamus and hippocampus could indirectly lead to the hyperfunction of AMPA and kainate glutamate receptors in the prefrontal cortex. In turn, prefrontal glutamatergic hyperfunction may contribute to the working memory deficits of schizophrenia patients [570, 571]. Hence, mGlu2/3 agonists might reverse these working memory deficits by attenuating synaptic glutamate release in the prefrontal cortex, and returning AMPA and kainite receptor activation to normal levels [572, 573]. In wildtype rodents, there is no prefrontal glutamatergic hyperfunction to reverse, so mGlu2/3 agonists have very different effects.

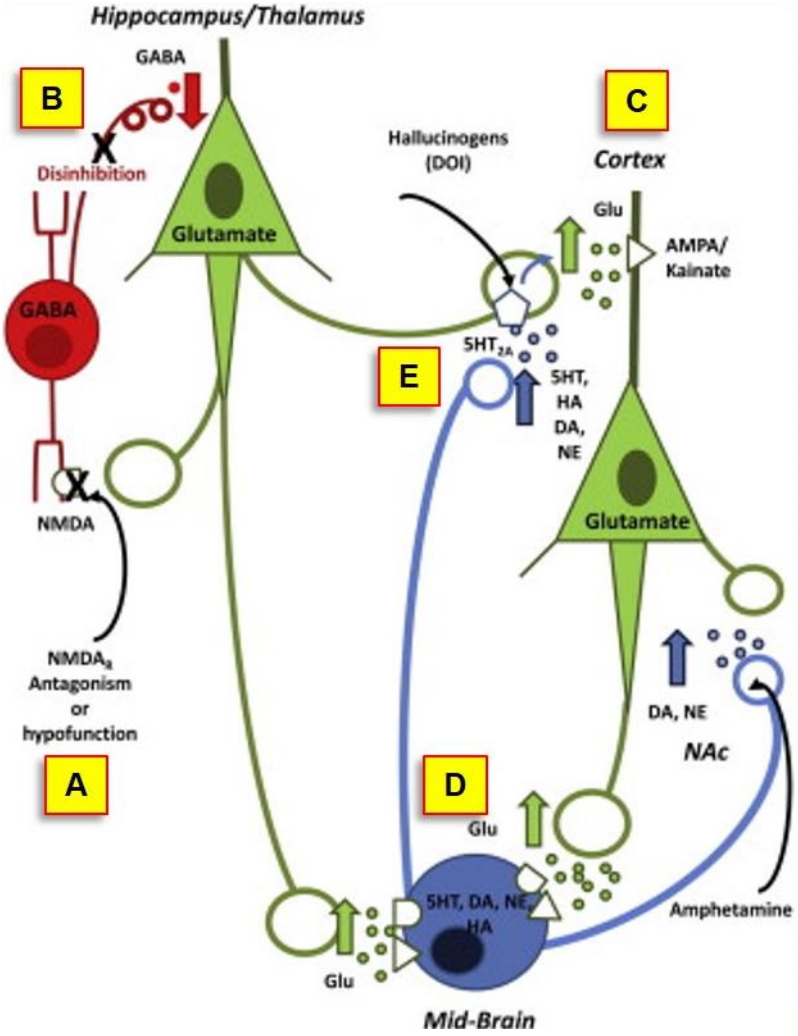

Fig. 1.14. Schematic depicting how NMDA receptor hypofunction in the thalamus and hippocampus could lead to AMPA and kainate receptor hyperfunction in the prefrontal cortex. (A) NMDAR hypofunction means that inhibitory GABAergic interneurons are not excited. (B) Reduced excitation of GABAergic interneurons disinhibits hippocampal and thalamic glutamatergic neurons that provide excitatory input to the prefrontal cortex. (C) Increased glutamate release in the prefrontal cortex leads to increased excitation of prefrontal glutamatergic pyramidal neurons. (D) Increased glutamate release from pyramidal neurons leads to increased excitation of aminergic neurons in the midbrain, which may drive the positive symptoms of schizophrenia. (E) Increased serotonin release in the prefrontal cortex activates $5HT_{2A}$ receptors which exacerbates the over-excitation of prefrontal AMPA and kainate receptors. Modified from Fell [572].

1.10.5. Sleep and circadian characterisation of the Grm2/3$^{-/-}$ mouse

At this point we will return to the 'shared neuropathophysiology' hypothesis of SCRD in schizophrenia, outlined in Section 1.7.2. According to this hypothesis, the co-morbidity of schizophrenia and SCRD stems from dysfunction in common brain mechanisms (e.g. specific neurotransmitter systems) [125, 343]. The glutamate system is one such candidate mechanism, given strong evidence of glutamatergic dysfunction in schizophrenia (see Section 1.2.5) and given that altered glutamatergic neurotransmission could impact on sleep and circadian function at multiple levels (see Section 5.1). At the receptor level, group II mGlus may be particularly relevant to the pathophysiology of schizophrenia (see Section 1.10.2), while there is also increasing evidence that implicates group II mGlus in sleep and circadian function (see Section 6.1). Based on this accumulated evidence, one might expect to observe significant SCRD in the *Grm2/3*$^{-/-}$ mouse. Specific predictions concerning the nature of the expected SCRD are outlined in Section 6.1. We elected to study the *Grm2/3*$^{-/-}$ mouse given that the behavioural phenotypes of *Grm2*$^{-/-}$ and *Grm3*$^{-/-}$ mice are mild in comparison [561, 574], possibly due to compensatory changes in gene expression [560]. The use of the double knockout also enables us to make direct comparisons with a comprehensive pharmacological literature examining the effects of mGlu2/3 modulating drugs on sleep, wherein most studies used drugs which act on mGlu2 and mGlu3 indiscriminately [575-582].

1.11. Summary of research aims

The primary research aims of my DPhil were as follows:

1) ***To characterise sleep, circadian rhythms and schizophrenia-relevant behaviour in the D-amino acid oxidase knockout (Dao$^{-/-}$) mouse.*** As described Section 1.9., DAO is a schizophrenia-relevant enzyme, the pharmacological inhibition of which been proposed as a novel treatment for the disorder. My goal was to investigate the behavioural consequences of DAO inactivation, using a transgenic mouse model lacking DAO expression and activity. My aim was to assess anxiety-like behaviour (Chapter 2), short-term memory performance (Chapter 2), long-term memory performance (Chapter 3), prepulse inhibition (Chapter 4), and sleep and circadian rhythms (Chapter 5). Specific predictions regarding each of these behaviours are outlined in the introduction to each chapter.

2) ***To characterise sleep and circadian rhythms in the metabotropic glutamate receptor 2 and 3 double-knockout (Grm2/3$^{-/-}$) mouse.*** Like DAO, these receptors are implicated in the pathophysiology and potential treatment of schizophrenia (see Section 1.10.). As described in Section 1.7.2., our 'shared neuropathophysiology' hypothesis of SCRD in schizophrenia predicts that the manipulation of schizophrenia-relevant genes in animal models should give rise to simultaneous SCRD and schizophrenia-relevant behavioural deficits. The *Grm2/3*$^{-/-}$ mouse has already been subjected to a battery of spatial memory tests, which revealed evidence of impaired memory performance (see Section 1.10.3), which may be relevant to the cognitive symptoms of schizophrenia. My goal was to establish whether *Grm2/3*$^{-/-}$ mice also demonstrate SCRD. Specific predictions relating to the sleep and circadian phenotype of the *Grm2/3*$^{-/-}$ mouse are outlined in Section 6.1.

2. Preliminary behavioural characterisation of the *Dao*$^{-/-}$ mouse: vision, anxiety, locomotor activity and short-term memory performance

2.1. Introduction

Standard laboratory tests of anxiety and memory for rodents typically involve the exploration of novel objects and/or arenas. Since these tasks are inherently visual, performance can be compromised by visual impairments. To confirm the suitability of these tests for *Dao*$^{-/-}$ mice, it was necessary to establish that their vision is unaltered relative to *Dao*$^{+/+}$ mice. This was particularly important given that NMDAR overactivity causes retinal apoptosis [583]. D-serine administration is known to potentiate this effect, while DAO administration is known to prevent it [584]. Since DAO is active in the wildtype retina [487], retinal D-serine is likely to be increased in *Dao*$^{-/-}$ mice, as it is in ddY/*Dao*$^{-}$ mice [487]. *Dao*$^{+/+}$ and *Dao*$^{-/-}$ mice were first tested in the visual cliff task, a test of depth perception. Elevation above the ground is a key anxiogenic property of standard anxiety tests such as the elevated plus maze, so it was important to confirm that depth perception is intact in *Dao*$^{-/-}$ mice. Subsequently, visual acuity was assessed with the optokinetic nystagmus (OKN) drum.

Following visual assessment, *Dao*$^{+/+}$ and *Dao*$^{-/-}$ mice were subjected to a battery of five standard laboratory tests of anxiety that generate 'approach/avoidance' conflict [585]. Behaviour in these tasks reflects a compromise between the motivation to explore the arena for useful resources (i.e. food, water, shelter, mates) and the motivation to remain stationary to avoid predation [585]. Performance in these tasks is thought to be dependent on ventral hippocampus function [585, 586], while recent neuroimaging data indicates that the same

region is engaged during an approach/avoidance conflict task in humans [587]. Moreover, performance in rodent approach/avoidance tasks is reliably altered by the administration of anxiolytic drugs such as benzodiazepines, which attests to their validity as a test of anxiety [588]. Significantly heightened anxiety was predicted in *Dao*$^{-/-}$ mice, given that anxiety is increased in ddY/*Dao*$^{-}$ mice and *Dao1*^{G181R} mice, and is also elevated in wildtype mice after D-serine administration [514]. In some cases, increased anxiety-like behaviour in approach/avoidance tasks may reflect a reduction in spontaneous locomotor activity, rather than a genuine anxiety phenotype. To eliminate this possibility, spontaneous locomotor activity was measured in a separate paradigm.

Dao$^{+/+}$ and *Dao*$^{-/-}$ mice were also subjected to three short-term spatial memory tasks. These tasks were selected on the basis that they rely on the animals' spontaneous preference for novelty, meaning that performance is not motivated by reward or punishment. The results of such tasks are easier to interpret, as they are not confounded by innate differences in sensitivity to reward or punishment, which is sometimes altered in transgenic models [131]. Nonetheless, performance *can* be affected by altered exploratory drive, so measures of locomotor activity and object exploration were also recorded in these tasks. There is currently little data that speaks to the relationship between DAO and short-term memory performance (see Section 1.9.5. & 1.9.6.), although in one study, D-serine administration was shown to enhance T-maze rewarded alternation in wildtype mice [522]. We expected that short-term memory performance might be altered in *Dao*$^{-/-}$ mice, based on the proposed involvement of NMDAR-dependent LTD in the habituation processes that are thought to underpin short-term memory performance in both spatial and non-spatial tasks [462-465]. Critically, hippocampal LTD is enhanced in wildtype rodents following D-serine administration [523, 533].

Finally, baseline plasma corticosterone levels were quantified in terminal blood samples taken from *Dao*$^{+/+}$ and *Dao*$^{-/-}$ mice. Corticosterone is a steroid hormone that is produced in the adrenal glands of rodents, and is released in response to stress [589]. Baseline levels of the human analogue, cortisol, are often increased in individuals with anxiety disorders [590]. Interestingly, altered plasma corticosterone levels have also been observed in rats following acute D-serine or D-alanine administration [Phil Burnet, *unpublished data*]. Hence, it was predicted that baseline plasma corticosterone might be increased in *Dao*$^{-/-}$ mice.

2.2. Methods

2.2.1. Animals

Dao knockout mice were generated as described previously [591]. Briefly, recombineering was used to replace 185 base pairs of *Dao* (encompassing exons 7 and 8) with a neomycin cassette, and the mutant allele was introduced into 129Sv/Ev mouse embryonic stem cells (TG-ES01-01 ESM07; Eurogentec, Seraing, Belgium) by standard homologous recombination. Male chimeric mice were generated by injecting the targeted embryonic stem cells into C57BL/6J blastocysts. Chimeric mice were bred with 129Sv/Ev mice (Taconic, Hudson, NY, USA) to produce F_1 heterozygotes, which in turn were mated to produce *Dao* knockout ($Dao^{-/-}$) mice and wildtype ($Dao^{+/+}$) littermate controls. $Dao^{-/-}$ mice exhibited normal development, longevity, and reproductive potential. A genotyping protocol is included in Appendix 8.5., while the mRNA and protein structure of DAO (showing the location of the sequence deletion in the $Dao^{-/-}$ mouse) is shown in Appendix 8.6.

Mice were at least 2 months old at the onset of all procedures, and no older than 9 months upon completion of testing. A total of 4 cohorts were used, full details of which are provided in Table 2.1. Males and females were subjected to behavioural testing, but only males participated in the sleep and circadian screen due to the potentially confounding influence of the oestrus cycle on wheel-running activity [592]. During behavioural testing, mice were housed under a 100 lux 12:12 h light/dark (12:12 LD) cycle, with access to food and water *ad libitum*. All behavioural procedures were performed in accordance with the United Kingdom Animals (Scientific Procedures) Act of 1986 and the University of Oxford Policy on the Use of Animals in Scientific Research. All experiments were approved by the University of Oxford Animal Welfare and Ethical Review Board, and were conducted under the PPLs 30/2812 and 30/3068 by PILs ICC0614BD (formerly 30/9339) and 40/8886.

Cohort	Housing	Animals	Behavioural Tests (in chronological order)	Time of Test
A1	Group	2 × *Dao*$^{+/+}$ ♂; 7 × *Dao*$^{+/+}$ ♀; 6 × *Dao*$^{-/-}$ ♀	Visual cliff	ZT13 – ZT18
			OKN drum	ZT13 – ZT18
			Open field test	ZT13 – ZT18
			Light/dark box	ZT13 – ZT18
A2	Group	5 × *Dao*$^{+/+}$ ♂; 7 × *Dao*$^{+/+}$ ♀; 6 × *Dao*$^{-/-}$ ♂; 5 × *Dao*$^{-/-}$ ♀	Visual cliff	ZT13 – ZT18
			Open field test	ZT13 – ZT18
			Light/dark box	ZT13 – ZT18
			Spontaneous recognition memory	ZT19 – ZT23
B1	Single	6 × *Dao*$^{+/+}$ ♂; 6 × *Dao*$^{+/+}$ ♀; 6 × *Dao*$^{-/-}$ ♂; 6 × *Dao*$^{-/-}$ ♀	Elevated plus maze	ZT3 – ZT7
			Successive alleys	ZT3 – ZT7
			Novelty-suppressed feeding	ZT1 – ZT4
			Spontaneous locomotor activity	ZT3 – ZT7
			T-maze spontaneous alternation	ZT3 – ZT4 and ZT7 – ZT8
			Y-maze spatial novelty preference	ZT3 – ZT7
B2	Single	6 × *Dao*$^{+/+}$ ♂; 6 × *Dao*$^{+/+}$ ♀; 6 × *Dao*$^{-/-}$ ♂; 6 × *Dao*$^{-/-}$ ♀	Elevated plus maze	ZT3 – ZT7
			T-maze spontaneous alternation	ZT3 – ZT4 and ZT7 – ZT8

Table 2.1. Summary of cohorts used for preliminary behavioural testing. Mice were at least 2 months old at the onset of all procedures, and no older than 9 months upon their completion. Cohorts A1 and A2 were group-housed (5-7 animals per cage). Cohorts B1 and B2 were singly-housed to allow direct comparison with other singly-housed cohorts in which long-term memory was assessed (see Chapter 3), PPI was assessed (see Chapter 4), and sleep and circadian rhythms were assessed (see Chapter 5). ZT = zeitgeber time; ZT0 refers to the onset of the light phase, while ZT12 denotes the onset of the dark phase. The OKN drum task was performed at ZT13-18, because this task is rod-dependent and should therefore be performed in dark-adapted animals. For consistency, all behavioural testing in cohorts A1 and A2 was performed during the dark phase (in illuminated arenas). Cohorts B1 and B2 were tested in an animal facility which lacked facilities to house mice under a reverse light/dark cycle, so all behavioural testing was performed during the light phase.

2.2.2. General behavioural protocol

Prior to behavioural testing, mice were handled for 2 min a day for 5 consecutive days, to habituate them to experimenter handling. For all experiments, mice were brought into the test room 5-10 min prior to the onset of testing. Test apparatus were cleaned with diluted ethanol between trials. Illuminance was 50 lux at the base of each apparatus, unless otherwise stated. With the exception of T-maze spontaneous alternation, novelty-suppressed feeding and spontaneous locomotor activity, all behavioural experiments were recorded with a webcam (Logitech, Morges, Switzerland) or a near-infrared CCTV camera (Maplin Electronics, Rotherham, UK). Automated tracking was conducted using ANY-maze 4.5 (Stoelting, Wood Dale, Illinois). The animal's *entire* body was tracked, and its position within the apparatus was determined on a frame-by-frame basis. An entry to a pre-defined zone was deemed to have occurred when at least 90% of the animal's body had entered the zone in question.

2.2.3. Visual tests

Visual Cliff

Vision in *Dao*$^{+/+}$ and *Dao*$^{-/-}$ mice was first assessed with the visual cliff experiment, a task which has been used to assess depth perception in both rodents and human infants [593-597]. In this task, normal depth perception is indicated by a significant preference for the raised half of the apparatus (i.e. animals should spend less than 50 % of the trial away from the raised platform). The apparatus was a rectangular arena measuring 60 cm by 30 cm, enclosed by four black walls, 25cm in height. The base of the arena was a sheet of transparent acrylic. On one side of the arena, the acrylic base sat directly atop a raised platform, measuring 30 cm by 30 cm. On the other side, the acrylic base prevented access to a lower platform of identical size, positioned 50 cm below the raised platform. The boundary between the two sides of the arena is referred to as the 'cliff'. The two platforms and vertical cliff edge were covered with a black and white chequerboard pattern, composed of squares measuring 3.33 cm^2, rendering the position and scale of the cliff clearly visible to an adult mouse with healthy vision. Mice were released in the centre of the raised platform, and allowed to explore the apparatus for 1 min. Distance travelled within the arena was extracted using ANY-maze. A number of additional variables were derived manually from the video recordings: time spent away from the raised platform, approaches to the cliff edge, cliff crossings relative to cliff approaches, and hesitation responses relative to cliff approaches. An approach to the cliff was deemed to have occurred whenever a mouse came within 5cm of the cliff edge. For a crossing to have taken place, all four feet had to be placed on the other side. Hesitation responses were defined as episodes where an animal broke stride to pause for at least 1 second during a cliff approach.

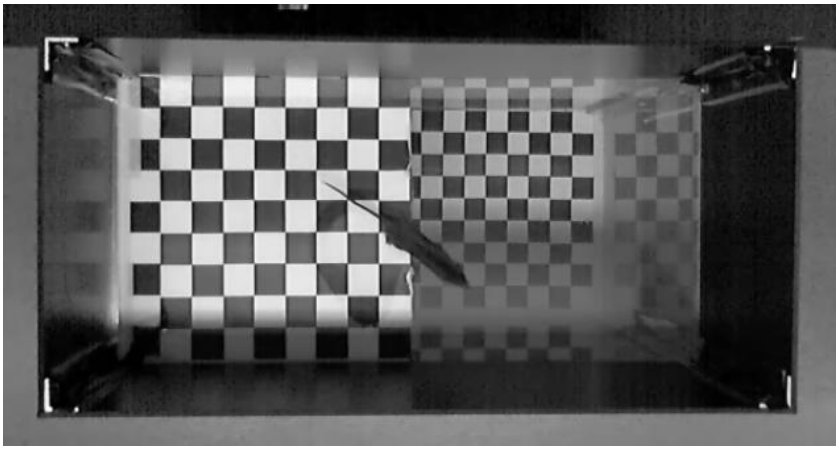

Figure 2.1. Aerial view of a mouse inside the visual cliff apparatus. Intact depth perception is indexed by a significant preference for the raised platform, and a reluctance to cross the 'cliff' edge between the two sides of the apparatus.

Optokinetic nystagmus drum

This simple test of visual acuity was performed according to a previously established protocol [598, 599]. The apparatus was a vertically-oriented transparent acrylic cylinder measuring 30 cm in diameter and 55 cm in height. Positioned centrally within the drum was a metal pedestal, 20cm in height. A plastic petri dish was mounted atop this pedestal. During testing, mice were placed inside the petri dish, which remained stationary, while the drum rotated at a speed of 2 revolutions per minute, driven by an electric motor. In each trial, the drum rotated for 90 s in a clockwise direction, then 90 s in an anti-clockwise direction. The inner surface of the drum was lined with white poster paper, which was either blank (sham trial), or printed with a black and white square wave grating pattern of a predefined spatial frequency (experimental trial). Three spatial frequencies were tested: 0.4, 0.5, and 0.6 cycles per degree of visual angle (cpd). Hence, each mouse completed four trials (one sham trial and three experimental trials) during the main experimental session. All mice encountered the grating patterns in the same pseudo-randomised order: sham, 0.6 cpd, 0.4 cpd, then 0.5 cpd. Prior to the main experimental session, each mouse completed two habituation sessions, spaced over two consecutive days. Each habituation session consisted of a single sham trial. Illumination was 200 lux at the top of the pedestal. Head-tracking responses were scored manually from the video recordings, with the

scorer blind to both genotype and spatial frequency. Manual scoring yielded two key variables. The first was the absolute limit of visual acuity; this was defined as the highest spatial frequency at which at least one head tracking response was observed in each direction. Secondly, the average head-tracking response rate was determined for each spatial frequency (expressed as head tracking responses per minute). No head-tracking responses were observed in any of the sham trials.

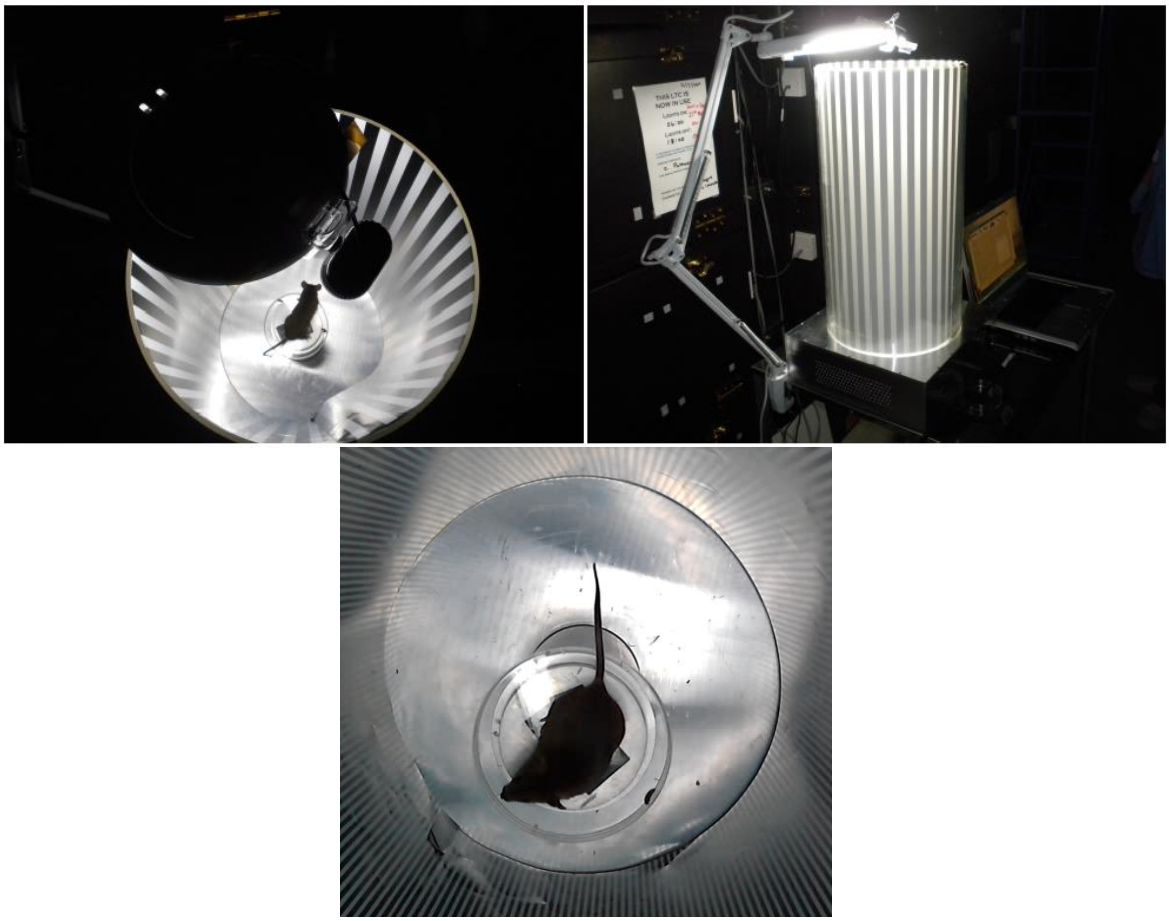

Figure 2.2. The optokinetic nystagmus (OKN) drum in operation. The mouse sits on a central pedestal and the drum rotates around it. If the mouse can perceive the grating pattern, it will show head tracking movements in the direction that the drum is rotating. Visual acuity is assessed both by the number of head tracking responses observed with grating patterns of different spatial frequencies, and as the highest spatial frequency at which head tracking responses are still observed.

2.2.4. Anxiety tests

Open field test

The open field test is one of the best known and most widely-used tests of rodent approach/avoidance conflict [588]. Ordinarily, wildtype mice will spend the majority of the experiment in the periphery of the maze, and will rarely venture into the centre. After benzodiazepine administration, wildtype mice are more likely to enter the apparatus' central zone, which confirms the relevance of this test to anxiety. The apparatus was a rectangular arena measuring 60 cm by 30 cm, enclosed by four black walls, 25cm in height. The base of the arena was a sheet of transparent acrylic, placed over a sheet of white card. Mice were released at the edge of the arena, facing towards the wall, and allowed to explore the apparatus for 5 min. Using ANY-maze, the apparatus was divided into nominal peripheral and central zones (central zone: 46.5 cm long × 16.5 cm wide). The key variables extracted were centre entries, latency to the first centre entry, percent time spent in the centre, percent distance travelled in the centre, and total distance travelled.

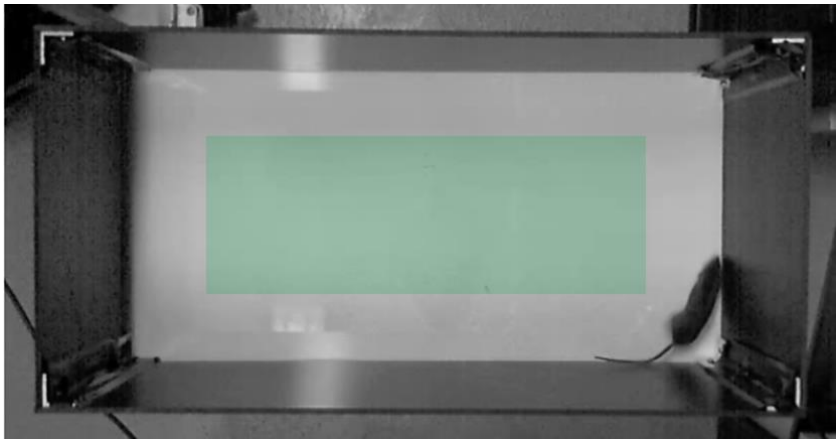

Figure 2.3. Aerial view of a mouse inside the open field apparatus. The extent of the imaginary central zone is represented by the green rectangle. Anxiety is indexed by the amount of time spent in this central zone, and the number of entries to the central zone.

Elevated plus maze

The elevated plus maze is another widely-used test of rodent approach/avoidance conflict that is sensitive to benzodiazepine administration [588]. Unlike the open field test, anxiety is indicated by the unwillingness of wildtype mice to leave the two closed arms of the apparatus, and enter the two open arms. The apparatus was a white wooden plus maze, elevated 72 cm above the floor. All four arms were 35 cm long and 6 cm wide. The two closed arms were enclosed by grey walls, 21 cm in height. The mouse was placed in the centre of the maze, so that its head and forepaws fell within one of the open arms. Mice were allowed to explore the arena for 5 min. The key variables extracted were open arm entries, closed arm entries, percent time spent in the open arms, latency to the first open arm entry, and total distance travelled.

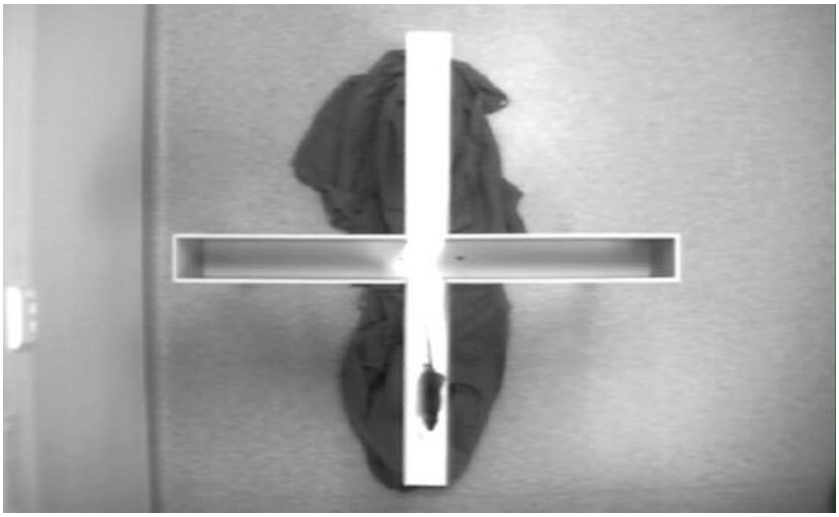

Figure 2.4. Aerial view of a mouse inside the elevated plus maze apparatus. Anxiety is indexed by the amount of time spent in the open arms, and the number of entries to the open arms.

Successive alleys

The successive alleys test is an approach/avoidance task that can be conceptualised as a modified version of the elevated plus maze. Like the plus maze, performance in this task is sensitive to benzodiazepine administration [600-602]. Unlike the plus maze, in which there are two open and two closed arms, the successive alleys apparatus consists of a single arm divided

into four sections, each of which is more anxiogenic than the last. This more subtle gradation between the most anxiogenic and least anxiogenic area of the apparatus means it may be better able to identify subtle anxiety phenotypes [600-602]. The apparatus consists of four linearly connected wooden alleys or 'zones', each 25cm in length. The four zones differ in their physical characteristics (e.g. stability, width and colour), rendering zone 1 the least anxiogenic, and zone 4 the most anxiogenic [600]. The apparatus was elevated 50cm above the floor. Mice were released from the enclosed end of zone 1, facing the back wall, and were allowed to explore the apparatus for 5 min. The key variables extracted were the amount of time spent in (and entries to) each of the four zones, in addition to total distance travelled.

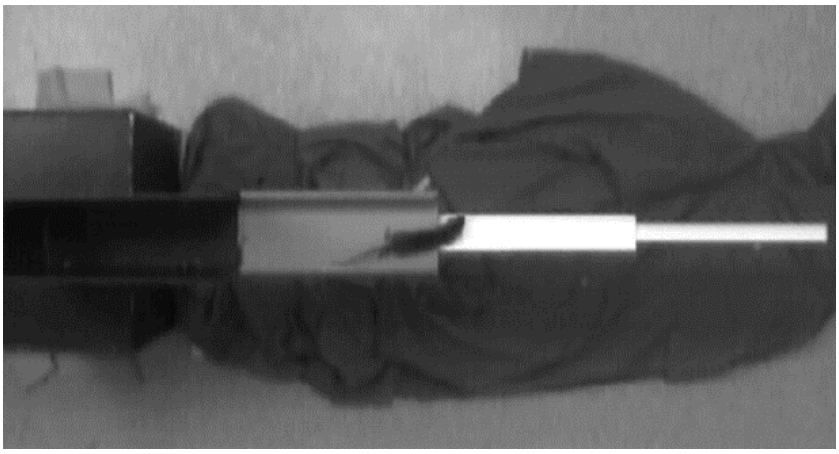

Figure 2.5. Aerial view of a mouse inside the successive alleys apparatus. Anxiety is indexed by the amount of time spent in the exposed, open zones of the apparatus, and the number of entries to these zones.

Light/dark box

The light/dark box is another test of rodent approach/avoidance conflict that is sensitive to benzodiazepine administration [588]. This time, anxiety is indicated by the unwillingness of wildtype mice to leave the dark side of the apparatus and spend time in the light side. The apparatus consisted of two identically-sized compartments, each 30 cm long, 15 cm wide and 30 cm high, connected by a small opening (4.5 cm wide and 3.5 cm high). One compartment was made of opaque black acrylic, while the other was made of transparent acrylic. The walls

of the transparent compartment were covered on the outside with white card. Mice were released in the centre of the light compartment, facing away from the opening, and were allowed to explore the arena for 5 min. The key variables extracted were percent time spent in the light compartment, the number of light/dark crossings, and latency to the first light/dark crossing. Note that 2 mice (both knockouts) were excluded from all light/dark box analyses as they froze for the entire trial and did not make any light/dark crossings ($\underline{M}$ = 14.9).

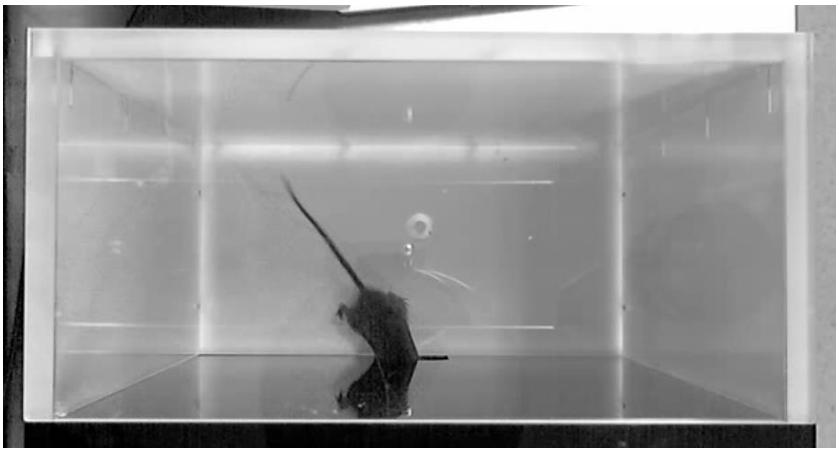

Figure 2.6. Aerial view of a mouse inside the light/dark box apparatus. Anxiety is indexed by the amount of time spent in the light half of the apparatus.

Novelty-suppressed feeding

The novelty suppressed feeding test is a rodent approach/avoidance task that relies on the natural wariness of rodents to eat novel foods. In this task, anxiety is indicated by the latency to begin eating a novel food item, a parameter which is sensitive to benzodiazepine administration [588]. All mice completed two trials, on separate days. Mice were partially food-restricted for the entirety of the preceding dark phase; all food was removed from the food hopper and 1g of standard chow was placed on the home-cage floor. Testing began one hour into the light phase. In the first trial, the novel food was a sucrose pellet, and the novel environment was the enclosed arm (25 cm long) of a black wooden Y-maze, elevated 80 cm above the floor, with 0.5 cm high walls. In the second trial, the novel food was a sweetcorn

niblet, and the novel environment was an unstable circular platform made of red acrylic (38 cm diameter), raised 64 cm above the floor, with no walls. Latency to first contact with the food was measured manually with a stopwatch, as was absolute latency to begin feeding. Feeding was defined as at least 2 s of continuous nibbling with the food held in the forepaws. Prior to analysis, latency to first contact with the food was subtracted from absolute latency to begin feeding, to control for differences in locomotor activity. Mice that did not feed within 2 min were removed from the apparatus and re-tested after 3 min. Each mouse was given a maximum of three attempts to feed, and a cumulative feeding latency was calculated, resulting in a maximum possible latency of 6 min.

2.2.5. Spontaneous locomotor activity

To confirm that the altered anxiety-like behaviour of *Dao*$^{-/-}$ mice was not an artefact of a hypolocomotor phenotype, *Dao*$^{+/+}$ and *Dao*$^{-/-}$ mice were subjected to a standard laboratory test of spontaneous locomotor activity. Testing was based on an established protocol [562]. Mice were transferred from their home-cage to a novel, open-top cage (42 cm long × 22 cm wide × 20 cm high), resting within a photobeam frame (San Diego Instruments, San Diego, USA). Locomotor activity was quantified as the number of beam breaks over a 2 h period, divided into twenty-four 5 min time bins. This interval was selected to enable direct comparison with the anxiety tests, 4 of which lasted 5 min.

2.2.6. Plasma corticosterone assay

Terminal blood samples were collected from 22 adult mice by cardiac puncture, under anaesthesia (isoflurane induction: 4.5 %; maintenance: 0.7–2.25 %). Samples were collected between ZT4 and ZT6 (i.e. 4 to 6 h after light onset during a standard 12:12 LD cycle). As plasma corticosterone levels show circadian and ultradian rhythmicity, *Dao*$^{+/+}$ and *Dao*$^{-/-}$ mice were sampled alternately to avoid temporal bias. Likewise, pairs of males and females were sampled alternately. Samples were collected as rapidly as possible following the experimenter's initial contact with each animal's cage, so that the results obtained represented baseline corticosterone levels rather than stress-induced corticosterone levels. (In rodents, there is no detectable rise in plasma corticosterone in the first 3-5 mins following acute stress [603]). 0.5 to 1 ml of blood was collected from each animal. Blood samples were stored in 1.5 ml eppendorf tubes containing 10 µl of the anticoagulant ethylenediamine tetraacetic acid (EDTA; 0.5 M) for 2-3 h at 5°C, and then centrifuged (at 2000 RCF (relative centrifugal force) for 15 mins) to separate plasma from leucocytes, thrombocytes and erythrocytes.

Corticosterone concentration was quantified using a mouse corticosterone enzyme-linked immunosorbent assay (ELISA) kit (ADI-900-097, Enzo Life Sciences, Farmingdale, NY, USA), following the manufacturer's instructions. Firstly, 10 µl of all plasma samples were transferred to micro-centrifuge tubes. 10 µl of 1:100 steroid displacement reagent (in deionised water) was added to each tube. Tubes were vortexed and left to stand for 5 mins. Samples were diluted with ELISA assay buffer and vortexed again (final dilution was 1:20). Next, 150 µl of assay buffer was pipetted into the 2 non-specific binding (NSB) wells of a 96–well microplate. 100 µl of standards 1 to 5 were pipetted into separate wells, as was 100 µl of each sample. (Note that all samples and standards were run in duplicate). Next, 50 µl of blue conjugate was

pipetted into each well, with the exception of the 2 blank wells. Lastly, 50 µl of yellow antibody was pipetted into each well, with the exception of the 2 blank wells and the 2 NSB wells.

The microplate was sealed and incubated at room temperature on a plate shaker for 2 h at 500 rpm. After incubation, the wells were emptied and washed by adding 400 µl of wash solution to every well. This wash procedure was performed 3 times. After the final wash, the wells were emptied and the plate was tapped firmly on paper towel to remove any remaining wash buffer. 200 µl of p-nitrophenyl phosphate (pNpp) substrate solution was added to every well. The plate was incubated at room temperature for a further hour without shaking. To stop the reaction, 50 µl of stop solution was added to every well. The optical density of each well was immediately determined with a microplate reader (Thermo Scientific, Waltham, MA, USA). Optical density in the blank wells and NSB wells was equivalent, confirming the absence of non-specific binding. The average optical density of the blank wells was subtracted from the average optical density of all standards and samples to yield average net optical densities (ODs). Average net ODs for standards 1 to 5 were plotted against their known corticosterone concentrations (in pg/ml), and a line of best fit was fitted to the data by nonlinear regression analysis (4 parameter logistic curve fit; see Fig. 2.7). Using the resulting formula, the corticosterone concentration of each sample (in pg/ml) was derived by interpolation, and converted to ng/ml. Note that Lindsay Benson assisted with blood sample collection, and Phil Burnet and Li Chen assisted with the corticosterone ELISA assay.

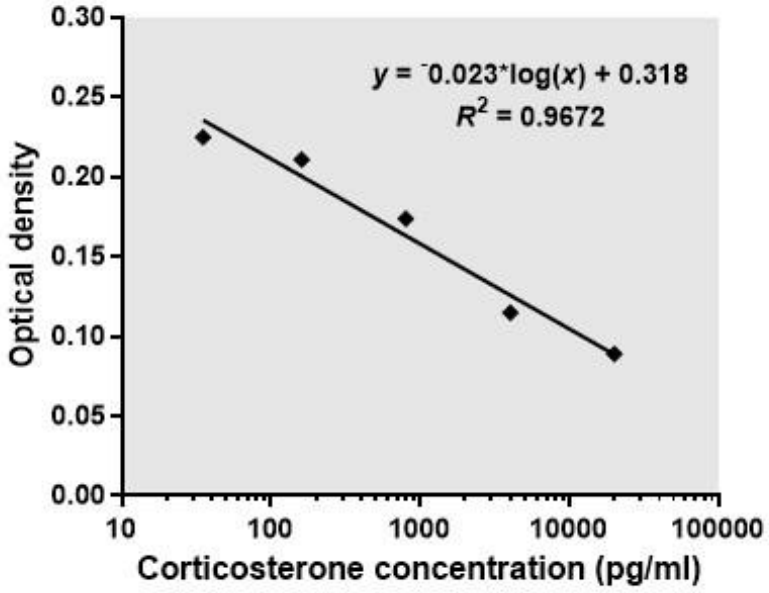

Figure 2.7. Standard curve used to derive corticosterone concentration of plasma samples by interpolation.

2.2.7. Short-term memory tests

Spontaneous recognition memory

Spontaneous recognition memory tasks rely on rodents' innate preference for novelty, and can be used to test short- or long-term memory of a spatial or a non-spatial nature [131]. In this case, we used them to test both spatial and non-spatial short-term memory performance. Spontaneous recognition memory testing took place in an open top arena (20 × 20 × 20 cm), made of transparent acrylic (Fig. 2.8A & 2.8B). To facilitate discrimination of the four corners, patterned wallpapers were attached to the outside of two walls. Velcro was attached to the base of the arena and the bottom of all experimental stimuli, so that they could be fixed in place during behavioural testing. Illumination was 200 lux at the base of the apparatus. All mice completed two habituation trials (on separate days) prior to testing. In these trials, mice were able to explore the empty apparatus for 9 min. Subsequently, all mice completed two trials of object recognition memory testing, two trials of spatial recognition memory testing, and two trials of odour recognition memory testing. Each trial was performed on a separate day, and the six trials were presented in a pseudo-randomised order, which was counterbalanced across genotype groups. Experimental trials consisted of a sample phase (10 min), a delay period (5 min), and a test phase (1 min).

In object recognition trials, mice explored two identical replicates of an object during the sample phase. During the delay period, the animal was removed from the arena and placed in an empty holding cage, while the arena was cleaned with diluted ethanol. One replicate was replaced by an entirely novel object, while the other was replaced by a third replicate of the familiar object (Fig. 2.8C). Multiple replicates were employed to prevent mice from re-encountering their own odour cues. Odour recognition trials were similar to object recognition trials, except that the stimulus was not a household object but 1 ml of food flavouring (Dr.

Oetker, Bielefeld, Germany) inside a transparent shot-glass. The to-be-discriminated object/odour pairings have been validated previously in our laboratory. Object pairings differed along multiple sensory dimensions (i.e. colour, size, shape, and texture). For each pairing, the identity of the novel object and its location at test (i.e. top or bottom) was counterbalanced across genotype groups. In spatial recognition trials, a novel object was not presented in the test phase. Instead, the test phase involved exposure to two replicates of the familiar object. One remained in the same location as in the sample phase, whereas the other was displaced to a novel location (Fig. 2.8C). The location selected for displacement (i.e. top or bottom) was counterbalanced across genotype groups

Total distance travelled during the habituation, sample and test phases was calculated using ANY-maze. The amount of time spent in contact with the experimental stimuli (during the sample and test phases) was derived manually from the videos, by an observer who was blind to both the genotype of the animals and the identity and location of the novel object. Recognition memory performance in each trial was expressed as a ratio, $n/(n+f)$, where f and n represent the total amount of time spent in contact with the familiar and novel stimuli during the test phase. A value of 0.5 indicates no preference for either object, a value > 0.5 indicates a preference for the novel object, and a value < 0.5 indicates a preference for the familiar object. One-sample *t*-tests (2-tailed) were used to compare recognition ratios against chance performance (0.5). Note that this experiment was conducted in collaboration with Eric Tam.

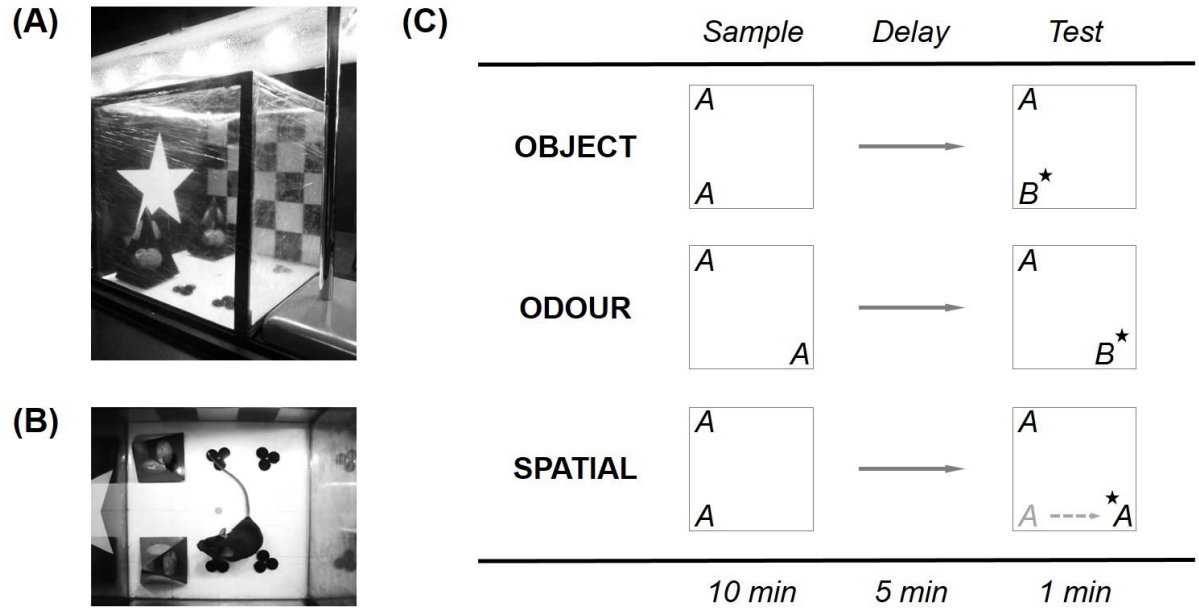

Figure 2.8. Apparatus and protocol for testing spontaneous recognition memory. Panels (A) and (B) show the side and top views of the apparatus, respectively. Patterned wallpapers were attached to two walls, to facilitate discrimination of the four corners of the arena. (C) A schematic showing the different versions of the spontaneous recognition task. In object and odour recognition trials, the mouse explored two identical replicates of an object or odour cue '*A*' for 10 min during the sample phase. After a 5-min delay (denoted by →), one replicate of '*A*' was replaced by a novel object or odour cue '*B*', and the animal was allowed to explore '*A*' and '*B*' for 1 min during the test phase. In spatial recognition trials, no novel object was introduced. Instead, one replicate of '*A*' was displaced to a novel location.

T-maze spontaneous alternation

Spontaneous alternation behaviour in the T-maze reflects rodents' innate preference for novelty, and can be used as a test of short-term spatial memory [131]. The apparatus was a black wooden T-maze. The walls were 21 cm high, while each of the arms was 30 cm long and 9 cm wide. A removable central partition (extending 14 cm into the start arm) was used during the sample phase but not the test phase of each trial. Guillotine doors were positioned at the entrance to each goal arm. At the beginning of the sample phase, both doors were raised, and the mouse was placed at the end of the start arm facing away from the goal arms. Each mouse was allowed to make a free choice between the two goal arms; after its tail had cleared the door of the chosen arm, the door was closed, and the mouse was allowed to explore the arm for 30 s. The mouse was then returned to the end of the start arm, with the central partition removed

and both guillotine doors raised, signalling the beginning of the test phase. Again the mouse was allowed to make a free choice between the two goal arms. Trials which were not completed within 90 s were terminated and disregarded during analysis. In such cases, mice were returned to their home-cage and re-tested after an interval of at least 10 min. All mice completed 2 trials per day over 3 consecutive days, with an inter-trial interval of 4 h. The principal dependent variable was the percentage of trials in which mice successfully alternated between the sample and test phases. One-sample *t*-tests (2-tailed) were used to compare these scores against chance performance (50%). Trial completion was also recorded (i.e. the proportion of trials completed within the 90 s cut-off at the first attempt).

Y-maze spatial novelty preference

This Y-maze task is another example of a short-term spatial memory test that relies on rodents' innate preference for novelty [131]. The apparatus was a transparent acrylic Y-maze lined with sawdust, mounted on a white acrylic base (64.5 cm x 56.5 cm). The walls of the maze were 20 cm high, while each of the three arms (the start arm and two goal arms) were 30 cm long and 8 cm wide. The maze was placed on a table-top in a room containing a variety of extra-maze cues. Each trial consisted of a sample phase (5 min), a delay period (1 minute), and a test phase (2 min). At the beginning of the sample and test phases, the mouse was placed at the end of the start arm facing away from the goal arms. During the sample phase, the entrance to one of the goal arms was blocked with an opaque acrylic guillotine door. Hence, mice could only explore the start arm and one of the two goal arms. During the delay period, the animal was removed from the arena and placed in an empty holding cage. In the test phase, the guillotine door was removed, so the mouse was free to explore the start arm, the familiar (previously accessible) goal arm, and the novel (previously inaccessible) goal arm. Sawdust was redistributed between mice and replaced between males and females. The identity of the novel arm (left or right) was

counterbalanced across genotype groups. Spatial novelty preference was expressed as a ratio, $n/(n+f)$, where f and n represent the total amount of time spent in (or the number of entries to) the familiar and novel goal arms during the test phase. A value of 0.5 indicates no preference for either arm, a value > 0.5 indicates a preference for the novel arm, and a value < 0.5 indicates a preference for the familiar arm. One sample *t*-tests (2-tailed) were conducted to compare spatial novelty preference against chance performance (0.5). Total distance travelled was calculated using ANY-maze during the test phase only.

2.2.8. Statistical analysis

All statistical analyses were performed with SPSS 22.0 (IBM, Armonk, New York). Unless otherwise stated, all reported statistics are the result of analyses of variance (ANOVAs), with genotype and sex included as independent variables, in addition to trial, day, stimulus type and time bin where applicable. Differences were considered to be statistically significant at p-values < 0.05. Greenhouse-Geisser corrections were applied where appropriate, but uncorrected degrees of freedom are reported in order to preserve the transparency of the statistical design. For analyses involving multiple cohorts, further ANOVAs were conducted with cohort included as an extra independent variable. No additional effects or interactions were observed, so these data are not shown. Defecation and urination were measured in all anxiety and memory experiments, but no effects were observed (data not shown). In all figures, * indicates a p-value ≤ 0.05, ** indicates a p-value ≤ 0.01, and *** indicates a p-value ≤ 0.001. Error bars depict the standard error of the mean. $\underline{M}$ = mean.

2.3. Results

2.3.1. Visual tests

Visual cliff

Both *Dao*$^{+/+}$ mice (Student's *t*-test, t_{20} = -4.440, *P* = <0.001, $\underline{M}$ = 29.1%) and *Dao*$^{-/-}$ mice (Student's *t*-test, t_{16} = -7.195, *P* = <0.001, $\underline{M}$ = 17.4%) spent significantly less than half of the trial away from the raised platform (Fig. 2.9A). This indicates that adult mice of both genotypes are capable of depth perception, and suggests that they found one side of the apparatus more anxiogenic than the other. Relative to *Dao*$^{+/+}$ mice, *Dao*$^{-/-}$ mice spent less time away from the raised platform, although this difference was not statistically significant ($F_{1,34}$ = 2.422, *P* = 0.129; Fig. 2.9A). Crucially, the proportion of cliff crossings relative to cliff approaches was lower in *Dao*$^{-/-}$ mice than *Dao*$^{+/+}$ mice ($F_{1,34}$ = 9.448, *P* = 0.004; Fig. 2.9B). Consistent with this, the proportion of hesitation responses relative to cliff approaches was higher in *Dao*$^{-/-}$ mice than *Dao*$^{+/+}$ mice ($F_{1,34}$ = 4.220, *P* = 0.048; Fig. 2.9C). By contrast, *Dao*$^{+/+}$ and *Dao*$^{-/-}$ mice were equally active in the visual cliff apparatus; genotype had no effect on distance travelled ($F_{1,19}$ = 0.341, *P* = 0.566; Fig. 2.9D), or on the total number of cliff approaches ($F_{1,34}$ = 1.746, *P* = 0.195; Fig. 2.9E). The altered behaviour of *Dao*$^{-/-}$ mice in this task could be a reflection of superior vision and/or heightened anxiety relative to *Dao*$^{+/+}$ mice. Females travelled a significantly shorter distance than males in the visual cliff apparatus ($F_{1,19}$ = 8.983, *P* = 0.007), and made significantly fewer cliff approaches ($F_{1,34}$ = 18.890, *P* = <0.001). Note that the video recordings for 15 mice did not include the periphery of the apparatus, so mice could not be tracked with ANY-maze. Hence, sample size is lower in the distance analyses than all other analyses.

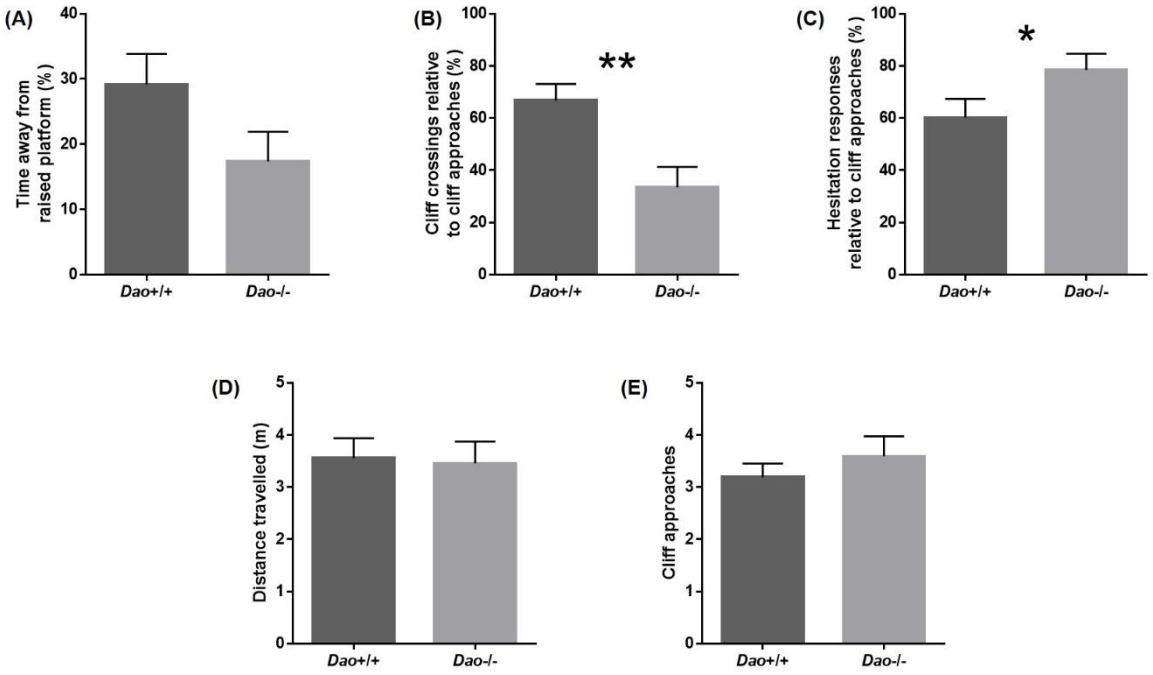

Figure 2.9. Altered behaviour in *Dao*$^{-/-}$ mice in the visual cliff task. (A) Time spent away from the raised platform was numerically but not significantly reduced in *Dao*$^{-/-}$ mice. (B) *Dao*$^{-/-}$ mice made significantly fewer cliff crossings than *Dao*$^{+/+}$ mice. (C) *Dao*$^{-/-}$ mice displayed significantly more hesitation responses than *Dao*$^{+/+}$ mice. (D) Distance travelled did not differ between *Dao*$^{+/+}$ and *Dao*$^{-/-}$ mice. (E) Total cliff approaches did not differ between *Dao*$^{+/+}$ and *Dao*$^{-/-}$ mice.

Optokinetic nystagmus drum

This test revealed no evidence of altered visual acuity in *Dao*$^{-/-}$ mice. Head-tracking response rate data were entered into a repeated-measures ANOVA, with genotype as a between-subjects variable, and spatial frequency as a within-subjects variable. There was a main effect of spatial frequency on head-tracking response rate ($F_{2,26} = 39.321$, $P = <0.001$; Fig. 2.10A), reflecting the reduced number of head-tracking responses seen at higher spatial frequencies. By contrast, there was no main effect of genotype on head-tracking response rate ($F_{1,13} = 0.149$, $P = 0.705$), and no interaction between spatial frequency and genotype ($F_{2,26} = 0.637$, $P = 0.537$). Likewise, genotype had no effect on the absolute limit of visual acuity ($F_{1,13} = 0.269$, $P = 0.613$; Fig. 2.10B).

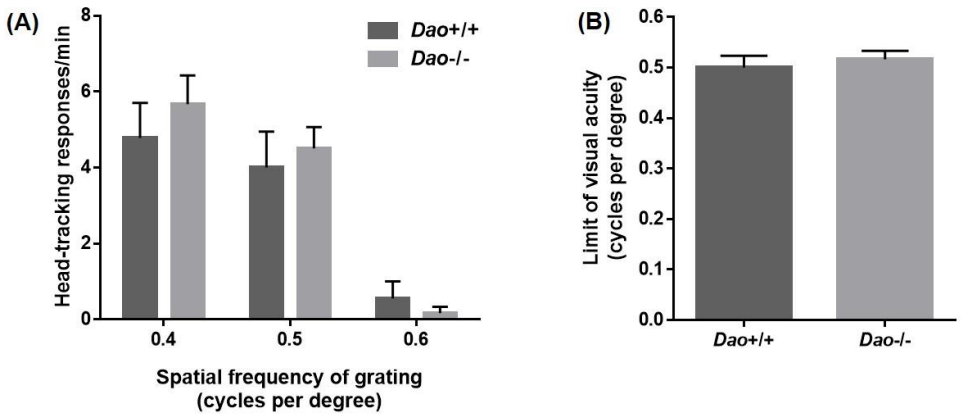

Figure 2.10. No evidence of altered visual acuity in *Dao*$^{-/-}$ mice. (A). Head-tracking response rate did not differ between *Dao*$^{+/+}$ and *Dao*$^{-/-}$ mice at any spatial frequency. (B) The absolute limit of visual acuity did not differ between *Dao*$^{+/+}$ and *Dao*$^{-/-}$ mice. Note that average visual acuity in laboratory mice is 0.53 cpd [604].

2.3.2. Anxiety tests

Open field test

Dao$^{-/-}$ mice showed elevated anxiety-like behaviour in the open field test. They made fewer centre entries than *Dao*$^{+/+}$ mice ($F_{1,34} = 4.765$, $P = 0.036$; Fig. 2.11A), despite the fact that there was no difference in overall locomotor activity, as measured by total distance travelled ($F_{1,34} = 0.035$, $P = 0.853$; Fig. 2.11B). Percent distance travelled in the centre of the arena was also lower in *Dao*$^{-/-}$ than *Dao*$^{+/+}$ mice, although this trend did not reach statistical significance ($F_{1,34} = 3.524$, $P = 0.069$; Fig. 2.11C). Genotype had no effect on percent time spent in the centre ($F_{1,34} = 1.728$, $P = 0.197$), or on latency to the first centre entry ($F_{1,34} = 1.500$, $P = 0.229$). Females made fewer centre entries than males ($F_{1,34} = 8.058$, $P = 0.008$), travelled less distance overall ($F_{1,34} = 23.566$, $P = <0.001$), and took longer to make their first centre entry ($F_{1,34} = 7.529$, $P = 0.010$). Percent distance travelled in the centre of the arena was also lower in females than males ($F_{1,34} = 6.495$, $P = 0.016$).

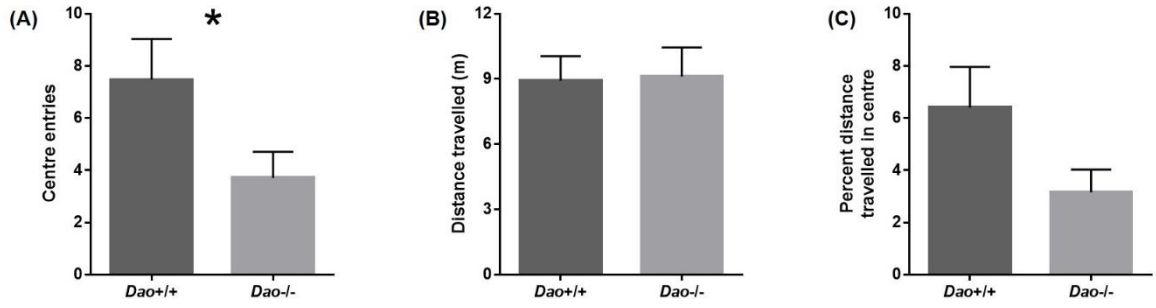

Figure 2.11. Evidence of heightened anxiety in *Dao*$^{-/-}$ mice in the open field test. (A) *Dao*$^{-/-}$ mice made significantly fewer centre entries than *Dao*$^{+/+}$ mice. (B) Distance travelled did not differ between *Dao*$^{+/+}$ and *Dao*$^{-/-}$ mice. (C) Percent distance travelled in the centre of the open field arena was numerically but not significantly reduced in *Dao*$^{-/-}$ mice.

Elevated plus maze

Dao$^{-/-}$ mice also demonstrated increased anxiety-like behaviour in the elevated plus maze. They made fewer open arm entries than *Dao*$^{+/+}$ mice ($F_{1,44} = 5.101$, $P = 0.029$; Fig. 2.12A), whereas there was no difference in closed arm entries ($F_{1,44} = 0.003$, $P = 0.958$; Fig 2.12B). *Dao*$^{-/-}$ mice also exhibited a non-significant tendency to spend less time than *Dao*$^{+/+}$ mice in the open arms of the maze ($F_{1,44} = 3.203$, $P = 0.080$; Fig. 2.12C). Genotype had no effect on latency to the first open arm entry ($F_{1,44} = 0.303$, $P = 0.585$), or on total distance travelled ($F_{1,44} = 3.015$, $P = 0.090$; Fig 2.12D). There were no main effects or interactions involving sex for any of the aforementioned variables (data not shown).

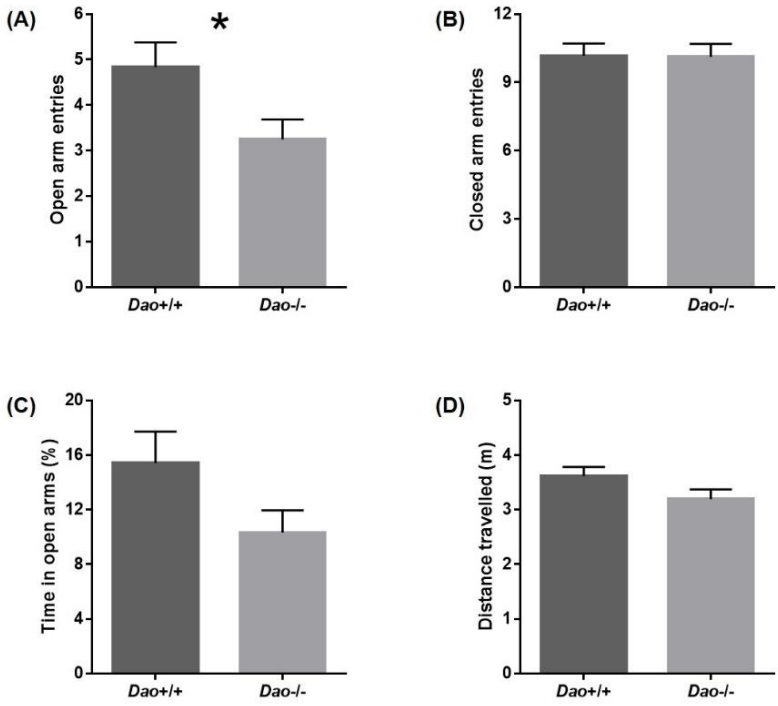

Figure 2.12. Evidence of heightened anxiety in *Dao*$^{-/-}$ mice in the elevated plus maze. (A) *Dao*$^{-/-}$ mice made significantly fewer open arm entries than *Dao*$^{+/+}$ mice. (B) The number of closed arm entries did not differ between *Dao*$^{+/+}$ and *Dao*$^{-/-}$ mice. (C) Time spent in the open arms of the elevated plus maze was numerically but not significantly reduced in *Dao*$^{-/-}$ mice. (D) Distance travelled did not differ between *Dao*$^{+/+}$ and *Dao*$^{-/-}$ mice.

Successive alleys

Dao$^{-/-}$ mice displayed heightened anxiety-like behaviour in the successive alleys test. They spent less time than *Dao*$^{+/+}$ mice in the exposed, open zones of the apparatus (i.e. zones 2 to 4) ($F_{1,20}$ = 7.072, P = 0.015; Fig. 2.13A). *Dao*$^{-/-}$ mice also made fewer entries to zone 3 than *Dao*$^{+/+}$ mice ($F_{1,20}$ = 4.370, P = 0.050; Fig. 2.13B). No mice of either genotype entered zone 4. Genotype had no effect on total distance travelled ($F_{1,20}$ = 1.030, P = 0.322; Fig. 2.13C). There were no main effects or interactions involving sex for any of the aforementioned variables (data not shown).

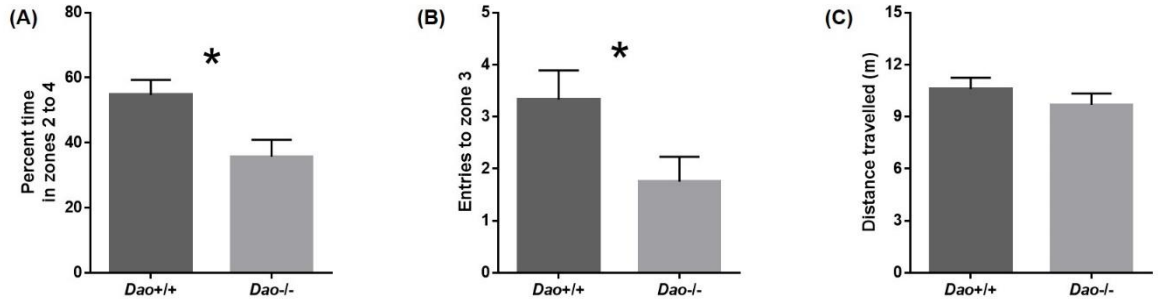

Figure 2.13. Evidence of heightened anxiety in *Dao*$^{-/-}$ mice in the successive alleys task. (A) *Dao*$^{-/-}$ mice spent significantly less time than *Dao*$^{+/+}$ mice in the exposed, open zones of the apparatus. (B) *Dao*$^{-/-}$ mice made significantly fewer entries to zone 3 of the successive alleys apparatus. (C) Distance travelled did not differ between *Dao*$^{+/+}$ and *Dao*$^{-/-}$ mice.

Light/dark box

Dao$^{-/-}$ mice also showed elevated anxiety-like behaviour in the light/dark box. They spent less time in the light compartment than *Dao*$^{+/+}$ mice ($F_{1,32}$ = 4.469, P = 0.042; Fig. 2.14A), although genotype had no effect on the number of light/dark crossings ($F_{1,32}$ = 2.476, P = 0.125; Fig. 2.14B), or on latency to the first crossing ($F_{1,32}$ = 1.993, P = 0.168; Fig. 2.14C). Males made more light/dark crossings than females ($F_{1,32}$ = 5.189, P = 0.030).

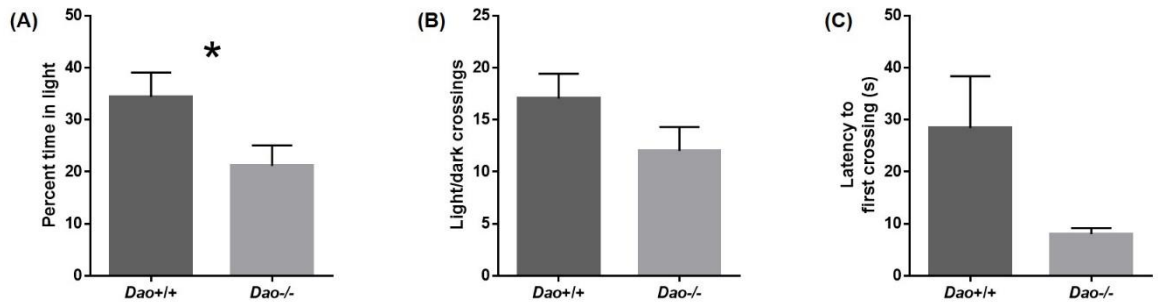

Figure 2.14. Evidence of heightened anxiety in *Dao*$^{-/-}$ mice in the light/dark box. (A) *Dao*$^{-/-}$ mice spent significantly less time than *Dao*$^{+/+}$ mice in light compartment of the light/dark box. (B) The number of light/dark crossings did not differ between *Dao*$^{+/+}$ and *Dao*$^{-/-}$ mice. (C) Latency to the first light/dark crossing did not differ between *Dao*$^{+/+}$ and *Dao*$^{-/-}$ mice.

Novelty-suppressed feeding

Dao$^{-/-}$ mice demonstrated heightened anxiety-like behaviour in the novelty-suppressed feeding test. Feeding latency data were entered into a repeated-measures ANOVA, with genotype and sex as between-subjects variables, and trial number as a within-subjects variable. There was a main effect of genotype, reflecting the longer feeding latencies in Dao$^{-/-}$ mice relative to *Dao*$^{+/+}$ mice ($F_{1,20}$ = 5.134, P = 0.035). This effect was driven exclusively by female *Dao*$^{-/-}$ mice. Amongst males, genotype had no effect on feeding latency ($F_{1,10}$ = 0.014, P = 0.908), but amongst females, feeding latency was greater in *Dao*$^{-/-}$ than *Dao*$^{+/+}$ mice ($F_{1,10}$ = 11.640, P = 0.007). Hence, there was a genotype-by-sex interaction for this variable ($F_{1,20}$ = 5.937, P = 0.024; Fig. 2.15). Interestingly, genotype-by-sex interactions were not evident in any of the other anxiety tests described in this manuscript (data not shown). In addition, there was a main effect of trial number on feeding latency ($F_{1,20}$ = 14.252, P = 0.001); feeding latencies were significantly greater in trial 2 than trial 1. This suggests that the sweetcorn niblet was less palatable than the sucrose pellet, and/or that the unstable circular platform was more anxiogenic than the Y-maze. Nonetheless, there was no interaction between genotype and trial number ($F_{1,20}$ = <0.001, P = 0.993). Note that feeding latency was calculated by subtracting the latency to the first contact with the food from the absolute latency to begin feeding. Importantly, genotype had no effect on latency to first contact with the novel food ($F_{1,20}$ = 0.014, P = 0.906).

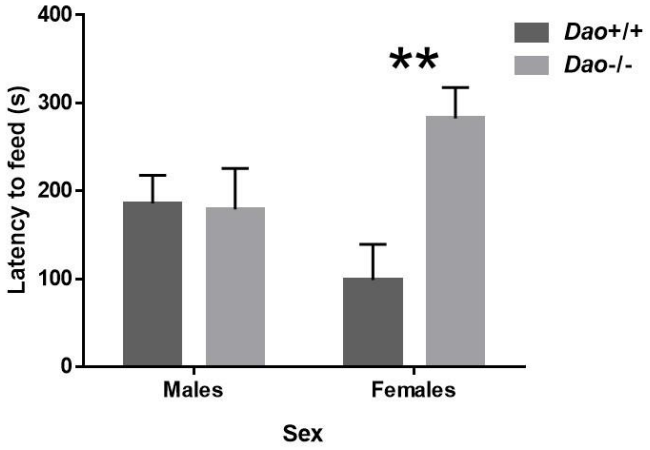

Figure 2.15. Evidence of heightened anxiety in *Dao*$^{-/-}$ mice in the novelty-suppressed feeding test. Female *Dao*$^{-/-}$ mice took significantly longer than female *Dao*$^{+/+}$ mice to begin feeding, although no such difference was evident in males. This figure represents average performance across both trials.

2.3.3. Spontaneous locomotor activity

Spontaneous locomotor activity was unaltered in *Dao*$^{-/-}$ mice (Fig. 2.16). Genotype had no effect on beam breaks during the first 5 min ($F_{1,20}$ = 1.462, P = 0.241), or the entire 2 h recording period ($F_{1,20}$ = 0.022, P = 0.884). With the 2 h session divided into twenty-four 5 min time bins, there was a main effect of time bin on beam breaks ($F_{23,460}$ = 57.229, P = <0.001), but no genotype-by-time bin interaction ($F_{23,460}$ = 0.790, P = 0.746), indicating that activity levels declined in *Dao*$^{-/-}$ and *Dao*$^{+/+}$ mice at a comparable rate. Males made more beam breaks than females during the first 5 min ($F_{1,20}$ = 12.855, P = 0.002), but not over the entire 2 h recording period ($F_{1,20}$ = 0.003, P = 0.959).

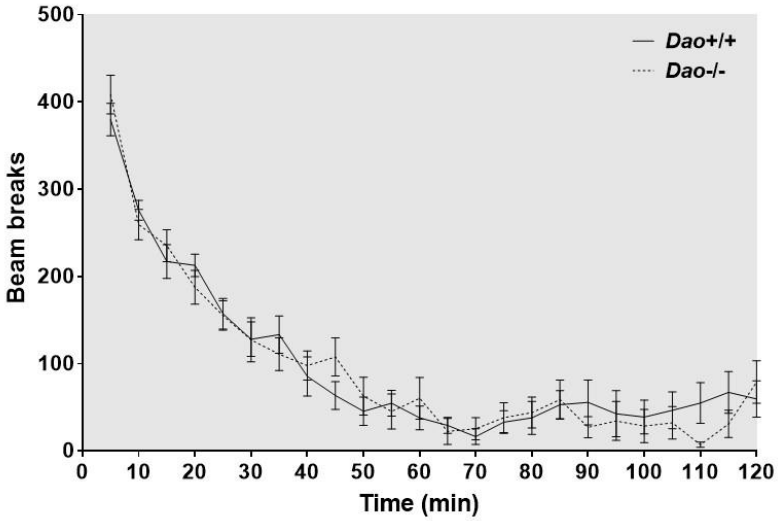

Figure 2.16. No evidence of altered spontaneous locomotor activity in *Dao*$^{-/-}$ mice. Activity is presented as the number of beam breaks across twenty-four 5 min time bins.

2.3.4. Plasma corticosterone assay

To evaluate the hypothesis that elevated corticosterone might contribute to the heightened anxiety phenotype of *Dao*$^{-/-}$ mice, plasma corticosterone levels were quantified with an ELISA assay. Genotype had no effect on plasma corticosterone concentration ($F_{1,18} = 0.469$, $P = 0.502$; Fig. 2.17). Similarly, there was no main effect of sex ($F_{1,18} = 1.942$, $P = 0.180$), and no interaction between genotype and sex ($F_{1,18} = 0.522$, $P = 0.479$).

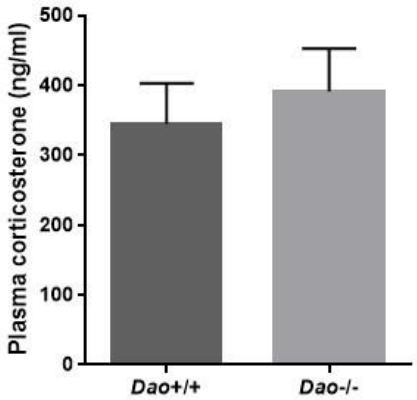

Figure 2.17. No evidence of altered plasma corticosterone levels in *Dao*$^{-/-}$ mice.

2.3.5. Short-term memory tests

Spontaneous recognition memory

Recognition ratios were entered into a repeated-measures ANOVA, with genotype as the principal between-subjects variable, and stimulus type (i.e. object, odour or spatial) as a within-subjects variable. This analysis yielded a main effect of genotype ($F_{1,19}$ = 11.394, P = 0.003; Fig. 2.18A), reflecting superior spontaneous recognition memory performance in *Dao*$^{-/-}$ mice. The enhanced recognition memory performance of *Dao*$^{-/-}$ mice reflects the fact that, during the test phase, *Dao*$^{-/-}$ mice spent more time than *Dao*$^{+/+}$ mice in contact with the novel stimulus, and less time than *Dao*$^{+/+}$ mice in contact with the familiar stimulus (Fig. 2.18E).

This enhancement was independent of stimulus type, since there was no interaction between genotype and stimulus type ($F_{2,38}$ = 0.656, P = 0.525). Likewise, there was no main effect of stimulus type ($F_{2,38}$ = 1.387, P = 0.262). With data collapsed across all three stimulus types, performance was above chance level (0.5) in *Dao*$^{-/-}$ mice (Student's *t*-test, t_{10} = 5.324, P = <0.001, $\underline{M}$ = 0.67), but in *Dao*$^{+/+}$ mice, this difference was only borderline-significant (Student's *t*-test, t_{11} = 2.189, P = 0.051, $\underline{M}$ = 0.54).

Subsequently, post-hoc ANOVAs were conducted to assess recognition ratios for each stimulus type in isolation. Relative to *Dao*$^{+/+}$ mice, *Dao*$^{-/-}$ mice showed improved spatial recognition memory performance ($F_{1,19}$ = 8.968, P = 0.007, Fig. 2.18B) and odour recognition memory performance ($F_{1,19}$ = 5.584, P = 0.029, Fig. 2.18C). Object recognition memory performance was numerically but not significantly enhanced in *Dao*$^{-/-}$ mice ($F_{1,19}$ = 0.763, P = 0.393, Fig. 2.18D).

In accordance with the results of these ANOVAs, a series of one-sample *t*-tests confirmed that recognition ratios were generally poorer in $Dao^{+/+}$ mice. $Dao^{+/+}$ mice did not perform above chance in either odour (Student's *t*-test, $t_{11} = 0.212$, $P = 0.836$, $\underline{M} = 0.51$) or spatial trials (Student's *t*-test, $t_{11} = {}^{-}0.059$, $P = 0.954$, $\underline{M} = 0.50$), whereas $Dao^{-/-}$ mice performed above chance in both odour (Student's *t*-test, $t_{10} = 3.444$, $P = 0.006$, $\underline{M} = 0.66$) and spatial trials (Student's *t*-test, $t_{10} = 4.898$, $P = 0.001$, $\underline{M} = 0.66$). In object trials, however, the performance of both $Dao^{+/+}$ mice (Student's *t*-test, $t_{11} = 3.045$, $P = 0.011$, $\underline{M} = 0.61$) and $Dao^{-/-}$ mice (Student's *t*-test, $t_{10} = 2.733$, $P = 0.021$, $\underline{M} = 0.69$) was above chance level.

With data collapsed across all three stimulus types, there was no effect of genotype on distance travelled during either the sample phase ($F_{1,19} = 1.824$, $P = 0.193$) or the test phase ($F_{1,19} = 0.471$, $P = 0.501$). Likewise, total stimulus contact time was no different between $Dao^{+/+}$ and $Dao^{-/-}$ mice during either the sample phase ($F_{1,19} = 0.045$, $P = 0.834$) or test phase ($F_{1,19} = 0.357$, $P = 0.557$). Hence, the superior recognition memory performance of $Dao^{-/-}$ mice did not result from increased exploration of the experimental stimuli during the sample phase.

Genotype had no effect on total distance travelled during habituation trials, when there were no experimental stimuli in the arena ($F_{1,19} = 2.026$, $P = 0.171$). However, males travelled a greater distance than females during habituation trials ($F_{1,19} = 4.908$, $P = 0.039$). Besides this result, there were no main effects or interactions involving sex for any of the aforementioned variables (data not shown).

Similarly, genotype had no effect on the rate of habituation to the test arena during habituation trials. When distance travelled was split into nine 1 min time bins, there was a main effect of both day ($F_{1,19} = 32.260$, $P = <0.001$) and time bin ($F_{8,152} = 37.558$, $P = <0.001$), reflecting a

progressive reduction in activity over time. However, there was no interaction between day and genotype ($F_{1,19}$ = 0.206, P = 0.655) or time bin and genotype ($F_{8,152}$ = 0.161, P = 0.894), indicating that *Dao*$^{-/-}$ and *Dao*$^{+/+}$ mice habituated to the arena at a similar rate.

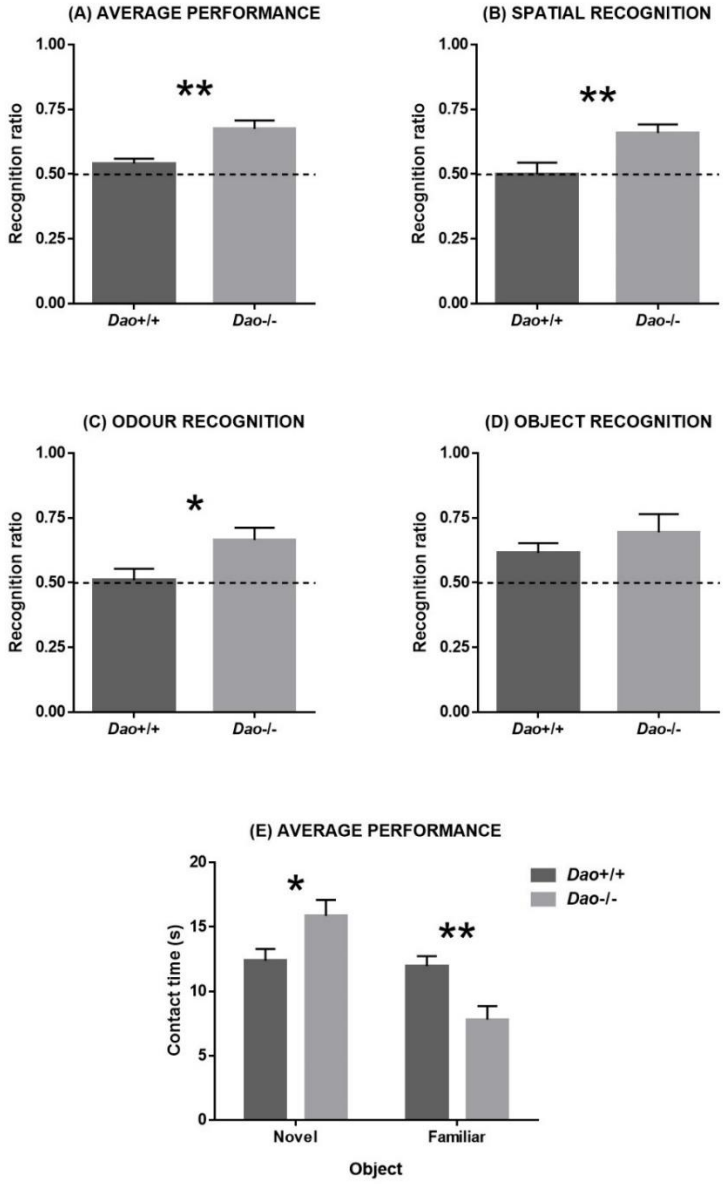

Figure 2.18. Evidence of enhanced spontaneous recognition memory performance in *Dao*$^{-/-}$ mice. (A) Average recognition memory performance was significantly enhanced in *Dao*$^{-/-}$ mice relative to *Dao*$^{+/+}$ mice. (B) Spatial recognition memory performance was significantly enhanced in *Dao*$^{-/-}$ mice. (C) Odour recognition memory performance was significantly enhanced in *Dao*$^{-/-}$ mice. (D) Object recognition memory performance was numerically but not significantly enhanced in *Dao*$^{-/-}$ mice. Dashed lines represent chance performance. (E) Analysis of recognition memory performance in terms of contact time with the novel and familiar stimuli during the test phase. *Dao*$^{-/-}$ mice spent more time than *Dao*$^{+/+}$ mice in contact with the novel stimulus, and less time than *Dao*$^{+/+}$ mice in contact with the familiar stimulus. This figure depicts average performance across all 6 trials of testing (i.e. 2 object recognition trials, 2 spatial recognition trials and 2 odour recognition trials).

T-maze spontaneous alternation

In the T-maze, *Dao*$^{-/-}$ mice demonstrated enhanced spontaneous alternation relative to *Dao*$^{+/+}$ mice ($F_{1,44}$ = 4.244, P = 0.045; Fig. 2.19A). Performance was above chance level (50%) in both *Dao*$^{+/+}$ mice (Student's *t*-test, t_{23} = 2.532, P = 0.019, $\underline{M}$ = 60.4%) and *Dao*$^{-/-}$ mice (Student's *t*-test, t_{23} = 5.784, P = <0.001, $\underline{M}$ = 72.2%). By contrast, there were no effects or interactions involving sex, day or trial number. The performance advantage of *Dao*$^{-/-}$ mice was more marked during the first trial ($F_{1,44}$ = 4.523, P = 0.039) than the second trial of each day($F_{1,44}$ = 0.540, P = 0.466), but the interaction between genotype and trial number was not significant ($F_{1,44}$ = 1.229, P = 0.274)**.**

Genotype had no effect on trial completion ($F_{1,44}$ = 1.431, P = 0.238; Fig. 2.19B). However, males completed fewer trials than females at the first attempt ($F_{1,44}$ = 5.724, P = 0.021). Besides this result, there were no main effects or interactions involving sex for any of the aforementioned variables (data not shown). Both day ($F_{2,88}$ = 7.391, P = 0.002) and trial number ($F_{1,44}$ = 6.707, P = 0.013) had a significant impact on trial completion, reflecting a gradual decline in trial completion across consecutive days and trials.

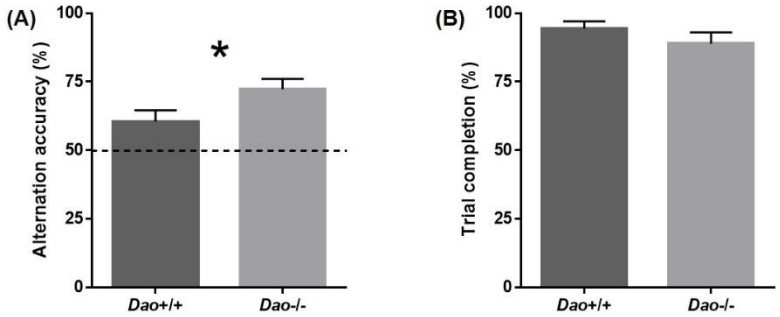

Figure 2.19. Evidence of enhanced T-maze spontaneous alternation in *Dao*$^{-/-}$ mice. (A) Alternation accuracy was significantly enhanced in *Dao*$^{-/-}$ mice relative to *Dao*$^{+/+}$ mice. Dashed lines represent chance performance. (B) Trial completion rate did not differ between *Dao*$^{+/+}$ and *Dao*$^{-/-}$ mice.

Y-maze spatial novelty preference

Genotype had no effect on the spatial novelty preference ratio, as derived from the time spent in each goal arm ($F_{1,20}$ = 0.039, P = 0.846; Fig. 2.20A), or the number of entries to each goal arm ($F_{1,20}$ = 0.010, P = 0.921; Fig. 2.20B). One sample *t*-tests (2-tailed) were conducted to compare mean novelty preference ratios against chance performance (0.5). Performance derived from the time spent in each arm was not above chance in either $Dao^{+/+}$ mice (Student's *t*-test, t_{11} = 1.822, P = 0.096, $\underline{M}$ = 0.59) or $Dao^{-/-}$ mice (Student's *t*-test, t_{11} = 1.154, P = 0.273, $\underline{M}$ = 0.57). Performance derived from arm entries was above chance in $Dao^{+/+}$ mice (Student's *t*-test, t_{11} = 3.755, P = 0.003, $\underline{M}$ = 0.59), but not in $Dao^{-/-}$ mice (Student's *t*-test, t_{11} = 1.676, P = 0.122, $\underline{M}$ = 0.59). Genotype had no effect on locomotor activity; distance travelled did not differ between $Dao^{+/+}$ and $Dao^{-/-}$ mice during the test phase ($F_{1,20}$ = 0.333, P = 0.570; Fig. 2.20C). Similarly, there was no difference in total arm entries during the test phase ($F_{1,20}$ = 0.731, P = 0.403; Fig. 2.20D). There were no main effects or interactions involving sex for any of the aforementioned variables (data not shown).

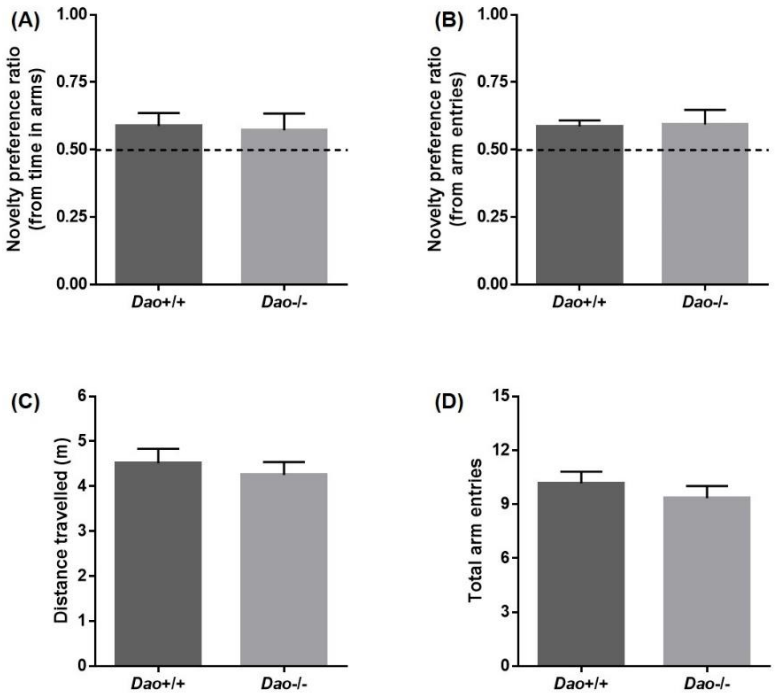

Figure 2.20. No evidence of altered Y-maze spatial novelty preference in *Dao*$^{-/-}$ mice. (A) The spatial novelty preference ratio (derived from the time spent in each goal arm) did not differ between *Dao*$^{+/+}$ and *Dao*$^{-/-}$ mice. (B) The spatial novelty preference ratio (derived from the number of entries to each goal arm) did not differ between *Dao*$^{+/+}$ and *Dao*$^{-/-}$ mice. (C) Distance travelled did not differ between *Dao*$^{+/+}$ and *Dao*$^{-/-}$ mice. (D) Total arm entries did not differ between *Dao*$^{+/+}$ and *Dao*$^{-/-}$ mice.

2.4. Discussion

Visual acuity is unaltered in Dao$^{-/-}$ mice

In the visual cliff task, *Dao*$^{-/-}$ mice made significantly fewer cliff crossings than *Dao*$^{+/+}$ mice, and displayed a significantly greater number of hesitation responses at the cliff edge. Theoretically, this behaviour could reflect enhanced visual function and/or increased anxiety. The latter explanation seemed the more likely, given that heightened anxiety has been observed in both *Dao* mutant mice and wildtype mice following D-serine administration [514]. However, to discount the former explanation, mice were subjected to an alternative visual task, the optokinetic nystagmus (OKN) drum. The performance of *Dao*$^{-/-}$ mice was unaltered in this test of visual acuity.

Dao$^{-/-}$ mice display heightened anxiety

Dao$^{-/-}$ mice demonstrated increased anxiety-like behaviour in the open field test, elevated plus maze, successive alleys, light/dark box, and novelty-suppressed feeding tasks. Since each of these tests involves the exploration of a relatively large arena, it could be argued that the increased anxiety-like behaviour of *Dao*$^{-/-}$ mice was an artefact of reduced locomotor activity. Contrary to this suggestion, locomotor activity was unaltered in *Dao*$^{-/-}$ mice in the three anxiety tests in which distance data were recorded (the open field test, elevated plus maze and successive alleys). Likewise, *Dao*$^{+/+}$ and *Dao*$^{-/-}$ mice demonstrated similar activity levels in a standard laboratory test of spontaneous locomotor activity.

Dao$^{-/-}$ mice demonstrate enhanced short-term memory performance

Dao$^{-/-}$ mice displayed improved short-term memory performance in both spatial and non-spatial tasks; they demonstrated enhanced spatial recognition memory performance, improved odour recognition memory performance, and enhanced spontaneous alternation in the T-maze.

Object recognition memory performance was also superior in *Dao*$^{-/-}$ mice, although this enhancement was not statistically significant. During recognition memory testing, *Dao*$^{-/-}$ mice did not show increased exploration of the experimental stimuli in the sample phase. Hence, their improved performance likely reflects a genuine enhancement of memory encoding and/or retrieval, rather than an increase in exploratory drive.

Y-maze spatial novelty preference is unaltered in Dao$^{-/-}$ *mice*

Despite showing enhanced T-maze spontaneous alternation, *Dao*$^{-/-}$ mice did not outperform *Dao*$^{+/+}$ mice in the Y-maze spatial novelty preference task. This is somewhat surprising, given that both tasks can be solved based on the relative familiarity of the previously-encountered goal arms. Indeed, it has been argued that the Y-maze spatial novelty preference task is conceptually equivalent to a single trial of T-maze spontaneous alternation [131]. One explanation for these negative results is that, as a single trial test, the Y-maze task had insufficient power to differentiate *Dao*$^{+/+}$ and *Dao*$^{-/-}$ mice. Moreover, it is important to note that the length of the sample, delay and test phases differed between the tasks. Consequently, it is possible that the Y-maze task was simply more difficult. Consistent with this explanation, neither *Dao*$^{+/+}$ or *Dao*$^{-/-}$ mice performed significantly above chance when the novelty preference ratio was derived from the amount of time spent in each of the goal arms. Finally, the walls of the T-maze were opaque, whereas the walls of the Y-maze were transparent. Hence, distal extramaze cues were visible in the latter task but not the former. For this reason, mice may have adopted different behavioural strategies in the two tasks.

Phenotypic comparison between Dao$^{-/-}$ *mice and Dao mutants*

The heightened anxiety phenotype of the *Dao*$^{-/-}$ mouse is broadly consistent with published data; heightened anxiety has previously been reported in *Dao1*^{G181R} mice and ddY/*Dao*$^{-}$ mice

in the elevated plus maze and open field test [514]. Moreover, this phenotype was more pronounced in females than males in both models [514]. In a separate study, ddY/*Dao*$^{-}$ mice did not show an increase in anxiety-like behaviour in either the elevated plus maze or novelty-suppressed feeding [520]. However, female ddY/*Dao*$^{-}$ mice were not tested, which, based on our results and those of Labrie and colleagues [514], would have been more likely to display an anxiety phenotype.

The enhanced short-term memory phenotype of the *Dao*$^{-/-}$ mouse is a completely novel addition to the literature. Although the natural ddY/*Dao*$^{-}$ mouse [521] and the related *Dao1*^{G181R} mouse [466] display improved performance in long-term spatial memory tasks such as the Morris watermaze, neither of these mice have been subjected to any tests of short-term memory, either spatial or non-spatial (see Section 1.9.5.). Hence, the present findings represent the first demonstration of enhanced *short-term* memory performance in a DAO deficient genetic mouse model. Our findings are consistent with the fact that rewarded alternation is enhanced in wildtype mice following D-serine administration [522].

The effects of DAO inactivity on anxiety appear relatively robust, given that heightened anxiety has now been witnessed across three different genetic constructs: ddY/*Dao*$^{-}$ mice (and presumably *Dao1*^{G181R} mice) show normal expression of a DAO enzyme rendered inactive by a point mutation [499, 512, 513], whereas *Dao*$^{-/-}$ mice show no detectable expression of *Dao* mRNA or DAO protein [534]. Hence, our use of a constitutive knockout precludes the possibility of any residual effects of the DAO protein. Moreover, there is phenotypic overlap between the models despite the use of different background strains (ddY, C57BL/6J and 129Sv/Ev), each of which differ in terms of baseline anxiety. 129 substrains, for example, are characterised by increased anxiety relative to other inbred strains [605-609].

In addition, the memory performance of 129 substrains in inferior to other inbred strains [605-609]. Hence, our use of the 129Sv/Ev strain may explain the generally poor recognition memory performance of *Dao*$^{+/+}$ mice, which did not exceed chance in either odour or spatial recognition trials. Nonetheless, the performance of *Dao*$^{+/+}$ mice did exceed chance in the T-maze spontaneous alternation task, so the significant advantage of *Dao*$^{-/-}$ mice in this task cannot be attributed to the poor performance of controls.

Mechanistic basis of altered memory performance and anxiety in Dao$^{-/-}$ *mice*

DAO is traditionally seen as a hindbrain enzyme [470, 610], and indeed, D-serine is not increased in the prefrontal cortex of ddY/*Dao*$^{-}$ mice [472], *Dao1*^{G181R} mice [466], or *Dao*$^{-/-}$ mice [591]. The behavioural phenotypes of these models may therefore reflect the absence of DAO activity in other brain regions, such as the cerebellum, wherein D-serine levels are markedly increased in all three models [466, 472, 591]. D-serine is also moderately elevated in the hippocampus of *Dao1*^{G181R} mice [466] and *Dao*$^{-/-}$ mice [Pfizer Inc., *unpublished data*]. Conceivably, altered hippocampal function could underlie aspects of both the anxiety and spatial memory phenotypes of *Dao*$^{-/-}$ mice, given that the ventral and dorsal hippocampus make dissociable contributions to anxiety and memory function, respectively [611]. More specifically, lesions to the ventral hippocampus reduce anxiety but spare memory performance in rodents, whereas lesions to the dorsal hippocampus impair memory performance but have no effect on anxiety [602, 612-619].

Despite evidence of elevated brain D-serine in *Dao*$^{-/-}$ mice and *Dao* mutants, it is not certain that D-serine is responsible for the behavioural phenotypes of these mice. Although D-serine is the most abundant substrate of DAO in the mammalian brain, DAO also metabolises D-alanine, another NMDAR co-agonist [489, 490]. D-alanine levels are increased uniformly

throughout the brain in ddY/*Dao*$^{-}$ mice [472], while D-alanine levels in *Dao1*^{G181R} and *Dao*$^{-/-}$ mice remain to be elucidated. Nonetheless, the increased anxiety-like behaviour of *Dao*$^{-/-}$ mice in the elevated plus maze closely resembles the increased anxiety-like behaviour of wildtype mice in the same test following the administration of D-serine [514]. These pharmacological data infer – but do not prove – that the anxiety phenotype of the *Dao*$^{-/-}$ mouse results from an increase in brain D-serine. They also imply that its behavioural phenotype is not merely a consequence of altered neurodevelopment or other long-term compensatory changes that can occur in constitutive knockout models.

Finally, despite evidence that D-serine and D-alanine administration can alter corticosterone levels in wildtype rats [Phil Burnet, *unpublished data*], there was no indication that baseline plasma corticosterone concentration was increased in *Dao*$^{-/-}$ mice, in either males or females. It therefore appears that a transient increase in brain D-serine has a different effect on the hypothalamic-pituitary-adrenal (HPA) stress axis to the chronic elevation of brain D-serine reported in the *Dao*$^{-/-}$ mouse [591,Pfizer Inc., *unpublished data*]. Alternatively, D-serine may affect the HPA axis differently in rats and mice.

Conclusions

Consistent with the elevated anxiety phenotypes of ddY/*Dao*$^{-}$ and *Dao1*^{G181R} mice, anxiety is significantly heightened in *Dao*$^{-/-}$ mice. Moreover, *Dao*$^{-/-}$ mice display enhanced spatial and non-spatial short-term memory. This is the first demonstration of improved short-term memory performance in a genetic mouse model of DAO inactivation.

3. Assessment of long-term spatial memory performance in the *Dao*$^{-/-}$ mouse

3.1. Introduction

As described in Section 1.9.5., long-term spatial memory performance has previously been assessed in two *Dao* mutant models. ddY/*Dao*$^{-}$ mice displayed enhanced performance in the Barnes maze [520], and improved spatial memory acquisition in the Morris watermaze [521]. The authors of the latter study attributed the enhanced spatial memory acquisition of ddY/*Dao*$^{-}$ mice to facilitated hippocampal long-term potentiation (LTP), which they demonstrated electrophysiologically in cultured hippocampal slices. By contrast, spatial memory acquisition in the Morris watermaze task was unaltered in *Dao1*^{G181R} mice [466], and was also unaltered in wildtype mice following D-serine administration [523]. In the experiments described in this chapter, we assessed long-term spatial memory acquisition in *Dao*$^{-/-}$ mice in the Morris watermaze. Our primary aim was to shed light on the inconsistencies in the *Dao* mutant literature.

We did not expect to observe enhanced spatial memory acquisition in the Morris watermaze, based on the results of a recent study from our own laboratory [620]. In this study, acquisition was *unimpaired* in transgenic mice lacking NMDARs in the hippocampus alone. These data gave rise to the suggestion that cortical NMDAR function is more important for long-term spatial memory acquisition than hippocampal NMDAR function [611]. According to this hypothesis, Morris watermaze performance should not be enhanced in *Dao*$^{-/-}$ mice, since D-serine levels are unchanged in the cortex of these animals [591,Pfizer Inc., *unpublished data*].

Our secondary aim was to assess reversal learning in the Morris watermaze, given that enhanced watermaze reversal learning has been observed in *Dao1*^{G181R} mice [466], and in wildtype mice after D-serine administration [523]. In both studies, enhanced reversal learning was attributed to the fact that D-serine facilitates hippocampal long-term depression (LTD), which has been demonstrated electrophysiologically in cultured hippocampal slices [523, 533]. We expected to observe enhanced reversal learning in *Dao*$^{-/-}$ mice, given that D-serine levels are increased in the hippocampus of these animals [Pfizer Inc., *unpublished data*].

3.2. Methods

3.2.1. Animals

Dao knockout mice were generated as described in Chapter 2. Mice were at least 7 weeks old at the onset of behavioural testing. A total of 4 cohorts were used, full details of which are provided in Sections 3.2.2 to 3.2.6. Prior to behavioural testing, mice were handled for 2 min a day for 5 consecutive days, to habituate them to experimenter handling. Mice were singly-housed under a 100 lux 12:12 h light/dark (12:12 LD) cycle with lights on at 07:00, with access to food and water *ad libitum*. All testing was conducted between 10:00 and 17:00 (i.e. between ZT3 and ZT10). For all experiments, mice were brought into the test room 5-10 min prior to the onset of testing. Animals were singly-housed to enable direct comparison with other singly-housed cohorts in which anxiety and short-term memory were assessed (see Chapter 2), PPI was assessed (see Chapter 4), and sleep and circadian rhythms were assessed (see Chapter 5). All behavioural procedures were performed in accordance with the United Kingdom Animals (Scientific Procedures) Act of 1986 and the University of Oxford Policy on the Use of Animals in Scientific Research. All experiments were approved by the University of Oxford Animal Welfare and Ethical Review Board, and were conducted under the PPL 30/3068 by PILs ICC0614BD (formerly 30/9339) and 30/6220.

3.2.2. Experiment 1: Spatial memory acquisition in the Morris watermaze

Experimentally-naïve control (*Dao*$^{+/+}$) and knockout (*Dao*$^{-/-}$) mice (*n*=6 males; *n*=6 females per genotype) were trained on the standard, fixed location, hidden escape platform version of the Morris watermaze escape task. Testing was based on an established protocol [620-622]. The watermaze was 2 m in diameter, with 90 cm high walls. Water level was 65 cm and water temperature was 20°C ± 2°C. Illumination of the apparatus was homogenous, measuring 180 lux at water level. The platform was 20 cm in diameter and was positioned 1.5 cm beneath the water surface. White paint was added to the water to obscure the platform from view. A variety of distal extra-maze cues were positioned around the laboratory (e.g. wall posters, racks of equipment, lights). All training trials (during acquisition and reversal) were 90 s in duration. Mice which did not locate the platform within this time were guided towards the platform by the experimenter's arm.

Mice were given a single session of training each day, consisting of four consecutive trials, with an inter-trial interval of 45 s (30 s spent on the platform and 15 s drying time). The platform was located in either the NW or SE quadrant, 50 cm from the side-wall (Fig. 3.1A), with the platform location counterbalanced across genotype groups. All mice completed acquisition sessions on days 1-4, 6-7 and 9-10 (i.e. 8 acquisition sessions in total). Reversal learning sessions, in which the platform location was switched to the diametrically opposite quadrant, were given on days 11-13 (i.e. 3 reversal learning sessions in total). Probe trials were conducted on days 5, 8 and 14, during which mice were able to swim freely for 60 s with the platform removed. In all trials, mice were released at the edge of the maze, facing towards the wall. Release point was varied pseudo-randomly across trials and test sessions, but the same sequence was used for all animals.

Trials were recorded with a CCTV camera (WV-BP334, Panasonic, Osaka, Japan) suspended above the pool, and automated tracking was conducted using the software package Watermaze 3.31 (Actimetrics, Illinois, USA). For acquisition and reversal learning trials, the key variables extracted were latency to the platform (s), pathlength to the platform (m), and average swim speed (m/s). For probe trials, the key variables extracted were platform crosses and percent time spent in the platform quadrant.

3.2.3. Experiment 2: The effect of radial platform distance on performance in the Morris watermaze

A separate cohort of experimentally-naïve control ($Dao^{+/+}$) and knockout ($Dao^{-/-}$) mice (n=11 males; n=12 females per genotype) were trained on the same standard, fixed location, hidden escape platform version of the Morris watermaze escape task as used in *Experiment 1*. In this experiment, however, half of the animals were trained to a find a hidden platform located in the periphery of the maze (25 cm from the side-wall; Fig. 3.1B), while the other half were trained to find a platform located towards the centre (75 cm from the side-wall; Fig. 3.1B). This variable is henceforth referred to as radial platform distance. Within each group, the platform was again located in either the NW or SE quadrant of the maze. All mice were given four training sessions over four consecutive days, followed by a single probe trial on day 5. All other aspects of the task's design were identical to *Experiment 1*.

A number of additional analyses were conducted on the data obtained from *Experiment 2*, using ANY-maze 4.5 (Stoelting, Wood Dale, Illinois). Firstly, the maze was subdivided into nominal central and peripheral zones, which took the form of concentric rings encompassing the central and peripheral platform locations employed in *Experiment 2* (Fig. 3.1C). The peripheral zone began 15 cm from the side-wall and ended 35 cm from the wall of the maze. The central zone began 65 cm from the side-wall and ended 85 cm from the wall of the maze. These choices were arbitrary, given that similar analyses have never been reported in previous experiments. Percent time spent swimming in each zone was computed for each mouse for each trial. Thigmotaxis, a standard measure of anxiety, was also calculated for all trials. This was defined as percent time spent swimming within 15 cm of the side-wall, consistent with the majority of publications in the Morris watermaze literature.

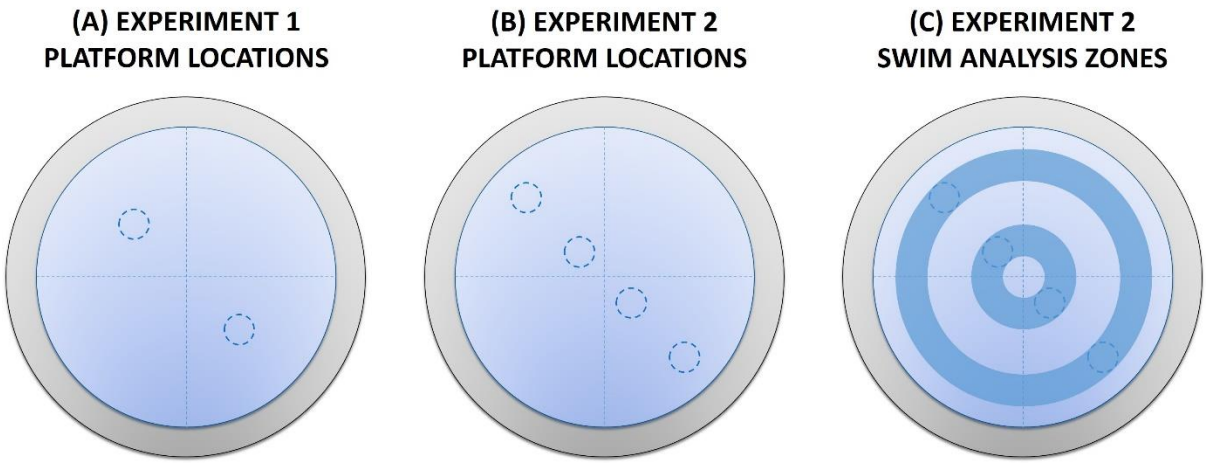

Figure 3.1. Morris watermaze platform locations and swim analysis zones. (A) In *Experiment 1*, the hidden platform was located 50 cm from the side-wall of the pool, in either the NW or SE quadrant. (B) In *Experiment 2*, the hidden platform was located either 25 cm or 75 cm from the side-wall, in either the NW or SE quadrant. (C) Using the software package ANY-maze, the pool was subdivided into nominal central and peripheral zones, encompassing the central and peripheral platform locations. Percent time spent in each of these zones was computed for each mouse for each trial of *Experiment 2*.

3.2.4. Experiment 3: Unconditioned anxiety in the anxiogenic open field test

A further cohort of experimentally-naïve control (*Dao*$^{+/+}$) and knockout (*Dao*$^{-/-}$) mice (*n*=14 males per genotype) were assessed in an anxiogenic, brightly lit open field test based on an established protocol [574, 601]. The apparatus was a white metal cylinder, with a diameter of 60 cm and a height of 60 cm. Illumination of the apparatus was homogenous, measuring 2000 lux at the base of the arena. Mice were released at the edge of the arena, facing towards the wall, and allowed to explore the apparatus for 1 min. Trials were recorded with a near-infrared CCTV camera (Maplin Electronics, Rotherham, UK) positioned above the apparatus, and automated tracking was performed using ANY-maze 4.5 (Stoelting, Wood Dale, Illinois). Using this software, the apparatus was divided into nominal peripheral and central zones (central zone diameter: 48 cm). The animal's *entire* body was tracked, and its position within the apparatus was determined on a frame-by-frame basis. A zone entry was deemed to have occurred when at least 90% of the animal's body had entered the zone in question. The key variables extracted were centre entries, latency to the first centre entry, percent distance travelled in the centre, and total distance travelled.

3.2.5. Experiment 4: Spatial memory acquisition in an aversively-motivated Y-maze (swim-escape) task

The same mice used in *Experiment 3* (*n*=14 males per genotype) were subsequently trained on an aversively-motivated spatial reference memory test in the form of a Y-maze swim-escape task. Testing was based on an established protocol [561]. The apparatus was a transparent acrylic Y-maze, with each arm measuring 30 cm in length, 9 cm in width, and 21 cm in height. The maze was filled with water, rendered opaque with white paint, to a depth of 12 cm. Water temperature was 20°C ± 2°C. Illumination of the apparatus was homogenous, measuring 250 lux at water level. A variety of distal extra-maze cues were positioned around the laboratory. As in the Morris watermaze, mice could escape from the water by climbing onto a hidden platform positioned 1.5 cm beneath the water surface. The platform was positioned at the end of one of the three arms, with the choice of target arm counterbalanced across genotype groups. In all trials, mice were released at the end of one of the two non-target arms, facing towards the wall. Release arm was varied pseudo-randomly across trials and test sessions, but the same sequence was used for all animals.

Acquisition trials were 90 s in duration, and mice which did not locate the platform within this time were guided towards the platform by the experimenter's arm. All mice completed a single session of training each day for 6 consecutive days. Each session consisted of 5 consecutive trials, with an inter-trial interval of 45 s (30 s spent on the platform and 15 s drying time). A probe trial was performed on day 7, during which mice were able to swim freely for 60 s with the platform removed. In acquisition trials, escape latency was measured manually with a stopwatch. Choice accuracy (i.e. whether the first arm entered was the target arm) was also recorded, as was the frequency of clinging behaviour (episodes where mice stopped swimming and clung to the walls of the maze). Probe trials were recorded with a near-infrared CCTV

camera (Maplin Electronics, Rotherham, UK) suspended above the apparatus, and automated tracking was conducted using ANY-maze 4.5 (Stoelting, Wood Dale, Illinois). The key variable extracted was percent time spent in the target arm. One *Dao*$^{-/-}$ mouse was excluded from probe trial analysis as it clung to the wall for the entirety of the trial. Note that *Experiments 3* and *4* were conducted in different test rooms. *Experiment 4* was performed by Amy Taylor.

3.2.6. Experiment 5: Spatial memory acquisition in an appetitively-motivated Y-maze task

A final cohort of experimentally-naïve control (*Dao*$^{+/+}$) and knockout (*Dao*$^{-/-}$) mice (*n*=12 males per genotype) were trained on a dry land, appetitively-motivated spatial reference memory Y-maze task. Testing was based on an established protocol [561, 621, 622]. The apparatus was a black wooden Y-maze, with each arm measuring 50 cm in length, 9 cm in width and 1 cm in height. The maze was elevated 80 cm above the ground. Illumination of the apparatus was homogenous, measuring 250 lux at the base of the arena. The design of *Experiment 5* was broadly analogous to that of *Experiment 4*, except mice were now running to receive to a food reward (sweetened condensed milk), rather than swimming to escape from water. Mice were maintained at 85-90% of their free-feeding weight throughout testing. In each trial, a mouse was released from one of the two non-baited arms and allowed to enter one of the other two arms. Mice which selected the baited arm were allowed to consume the milk reward before being returned to the home-cage, whereas mice which entered the incorrect arm were immediately returned to the home-cage. All mice completed a single session of training each day for 10 consecutive days. Each session consisted of 5 consecutive trials, with an inter-trial interval of approximately 5 min. On days 11 and 12, mice completed a session of 5 post-choice bait trials (i.e. 10 post-choice bait trials in total). In these trials, the milk reward was not administered to the target arm until after the mouse had entered this arm; this ensures that mice cannot solve the task based on the sight or smell of the milk reward. All other aspects of the task's design were identical to *Experiment 4*. In all trials, reward latency was measured manually with a stopwatch. Choice accuracy (i.e. whether the first arm entered was the target arm) was also recorded. Note that *Experiment 5* was performed by Amy Taylor.

3.2.7. Statistical analysis

All statistical analyses were performed with SPSS 22.0 (IBM, Armonk, New York). Unless otherwise stated, all reported statistics are the result of analyses of variance (ANOVAs), with genotype as the principal independent variable, in addition to sex, day, trial number (i.e. trials 1-4 or 5 within a given day of testing), radial platform distance and swim zone where applicable. Differences were considered to be statistically significant at p-values < 0.05. Greenhouse-Geisser corrections were applied where appropriate, but uncorrected degrees of freedom are reported in order to preserve the transparency of the statistical design. For all Morris watermaze experiments, further ANOVAs were conducted with the quadrant location of the hidden platform (i.e. NW or SE) included as an extra independent variable. No additional effects or interactions were observed, so these data are not shown. Defecation and urination were measured in *Experiment 3*, but no effects were observed (data not shown). In all figures, * indicates a p-value ≤ 0.05, ** indicates a p-value ≤ 0.01, and *** indicates a p-value ≤ 0.001. Error bars depict the standard error of the mean. $\underline{M}$ = mean.

3.3. Results

3.3.1. Experiment 1: Enhanced Morris watermaze performance in Dao$^{-/-}$ mice

Across the first four days of acquisition training, *Dao*$^{-/-}$ mice significantly outperformed *Dao*$^{+/+}$ mice on the first trial of each day. Relative to *Dao*$^{+/+}$ mice, their escape latencies on trial 1 were shorter ($F_{1,20}$ = 8.517, P = 0.008; Fig. 3.2A), and they travelled less distance before reaching the hidden platform ($F_{1,20}$ = 7.305, P = 0.014; Fig. 3.2B). By contrast, *Dao*$^{-/-}$ mice did not outperform *Dao*$^{+/+}$ mice on trials 2, 3 or 4, in terms of either escape latency or pathlength (Ps = $\geq$ 0.133). Consequently, there were trial number-by-genotype interactions for both escape latency ($F_{3,60}$ = 5.566, P = 0.002) and pathlength ($F_{3,60}$ = 5.594, P = 0.002) across the first four days of acquisition. These interactions were also evident when all eight days of acquisition were considered (escape latency: $F_{3,60}$ = 3.714, P = 0.016; pathlength: $F_{3,60}$ = 3.950, P = 0.012), and, more remarkably, remained significant when day 1 was analysed alone (escape latency: $F_{3,60}$ = 3.098, P = 0.033; pathlength: $F_{3,60}$ = 3.537, P = 0.020; Fig. 3.2C & 3.2D). Indeed, post-hoc analyses revealed that *Dao*$^{-/-}$ mice had outperformed *Dao*$^{+/+}$ mice on the first trial of the first day of acquisition training, presumably before any associative spatial learning could have taken place (escape latency: $F_{1,20}$ = 5.733, P = 0.027; pathlength: $F_{1,20}$ = 5.393, P = 0.031).

The results of *experiment 1* underline the importance of analysing Morris watermaze data on a trial-by-trial basis as well as a day-by-day basis. With data collapsed across the four trials of each training session, genotype had no effect on either escape latency ($F_{1,20}$ = 0.114, P = 0.739; Fig. 3.2E) or pathlength ($F_{1,20}$ = 0.539, P = 0.471; Fig. 3.2F) during the eight-day acquisition phase, and there were no interactions between day and genotype (escape latency: $F_{7,140}$ = 0.423, P = 0.777; pathlength: $F_{7,140}$ = 0.483, P = 0.724). By contrast, there was an overall main effect of genotype on swim speed; *Dao*$^{-/-}$ mice swam consistently faster than *Dao*$^{+/+}$ mice throughout

acquisition training ($F_{1,20}$ = 5.345, P = 0.032). However, this cannot explain the enhanced first trial performance of the *Dao*$^{-/-}$ mice, as their superiority was also evident in the pathlength data.

The spatial memory performance of the two genotype groups was well matched in the two probe trials that were conducted after 16 and 24 acquisition trials, respectively. During these trials, genotype had no effect on platform crosses ($F_{1,20}$ = 1.918, P = 0.181) or percent time spent in the platform quadrant ($F_{1,20}$ = 0.342, P = 0.565; Fig. 3.3A).

The performance of the two genotype groups was also indistinguishable when the platform was moved to a novel spatial location in the diametrically opposite quadrant. During this three-day reversal learning phase, genotype had no effect on either escape latency ($F_{1,20}$ = 2.519, P = 0.128; Fig. 3.2E) or pathlength ($F_{1,20}$ = 2.239, P = 0.150; Fig. 3.2F), and there were no interactions between day and genotype (escape latency: $F_{2,40}$ = 0.292, P = 0.748; pathlength: $F_{2,40}$ = 0.100, P = 0.905) or trial number and genotype (escape latency: $F_{3,60}$ = 1.344, P = 0.269; pathlength: $F_{3,60}$ = 1.339, P = 0.270). Genotype no longer had an effect on swim speed during the reversal learning phase ($F_{1,20}$ = 0.009, P = 0.926). The spatial memory performance of the two genotype groups was also well matched in the probe trial that followed the reversal learning phase; genotype had no effect on platform crosses ($F_{1,20}$ = 0.062, P = 0.806) or percent time spent in the platform quadrant ($F_{1,20}$ = 0.982, P = 0.334; Fig. 3.3B).

In *Experiment 1*, sex did not influence escape latency, pathlength or swim speed during the acquisition phase or reversal learning phase, and there were no interactions involving sex in any of the aforementioned analyses.

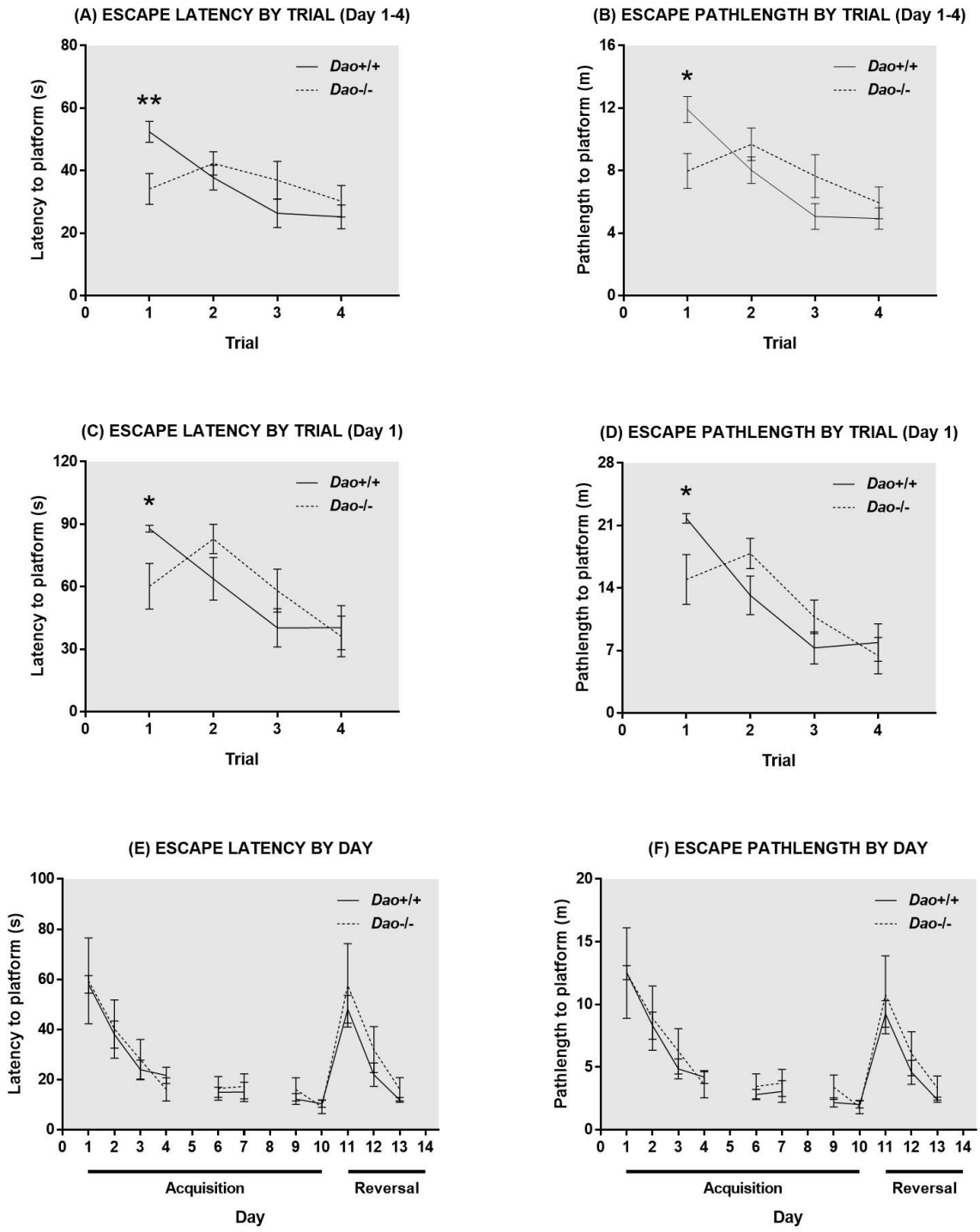

Figure 3.2. Morris watermaze performance in control (*Dao*$^{+/+}$) and knockout (*Dao*$^{-/-}$) mice (*n*=6 males; *n*=6 females per genotype; *Experiment 1*). Acquisition training took place on days 1-4, 6-7 and 9-10. Reversal learning began on day 11. Probe trials were performed on days 5 and 8, and a reversal probe trial was conducted on day 14. (A-B) Across the first four days of acquisition training, *Dao*$^{-/-}$ mice significantly outperformed *Dao*$^{+/+}$ mice on the first trial of each day, but not on the subsequent three trials. (C-D) On the first day of acquisition training, the same pattern of performance was evident. (E-F) With data collapsed across the four trials of each training session, genotype had no apparent impact on watermaze performance during the acquisition phase or the reversal learning phase.

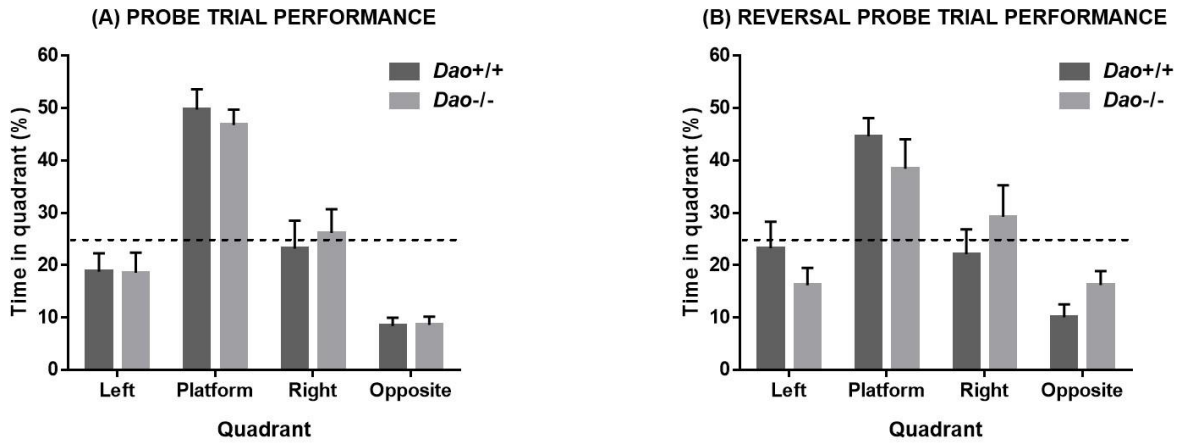

Figure 3.3. Probe trial and reversal probe trial performance in *Experiment 1*. (A) Genotype had no effect on probe trial performance. Mice of both genotypes displayed a strong preference for the platform quadrant; time spent in this quadrant exceeded chance level (25%) in both *Dao*$^{+/+}$ mice (Student's *t*-test, t_{11} = 6.362, *P* = <0.001, *M* = 49.7%) and *Dao*$^{-/-}$ mice (Student's *t*-test, t_{11} = 7.307, *P* = <0.001, *M* = 46.8%). (B) Genotype had no effect on reversal probe trial performance. Mice of both genotypes demonstrated a clear preference for the platform quadrant; time spent in this quadrant exceeded chance level (25%) in both *Dao*$^{+/+}$ mice (Student's *t*-test, t_{11} = 5.623, *P* = <0.001, *M* = 44.6%) and *Dao*$^{-/-}$ mice (Student's *t*-test, t_{11} = 2.279, *P* = 0.044, *M* = 37.9%).

3.3.2. Experiment 2: Morris watermaze performance in Dao$^{-/-}$ mice is critically dependent on radial platform distance

The observation that *Dao*$^{-/-}$ mice outperformed *Dao*$^{+/+}$ mice on the first trial of the first day of acquisition training, before any associative spatial learning is likely to have taken place, suggests that performance levels may be shaped by animals' innate preferences for particular zones of the pool (as defined by their distance from the side-wall). To investigate this possibility, we trained separate groups of experimentally-naïve mice to distinct platform locations at different radial distances from the side-wall.

In this modified watermaze experiment, *Dao*$^{-/-}$ mice outperformed *Dao*$^{+/+}$ mice in the peripheral platform condition, but were outperformed by *Dao*$^{+/+}$ mice in the central platform condition. Consequently, analysis of all 16 acquisition trials (i.e. 4 trials per day for 4 days) revealed interactions between radial platform distance and genotype (escape latency: $F_{1,38}$ = 4.263, P = 0.046; pathlength: $F_{1,38}$ = 4.020, P = 0.052; Fig. 3.4A-D). These interactions were clearly evident in males (escape latency: $F_{1,18}$ = 5.025, P = 0.038; pathlength: $F_{1,18}$ = 5.728, P = 0.028; Appendix Fig. 8.1A-D), but completely absent in females (escape latency: $F_{1,20}$ = 0.048, P = 0.828; pathlength: $F_{1,20}$ = 0.007, P = 0.932; Appendix Fig. 8.2A-D). Thus, there were also *three*-way interactions between radial platform distance, genotype and sex (pathlength: $F_{1,38}$ = 4.409, P = 0.042; escape latency: $F_{1,38}$ = 3.345, P = 0.075).

As in *Experiment 1*, the altered performance of *Dao*$^{-/-}$ mice was evident on the first trial of the first acquisition session, seemingly before any associative spatial learning could have taken place. Hence, there were also interactions between radial platform distance and genotype when the opening trial was analysed in isolation (escape latency: $F_{1,38}$ = 5.419, P = 0.025; pathlength: $F_{1,38}$ = 4.997, P = 0.031; Appendix Fig. 8.3).

In *Experiment 1*, *Dao*$^{-/-}$ mice outperformed *Dao*$^{+/+}$ mice on the first trial of each day, but not on trials 2, 3, or 4. A complementary pattern of performance was evident in the central platform condition in *experiment 2*; this time, *Dao*$^{+/+}$ mice significantly outperformed *Dao*$^{-/-}$ mice on the first trial of each day (escape latency: $F_{1,18} = 6.061$, $P = 0.024$; pathlength: $F_{1,18} = 8.184$, $P = 0.010$), but not on trials 2, 3, or 4 (Ps = ≥ 0.208). Accordingly, there were trial number-by-genotype interactions in the central platform condition (escape latency: $F_{3,54} = 3.074$, $P = 0.035$; pathlength: $F_{3,54} = 3.495$, $P = 0.022$; Fig. 3.4A & 3.4B). By contrast, there were no trial number-by-genotype interactions in the peripheral platform condition (escape latency: $F_{3,60} = 0.484$, $P = 0.694$; pathlength: $F_{3,60} = 0.441$, $P = 0.724$; Fig. 3.4C & 3.4D); here, the performance of *Dao*$^{-/-}$ mice was numerically superior to that of *Dao*$^{+/+}$ mice on all four trials. Hence, there were also *three*-way interactions between trial number, genotype and radial platform distance (escape latency: $F_{3,114} = 3.128$, $P = 0.029$; pathlength: $F_{3,114} = 3.368$, $P = 0.021$).

The results of *experiment 2* further emphasise the importance of analysing Morris watermaze data on a trial-by-trial basis as well as a day-by-day basis. With data collapsed across the four trials of each training session, genotype had no effect on either escape latency ($F_{1,38} = 0.508$, $P = 0.480$; Fig. 3.4E) or pathlength ($F_{1,38} = 0.161$, $P = 0.690$; Fig. 3.4F) during the four-day acquisition phase, and there were no interactions between day and genotype (escape latency: $F_{3,114} = 0.152$, $P = 0.928$; pathlength: $F_{3,114} = 0.280$, $P = 0.840$). This remained the case when males and female mice were analysed separately (Appendix Fig. 8.4).

The spatial memory performance of the two genotype groups was well matched in the probe trial that was conducted at the end of acquisition training; genotype had no effect on platform crosses ($F_{1,38} = 0.915$, $P = 0.345$) or percent time spent in the platform quadrant ($F_{1,38} = 0.483$, $P = 0.492$; Fig. 3.5). Likewise, there were no interactions involving genotype, and no main

effects or interactions involving sex for either variable (*P*s = ≥ 0.506). By contrast, the probe trial performance of mice in the peripheral platform condition was superior to that of mice in the central platform condition (Appendix Fig. 8.5).

To directly test whether the differential performance of *Dao*$^{+/+}$ and *Dao*$^{-/-}$ mice in the two radial platform distance conditions was a reflection of differing spatial swimming preferences, we next analysed the percentage of time spent in the peripheral and central zones of the pool during the 16-trial acquisition phase. As expected, *Dao*$^{-/-}$ mice spent more time than *Dao*$^{+/+}$ mice in the peripheral zone ($F_{1,38}$ = 8.097, P = 0.007; Fig. 3.6A), but less time than *Dao*$^{+/+}$ mice in the central zone ($F_{1,38}$ = 2.735, P = 0.106). Interestingly, peripheral swimming increased between trials 1 and 2, regardless of genotype, sex or radial platform distance (Appendix Fig. 8.6). Given the increased preference of the *Dao*$^{-/-}$ mice for the peripheral zone of the pool, it was somewhat surprising to find that genotype had no effect on thigmotaxis ($F_{1,38}$ = 0.018, P = 0.893; Fig. 3.6B); *Dao*$^{-/-}$ and *Dao*$^{+/+}$ mice spent a similar amount of time in the immediate vicinity of the wall (i.e. within 15 cm).

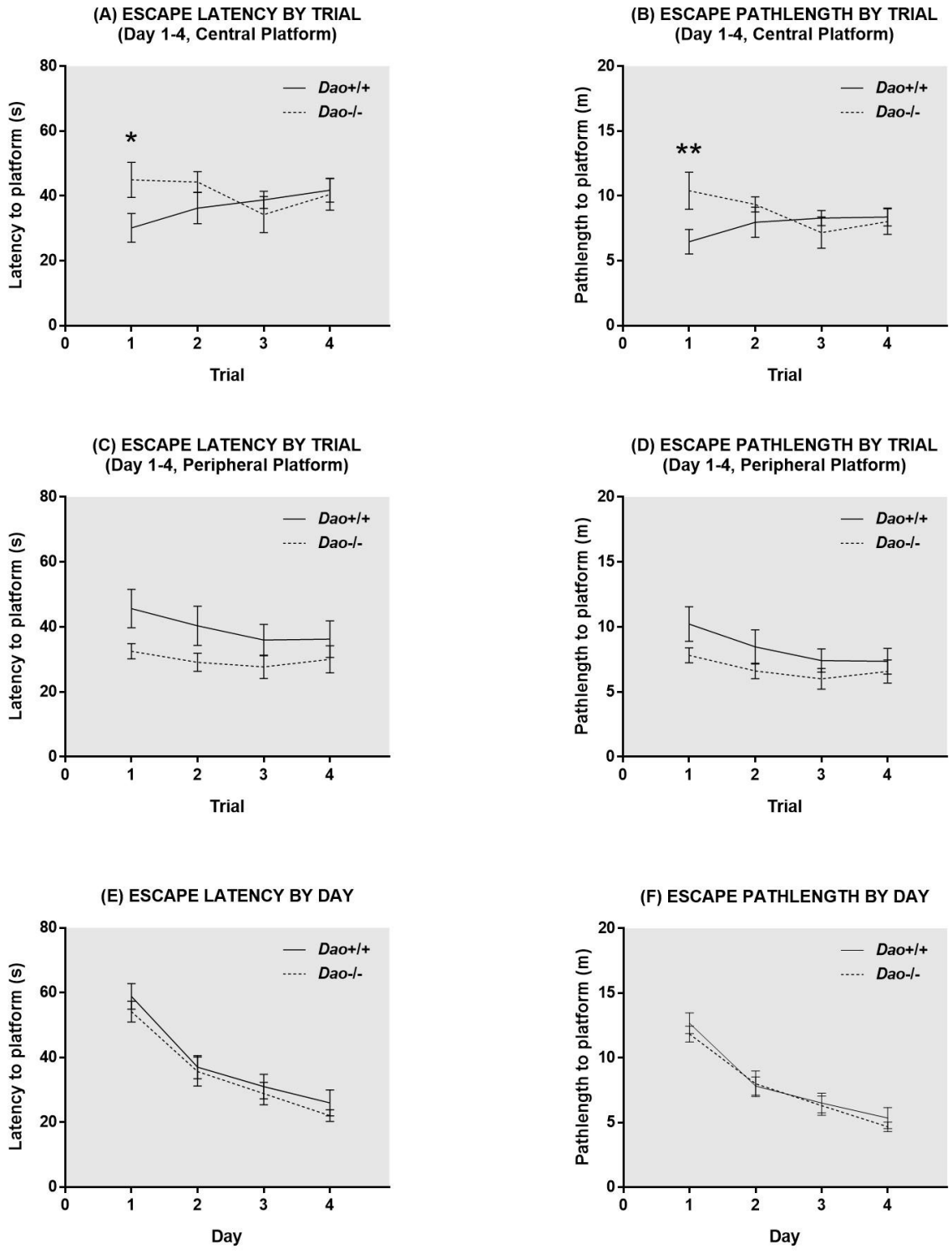

Figure 3.4. Morris watermaze performance in control (*Dao*$^{+/+}$) and knockout (*Dao*$^{-/-}$) mice (*n*=11 males; *n*=12 females per genotype; *Experiment 2*). Acquisition training took place on days 1-4 and a probe trial was performed on day 5. (A-B) Across the four days of acquisition training, *Dao*$^{+/+}$ mice in the central platform condition significantly outperformed *Dao*$^{-/-}$ mice on trial 1, but not on the subsequent three trials. (C-D) In the peripheral platform condition, *Dao*$^{-/-}$ mice outperformed *Dao*$^{+/+}$ mice on all 4 trials, although this advantage was not statistically significant for any trial. (E-F) With data collapsed across the four trials of each training session, genotype had no apparent impact on watermaze performance during the acquisition phase.

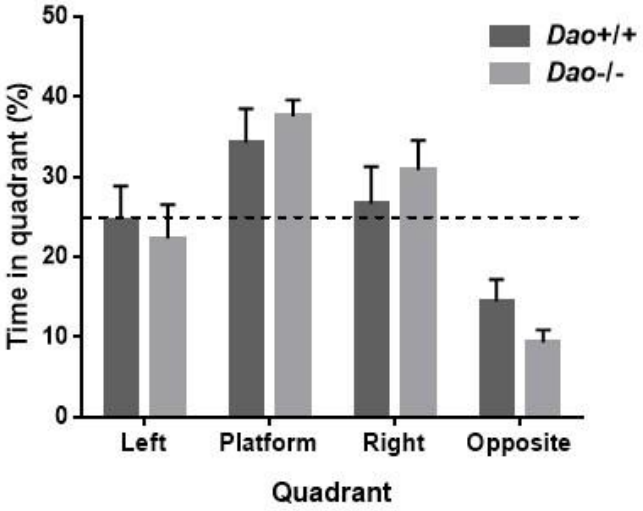

Figure 3.5. Genotype had no effect on probe trial performance in *Experiment 2*. Mice of both genotypes displayed a strong preference for the platform quadrant; time spent in this quadrant exceeded chance level (25%) in both *Dao*$^{+/+}$ mice (Student's *t*-test, t_{22} = 2.199, *P* = 0.039, *M* = 34.3%) and *Dao*$^{-/-}$ mice (Student's *t*-test, t_{22} = 6.124, *P* = <0.001, *M* = 37.6%).

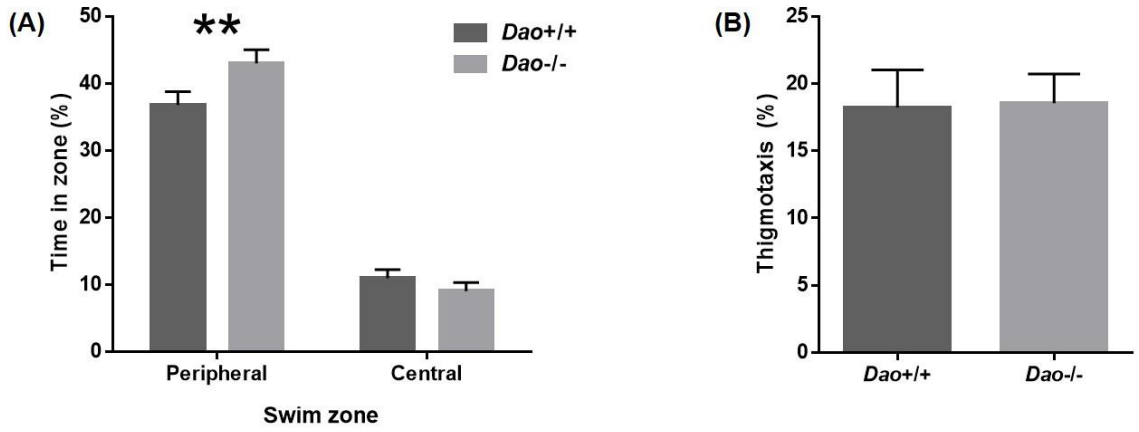

Figure 3.6. Spatial analyses of swimming behaviour during the acquisition phase of *Experiment 2*. (A) *Dao*$^{-/-}$ mice spent more time than *Dao*$^{+/+}$ mice in the peripheral zone of the watermaze pool, but less time than *Dao*$^{+/+}$ mice in the central zone. (B) Genotype had no effect on thigmotaxis.

3.3.3. Experiment 3: Elevated unconditioned anxiety in Dao$^{-/-}$ mice in the anxiogenic open field test

To evaluate whether the differing spatial swimming preferences of *Dao*$^{+/+}$ and *Dao*$^{-/-}$ mice could reflect differences in emotionality, we assessed anxiety in a brightly lit open field test. Although we had previously observed increased anxiety-like behaviour in *Dao*$^{-/-}$ mice in an open field test (see Chapter 2), the present protocol was more comparable to the Morris watermaze protocol for a number of reasons. Firstly, the arena was circular rather than rectangular. Secondly, this test was performed in the same animal facility as the Morris watermaze, whereas the previous open field test had been performed in another animal facility. Thirdly, this test was performed during the same period of the light phase as the Morris watermaze (ZT3 – ZT8), whereas the previous open field test had been performed during the dark phase (ZT13 – ZT18). Finally, singly-housed animals participated in this test, whereas group-housed animals had been tested previously.

Again, *Dao*$^{-/-}$ mice were significantly more anxious than their *Dao*$^{+/+}$ littermates; they spent less time than *Dao*$^{+/+}$ mice in the centre zone of the arena ($F_{1,26} = 5.945$, $P = 0.022$; Fig. 3.7A), and took longer to make their first centre zone entry ($F_{1,26} = 6.132$, $P = 0.020$; Fig. 3.7B). In addition, genotype had a borderline-significant effect on percent distance travelled in the centre zone ($F_{1,26} = 4.067$, $P = 0.054$); this was lower in *Dao*$^{-/-}$ than *Dao*$^{+/+}$ mice. The increased anxiety-like behaviour of *Dao*$^{-/-}$ mice was not an artefact of reduced locomotor activity, as genotype had no effect on total distance travelled ($F_{1,26} = 0.099$, $P = 0.756$; Fig. 3.7C).

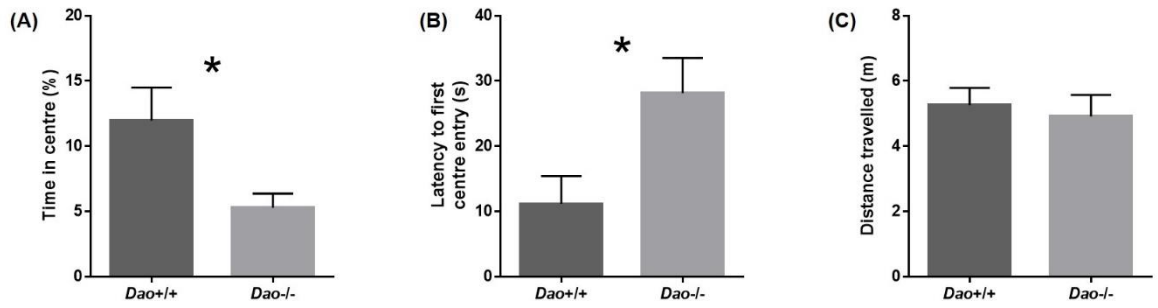

Figure 3.7. Unconditioned anxiety in the anxiogenic open field test in control (*Dao*$^{+/+}$) and knockout (*Dao*$^{-/-}$) mice (*n*=14 males per genotype; *Experiment 3*). Relative to *Dao*$^{+/+}$ mice, *Dao*$^{-/-}$ mice demonstrated increased anxiety-like behaviour. (A) *Dao*$^{-/-}$ mice spent less time than *Dao*$^{+/+}$ mice in the centre zone of the arena, and (B) took longer to make their first centre zone entry. (C) Genotype had no effect on total distance travelled.

3.3.4. Experiment 4: Unaltered choice accuracy in Dao$^{-/-}$ mice in an aversively-motivated Y-maze (swim-escape) task

We next assessed associative spatial memory performance in a Y-maze swim-escape task. Unlike the Morris watermaze, in which the centre of the arena is more exposed than the periphery, all three arms of the Y-maze are narrow and enclosed by high walls. Within the Y-maze therefore, all potential target locations (i.e. the end of each arm) should be equally anxiogenic, so performance in this task this should not be confounded by innate differences in spatial swimming preferences. On this basis, we did not expect *Dao*$^{-/-}$ mice to outperform *Dao*$^{+/+}$ mice in the Y-maze, assuming they have no enhancement in long-term spatial memory.

As predicted, genotype had no effect on choice accuracy during the six-day acquisition phase ($F_{1,26}$ = 0.721, P = 0.404; Fig. 3.8A). Likewise, there were no interactions between day and genotype ($F_{5,130}$ = 0.498, P = 0.697) or trial number and genotype ($F_{4,104}$ = 0.760, P = 0.553). Importantly, although the performance of both *Dao*$^{+/+}$ mice (Student's *t*-test, t_{13} = 5.740, P = <0.001, $\underline{M}$ = 72.9%) and *Dao*$^{-/-}$ mice (Student's *t*-test, t_{13} = 4.305, P = 0.001, $\underline{M}$ = 67.1%) exceeded chance level (50%) on day 1, the proportion of mice that selected the target arm on the opening trial did not deviate from chance (50%) in either the *Dao*$^{+/+}$ group (Student's *t*-test, t_{13} = 0.000, P = 1.000, $\underline{M}$ = 50.0%) or the *Dao*$^{-/-}$ group (Student's *t*-test, t_{13} = 1.075, P = 0.302, $\underline{M}$ = 64.3%). Consistent with this, opening trial performance did not vary significantly between the two genotype groups ($F_{1,26}$ = 0.553, P = 0.464).

Although choice accuracy was unaffected in *Dao*$^{-/-}$ mice, they took consistently longer to reach the escape platform than *Dao*$^{+/+}$ mice ($F_{1,26}$ = 5.488, P = 0.027; Fig. 3.8B). This difference was present on the first trial of the first acquisition session, presumably before any associative spatial learning could have taken place ($F_{1,26}$ = 5.131, P = 0.032). The escape latencies of *Dao*$^{-}$

$^{/-}$ mice were significantly greater than those of *Dao*$^{+/+}$ mice on day 1 of acquisition training ($F_{1,26}$ = 5.137, P = 0.032), but not on any subsequent day (Ps = ≥ 0.083). Hence, there was an interaction between day and genotype for escape latency ($F_{5,130}$ = 2.845, P = 0.049). By contrast, there was no interaction between trial number and genotype ($F_{4,104}$ = 1.503, P = 0.223).

The greater escape latencies of the *Dao*$^{-/-}$ mice were likely a reflection of heightened anxiety, since average escape latency was positively associated with the frequency of clinging episodes in both *Dao*$^{+/+}$ mice (Pearson's correlation, R_{12} = 0.737, P = 0.003; Fig. 3.8C) and *Dao*$^{-/-}$ mice (Pearson's correlation, R_{12} = 0.884, P = <0.001; Fig. 3.8D). *Dao*$^{-/-}$ mice demonstrated significantly more clinging episodes than *Dao*$^{+/+}$ mice on day 2 ($F_{1,26}$ = 4.357, P = 0.047) and day 3 ($F_{1,26}$ = 6.158, P = 0.020), although the overall main effect of genotype on the frequency of clinging episodes was not significant ($F_{1,26}$ = 2.184, P = 0.152).

The spatial memory performance of the two genotype groups was well matched in the probe trial that was conducted at the end of acquisition training; genotype had no effect on time spent in the target arm ($F_{1,25}$ = 0.398, P = 0.534; Fig. 3.9).

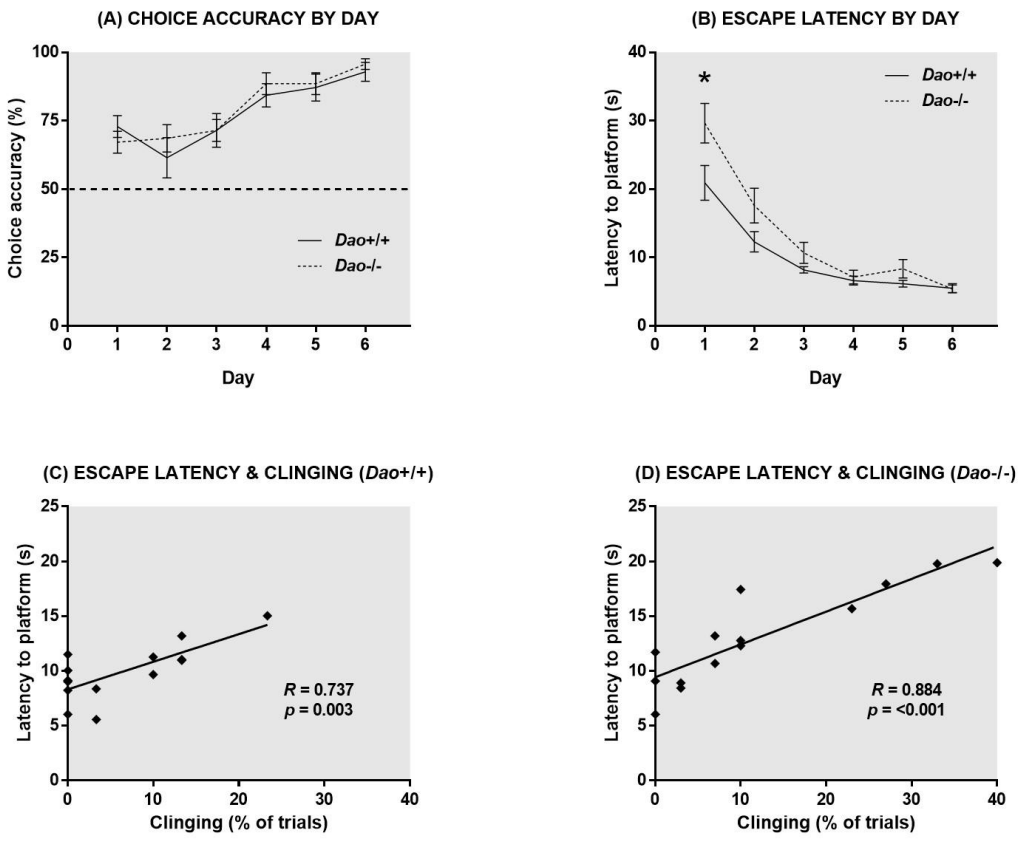

Figure 3.8. Spatial memory acquisition in a Y-maze swim-escape task in control (*Dao*$^{+/+}$) and knockout (*Dao*$^{-/-}$) mice (*n*=14 males per genotype; *Experiment 4*). Acquisition training took place on days 1-6 and a probe trial was performed on day 7. (A) Genotype had no effect on choice accuracy in this task. (B) *Dao*$^{-/-}$ mice took longer than *Dao*$^{+/+}$ mice to reach the hidden escape platform, particularly on the first day of acquisition training. (C-D). Average escape latency was positively associated with the frequency of clinging episodes in both *Dao*$^{+/+}$ and *Dao*$^{-/-}$ mice.

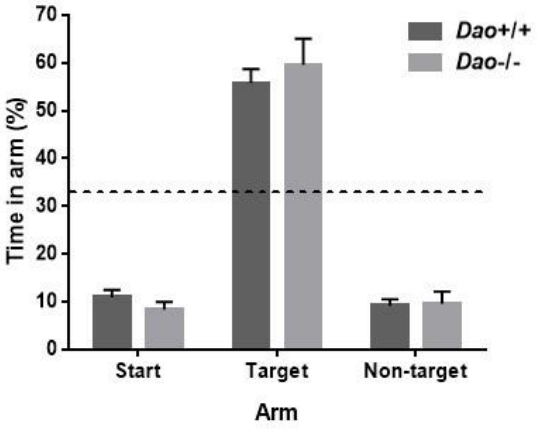

Figure 3.9. Genotype had no effect on probe trial performance in *Experiment 4*. Mice of both genotypes displayed a strong preference for the target arm; time spent in this arm exceeded chance level (33.3%) in both *Dao*$^{+/+}$ mice (Student's *t*-test, t_{13} = 7.527, *P* = <0.001, *M* = 55.8%) and *Dao*$^{-/-}$ mice (Student's *t*-test, t_{12} = 4.827, *P* = <0.001, *M* = 59.6%).

3.3.5. Experiment 5: Unaltered choice accuracy in Dao$^{-/-}$ mice in an appetitively-motivated Y-maze task

Finally, we assessed associative spatial memory performance in an appetitively-motivated Y-maze task. Due to the physical similarity of the aversive and appetitive Y-maze arenas, we again predicted that *Dao*$^{-/-}$ mice would not outperform *Dao*$^{+/+}$ mice. As expected, genotype did not affect choice accuracy in this task ($F_{1,22}$ = 0.002, P = 0.962; Fig. 3.9A). Likewise, there were no interactions between day and genotype ($F_{9,198}$ = 0.687, P = 0.646) or trial number and genotype ($F_{4,88}$ = 1.797, P = 0.137). Moreover, the proportion of mice that selected the target arm on the opening trial did not deviate from chance (50%) in either the *Dao*$^{+/+}$ group (Student's *t*-test, t_{11} = -1.173, P = 0.266, $\underline{M}$ = 33.3%) or the *Dao*$^{-/-}$ group (Student's *t*-test, t_{11} = 0.561, P = 0.586, $\underline{M}$ = 58.3%). Consistent with this, opening trial performance did not vary significantly between the two genotype groups ($F_{1,22}$ = 1.478, P = 0.237).

In general, *Dao*$^{-/-}$ mice took slightly longer than *Dao*$^{+/+}$ mice to reach the reward, although this difference was not significant ($F_{1,22}$ = 1.954, P = 0.176; Fig. 3.9B). Likewise, genotype did not influence reward latency on the first trial of the first day ($F_{1,22}$ = 0.393, P = 0.537). There were no interactions between day and genotype ($F_{9,198}$ = 0.932, P = 0.423) or trial number and genotype ($F_{4,88}$ = 1.146, P = 0.336) for reward latency.

To eliminate the possibility that mice were selecting which arm to enter based on odour cues from the milk, 10 post-choice bait trials were conducted over two further days of testing. During these trials, average choice accuracy remained high in both *Dao*$^{+/+}$ mice ($\underline{M}$ = 98.3%) and *Dao*$^{-/-}$ mice ($\underline{M}$ = 95.0%), which indicates that mice were not solving the task by smelling the milk reward.

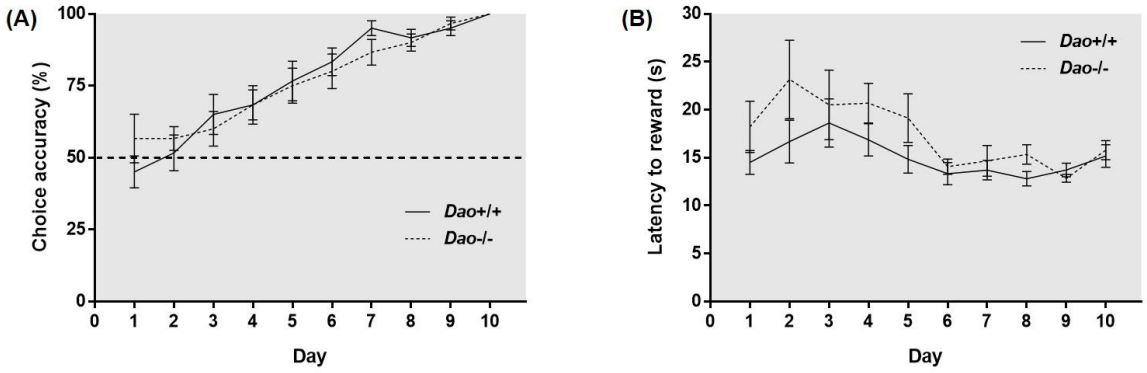

Figure 3.10. Spatial memory acquisition in in an appetitively-motivated Y-maze task in control (*Dao*$^{+/+}$) and knockout (*Dao*$^{-/-}$) mice (*n*=12 males per genotype; *Experiment 5*). Acquisition training took place over 10 days. (A) Genotype had no effect on choice accuracy in this task. (B) In general, reward latencies were greater in *Dao*$^{-/-}$ than *Dao*$^{+/+}$ mice, but this difference was not significant.

3.4. Discussion

The preceding experiments compared the Morris watermaze performance of *Dao* knockout (*Dao*$^{-/-}$) mice with their wildtype (*Dao*$^{+/+}$) littermates. We found that the performance of *Dao*$^{-/-}$ mice could either be enhanced *or* impaired, depending on the radial distance of the hidden platform from the side-wall. *Dao*$^{-/-}$ mice outperformed *Dao*$^{+/+}$ mice (in terms of both escape latencies and pathlengths) when the hidden platform was positioned in a peripheral location within the maze, but were outperformed by *Dao*$^{+/+}$ mice when the platform was positioned in a more central location. These results likely reflect the fact that *Dao*$^{-/-}$ mice spent more time in the periphery of the pool than *Dao*$^{+/+}$ mice, rendering them more likely to encounter the peripheral platform by chance, but less likely to discover the central platform. The altered spatial swimming behaviour of *Dao*$^{-/-}$ mice may be a consequence of heightened anxiety, since they also demonstrated an increased preference for the periphery of a brightly lit, open field arena; an established indicator of anxiety. Finally, choice accuracy was unaffected by genotype in both the aversive and appetitive Y-maze tasks. Like the Morris watermaze, these are tests of long-term spatial memory, which further suggests that long-term spatial memory is unaltered in *Dao*$^{-/-}$ mice.

Increased anxiety in Dao$^{-/-}$ *mice*

The increased preference of *Dao*$^{-/-}$ mice for the periphery of the Morris watermaze was mirrored by an increased preference for the periphery of the anxiogenic open field. The open field test is an established test of anxiety, in which performance is predictably altered by anxiolytic compounds such as benzodiazepines [623]. Hence, the increased peripheral swimming of *Dao*$^{-/-}$ mice in the Morris watermaze could be a manifestation of increased anxiety. This conclusion is consistent with our observation of heightened anxiety-like behaviour in *Dao*$^{-/-}$ mice across five standard tests of unconditioned anxiety that generate

approach/avoidance conflict: the open field, successive alleys, light/dark box, elevated plus maze and novelty-suppressed feeding tasks (see Chapter 2). Likewise, anxiety is elevated in ddY/*Dao*$^{-}$ mice and *Dao1*^{G181R} mice, and in wildtype mice following D-serine administration [514]. Heightened anxiety could also account for the increased swim speed of *Dao*$^{-/-}$ mice in *Experiment 1*, and their increased clinging behaviour in *Experiment 4*.

Surprisingly, despite spending more time than *Dao*$^{+/+}$ mice in the peripheral zone of the maze (15–35 cm from the wall), *Dao*$^{-/-}$ mice did not display greater thigmotaxis (i.e. swimming within 15 cm of the wall). Hence, their behaviour in the watermaze was not entirely consistent with their behaviour in the open field test. This suggests *either* that heightened anxiety is not responsible for the altered watermaze performance of *Dao*$^{-/-}$ mice, *or* that anxiety can affect swimming behaviour in a manner that is more complex than simply compelling anxious mice to swim directly against the side-wall of the maze. If the latter explanation is correct, this would be particularly significant, as thigmotaxis is typically the only measure of spatial swimming preferences reported in Morris watermaze experiments, and is often used to rule out innate differences in swimming behaviour.

Explaining the inconsistency in the Dao mutant literature

Spatial memory acquisition in the Morris watermaze has previously been assessed in two *Dao* mutant models. As described in Section 3.1., acquisition was enhanced in ddY/*Dao*$^{-}$ mice [520], but unaltered in *Dao1*^{G181R} mice [466]. The dissimilar performance of these two mutant models could have been due to any one of several methodological differences between these earlier studies [466, 521] (see Table 3.1). Our data suggest that experimental factors such as pool diameter and radial platform distance could easily affect the likelihood of mice encountering the hidden platform by chance, and thereby influence learning about its spatial

location. Therefore, our results cast doubt over whether the inactivation of DAO yields *genuine* improvements in long-term associative spatial memory. Instead, the apparently enhanced watermaze acquisition of ddY/*Dao*$^{-}$ mice [520] may have been an artefact of anxiety-mediated alterations in swimming behaviour, as we observed in own experiments.

Moreover, escape latencies and pathlengths were not presented on a trial-by-trial basis in either previous study [464,519]. It is therefore possible that in *both* studies, *Dao* mutants outperformed wildtype mice on the first trial of each acquisition session, just as we observed in our dataset. By collapsing data across trials, such an effect may have been masked in the study involving the *Dao1*^{G181R} mouse [466], but not in the study involving the ddY/*Dao*$^{-}$ mouse [521]. This seems plausible given that the former study included more trials per session (see Table 3.1).

Unfortunately, neither ddY/*Dao*$^{-}$ nor *Dao1*^{G181R} mice have, to our knowledge, been subjected to any tests of long-term spatial memory besides the Morris watermaze, with the exception of ddY/*Dao*$^{-}$ mice, which have also been assessed in the Barnes maze [520]. Interestingly, the authors concede that the apparently enhanced spatial memory performance of ddY/*Dao*$^{-}$ mice in this task may not have been related to memory at all; instead, it might have been explained by their *'increased preference for the periphery of the maze'* [520]. This assessment strikes a clear parallel with our own observations in the Morris watermaze. Then again, the Barnes maze apparatus can be conceptualised as an unprotected open field. It is unclear why ddY/*Dao*$^{-}$ mice would demonstrate a preference for the edge of such an arena, given their established anxiety phenotype [514].

If the enhanced Morris watermaze acquisition of ddY/*Dao*$^{-}$ mice was reflective of altered anxiety rather than a genuine memory enhancement, how can one explain their facilitated hippocampal LTP? In a recent review, it was argued that although facilitated hippocampal LTP is often correlated with Morris watermaze acquisition performance, this does not prove that it makes a direct contribution to it [611]. Instead, LTP may be upregulated in several brain areas *including* the hippocampus, with facilitated cortical LTP being the *true* substrate of long-term spatial memory acquisition [611]. If this hypothesis is correct, it would further suggest that the enhanced watermaze acquisition of ddY/*Dao*$^{-}$ mice was an artefact of anxiety, since D-serine levels are not increased in the cortex in ddY/*Dao*$^{-}$ mice [472].

Parameter	Maekawa *et al.*, 2005	Labrie *et al.*, 2009b
Mutant model	ddY/*Dao*$^{-}$	*Dao1*^{G181R}
Background strain	ddY	C57BL/6J
Pool diameter (cm)	70	185
Radial platform distance (cm)	17.5	25
Acquisition trial duration (s)	120	90
Trials per session	3	4
Sessions per day	2	1
Inter-trial interval (h)	Unspecified	1
Sex(es)	Males only	Males and females
Index of probe trial performance	Percent time in the platform quadrant	Percent time within 5 cm of the platform location
Age at test (weeks)	8-16	11-16

Table 3.1. Methodological differences between two previous studies of Morris watermaze performance in two related *Dao* mutants; the ddY/*Dao*$^{-}$ mouse [521] and the *Dao1*^{G181R} mouse [466].

The influence of sex on the watermaze performance of Dao$^{-/-}$ *mice*

Interestingly, the interaction between genotype and radial platform distance was far more pronounced in males than females in *Experiment 2*. There was also little resemblance between the male and female data in terms of the changes in latencies and pathlengths across trials. It is unclear whether these differences reflect the influence of sex on anxiety, memory, a combination of the two, or another, as-yet-unidentified factor. A straightforward anxiety-based explanation would appear inadequate, since male and female *Dao*$^{-/-}$ mice perform similarly in

a range of anxiety tests, including the open field (see Chapter 2). It has previously been suggested that male and female rodents use different strategies to solve watermaze tasks; males are thought to navigate using 'geometric' cues, while females rely more heavily upon 'landmark' cues [624]. Perhaps anxiety modulates the former strategy more than the latter. To add a further layer of complexity, a comprehensive account would need to explain why sex influenced the performance of *Dao*$^{-/-}$ mice in the peripheral and intermediate platform conditions (c.f. *Experiment 2*), but not in the intermediate platform condition (c.f. *Experiment 1*).

Notably, sex differences may also have contributed to the inconsistent findings concerning *Dao* mutants in the watermaze, since one study included only male mice [521], while the other employed males and females [466]. As explained, genotype had a stronger impact on the watermaze performance of male mice in our own dataset; this is clearly consistent with the fact that enhanced acquisition was reported in the male-only study involving the ddY/*Dao*$^{-}$ mouse [521], but not in the mixed sex study involving the *Dao1*^{G181R} mouse [466].

Implications for the Morris watermaze task with mice

Since its introduction in 1981 [625], the Morris watermaze has been used to evaluate the impact of countless genetic, pharmacological, environmental and lesion-based manipulations on rodent spatial memory. To date, the task has been mentioned in at least 6,250 publications[3], which attests to its importance within the field of behavioural neuroscience. The findings of the present study have a number of implications for the design and interpretation of Morris watermaze experiments, particularly when using mice. Firstly, our data suggest that the

[3] Based on a search of the PubMed database (http://www.ncbi.nlm.nih.gov/) in May 2015, using the search term 'Morris water maze'.

variation (and counterbalancing) of radial platform distance might be a useful addition to future studies. While it is generally accepted as best practice to train different animals to different platform locations as defined by the quadrant of the pool in which they are located (e.g. NW versus SE; and to counterbalance this across groups), it is normally the case that all animals are trained to locate platforms positioned a set distance from the side-wall. However, our data clearly suggest that the use of a single radial platform distance could unintentionally bias the outcome of a study.

The number of trials per session and the timing of the probe trial are two further aspects of the task's design which require careful consideration; the fact that Morris watermaze performance can converge (and presumably also diverge) over consecutive trials implies that these factors could have considerable bearing on the results obtained. For the same reason, it is important to analyse Morris watermaze data on a trial-by-trial basis as well as a day-by-day basis. Likewise, it is preferable to test both males and female animals in the Morris watermaze (see above). Finally, our data emphasise the utility of employing a battery of long-term spatial memory tests in addition to the Morris watermaze, although it is important to note that different spatial memory tasks are likely to recruit distinct psychological processes, and may be subserved by different neurobiological substrates [620].

Trial-by-genotype interactions in Morris watermaze performance

Perhaps the most puzzling findings of the present study were the trial-by-genotype interactions in the intermediate platform condition in *Experiment 1*, and the central platform condition in *Experiment 2*. Why did the performance of *Dao*$^{-/-}$ and *Dao*$^{+/+}$ mice only differ significantly on the first trial of each four-trial acquisition session? We would argue that in any given trial, escape latency and pathlength are dependent on at least two contributory factors: memory and

anxiety. In addition, escape latency is influenced by swim speed. Memory for the platform location is likely increase from trial to trial, which should serve to reduce both latency and pathlength. Anxiety, on the other hand, might promote peripheral swimming. Hence, anxiety could serve either to increase *or* decrease escape latency and pathlength across consecutive trials, depending on the platform's location within the pool. The picture is further complicated by the fact that baseline anxiety is likely to differ between *Dao*$^{+/+}$ and *Dao*$^{-/-}$ mice (see Chapter 2). In order to make sense of this puzzle, one would need an objective measure of anxiety that could recorded be on a trial-by-trial basis (and could be performed without influencing anxiety itself). Alternatively, one could use a computational model to predict escape latencies and pathlengths for platforms positioned at various distances from the side-wall. These predictions could then be tested experimentally.

Interestingly, our observation of a trial-by-genotype interaction in *Dao*$^{-/-}$ mice has a precedent. In an unpublished study, long-term spatial memory acquisition in the Morris watermaze was tested in wildtype rats after D-cycloserine administration [David Bannerman, *unpublished data*]. D-cycloserine, like D-serine, is an NMDAR co-agonist that acts at the glycine site [472]. Just like *Dao*$^{-/-}$ mice, D-cycloserine-treated rats outperformed vehicle-treated rats on the first trial of each acquisition session. However, on the second and third trials of each three-trial session, D-cycloserine-treated rats were outperformed by vehicle-treated rats. Hence, there was a borderline-significant trial-by-treatment interaction for both escape latency and pathlength in this dataset (see Appendix Fig. 8.7). This remarkable convergence with our own data indicate that glycine-site-mediated NMDAR co-agonism has robust effects on the progression of Morris watermaze performance across trials. They also suggest that the observed phenotype of the *Dao*$^{-/-}$ mouse was not a consequence of altered neurodevelopment or other long-term compensatory changes that can occur in constitutive knockout models.

Reversal learning

Contrary to our prediction, we observed no enhancement in Morris watermaze reversal learning in *Dao*$^{-/-}$ mice. This is in contrast to reports of enhanced watermaze reversal learning in *Dao1*^{G181R} mice [466], and in wildtype mice after D-serine administration [523]. Note that watermaze reversal learning has yet to be tested in ddY/*Dao*$^{-}$ mice. In future, it would be useful to test reversal learning in *Dao*$^{-/-}$ mice in another apparatus, such as the radial arm maze or Barnes maze. This would establish whether reversal learning is genuinely unaltered in *Dao*$^{-/-}$ mice, or whether our negative findings in the Morris watermaze were simply the result of methodological differences between our study and previous studies [466, 523]. In addition, *Dao1*^{G181R} mice display more rapid extinction in the Morris watermaze, and more rapid extinction of a conditioned contextual fear response [466]. Hence, it would be useful to test extinction in *Dao*$^{-/-}$ mice in the future. Lastly, one could subject *Dao*$^{-/-}$ mice to the 'beacons task', a recently-developed test of 'behavioural inhibition' that is performed in the Morris watermaze [620]. Behavioural inhibition is a form of cognitive flexibility that is closely related to reversal learning, and is known to be dependent on hippocampal NMDARs [620]. Hence, performance in this task may be enhanced in *Dao*$^{-/-}$ mice.

Conclusions

To conclude, we have demonstrated that Morris watermaze performance in *Dao*$^{-/-}$ mice is critically dependent on the radial distance of the hidden platform from the side-wall. This may be a reflection of heightened anxiety in the *Dao*$^{-/-}$ mouse, rather than altered long-term associative spatial memory. Our results have implications for the understanding of the role of DAO in brain function and dysfunction, and, more generally, for the design and interpretation of Morris watermaze experiments with mice.

4. Prepulse inhibition, startle amplitude and startle habituation in the *Dao*$^{-/-}$ mouse

4.1. Introduction

Prepulse inhibition (PPI) is the phenomenon by which a weaker pre-stimulus (referred to as the 'prepulse') inhibits the response of an organism to a subsequent, startling stimulus (known as the 'pulse') [138]. Acoustic stimuli are typically used in PPI protocols, but tactile and light stimuli can also be used. PPI is an oft-cited example of 'sensorimotor gating', which is *"a form of central nervous system inhibition wherein irrelevant sensory information is filtered out during the early stages of processing, so that attention can be focused on more salient features of the environment"* [483]. One of the main attractions of PPI is that it can be assessed with virtually identical protocols in humans and rodents, in stark contrast to tests of anxiety, memory and depression. In addition, PPI appears to be modulated by the same cortical, limbic and striatal brain loci in rodents [626] as in humans [627-631]. Therefore, PPI has good construct validity in addition to excellent face validity.

There have been reports of decreased PPI in a wide range of clinical populations, including individuals with obsessive-compulsive disorder, Tourette's syndrome, Huntington's disease, bipolar disorder, panic disorder and autism [632]. However, schizophrenia is the disorder in which reduced PPI has been most widely replicated [137-141]. Decreased PPI has also been observed in schizotypal personality disorder [633], in the unaffected first-degree relatives of schizophrenia patients [634], and in subjects at ultra-high risk (UHR) for psychosis [635, 636].

Although PPI is consistently reduced in schizophrenia, its relationship to the positive, negative and cognitive symptoms of the disorder is somewhat controversial. In rodent studies, PPI

results are often presented as a model of the positive symptoms of schizophrenia, yet there is little evidence that PPI is correlated with either the positive or negative symptoms of the disorder [637]. This common misrepresentation likely stems from the fact that PPI deficits can be induced by psychotomimetic drugs in rodents, and can be reversed by antipsychotic medication [632]. PPI can also be potentiated above baseline by antipsychotic administration in rats and mice [638-640].

In reality, PPI may be more relevant to the cognitive symptoms of schizophrenia, although evidence for this hypothesis is also equivocal. Certainly, PPI does not seem to be correlated with performance in simple 'pen and paper' cognitive tasks in schizophrenia patients [641]. By contrast, PPI levels accurately predict performance in more advanced tests of executive function in healthy individuals [642-644]. Future studies should determine whether similar correlations exist in clinical populations. Finally, negative correlations have been reported between PPI and more general cognitive measures in schizophrenia patients, such as 'distractibility' [645] and 'thought disorder' [646-648]. Therefore, PPI represents a promising biomarker for use in the development of novel treatments for the cognitive symptoms of schizophrenia [649]. However, it would be incorrect to present PPI as a direct analogue of the positive, negative or cognitive symptoms of the disorder [137, 632, 649].

A number of previous studies have quantified PPI in mouse models with altered DAO activity and/or brain D-serine levels. Taken together, the results of these studies are suggestive of a positive association between brain D-serine concentration and PPI levels. Firstly, increased PPI has been observed in wildtype mice following D-serine administration [531], and in ddY/*Dao*$^{-}$ mutants [520], although another study reported no difference between ddY/*Dao*$^{-}$ mice and wildtypes [499]. Secondly, D-serine administration and pharmacological DAO inhibition can

both reverse NMDAR antagonist-induced PPI deficits in wildtype rodents [508, 530, 532, 650]. Thirdly, *Srr*^{Y269} mutant mice, in which brain D-serine levels are significantly depleted, demonstrate significantly *reduced* PPI [650]. Importantly, there is an association between DAO and PPI in humans as well as rodents; in a recent clinical study, reduced PPI was significantly associated with two single-nucleotide polymorphisms (SNPs) in *Dao* in a healthy adult population [483].

Notably, there was a key methodological difference between the two previous PPI studies involving ddY/*Dao*$^{-}$ mice. In one of these studies, intraperitoneal vehicle injections were administered 15 minutes before behavioural testing, while in the other, no injections were employed (see Table 4.1). The assessment of PPI in D-serine-treated wildtype mice also involved intraperitoneal injections (see Table 4.1). Hence, it is possible that the positive findings in the literature reflect an interaction between DAO inactivity/elevated brain D-serine and the stress response evoked by intraperitoneal injection. According to this hypothesis, one would expect PPI to be elevated in vehicle-injected male *Dao*$^{-/-}$ mice relative to vehicle-injected male *Dao*$^{+/+}$ mice, but to be unaltered in untreated male *Dao*$^{-/-}$ mice relative to untreated male *Dao*$^{+/+}$ mice. To test this prediction, we quantified PPI in *Dao*$^{-/-}$ mice, both with and without a stressful intraperitoneal injection prior to testing. We also tested female mice, since the aforementioned studies included only males. The characterisation of both sexes was important given prior evidence of sex-specific behavioural phenotypes in *Dao*$^{-/-}$ mice (cf. novelty-suppressed feeding, described in Chapter 2, and the Morris watermaze, described in Chapter 3).

In both PPI studies involving ddY/*Dao*$^{-}$ mice, the genetic inactivation of DAO was associated with increased baseline startle amplitude [499, 520]. Therefore, an additional objective of the

present chapter was to confirm this finding in *Dao*$^{-/-}$ mice. We assessed startle amplitude both within the PPI paradigm itself, and with a separate acoustic startle protocol. Schizophrenia patients often show a reduction in baseline startle amplitude, and this finding has been linked to the affective flattening seen in the disorder [651]. Some antipsychotic drugs (e.g. amisulpride) increase baseline startle amplitude in schizophrenia patients, although others (e.g. olanzapine) have no effect [651].

Finally, we assessed acoustic startle habituation in *Dao*$^{+/+}$ and *Dao*$^{-/-}$ mice of both sexes. Startle habituation refers to the progressive reduction in the amplitude of the startle response that occurs with repeated exposures to the startling stimulus. We elected to study this process given evidence that it occurs more slowly in individuals with schizophrenia [652, 653]. Some antipsychotic drugs (e.g. amisulpride) accelerate acoustic startle habituation in schizophrenia patients, although others (e.g. olanzapine) do not [651]. To the best of our knowledge, nobody has investigated the relationship between acoustic startle habituation and DAO activity.

Study	Model	Strain	Sex	Age	Housing	Stimuli	Injection stress	PPI	Baseline Startle Amplitude
Lipina *et al.* (2005) [531]	D-serine administered to wildtype mice	C57Bl/6J	Male	7 to 9 weeks	Group-housed	120 dB pulse; 69, 73 or 81 dB prepulse	Yes (i.p. injection 20 mins prior to test)	↑	↔
Almond *et al.* (2006) [499]	ddY/*Dao*$^{-}$ mice	ddY	Male	3 to 4 months	Singly- or group-housed	120 dB pulse; 71, 74 or 78 dB prepulse	No	↔	↑
Zhang *et al.* (2011) [520]	ddY/*Dao*$^{-}$ mice	ddY	Male	Unspecified	Group-housed	120 dB pulse; 70, 75 or 80 dB prepulse	Yes (i.p. injection 15 mins prior to test)	↑	↑

Table 4.1. Summary of experiments investigating the relationship between prepulse inhibition (PPI) and DAO activity or brain D-serine levels in mice. ↔ denotes no difference in PPI or baseline startle amplitude between experimental animals and controls; ↑ indicates a significant increase in PPI or baseline startle amplitude in experimental animals relative to controls. I.p. = intraperitoneal.

4.2. Methods

4.2.1. Animals

Dao knockout mice were generated as described in Chapter 2. Two cohorts of mice participated in the prepulse inhibition paradigm. Cohort 1 consisted of 22 mice (6 male $Dao^{+/+}$ mice, 6 female $Dao^{+/+}$ mice, 6 male $Dao^{-/-}$ mice and 4 female $Dao^{-/-}$ mice), while cohort 2 was comprised of 24 mice (*n*=6 males; *n*=6 females per genotype). Only cohort 1 completed the acoustic startle protocol. All mice were singly-housed throughout testing. Mice in cohort 1 were aged 6 to 9 months at the time of PPI testing ($\underline{M}$ = 7.2 months). Mice in cohort 2 were aged 6 to 10 months at the time of PPI testing ($\underline{M}$ = 7.7 months). Prior to behavioural testing, mice were handled for 2 min a day for 5 consecutive days, to habituate them to experimenter handling. Mice were singly-housed under a 100 lux 12:12 h light/dark (12:12 LD) cycle with lights on at 07:00, with access to food and water *ad libitum*. All testing was conducted between 13:30 and 17:30 (i.e. between ZT6.5 and ZT10.5). For all experiments, mice were brought into the test room 5-10 min prior to the onset of testing. Animals were singly-housed to enable direct comparison with other singly-housed cohorts in which anxiety and short-term memory were assessed (see Chapter 2), long-term memory was assessed (see Chapter 3), and sleep and circadian rhythms were assessed (see Chapter 5). All behavioural procedures were performed in accordance with the United Kingdom Animals (Scientific Procedures) Act of 1986 and the University of Oxford Policy on the Use of Animals in Scientific Research. All experiments were approved by the University of Oxford Animal Welfare and Ethical Review Board, and were conducted under the PPL 30/3068 by PIL ICC0614BD (formerly 30/9339).

4.2.2. Prepulse inhibition of acoustic startle

Testing was based on an existing protocol [654], which was very similar to that used to test PPI in *Dao* mutants and in wildtype rodents after D-serine administration [499, 520, 531]. PPI testing was performed using the SR-Lab System (San Diego Instruments, San Diego, CA, USA), and took place inside six sound-isolating startle chambers. The door of each chamber was lined with foam for further sound-dampening. A cylindrical transparent acrylic mouse holder with ventilation slots (internal diameter: 5 cm; length: 10 cm) was fixed to a central platform within each chamber. Mice were confined to these holders during testing. Mouse holders and platforms were cleaned with diluted ethanol before and after each session. Each chamber contained a speaker to emit sounds, and a piezoelectric motion sensor to measure the amplitude of each startle response. Chambers were also equipped with a fan for ventilation and a white light that remained on for the duration of testing. Illumination was 200 lux at the level of the mouse holder. The presentation of auditory events was controlled by the SR-Lab software package (San Diego Instruments, San Diego, CA, USA). This software was also used to record the amplitude of each startle response.

Background white noise (65 dB) was played for the entirety of each session. Five types of trial were employed. Pulse alone (P) trials consisted of a 40 ms white noise burst at 120 dB, while prepulse alone (PP) trials consisted of a 20 ms white noise burst at either 69, 73, 77 or 81 dB (i.e. 4, 8, 12 or 16 dB above background noise). Prepulse inhibition (PPI) trials comprised of 20 ms prepulse at either 69, 73, 77 or 81 dB, followed 100 ms later by a 40 ms pulse at 120 dB. 'Silent' (S) trials consisted of background white noise only (65 dB). Each session began with a short acclimatisation period, consisting of 5 mins of background white noise at 65 dB. This was followed by a brief habituation period, in which 5 P trials were presented in succession. (These trials were not included in data analysis, but were presented to standardise startle

responding as there is always a rapid decline in the amplitude of the startle reflex across the first few P trials [655]). The main experimental session included 9 P trials, 36 PP trials (9 of each prepulse intensity), 36 PPI trials (9 of each prepulse intensity), and 9 S trials. Trials were presented in a pseudo-randomised order, with a variable inter-trial interval (ITI; 10-20 s); this meant that the timing of trial presentation was not predictable, which prevented anticipatory responding. The S trials also served to increase the variability of the ITI, making the timing of trial presentation less predictable.

Startle amplitude was recorded in each trial, and was defined as the average amplitude of the startle reflex waveform (henceforth referred to as V^{avg}). In P and PPI trials, waveform analysis was restricted to a 65 ms sampling window starting at the onset of the pulse. The average V^{avg} value from all P trials (excluding those from the habituation period) is henceforth referred to as 'startle amplitude'. An average V^{avg} value was also computed from all PP trials, henceforth referred to as 'prepulse responsivity'. Here, waveform analysis was confined to a 65 ms sampling window starting at the onset of the prepulse. In addition, an average V^{avg} value was computed from all S trials, to provide an index of baseline locomotor activity within the mouse holder. This value is henceforth referred to as 'baseline movement'. Here, waveform analysis was confined to a 65 ms sampling window starting at the onset of the trial. Baseline movement data are included in Appendix Fig. 8.8.

To calculate the degree of prepulse inhibition itself (i.e. the percent reduction in startle intensity between P trials and PPI trials), the following formula was used: ((average V^{avg} value from P trials – average V^{avg} value from PPI trials)/average V^{avg} value from P trials) × 100. Once again, note that V^{avg} values from P trials in the habituation period were not included in this calculation.

All mice completed a single PPI session on two separate days, 7 days apart. Each session lasted approximately 30 mins. Since only six startle chambers were available, mice from each cohort were tested in four batches. Each batch contained an equal number of *Dao*$^{+/+}$ and *Dao*$^{-/-}$ mice, while the two male and two female batches were tested in an alternating fashion. On day 1, half of the mice received an intraperitoneal saline injection 15 min prior to the onset of the PPI session, while the other half received no injection. On day 2, the roles were reversed; those that had received no injection on day 1 received an injection on day 2, and those that had received an injection on day 1 received no injection on day 2. The purpose of this counterbalanced design was to prevent an effect of session from being misinterpreted as an effect of injection stress. The identities of those mice receiving injections on days 1 and 2 were counterbalanced across sex and genotype. Each mouse was injected with 0.3 ml of sterile saline solution, corresponding to a final injection volume of approximately 10ml/kg. The 15 min interval between injection and PPI testing was chosen to enable direct comparison with the experiments described in the introduction [520, 531]. Note that Katie Hewitt assisted with the intraperitoneal saline injections.

4.2.3. Acoustic startle habituation protocol

This experiment was based on an established protocol [654]. Testing took place in the same startle chambers as the PPI paradigm, and was conducted 13 days after the second day of PPI testing. Again, background white noise (65 dB) was played for the entirety of the session, and once more, the session began with a short acclimatisation period, consisting of 5 mins of background white noise at 65 dB. Two types of trial were employed. Mice were presented with 84 startle trials, which consisted of a 40 ms white noise burst at 100 dB. Startle trials were interspersed with 21 'silent' trials, which were identical to those used in the PPI paradigm. Trials were presented in a pseudo-randomised order, with a variable inter-trial interval 10-20 s); this meant that the timing of startle trial presentation was not predictable, which prevented anticipatory responding. All mice completed a single acoustic startle session on the same day. Each session lasted approximately 35 mins. Since only six startle chambers were available, mice were tested in four batches. Each batch contained an equal number of *Dao*$^{+/+}$ and *Dao*$^{-/-}$ mice, while the two male and two female batches were tested in an alternating fashion. Average 'startle amplitude' and 'baseline movement' values were computed for each mouse using the same procedure as described for the PPI paradigm. Baseline movement data are included in Appendix Fig. 8.9.

4.2.4. Statistical analysis

All statistical analyses were performed with SPSS 22.0 (IBM, Armonk, New York). Unless otherwise stated, all reported statistics are the result of analyses of variance (ANOVAs), with genotype and sex included as independent variables, in addition to injection stress where applicable. Differences were considered to be statistically significant at p-values < 0.05. Greenhouse-Geisser corrections were applied where appropriate, but uncorrected degrees of freedom are reported in order to preserve the transparency of the statistical design. For experiments involving multiple cohorts, further ANOVAs were conducted with cohort included as an extra independent variable. No additional effects or interactions were observed, so these data are not shown. Note that in the PPI experiment, data for PPI trials represent the average of all 36 trials across all 4 prepulse intensities. A separate ANOVA was conducted with prepulse intensity included as an additional within-subjects variable. This ANOVA revealed a significant main effect of prepulse intensity (P = < 0.05), reflecting the fact that PPI was greater at higher intensity prepulses. However, there were no significant interactions between prepulse intensity and any other variable (Ps > 0.05), as this effect was unaltered by genotype, sex or injection stress. In all figures, * indicates a p-value ≤ 0.05, ** indicates a p-value ≤ 0.01, and *** indicates a p-value ≤ 0.001. Error bars depict the standard error of the mean. $\underline{M}$ = mean.

4.3. Results

4.3.1. Prepulse inhibition of acoustic startle

Prepulse inhibition with and without injection stress

Average PPI values for each mouse were entered into an ANOVA, with genotype and sex as between-subjects variables, and injection stress as a within-subjects variable. This ANOVA yielded no main effect of genotype or injection stress (*P*s = > 0.363). There was, however, a main effect of sex ($F_{1,42}$ = 4.967, P = 0.031), reflecting the fact that PPI was generally higher in males than females. This is consistent with previous findings in humans [656] and rodents [657]. In addition, there was a significant three-way interaction between genotype, sex and injection stress ($F_{1,42}$ = 9.538, P = 0.004; Fig. 4.1A & 4.1B). In the absence of injection stress, PPI was lower in male *Dao*$^{-/-}$ mice than male *Dao*$^{+/+}$ mice ($F_{1,22}$ = 2.270, P = 0.146), but higher in female *Dao*$^{-/-}$ mice than female *Dao*$^{+/+}$ mice ($F_{1,20}$ = 0.178, P = 0.678). These baseline contingencies were completely reversed by injection stress. PPI became higher in male *Dao*$^{-/-}$ mice than male *Dao*$^{+/+}$ mice after injection stress ($F_{1,22}$ = 0.116, P = 0.736), but lower in female *Dao*$^{-/-}$ mice than female *Dao*$^{+/+}$ mice ($F_{1,20}$ = 4.270, P = 0.052). Consistent with this picture, there was a significant genotype-by-injection stress interaction in both males ($F_{1,22}$ = 4.739, P = 0.041; Fig. 4.1A) and females ($F_{1,20}$ = 4.770, P = 0.041; Fig. 4.1B).

An alternative way to analyse these data is to calculate the percent change in PPI (from baseline) that occurs as the result of injection stress. Percent change values for each mouse were entered into an ANOVA, with genotype and sex as between-subjects variables. This analysis yielded no main effect of genotype or sex (*Ps* = > 0.335), but there was a significant interaction between genotype and sex ($F_{1,42}$ = 5.906, P = 0.020; Fig. 4.1C). This reflects the fact that injection stress decreased PPI in male *Dao*$^{+/+}$ mice and female *Dao*$^{-/-}$ mice, but increased PPI in male *Dao*$^{-/-}$ mice and female *Dao*$^{+/+}$ mice.

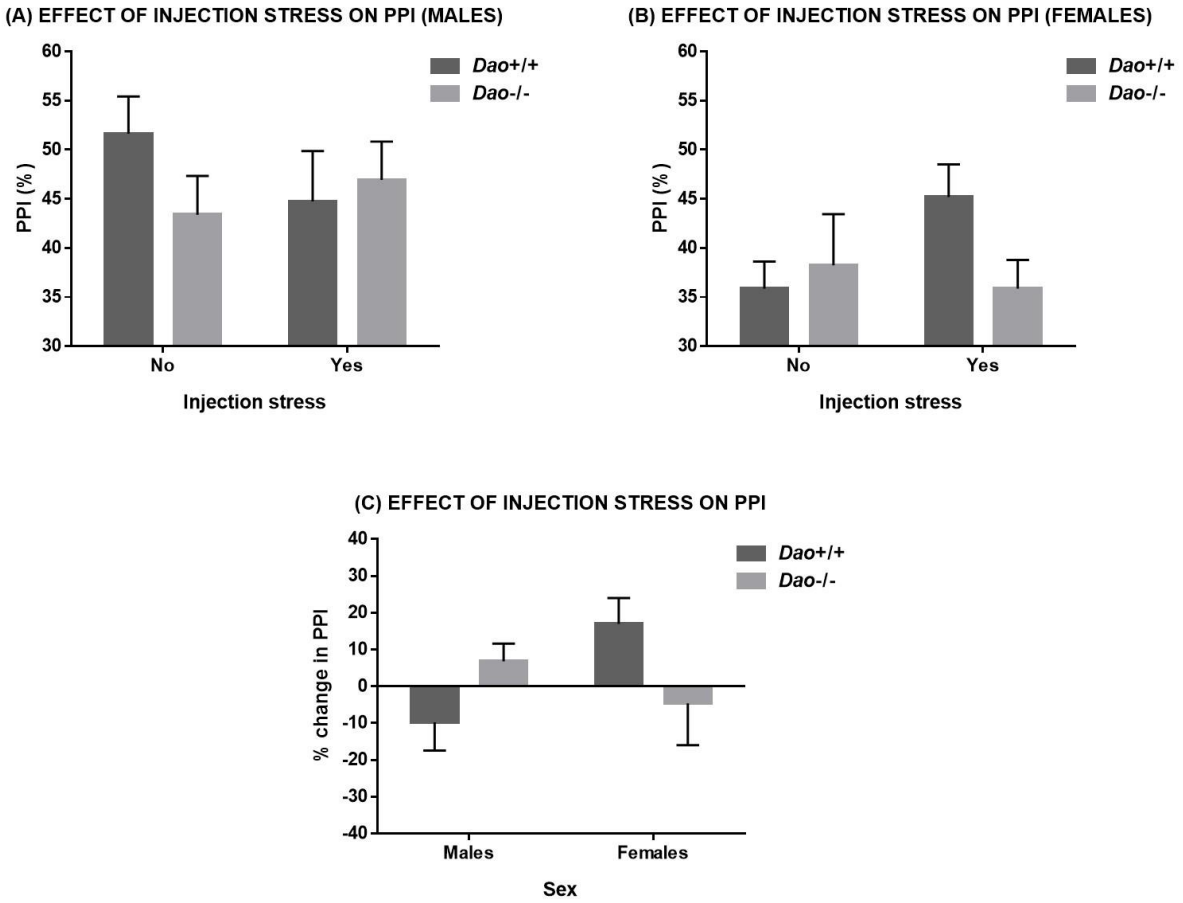

Figure 4.1. Prepulse inhibition of the acoustic startle reflex in *Dao*$^{+/+}$ and *Dao*$^{-/-}$ mice, with and without injection stress. (A) In the absence of injection stress, PPI is lower in male *Dao*$^{-/-}$ mice than male *Dao*$^{+/+}$ mice. Following injection stress, PPI is higher in male *Dao*$^{-/-}$ mice than male *Dao*$^{+/+}$ mice. (B) In the absence of injection stress, PPI is higher in female *Dao*$^{-/-}$ mice than female *Dao*$^{+/+}$ mice. After injection stress, PPI is lower in female *Dao*$^{-/-}$ mice than female *Dao*$^{+/+}$ mice. (C) Relative to PPI under standard conditions, injection stress reduces PPI in male *Dao*$^{+/+}$ mice and female *Dao*$^{-/-}$ mice, but increases PPI in male *Dao*$^{-/-}$ mice and female *Dao*$^{+/+}$ mice.

Startle amplitude

Average startle amplitude values for each mouse were entered into an ANOVA, with genotype and sex as between-subjects variables, and injection stress as a within-subjects variable. Average startle amplitude was unaffected by genotype ($F_{1,42}$ = 0.426, P = 0.517; Fig. 4.2A), sex ($F_{1,42}$ = 0.462, P = 0.500; Fig. 4.2B), and injection stress ($F_{1,42}$ = 0.056, P = 0.814; Fig. 4.2C). There were no significant interactions between any of the variables (Ps = > 0.111). Hence, it seems unlikely that the complex PPI phenotype of the *Dao*$^{-/-}$ mouse was a consequence of changes in baseline startle amplitude. This possibility was important to exclude given evidence that PPI is significantly negatively associated with baseline startle amplitude in both humans and mice [658].

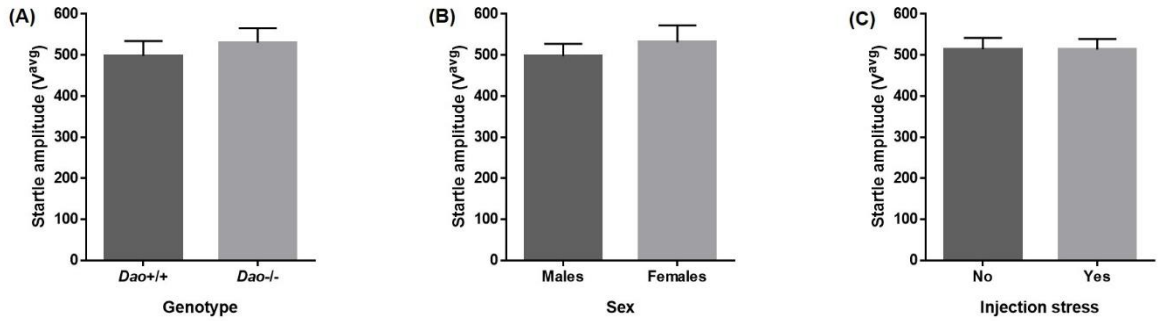

Figure 4.2. Startle amplitude within the prepulse inhibition paradigm. (A) Startle amplitude did not differ between *Dao*$^{+/+}$ and *Dao*$^{-/-}$ mice. (B) Startle amplitude did not differ between male and female mice. (C) Injection stress had no impact on startle amplitude.

Prepulse responsivity

Average prepulse responsivity values for each mouse were entered into an ANOVA, with genotype and sex as between-subjects variables, and injection stress as a within-subjects variable. Average prepulse responsivity was unaffected by genotype ($F_{1,42}$ = 0.160, P = 0.691; Fig. 4.3A), sex ($F_{1,42}$ = 0.360, P = 0.552; Fig. 4.3B), and injection stress ($F_{1,42}$ = 0.324, P = 0.572; Fig. 4.3C). There were no significant interactions between any of the variables (Ps = >0.760). Hence, the altered PPI levels witnessed in the current experiment do not appear to be a consequence of facilitated or impaired hearing or altered sensory processing of the prepulse stimuli.

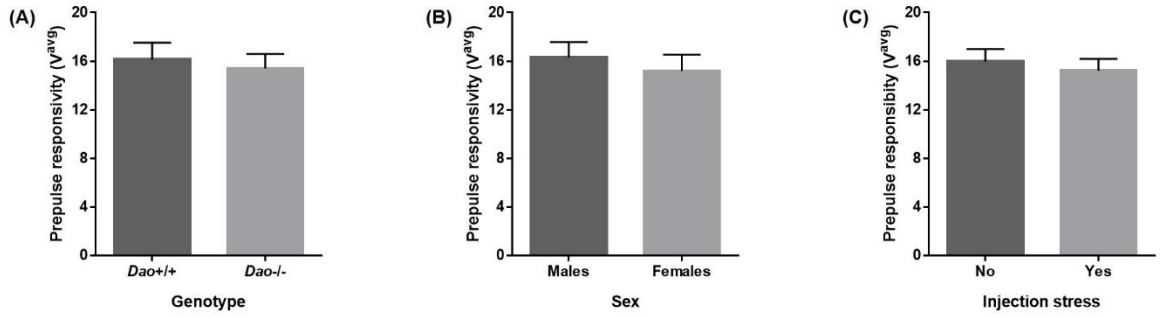

Figure 4.3. Prepulse responsivity within the prepulse inhibition paradigm paradigm. (A) Prepulse responsivity did not differ between *Dao*$^{+/+}$ and *Dao*$^{-/-}$ mice. (B) Prepulse responsivity did not differ between male and female mice. (C) Injection stress had no impact on prepulse responsivity.

4.3.2. Acoustic Startle Habituation Protocol

When all 84 startle trials were considered, there was no main effect of genotype on average startle amplitude ($F_{1,18}$ = 0.146, P = 0.707). By contrast, average startle amplitude was higher in males than females, although this difference was not statistically significant ($F_{1,18}$ = 4.187, P = 0.056). To provide an index of startle habituation, average startle amplitude during the first 21 startle trials was contrasted with average startle amplitude during the final 21 startle trials. These values entered into an ANOVA, with genotype and sex as between-subjects variables, and time (i.e. start vs. end) as a within-subjects variable. Once again, genotype had no impact on startle amplitude ($F_{1,18}$ = 0.134, P = 0.719 Fig. 4.4A), but there was a trend-level effect of sex ($F_{1,18}$ = 3.639, P = 0.073; Fig. 4.4B), since average startle amplitude was higher in males than females. There was a significant main effect of time ($F_{1,18}$ = 6.316, P = 0.022; Fig. 4.4C), reflecting the decline in average startle amplitude between the start and the end of the session. Crucially, there was no interaction between genotype and time, sex and time, or genotype, sex and time (Ps = > 0.346). Hence, the degree of startle habituation was unaffected by genotype and sex (Fig. 4.4D & 4.4E).

An alternative way to analyse these data is to calculate the percent change in average startle amplitude between the first 21 startle trials and the final 21 startle trials. Percent change values for each mouse were entered into an ANOVA, with genotype and sex as between-subjects variables. This analysis yielded no main effect of genotype ($F_{1,18}$ = 0.170, P = 0.685) or sex ($F_{1,18}$ = 1.109, P = 0.306), and no interaction between genotype and sex ($F_{1,18}$ = 0.235, P = 0.634). Again, this indicates that the degree of startle habituation was unaffected by genotype and sex.

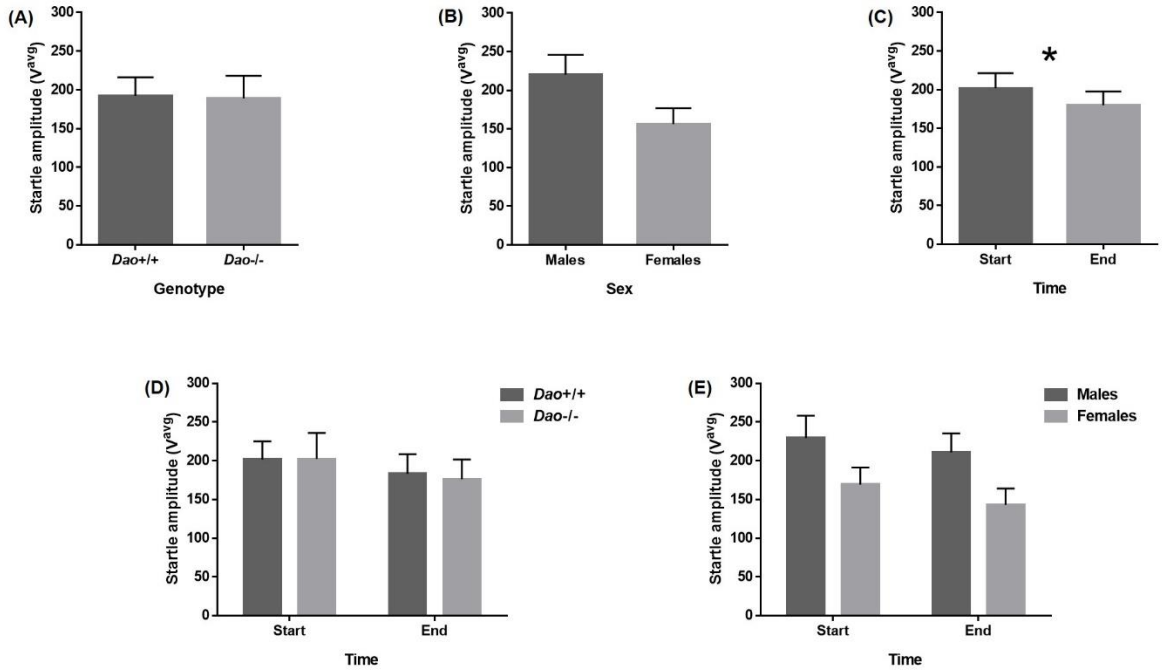

Figure 4.4. Startle amplitude within the acoustic startle habituation protocol. (A) Startle amplitude did not differ between *Dao*$^{+/+}$ and *Dao*$^{-/-}$ mice. (B) Startle amplitude was numerically but not significantly higher in male than female mice. (C) Startle amplitude was significantly greater at the start than at the end of the habituation session. (D) Habituation of the acoustic startle reflex was evident in both *Dao*$^{+/+}$ and *Dao*$^{-/-}$ mice, but the degree of startle habituation was unaffected by genotype. (E) Habituation of the acoustic startle reflex was evident in both males and females, but the degree of startle habituation was unaffected by sex.

4.4. Discussion

The present chapter describes the characterisation of baseline acoustic startle amplitude, acoustic startle habituation, and prepulse inhibition (PPI) of the acoustic startle reflex in *Dao*$^{+/+}$ and *Dao*$^{-/-}$ mice. While genotype had no significant effect on startle amplitude or startle habituation, a highly complex PPI phenotype was revealed, challenging the hypothesis that there is a simple positive association between brain D-serine concentration and PPI levels.

Prepulse inhibition with and without injection stress

Two previous studies measured PPI in ddY/*Dao*$^{-}$ mice [499, 520]. In the former, no alteration in PPI was reported [499], but in the latter, PPI was increased in mutant mice relative to wildtypes [520]. Despite using the same mouse model and similar PPI protocols, there was one major difference between the experiments; all mice in the latter study received an intraperitoneal vehicle injection prior to PPI testing [520]. We therefore hypothesised that the increased PPI witnessed in the latter study reflected an interaction between DAO inactivity/increased brain D-serine and the stress response evoked by intraperitoneal injection.

This prediction proved to be accurate; in the absence of injection stress, PPI was lower in male *Dao*$^{-/-}$ mice than male *Dao*$^{+/+}$ mice. However, following an intraperitoneal saline injection, PPI was higher in male *Dao*$^{-/-}$ mice than male *Dao*$^{+/+}$ mice. Although neither of these differences were statistically significant, the genotype-by-injection stress interaction *was* significant. This result indicates that the effect of DAO inactivity on PPI is strongly modulated by stress, to the extent that heightened stress can completely reverse the behavioural phenotype.

Since the aforementioned studies included only male mice, we also assessed PPI in female *Dao*$^{+/+}$ and *Dao*$^{-/-}$ mice. As in males, we observed a significant genotype-by-injection stress

interaction, whereby the relative PPI performance of the two genotypes was completely reversed after injection stress. Remarkably, however, the pattern was the exact opposite of that seen in males; in the absence of injection stress, PPI was higher in female *Dao*$^{-/-}$ mice than female *Dao*$^{+/+}$ mice, but, following an intraperitoneal saline injection, PPI was lower in female *Dao*$^{-/-}$ mice than female *Dao*$^{+/+}$ mice. Consequently, our experiment yielded a significant three-way interaction between genotype, sex and injection stress.

To the best of our knowledge, such an effect has never been reported in a published PPI study. However, we are not the first to demonstrate that injection stress can differentially affect rodents of the same sex. In the absence of injection stress, PPI levels do not differ between male Sprague Dawley (SD) rats and male Long Evans (LE) rats, which, like *Dao*$^{+/+}$ and *Dao*$^{-/-}$ mice, perform differently in standard laboratory tests of anxiety and cognition [659]. Following an intracerebral vehicle injection, PPI is significantly reduced in LE rats relative to SD rats. This effect is attributable to a differential stress response in SD and LE rats, since the same effect was produced by a 'mock infusion' procedure involving restraint stress, light pressure to the top of the head, and the noise of a pump.

Our findings of differential effects in males and females are also not without precedent; amongst patients with bipolar disorder, for example, males show reduced PPI, whereas females exhibit increased PPI [660]. In addition, a recent study unearthed a SNP in *Dao* that confers increased risk of schizophrenia in females, but decreased risk in males [661].

Baseline acoustic startle amplitude

Increased baseline startle amplitude is observed in male ddY/*Dao*$^{-}$ mice [499, 520], but not in wildtype mice following D-serine administration [531]. Consistent with the latter study, we

found no evidence of altered baseline startle amplitude in either male or female *Dao*$^{-/-}$ mice, in either the PPI paradigm or the acoustic startle habituation protocol. Importantly, there were no significant effects or interactions involving genotype, sex or injection stress for baseline startle amplitude. This implies that the complex PPI phenotype of the *Dao*$^{-/-}$ mouse was not an artefact of alterations in baseline startle amplitude [658].

Habituation of the acoustic startle reflex

In the acoustic startle habituation protocol, the degree of startle habituation was unaffected by genotype and sex. To the best of our knowledge, this experiment represents the first attempt to characterise the relationship between DAO activity and acoustic startle habituation. Our results indicate that the former has no influence over the latter. This tentatively suggests that DAO inhibition should not exacerbate the startle habituation deficits of schizophrenia patients [652, 653].

Mechanistic basis of altered PPI in Dao$^{-/-}$ *mice*

To falsify our hypothesis that PPI levels are dependent on an interaction between D-serine concentration and stress levels, one would need to administer D-serine by a means that does not cause a concordant stress response. One possibility would be to release D-serine from a previously-implanted minipump. Alternatively, a transitory increase in D-serine could be induced through the optogenetic inactivation of the DAO enzyme. One would predict that after either of these stress-free manipulations, PPI should be reduced in treated males relative to sham males, but increased in treated females relative to sham females. With the addition of an intraperitoneal saline injection to the same protocol, PPI should be increased in treated males relative to sham males, but decreased in treated females relative to sham females.

The neurotransmitter(s) responsible for altered PPI in *Dao*$^{-/-}$ mice remain to be elucidated, but the dopaminergic, glutamatergic and serotonergic systems are all possible candidates. Dopamine in particular is strongly implicated in the modulation of PPI; in rodents, PPI is typically reduced by the administration of dopamine agonists, and increased by the administration of antipsychotic drugs, which are dopamine antagonists [638-640, 662-667]. Having said this, the opposite effects can also be observed, depending on the stimulus conditions and doses [664]. The fact that dopamine can have bilateral effects on PPI is potentially relevant to our own bidirectional results. In healthy humans, PPI is also modulated by dopamine agonists, antagonists and other substances that influence dopamine metabolism [668]. The glutamatergic system may also be involved in the modulation of PPI, since PPI is reduced by the administration of NMDAR antagonists [638, 669-671], although relatively little is known about the effect of NMDAR agonists on PPI [670]. Interestingly, atypical antipsychotics are more effective than typical antipsychotics at reversing PPI deficits induced by NMDAR antagonists [672-674], which hints at a role for serotonin receptors in the modulation of PPI.

PPI is modulated by multiple brain regions in rodents, including cortical, limbic and striatal brain areas [626]. Increased striatal dopamine concentration has been observed in patients with schizophrenia [675], while the direct infusion of dopamine agonists into the nucleus accumbens (NAc) of the striatum reduces PPI in Sprague Dawley rats, an effect counteracted by the administration of dopamine antagonists [664]).

Indeed, the NAc is a possible point of convergence for the D-serine pathway, the stress axis and PPI neurocircuitry. Systemic D-serine administration attenuates NAc dopamine release in wildtype rats [526], while dopamine levels are significantly decreased in the NAc of *Dao*$^{-/-}$

mice [676]. In rodents, increased striatal dopamine release is associated with a variety of stressors including restraint, foot and tail shock, and exhaustion [677]. Increased striatal dopamine release also accompanies psychological stress in healthy human volunteers [678]. Glucocorticoids likely mediate this effect; in humans, striatal dopamine release is significantly correlated with stress-induced cortisol release [679], while in rats, extracellular dopamine in the NAc is increased after foot-shock stress, systemic corticosterone administration, and intra-NAc corticosterone administration [680]. The striatum is also a plausible conduit for the effect of sex on PPI in *Dao*$^{-/-}$ mice, given that oestrogen enhances dopaminergic activity in the NAc [681].

Functional imaging studies in human subjects have also identified the prefrontal cortex, hippocampus and cerebellum as brain regions activated during PPI paradigms [627, 628, 630, 631]. In rats, direct infusion of dopamine antagonists into the orbitofrontal cortex reduces PPI [667]. Interestingly, injection of the DAO inhibitor sodium benzoate into the ventral tegmental area (VTA) of rats increases extracellular dopamine in the frontal cortex [682], while the intra-VTA injection of D-serine alters the levels of dopamine metabolites in the same region [682]. However, increased frontal dopamine is unlikely to be the cause of the altered PPI witnessed in the current experiment, since dopamine levels are unchanged in the prefrontal cortex of *Dao*$^{-/-}$ mice [676].

Clinical implications

Although it is risky to extrapolate from a transgenic mouse model to a complex neuropsychiatric disorder such as schizophrenia, these results have potentially important clinical implications. They suggest that the effect of pharmacological DAO inhibition on PPI performance in humans may depend on both the sex and stress levels of the patient in question.

Although reduced PPI is not considered a symptom of schizophrenia in and of itself [137, 632, 649], it may be related to executive function [642-644], which is significantly impaired in schizophrenia [683]. Therefore, the possibility exists that DAO inhibition could exacerbate the cognitive impairments of schizophrenia patients under specific circumstances (i.e. periods of low stress in men and high stress in women). If true, this would severely limit the therapeutic utility of DAO inhibition, given that stress is an inherently unstable parameter. Having said this, significantly enhanced cognitive performance was recently reported in an early clinical trial of the DAO inhibitor sodium benzoate in a small sample of schizophrenia patients [502]. This sample included both males and females, and it is safe to assume that stress levels varied both within and between individuals over the course of the study (6 weeks).

Conclusion

Previous studies of PPI in *Dao* mutants have yielded inconsistent results. To explore whether this reflects methodological differences between the studies, we assessed PPI in $Dao^{+/+}$ and $Dao^{-/-}$ mice, both with and without injection stress. In males, the effect of genotype on PPI was reversed by injection stress. Importantly, the direction of this effect was compatible with the results of the aforementioned studies. Since PPI has not been tested in female *Dao* mutants, we also quantified PPI in female $Dao^{+/+}$ and $Dao^{-/-}$ mice, both with and without injection stress. Again, the effect of genotype on PPI was reversed by injection stress. Remarkably, however, the observed contingencies were the complete opposite of those seen in males. Hence, PPI performance in $Dao^{-/-}$ mice reflects a complex interplay between genotype, sex and stress levels.

5. Sleep and circadian characterisation of the *Dao*$^{-/-}$ mouse

5.1. Introduction

As outlined in Chapter 1, sleep and circadian rhythm disruption (SCRD) is reported in 30–80% of patients with schizophrenia, and is increasingly recognised as one of the most common features of the disorder [326]. Schizophrenia patients with SCRD score badly on many quality-of-life clinical subscales [326,338,339], while many schizophrenia patients comment that an improvement in sleep is one of their highest priorities during treatment [340]. In this context, it is important that novel treatments for schizophrenia do not exacerbate SCRD. In recent years, DAO inhibition has been championed as a potential treatment for the cognitive symptoms of schizophrenia [502, 684-686], yet not a single published study has investigated the relationship between DAO function and sleep or circadian rhythms, in either rodents or humans.

This chapter describes the sleep and circadian characterisation of the *Dao* knockout (*Dao*$^{-/-}$) mouse. We expected to observe SCRD in this model, for a number of reasons. Firstly, *Dao*$^{-/-}$ mice display a robust anxiety phenotype (see Chapter 2), and there is evidence of a bidirectional relationship between anxiety and sleep and circadian function in rodents. In one direction, sleep deprivation alters behaviour in standard tests of anxiety such as the elevated plus maze [687], while in the other, exposure to environmental stressors impacts on subsequent sleep, particularly REM sleep [688-690]. In addition, mice selectively bred to show high trait anxiety demonstrate sleep irregularities such as increased dark phase sleep and increased sleep fragmentation in 12:12 LD [691]. They also display circadian abnormalities such as increased activity fragmentation in 12:12 LD and DD, and increased period length in DD [692]. SCRD has also been observed in mice selectively bred to show high stress reactivity [693, 694].

Secondly, through its modulation of NMDAR-mediated neurotransmission [499, 501], DAO has the potential to influence inputs to the SCN, the function of the SCN itself, and the outputs of the SCN. At the level of the retina, bipolar cells send excitatory glutamatergic inputs to retinal ganglion cells [584], which express NMDA receptors, as well as a range of other ionotropic and metabotropic glutamate receptors [695]. Consequently, the application of D-serine enhances light-evoked, NMDAR-mediated synaptic currents in the retinal ganglion cells of rats, while the application of SRR inhibitors or DAO attenuates these currents, presumably via a reduction in D-serine levels [696-698]. Likewise, D-serine administration enhances glutamate-induced calcium influx in retinal ganglion cells [699]. D-serine and its synthesising enzyme, SRR, are located in Müller cells and astrocytes (two types of glial cell) in the rodent retina [697], while it has been known for several decades that DAO is expressed in the Müller cells of amphibians [700, 701]. By contrast, it was only very recently that retinal DAO activity was first reported in mice [487]. This activity is restricted to the inner plexiform layer, which, appropriately, is the region in which retinal ganglion cells receive bipolar cell input via their NMDAR-containing dendrites. In the same study, it was confirmed that retinal D-serine concentration is significantly elevated in ddY/*Dao*$^{-}$ mice relative to wildtype controls [487].

In turn, the axons of retinal ganglion cells – collectively known as the retinohypothalamic tract (RHT) – synapse directly with SCN neurons [186, 187]. Together with PACAP, glutamate is the principal neurotransmitter at these synapses, and mediates the transduction of light information from the retina to the SCN [188-193]. The evidence for this is fivefold [180, 702-704]: (1) glutamate is released in the SCN upon electrical stimulation of the RHT; (2) RHT terminals innervating the SCN show glutamate immunoreactivity; (3) a variety of ionotropic and metabotropic glutamate receptors are expressed in the SCN; (4) the administration of glutamate or NMDA activates SCN neurons and mimics the effect of light by inducing phase

shifts in rest-activity rhythms; and (5) the administration of NMDAR antagonists blocks light-induced phase-shifts in rest-activity rhythms. More specifically, the NMDAR antagonists MK-801 and CPP block the phase-shifting effects of light on the wheel-running rhythms of mice and hamsters [189, 705], and prevent the light-induced expression of the immediate early gene *c-Fos* within the SCN [188, 706]. Recently, the importance of glutamatergic signalling from intrinsically photosensitive retinal ganglion cells (ipRGCs) to the SCN was confirmed with the generation of mice lacking vesicular glutamate transporter 2 expression in these cells [707, 708]. This manipulation prevents ipRGCs from packaging glutamate into synaptic vesicles, and results in impaired entrainment to a 12:12 LD cycle, slower re-entrainment after a 6 h phase advance or delay, attenuated negative masking and an absence of light induced phase delays [707, 708]. Based on this accumulated evidence, and since D-serine is an NMDAR co-agonist, we expected *Dao*$^{-/-}$ mice to demonstrate increased sensitivity to the circadian effects of light (i.e. increased phase-shifting and negative masking in response to nocturnal light pulses), together with more rapid re-entrainment following a 6 h phase advance in a standard 12:12 LD cycle.

The SCN contains a variety of neurotransmitters, including GABA, galanin, and serotonin, together with a range of neuropeptides including arginine vasopressin and vasoactive intestinal polypeptide [709]. It is well established that glutamate is involved in inputs to the SCN (see above) and outputs from it (see below), but there is little evidence that glutamate is involved in inter-neuronal signalling within the SCN [710]. However, recent evidence challenges this dogma. Glutamatergic signalling is important for bilateral communication between the left and right SCN, as this is impaired by the AMPA receptor antagonist CNQX [711]. There is also unpublished data which indicates that glutamatergic neurotransmission may be important to neuronal synchrony within the SCN; the inhibition of the glutamate transporter EAAT reduces

glial glutamate uptake and de-synchronises the firing of neighbouring SCN neurons [Marco Brancaccio, *unpublished data*].

DAO inactivation could also affect the glutamatergic outputs of the SCN. During the dark phase, for example, the SCN stimulates the paraventricular nucleus (PVN) via glutamatergic efferents, which in turn promotes melatonin synthesis in the pineal gland [712-716]. Consistent with this, dark phase administration of the NMDAR antagonist MK-801 (both systemic and intra-PVN) inhibits pineal melatonin production [715, 717]. The SCN may also influence the sleep-wake cycle via a small number of direct glutamatergic projections to the VLPO [718-720], the primary inhibitor of the ascending arousal system. (However, most input to the VLPO from the SCN is thought be indirect, as described in section 1.5.3.). It is not known if DAO is expressed in the PVN or the VLPO, so it is uncertain whether these mechanisms are likely to be disrupted in *Dao*$^{-/-}$ mice. However, light-induced *c-Fos* expression in the VLPO is significantly increased in ddY/*Dao*$^{-}$ mice relative to wildtype mice [Melanie Sobczyk, *unpublished data*], which suggests that it might be expressed in the VLPO. (Note that *c-Fos* induction in the VLPO is a normal response to a light pulse [290, 721, 722]). Finally, it should be noted that glutamate release in the prefrontal cortex displays rhythmic fluctuations during the sleep-wake cycle; it increases during wakefulness and REM sleep episodes, but decreases during non-REM sleep [723-725].

A further reason to expect SCRD in *Dao*$^{-/-}$ mice is that altered rest-activity rhythms have previously been observed in ddY/*Dao*$^{-}$ mutant mice [Melanie Sobczyk, *unpublished data*]. Relative to wildtype mice, ddY/*Dao*$^{-}$ mutants show less robust rest-activity rhythms, as determined with running wheels (see Table 5.1.). The wheel-running rhythms of ddY/*Dao*$^{-}$ mice are characterised by increased light phase activity (relative to wildtype mice), and

increased activity fragmentation. In addition, ddY/*Dao*$^{-}$ mutants demonstrate increased free-running period length in constant dark, and are quicker to re-entrain following a 6-hr phase advance in a 12:12 LD cycle. They also display increased period lengthening in constant light, and greater activity suppression in constant light, both of which are indicative of increased sensitivity to the circadian effects of light. Somewhat counterintuitively, ddY/*Dao*$^{-}$ mice show *reduced* activity suppression during type II phase-shifting light pulses. The magnitude of the phase delays induced by type II light pulses is unaltered in ddY/*Dao*$^{-}$ mice.

Light Schedule(s)	Capacity under Investigation	Observation in ddY/*Dao*$^{-}$ mice
12:12 LD	Entrainment	Increased light phase activity
6-hr phase advance in 12:12 LD	Speed of re-entrainment	Quicker re-entrainment
DD	Free-running period length	Increased period length
LL	Activity suppression	Enhanced activity suppression
	Period lengthening	Greater period lengthening
Type II phase-shifting light pulse	Activity suppression	Reduced activity suppression
	Size of phase delay	No effect
All light schedules	Activity fragmentation	Increased fragmentation

Table 5.1. The circadian phenotype of (male) ddY/*Dao*$^{-}$ mutant mice [Melanie Sobczyk, *unpublished data*]. Phenotyping was performed with running wheels.

5.2. Methods

5.2.1. Animals

Dao knockout mice were generated as described in Chapter 2. Age-matched males were used in all experiments. Only males were tested due to the potentially confounding influence of the oestrus cycle on wheel-running activity [592]. Three cohorts of mice participated in sleep and circadian screening. Cohorts 1 and 2 completed a wheel-running (circadian) screen prior to a video-tracking (sleep) screen, while cohort 3 was subjected to EEG-based sleep analysis only. Cohorts 1 and 2 both consisted of 12 mice (6 male $Dao^{+/+}$ mice and 6 male $Dao^{-/-}$ mice), while cohort 3 was comprised of 6 mice (3 male $Dao^{+/+}$ mice and 3 male $Dao^{-/-}$ mice). Mice in cohorts 1 and 2 were at least 2 months old at the onset of behavioural screening, and no older than 9 months upon completion of testing. Mice in cohort 3 were 13 to 16 weeks (i.e. 3 to 4 months) old when they underwent surgery, and sleep analysis was performed on a single day approximately two weeks later. Mice were singly-housed throughout testing (as is necessary for sleep and circadian screening), and had access to food and water *ad libitum*. All behavioural procedures were performed in accordance with the United Kingdom Animals (Scientific Procedures) Act of 1986 and the University of Oxford Policy on the Use of Animals in Scientific Research. All experiments were approved by the University of Oxford Animal Welfare and Ethical Review Board, and were conducted under the PPL 30/2812 by PILs ICC0614BD (formerly 30/9339) and I459D3D59.

5.2.2. Wheel-running (circadian) analyses

This screen was based on an established protocol [309, 311, 355]. Only cohorts 1 and 2 were tested. Mice were individually housed in large cages (44 cm long × 26 cm wide × 12 cm high) fitted with running wheels (18 cm diameter), positioned within light-tight chambers (LTCs), illuminated by an overhead cool white LED light-source. Illuminance was 100 lux at the base of each cage. LTCs were maintained at constant temperature (21°C) and humidity (50%). Each LTC contained 6 cages, with 3 mice of each genotype housed in alternating positions. Cohort 1 was exposed to the following light schedules (see Fig. 5.1): 14 days of 12:12 h light/dark (12:12 LD), a 6 h phase advance during 12:12 LD, 11 days of constant dark (DD), and 7 days of constant light (LL). Cohort 2 was exposed to 12:12 LD only.

Activity levels (i.e. wheel rotations) were recorded with the software package ClockLab (Actimetrics, Illinois, USA). Standard circadian parameters were extracted from the raw wheel-running data using the ClockLab toolbox (Actimetrics, Illinois, USA) for MatLab (MathWorks, Massachusetts, USA). Average daily activity counts (i.e. wheel rotations) provided a measure of spontaneous locomotor activity. Circadian rhythm fragmentation was also assessed, given evidence of increased activity fragmentation in schizophrenia [349]. Fragmentation was estimated by calculating the average number of activity bouts (maximum gap: 18 min; threshold: 5 counts/min) per day. Intradaily variation provided another indicator of fragmentation; this non-parametric measure quantifies the frequency and extent of transitions between rest and activity within each 24 h period [309].

To assess entrainment during 12:12 LD, multiple parameters were extracted: onset tau (henceforth referred to as period length), onset tau error, alpha, chi-square periodogram amplitude, phase of entrainment, relative light phase activity, and interdaily stability. Interdaily

stability is a non-parametric measure that quantifies the consistency of activity patterns across multiple days [310]. Period length was also computed under constant dark conditions (DD). Period length in constant light (LL) was calculated manually by extrapolation (see Fig. 5.5D), since activity levels were too low to use the automated method based on activity onsets. Re-entrainment following the 6 h phase advance was scored manually from individual actograms as the number of days taken to re-entrain. Note that interdaily stability and intradaily variation were computed using Actiwatch Activity & Sleep Analysis 7 (Cambridge Neurotechnology, Cambridge, UK).

Cohort 1 was also subjected to a type II phase-shifting light pulse [726] (using a previously described protocol [309, 727]) to induce a phase delay in their wheel-running rhythms, providing an indication of circadian photosensitivity. Mice were exposed to 100 lux light for one hour at zeitgeber time (ZT) 16 during a standard 12:12 LD cycle. (ZT0 refers to the onset of the light phase, while ZT12 denotes the onset of the dark phase). Following the pulse, mice were released into DD. The magnitude of the phase delay was quantified by fitting one regression line through 6 consecutive activity onsets preceding the light pulse, and another through 6 consecutive activity onsets following the pulse. The first activity onset following the light pulse was disregarded because of possible transition effects [309]. The magnitude of the phase delay was calculated as the time difference between the two regression lines on the first day after the light pulse. Negative masking – percent activity suppression induced by the light pulse – was also calculated, yielding an additional measure of circadian photosensitivity [728]. This parameter was computed by comparing the number of activity counts during the light pulse with the average number of counts during the same time window (ZT16-17) across the previous 3 days.

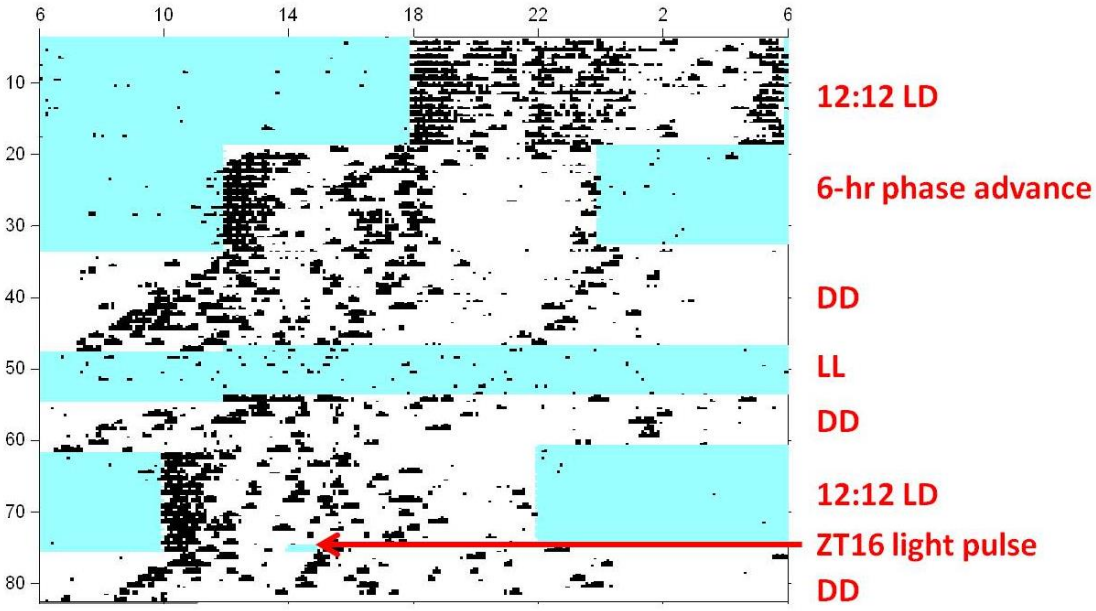

Figure 5.1. Representative wheel-running actogram of a *Dao*$^{+/+}$ mouse progressing through the various light schedules of the wheel-running (circadian) screen. The x-axis denotes clock-time in hours, while the y-axis denotes time in days. The blue and white shading corresponds to periods of light and dark, respectively. The black bars denote periods of wheel-running activity, presented in 6 min epochs. The height of the bars corresponds to the number of wheel rotations within each epoch.

Parameter	Units	Definition
Daily activity	Wheel rotations	The average number of activity counts occurring in the complete 24 h cycle. An activity count corresponds to one revolution of the cage wheel.
Daily activity bouts	Bouts	Activity bouts were quantified using predefined criteria (maximum gap: 18 min; threshold: 5 counts/min)
Activity bout durations	min	The average length of activity bouts.
Intradaily variation	AU	A non-parametric circadian variable which quantifies the fragmentation of the rhythm; i.e. the frequency and extent of transitions between rest and activity [310]. The higher this value, the more fragmented the rhythm.
Period length (onset tau)	h	Circadian period length (tau), derived from activity onsets.
Onset tau error	h	A measure of period consistency/stability, derived from automatically positioned activity onsets.
Alpha	h	The length of the animal's active phase.
Chi-square periodogram amplitude	AU	A measure of period consistency/stability. Corresponds to the peak of the chi-square periodogram curve [729].
Phase of entrainment	h	A measure of the accuracy of entrainment. Corresponds to the average amount of time separating the onset of the dark phase and the onset of wheel-running activity.
Relative light phase activity	%	The proportion of total activity occurring in the light phase of the 24 h cycle.
Interdaily Stability	AU	A non-parametric circadian variable, which quantifies the stability of the rhythm across multiple days; i.e. the consistency of the waveform [310]. The higher this value, the more consistent the rhythm.

Table 5.2. A description of the various circadian parameters computed for each mouse during the 12:12 LD light schedule of the circadian wheel-running screen. All circadian parameters were calculated using the ClockLab toolbox (Actimetrics, Illinois, USA) for MatLab (MathWorks, Massachusetts, USA), with the exception of the two non-parametric circadian variables (interdaily stability and intradaily variation), which were calculated with the software package Actiwatch Activity & Sleep Analysis 7 (Cambridge Neurotechnology, Cambridge, UK). AU = arbitrary units.

5.2.3. Video-tracking (sleep) analyses

Video-tracking analyses were based on an established protocol (see Fig. 5.2.) [307]. Only cohorts 1 and 2 were tested. At the end of the wheel-running screen, mice were entrained to a 100 lux 12:12 LD cycle for 14 days and then transferred to identically-sized cages (without running wheels) in new light-tight chambers (see Fig. 5.3). Housing conditions were otherwise identical to that of the wheel-running protocol described above. A standard 12:12 h light/dark (12:12 LD) cycle was employed and illuminance was 100 lux at the base of each cage. Recording began within 48 h of the transfer to the new cage. A single 12:12 LD cycle was recorded with a near-infrared CCTV camera (Maplin Electronics, Rotherham, UK), at 3 frames per second, in the AVI file format. An acrylic block was placed under the food hopper to keep the mouse in the recording field at all times.

Video files were stored on a digital hard drive recorder (Samsung, Suwon, South Korea) prior to analysis with ANY-maze 4.5 (Stoelting, Wood Dale, Illinois). Multiple immobility-determined sleep parameters were extracted from the video footage: total sleep time, light and dark phase sleep time, total sleep bouts, and light and dark phase sleep bouts. Sleep was defined as a period of immobility of at least 40 s, a previously established proxy measure of sleep [307]. This measure has an extremely high concordance (>95%) with electroencephalography (EEG)-based sleep determination [307]. Immobility sensitivity was set at 95% to prevent the detection of movements caused by breathing during sleep. Note that sleep time is expressed as a percentage of recording time. In addition to the sleep parameters outlined above, three activity parameters were extracted from the video footage using ANY-maze 4.5: total activity, light phase activity, and dark phase activity (distance travelled in metres).

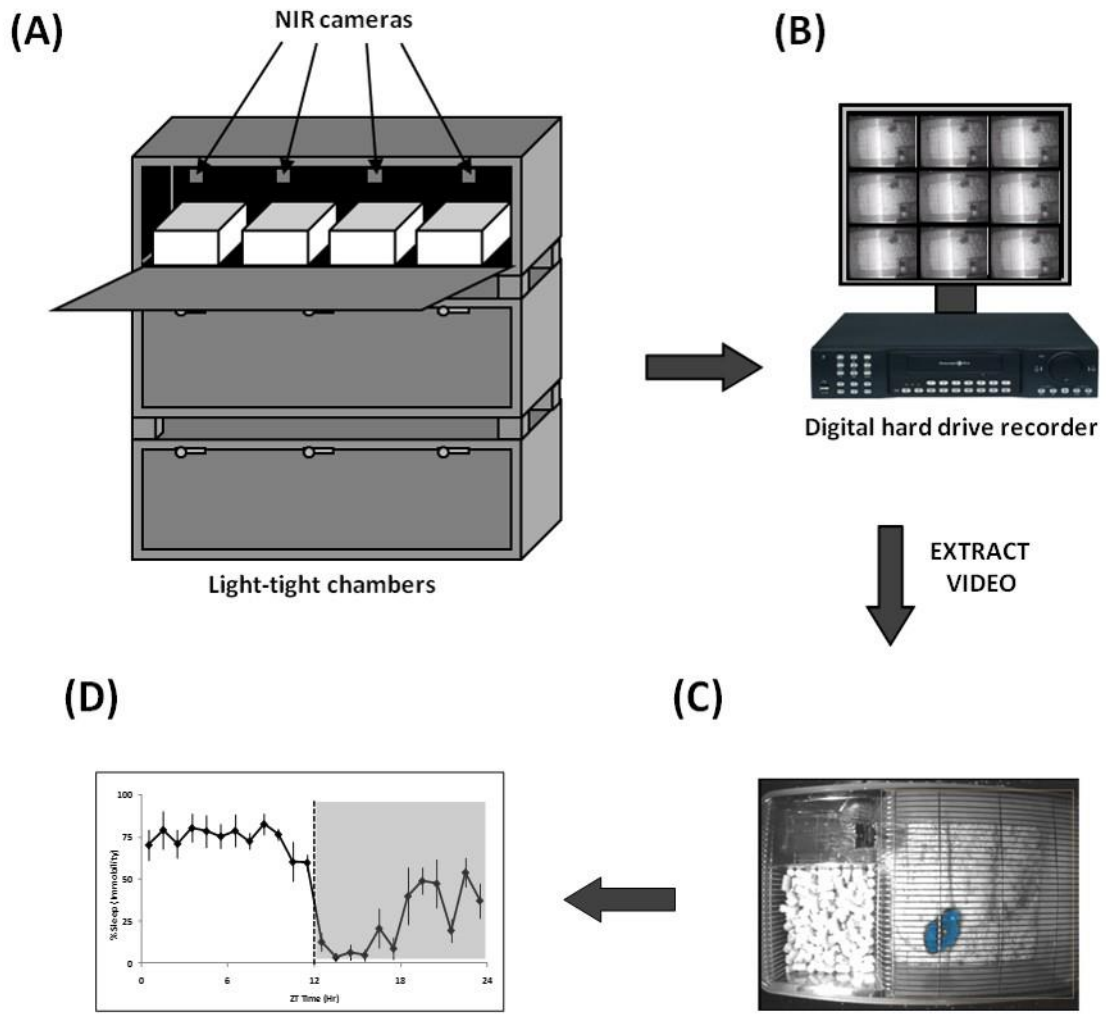

Figure 5.2. Experimental procedure for the video-tracking (sleep) screen. (A) Locomotor activity was monitored continuously over a 24 h recording period, using a small, near-infrared (NIR) camera fitted above each cage. In reality, 6 cages were housed within each light-tight chamber. (B) The resulting video data was stored on a digital hard drive recorder. (C) These files were subsequently analysed using the software package ANY-maze 4.5 (Stoelting, Wood Dale, Illinois). (D) Multiple immobility-determined sleep parameters were extracted from the video footage.

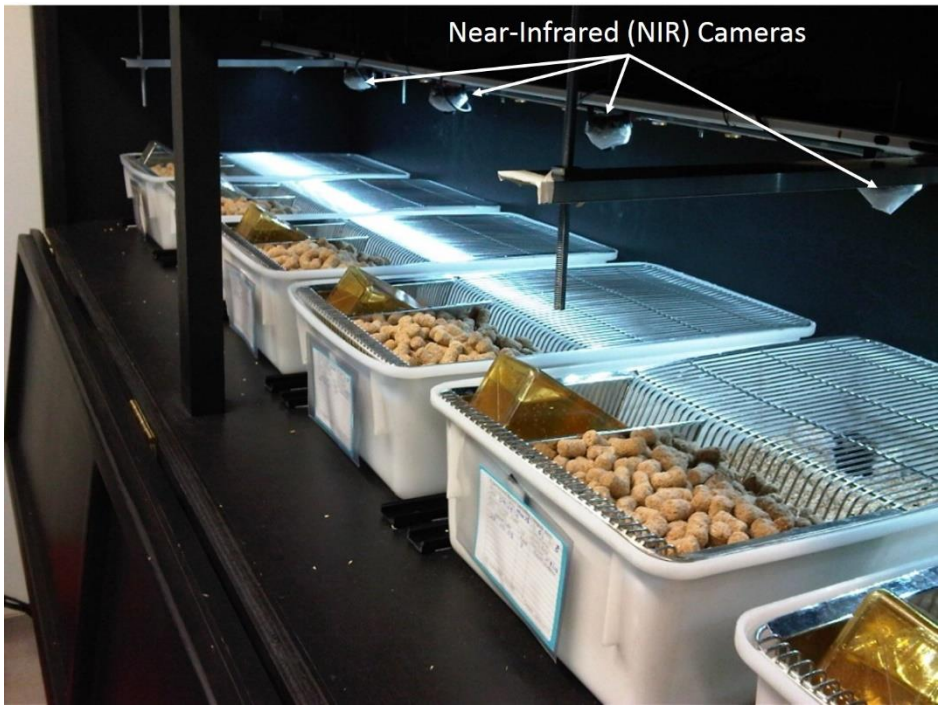

Figure 5.3. Photograph of a single light-tight chamber (LTC) containing singly-housed mice in large cages (44 cm long × 26 cm wide × 12 cm high). LTCs were illuminated by an overhead cool white LED light-source. Illuminance was 100 lux at the base of each cage. LTCs were maintained at constant temperature (21°C) and humidity (50%). Each LTC contained 6 cages, with 3 mice of each genotype housed in alternating positions.

5.2.4. EEG-based (sleep) analyses

Since immobility-determined sleep analyses do not distinguish rapid eye movement (REM) and non-REM (NREM) sleep, EEG-based sleep analyses were performed in an additional cohort of mice (cohort 3). Six adult male mice (*Dao*$^{+/+}$: *n* = 3; *Dao*$^{-/-}$: *n* = 3; 3 to 4 months old) were implanted with a telemetric transmitter (volume: 1.9 cm^3; total weight: 3.9 g; TL11M2-F20-EET; DSI, St. Paul, MN, USA) connected to EEG and electromyography (EMG) electrodes, as described previously [730]. Surgery was performed under anaesthesia (isoflurane induction: 4.5 %; maintenance: 0.7–2.25 %). Two stainless-steel EEG electrodes (screw shaft length: 2.4 mm; screw thread outer diameter: 1.19 mm) were implanted epidurally over the right frontal and right parietal cortices (see Fig. 5.4) [315], and connected to the telemetric transmitter with medical-grade stainless-steel wires encased in silicone tubing. The EEG electrodes and connections to the subcutaneous wiring were covered with dental cement (RelyX Arc, Kent Express, Kent, UK). Two stainless-steel EMG leads were inserted into the neck muscle ~5 mm apart and sutured in place. The telemetric transmitter was inserted into the peritoneal cavity. Perioperative analgesics were administered at the onset of surgery (buprenorphine, 0.1 mg/kg; meloxicam, 5 mg/kg), and on the following day (meloxicam, 5 mg/kg). Saline (0.9 %; 500 µl) was administered by subcutaneous injection immediately after surgery. Animals were given 12 to 15 days to recover after surgery, and the telemetric transmitters were activated 2 days prior to data collection. EEG/EMG signals were recorded continuously for 24 h, starting at light onset (ZT0), using the software package Dataquest ART (DSI). The EEG and EMG signals were filtered with high-pass (3 dB, 1.0 Hz) and low-pass anti-aliasing (49.5 Hz) analog filters. Wakefulness, REM sleep and NREM sleep were visually classified according to standard criteria [315], in 4 s epochs, without knowledge of the animal's genotype. Three parameters were extracted from the EEG/EMG data: total sleep time, REM sleep time, and NREM sleep time (all three are expressed as a percentage of recording time).

Note that surgeries were conducted by Sibah Hasan and Eric Tam, and sleep scoring was performed by Sibah Hasan.

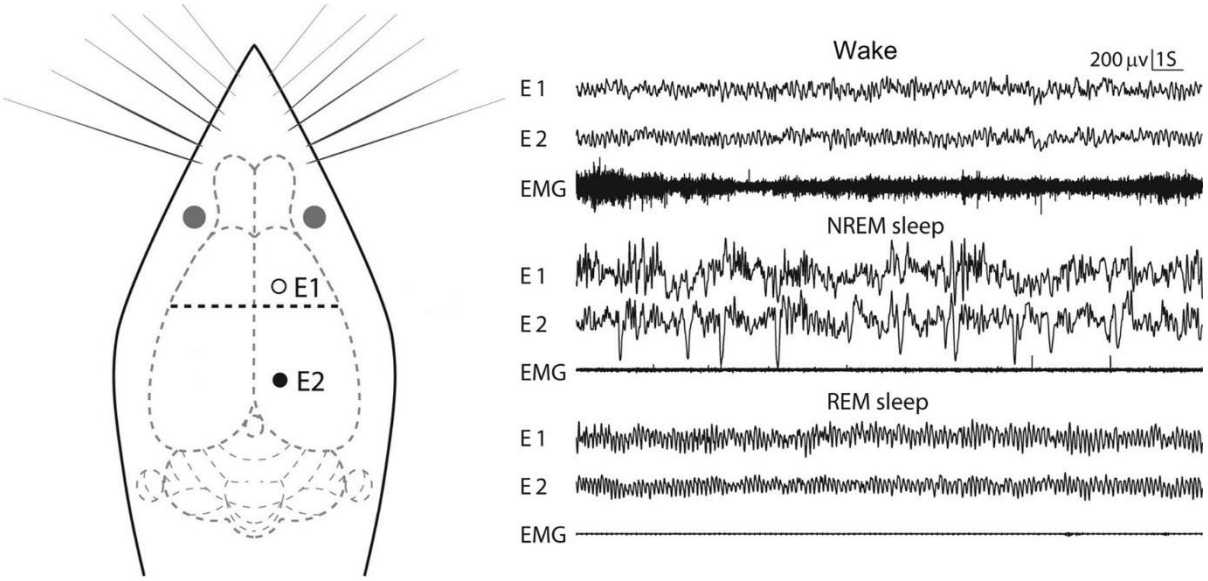

Figure 5.4. Electrode placements and 20 s of representative EEG–EMG traces of different sleep–wake stages for the two EEG electrodes. The horizontal dashed line in bold denotes the position of the bregma. E1 is the right frontal electrode (1.7 mm lateral to midline, 1.5 mm anterior to bregma). E2 is the right parietal electrode (1.7 mm lateral to midline, 3.2 mm posterior to bregma). EEG = electroencephalogram; EMG = electromyogram; REM = rapid eye movement; NREM = non-rapid eye movement. Figure adapted from Fang and colleagues [731].

5.2.5. Statistical analysis

All statistical analyses were performed with SPSS 22.0 (IBM, Armonk, New York). Unless otherwise stated, all reported statistics are the result of analyses of variance (ANOVAs), with genotype included as the independent variable, in addition to time bin where applicable. Differences were considered to be statistically significant at p-values < 0.05. Greenhouse-Geisser corrections were applied where appropriate, but uncorrected degrees of freedom are reported in order to preserve the transparency of the statistical design. For experiments involving multiple cohorts, further ANOVAs were conducted with cohort included as an extra independent variable. No additional effects or interactions were observed, so these data are not shown. In all figures, * indicates a p-value ≤ 0.05, ** indicates a p-value ≤ 0.01, and *** indicates a p-value ≤ 0.001. Error bars depict the standard error of the mean. $\underline{M}$ = mean.

5.3. Results

5.3.1. Wheel-running (circadian) analyses

Spontaneous locomotor activity in wheel-running cages was unaltered in *Dao*$^{-/-}$ mice; genotype had no effect on average daily activity counts under DD ($F_{1,10}$ = 1.484, P = 0.251), LL ($F_{1,10}$ = 3.122, P = 0.108) or 12:12 LD ($F_{1,22}$ = 0.033, P = 0.858). (Note that mean values for all circadian analyses are included in Table 5.3 and Table 5.4). Furthermore, the temporal distribution of activity over the 24 h day was almost identical in *Dao*$^{+/+}$ and *Dao*$^{-/-}$ mice under 12:12 LD (Fig. 5.5A).

There was also no evidence of altered circadian rhythm fragmentation in *Dao*$^{-/-}$ mice; genotype had no effect on average daily activity bouts in either DD ($F_{1,10}$ = 0.991, P = 0.343), LL ($F_{1,10}$ = 4.140, P = 0.069) or 12:12 LD ($F_{1,22}$ = 2.780, P = 0.110). Likewise, there was no difference in average bout duration in DD ($F_{1,10}$ = 0.726, P = 0.414), LL ($F_{1,10}$ = 2.253, P = 0.164) or 12:12 LD ($F_{1,22}$ = 0.181, P = 0.674). Intradaily variation – another measure of circadian fragmentation – was also unaffected by genotype in 12:12 LD ($F_{1,22}$ = 1.158, P = 0.294).

Dao$^{+/+}$ and *Dao*$^{-/-}$ mice were equally able to entrain to a standard 12:12 LD cycle (Fig. 5.5A & 5.5B). In 12:12 LD, genotype had no effect on period length, onset tau error, alpha, chi-square periodogram amplitude, phase of entrainment, relative light phase activity, or interdaily stability (see Table 5.3). Similarly, *Dao*$^{+/+}$ and *Dao*$^{-/-}$ mice were equally able to adjust to a shift in the light/dark cycle. Following a 6 h phase advance in 12:12 LD, genotype had no effect on the number of days required for re-entrainment ($F_{1,10}$ = 0.031, P = 0.864).

Finally, there was no evidence of altered photosensitivity in *Dao*$^{-/-}$ mice. When exposed to a type II phase-shifting light pulse from ZT16 to ZT17, percent activity suppression (negative

masking) was comparable in *Dao*$^{+/+}$ and *Dao*$^{-/-}$ mice ($F_{1,9}$ = 1.354, P = 0.274), as was the magnitude of the phase delay induced by the light pulse ($F_{1,7}$ = 0.318, P = 0.590). Similarly, genotype had no effect on free-running period length in either DD ($F_{1,10}$ = 0.330, P = 0.579, Fig. 5.5C) or LL ($F_{1,10}$ = 1.160, P = 0.307; Fig. 5.5D).

Parameter	*Dao*$^{+/+}$ (mean ± SEM)	*Dao*$^{-/-}$ (mean ± SEM)	p-value
Daily activity (wheel rotations)	5289 ± 1023	5504 ± 603	0.858
Daily activity bouts	5.6 ± 0.6	6.8 ± 0.4	0.110
Activity bout duration (min)	48 ± 7	52 ± 6	0.674
Intradaily variation (AU)	1.53 ± 0.08	1.66 ± 0.09	0.294
Period length (h)	24.02 ± 0.03	24.00 ± 0.01	0.347
Onset tau error (h)	0.82 ± 0.37	0.28 ± 0.10	0.172
Alpha (h)	10.98 ± 0.81	12.26 ± 0.32	0.156
Chi-square periodogram amplitude (AU)	1177 ± 100	1198 ± 91	0.883
Phase of entrainment (h)	0.074 ± 0.022	0.086 ± 0.021	0.691
Relative light phase activity (%)	4.8 ± 1.0	6.1 ± 1.9	0.527
Interdaily stability (AU)	0.63 ± 0.06	0.71 ± 0.05	0.326

Table 5.3. Descriptive statistics for selected wheel-running (circadian) parameters. Statistics are derived from 14 consecutive days of recording under a 12:12 h light/dark (12:12 LD) cycle at 100 lux. Sample size is 12 for *Dao*$^{+/+}$ mice and 12 for *Dao*$^{-/-}$ mice in all analyses. Units of measurement are indicated in brackets. AU = arbitrary units. SEM = standard error of the mean.

Parameter	*Dao*$^{+/+}$ (mean ± SEM)	*Dao*$^{-/-}$ (mean ± SEM)	p-value
Daily activity in DD (wheel rotations)	2854 ± 748 (*n* = 6)	4150 ± 756 (*n* = 6)	0.251
Daily activity bouts in DD	4.4 ± 0.8 (*n* = 6)	5.2 ± 0.2 (*n* = 6)	0.343
Activity bout duration in DD (min)	44 ± 9 (*n* = 6)	54 ± 7 (*n* = 6)	0.414
Period length in DD (h)	23.77 ± 0.10 (*n* = 6)	23.69 ± 0.10 (*n* = 6)	0.579
Daily activity in LL (wheel rotations)	61 ± 15 (*n* = 6)	248 ± 105 (*n* = 6)	0.108
Daily activity bouts in LL	0.3 ± 0.2 (*n* = 6)	1.0 ± 0.3 (*n* = 6)	0.069
Activity bout duration in LL (min)	4 ± 2 (*n* = 6)	13 ± 6 (*n* = 6)	0.164
Period length in LL (h)	25.89 ± 0.23 (*n* = 6)	25.50 ± 0.27 (*n* = 6)	0.307
Days to re-entrain after a 6 h phase advance	4.7 ± 0.6 (*n* = 6)	4.5 ± 0.8 (*n* = 6)	0.864
Type II light pulse – negative masking (%)	81.3 ± 9.0 (*n* = 6)	93.3 ± 2.8 (*n* = 5)	0.274
Type II light pulse – phase delay (h)	0.86 ± 0.36 (*n* = 4)	0.63 ± 0.21 (*n* = 5)	0.590

Table 5.4. Descriptive statistics for selected wheel-running (circadian) parameters. Units of measurement and sample sizes are indicated in brackets. SEM = standard error of the mean.

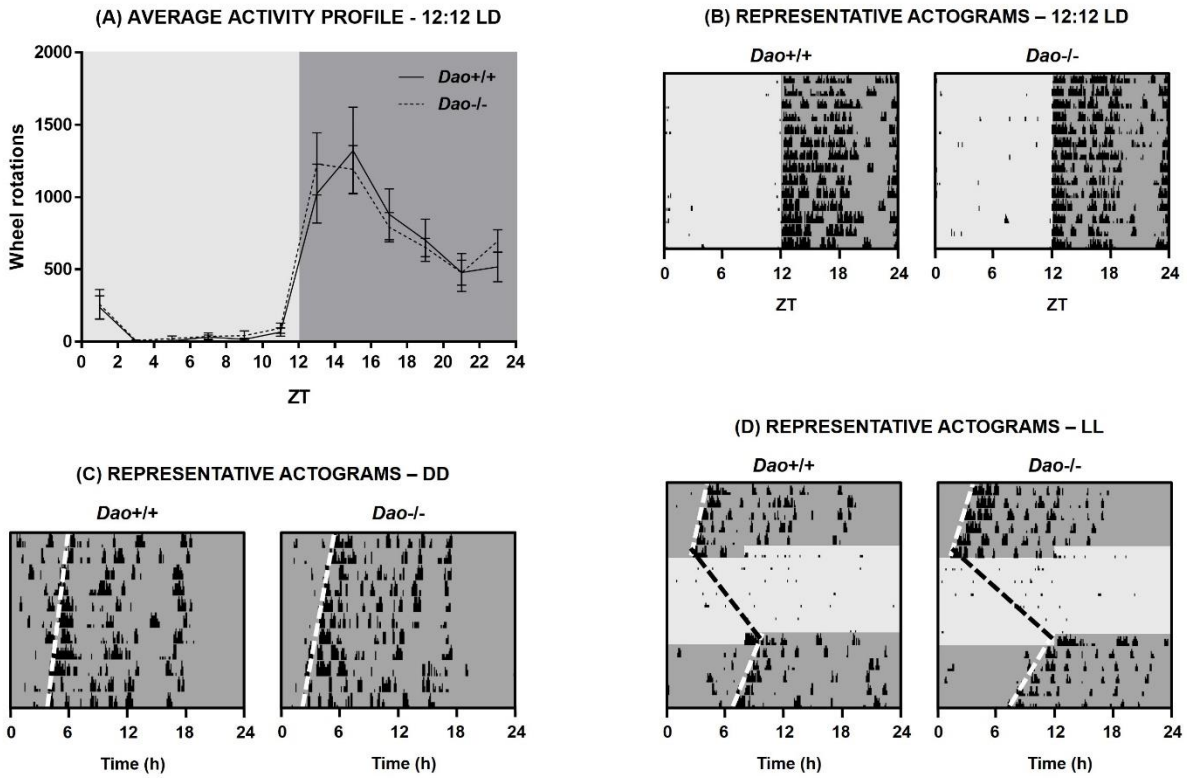

Figure 5.5. No evidence of circadian rhythm disruption in *Dao*$^{-/-}$ mice. (A) Average activity profiles for *Dao*$^{+/+}$ and *Dao*$^{-/-}$ mice during a 12:12 h light/dark (12:12 LD) cycle at 100 lux. Activity profiles are based on 14 consecutive days of wheel-running data. Data are presented in 2 h time bins. (B-D) Representative wheel-running actograms of *Dao*$^{+/+}$ and *Dao*$^{-/-}$ mice during 12:12 LD (Fig. 4B), constant dark (DD; Fig. 4C), and constant light (LL; Fig. 4D). Each row depicts a single 24 h period. The light and dark grey shading corresponds to periods of (100 lux) light and dark, respectively. The black bars denote periods of wheel-running activity, presented in 6 min epochs. The height of the bars corresponds to the number of wheel rotations within each epoch. ZT = zeitgeber time.

5.3.2. Video-tracking (sleep) analyses

These analyses revealed no evidence of altered sleep in *Dao*$^{-/-}$ mice. As expected, there was a significant main effect of time bin on sleep time, sleep bouts and distance travelled (*P*s = <0.001), but genotype had no effect on sleep time ($F_{1,22} = 0.028$, $P = 0.868$), sleep bouts ($F_{1,22} = 0.055$, $P = 0.816$), or distance travelled ($F_{1,22} = 0.210$, $P = 0.652$). With the light and dark phases considered in isolation, these variables still did not vary according to genotype (see Table 5.5). Moreover, the temporal distribution of immobility-determined sleep was broadly consistent between *Dao*$^{+/+}$ and *Dao*$^{-/-}$ mice (Fig. 5.6A). The same was true of the temporal distribution of sleep bouts (Fig. 5.6B). Consistent with this, there were no significant interactions between genotype and time bin for any of the dependent variables.

Parameter	*Dao*$^{+/+}$ (mean ± SEM)	*Dao*$^{-/-}$ (mean ± SEM)	p-value
Total sleep time (%)	55.0 ± 2.4	54.5 ± 2.0	0.868
Light phase sleep time (%)	69.0 ± 3.0	69.4 ± 1.9	0.907
Dark phase sleep time (%)	41.1 ± 2.3	39.6 ± 2.6	0.679
Total sleep bouts	274 ± 11	269 ± 16	0.816
Light phase sleep bouts	149 ± 7	144 ± 6	0.553
Dark phase sleep bouts	125 ± 10	126 ± 13	0.964
Total distance travelled (m)	112.9 ± 16.2	102.9 ± 15.0	0.652
Light phase distance travelled (m)	24.8 ± 4.7	24.5 ± 6.8	0.971
Dark phase distance travelled (m)	88.2 ± 14.3	78.4 ± 9.8	0.577

Table 5.5. Descriptive statistics for selected immobility-determined sleep parameters. Statistics are derived from 24 h of recording during a 12:12 h light/dark (12:12 LD) cycle at 100 lux. Sample size is 12 for *Dao*$^{+/+}$ mice and 12 for *Dao*$^{-/-}$ mice in all analyses. Units of measurement are indicated in brackets. SEM = standard error of the mean.

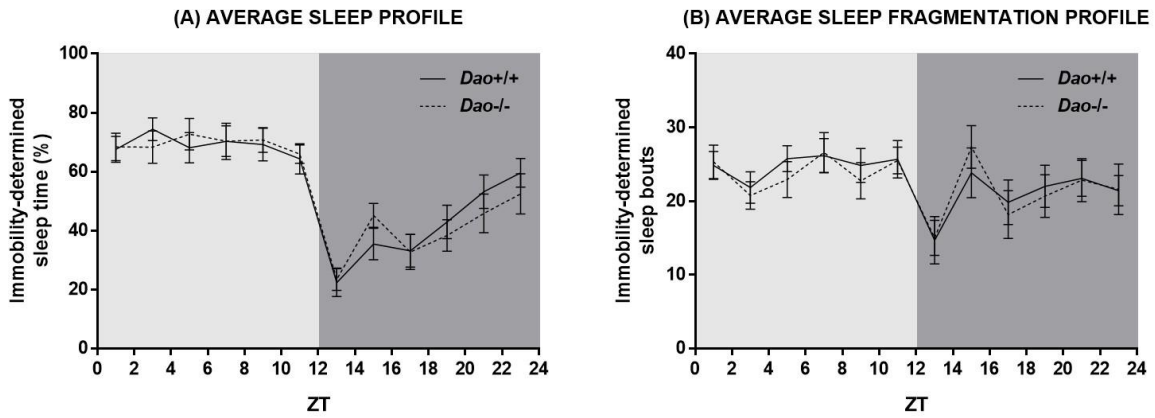

Figure 5.6. No evidence of sleep disruption in *Dao*$^{-/-}$ mice. (A) Average immobility-determined sleep profiles for *Dao*$^{+/+}$ and *Dao*$^{-/-}$ mice during a 12:12 h light/dark (12:12 LD) cycle at 100 lux. (B) Average temporal distribution of immobility-determined sleep bouts in *Dao*$^{+/+}$ and *Dao*$^{-/-}$ mice during 12:12 LD. A sleep bout was defined as a period of immobility of at least 40 s. All plots are based on 24 h of data, presented in 2 h time bins. ZT = zeitgeber time.

5.3.3. EEG-based (sleep) analyses

Immobility-determined sleep analyses do not differentiate REM and NREM sleep. Hence, although we witnessed no difference in total sleep duration between *Dao*$^{+/+}$ and *Dao*$^{-/-}$ mice, the possibility exists that REM sleep is reduced and NREM sleep increased in *Dao*$^{-/-}$ mice, or vice versa. To investigate this possibility, EEG-based sleep analyses were performed. Again, we found no evidence of altered sleep in *Dao*$^{-/-}$ mice. As expected, there was a significant main effect of time bin on total sleep, REM sleep and NREM sleep time (*P*s = <0.001), but genotype had no effect on total sleep ($F_{1,4}$ = 1.472, P = 0.292), REM sleep ($F_{1,4}$ = 0.131, P = 0.735), or NREM sleep time ($F_{1,4}$ = 2.658, P = 0.178). These variables still did not vary according to genotype when the light and dark phases were considered separately (see Table 5.6). Furthermore, the temporal distribution of EEG-determined sleep was broadly consistent between *Dao*$^{+/+}$ and *Dao*$^{-/-}$ mice (Fig. 5.7A). The same was true of the temporal distribution of REM sleep (Fig. 5.7B) and NREM sleep (Fig. 5.7C). Consistent with this, there were no significant interactions between genotype and time bin for any of the dependent variables.

Parameter	*Dao*$^{+/+}$ (mean ± SEM)	*Dao*$^{-/-}$ (mean ± SEM)	p-value
Total sleep time (%)	50.0 ± 1.4	52.1 ± 1.1	0.292
Light phase sleep time (%)	57.4 ± 4.3	65.1 ± 3.0	0.218
Dark phase sleep time (%)	42.6 ± 4.1	39.2 ± 4.7	0.606
Total REM sleep time (%)	10.0 ± 0.5	9.8 ± 0.4	0.735
Light phase REM sleep time (%)	12.3 ± 1.7	13.8 ± 0.7	0.440
Dark phase REM sleep time (%)	7.8 ± 1.1	5.8 ± 0.7	0.204
Total NREM sleep time (%)	40.0 ± 0.9	42.3 ± 1.2	0.178
Light phase NREM sleep time (%)	45.1 ± 2.8	51.3 ± 3.0	0.209
Dark phase NREM sleep time (%)	34.9 ± 3.0	33.4 ± 4.1	0.785

Table 5.6. Descriptive statistics for selected EEG-determined sleep parameters. Statistics are derived from 24 h of recording during a 12:12 h light/dark (12:12 LD) cycle at 100 lux. Sample size is 3 for *Dao*$^{+/+}$ mice and 3 for *Dao*$^{-/-}$ mice in all analyses. Units of measurement are indicated in brackets. SEM = standard error of the mean.

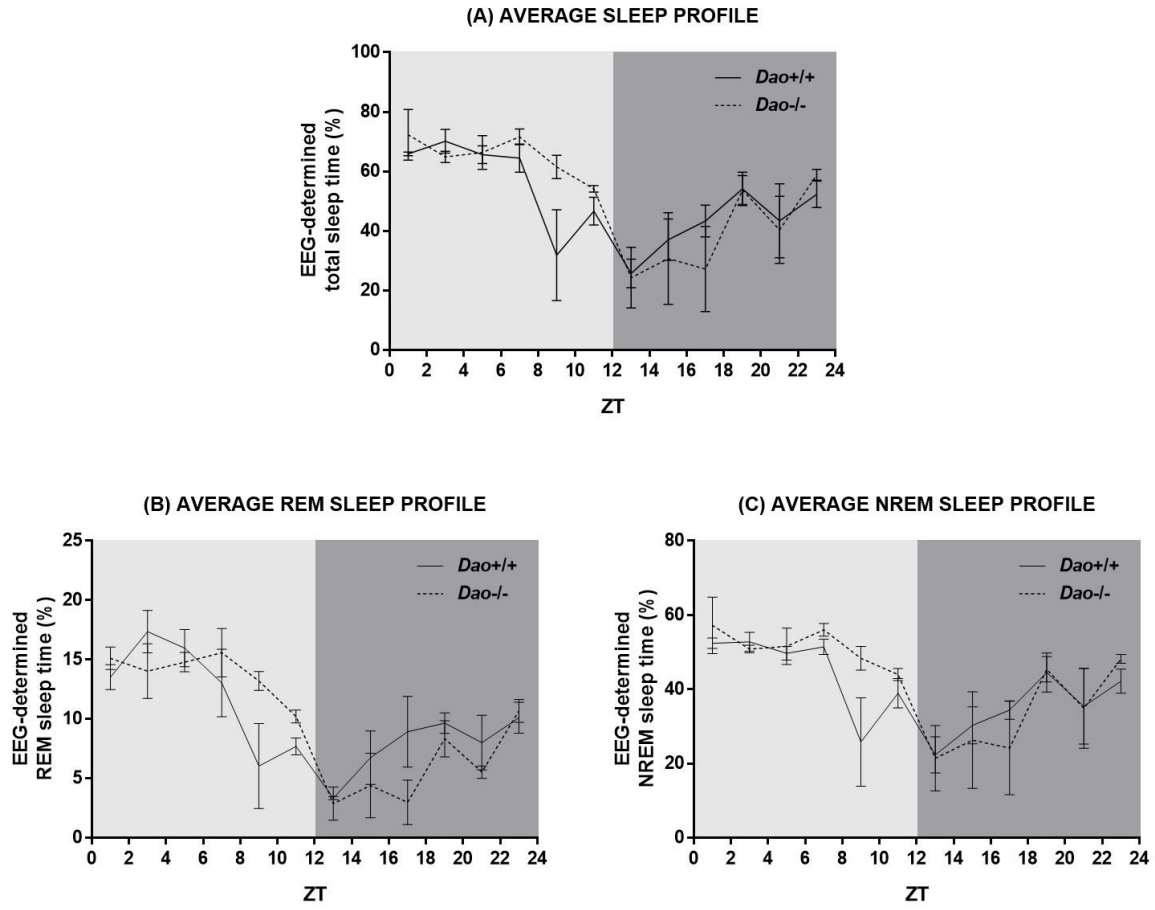

Figure 5.7. No evidence of sleep disruption in *Dao*$^{-/-}$ mice. (A) Average EEG-determined sleep profiles for *Dao*$^{+/+}$ and *Dao*$^{-/-}$ mice during a 12:12 h light/dark (12:12 LD) cycle at 100 lux. (B-C) Average EEG-determined REM sleep profiles (Fig. 5C) and NREM sleep profiles (Fig. 5D) for *Dao*$^{+/+}$ and *Dao*$^{-/-}$ mice during 12:12 LD. The increased variance at ZT8-10 was due to one *Dao*$^{+/+}$ mouse sleeping for only 2.7 % of this time bin. All plots are based on 24 h of data, presented in 2 h time bins. ZT = zeitgeber time.

5.4. Discussion

Contrary to our expectations, we found no evidence of circadian rhythm disruption in *Dao*$^{-/-}$ mice, as determined with running wheels, and no evidence of altered sleep, as assayed by video-tracking and EEG.

The relationship between anxiety and sleep and circadian rhythm disruption

In rodents, there is evidence of a bidirectional relationship between anxiety and sleep and circadian function, as outlined in the introduction to this chapter. In light of these findings, it was somewhat surprising to find no evidence of sleep or circadian rhythm disruption in *Dao*$^{-/-}$ mice, given their robust anxiety phenotype (see Chapter 2). Instead, our data indicate that altered sleep or circadian rhythms are neither a cause nor a consequence of the elevated anxiety seen in *Dao*$^{-/-}$ mice. More generally, our data reveal that sleep and circadian rhythm disruption are not inevitable correlates of heightened anxiety in mice.

DAO in the retina

Despite the fact that DAO has an established physiological role in the inner plexiform layer of the mammalian retina [487, 696, 697], the absence of a circadian phenotype in the *Dao*$^{-/-}$ mouse indicates that DAO is not essential for non-image-forming visual function. This is perhaps unsurprising given that circadian photoentrainment is resistant to dramatic retinal changes, including the complete ablation of rods and cones, which renders mice visually blind [732].

Interestingly, an altered electroretinography (ERG) profile was recently observed in ddY/*Dao*$^{-}$ mutant mice [Alun Barnard & Melanie Sobczyk, *unpublished data*], although this phenotype was not shared by *Dao*$^{-/-}$ mice [Alun Barnard, *unpublished data*]. Under scotopic (i.e. dim light) conditions, a-wave amplitude was significantly increased in ddY/*Dao*$^{-}$ mice relative to

wildtype controls, hinting at a previously-unreported role for DAO in rod photoreceptor function. Although DAO activity has been detected in the inner plexiform layer of the mouse retina [487], DAO *expression* has yet to be characterised in the mammalian retina. However, NMDAR subunits are known to be expressed in mammalian photoreceptor outer segments [733], photoreceptor terminals [734, 735], and rod bipolar cells [736-738].

Synapses between the retinohypothalamic tract and the suprachiasmatic nucleus

Another reason to evaluate circadian function in *Dao*$^{-/-}$ mice was that NMDARs play a critical role at the junction between the retinohypothalamic tract (RHT) and the SCN. Since the NMDAR antagonists MK-801 and CPP block the phase-shifting effects of light on the wheel-running rhythms of mice [189], we predicted that *Dao*$^{-/-}$ mice would demonstrate heightened sensitivity to the circadian effects of light. We found no evidence to support this hypothesis, suggesting that DAO does not modulate glutamatergic neurotransmission at RHT-SCN synapses. Indeed, although *Dao* is widely expressed in the brain [485], it is not known whether it is expressed in the SCN. *Dao* is certainly expressed in the hypothalamus of primates [739], while D-serine and D-alanine levels are significantly increased in the hypothalamus of ddY/*Dao*$^{-}$ mice [517]. However, both studies sampled the hypothalamus as a whole [517, 739], so these results cannot be generalised to specific sub-regions of the hypothalamus. In future, one could resolve this issue by quantifying *Dao* expression, DAO activity and/or D-serine concentration within SCN tissue.

Phenotypic comparison with the ddY/*Dao*$^{-}$ mutant *mouse*

In stark contrast to *Dao*$^{-/-}$ mice, ddY/*Dao*$^{-}$ mutant mice have a complex circadian phenotype, as outlined in the introduction to this chapter [Melanie Sobczyk, *unpublished data*]. Unfortunately, the rest-activity rhythms of ddY/*Dao*$^{-}$ mice have not been characterised in cages

lacking running wheels, with either video cameras or passive infrared (PIR) motion detectors. Hence, it is impossible to determine whether the complex rest-activity phenotype of the ddY/*Dao*$^{-}$ mouse is a reflection of underlying circadian dysregulation, or an artefact of the use of the running wheels. Another schizophrenia-relevant model, the *Grm2/3*$^{-/-}$ mouse, displays significantly perturbed wheel-running rhythms, but shows no evidence of circadian disruption in its general homecage activity (see Chapter 6). This issue could be easily resolved by testing ddY/*Dao*$^{-}$ mice in cages lacking running wheels. Additionally, one could establish whether the altered wheel-running behaviour of the ddY/*Dao*$^{-}$ mouse is accompanied by corresponding alterations in rhythmic clock gene expression or electrical activity within the SCN.

There are several possible explanations for the contrasting wheel-running phenotypes of the ddY/*Dao*$^{-}$ mouse and the *Dao*$^{-/-}$ mouse. Firstly, and perhaps most importantly, the two models utilise different background strains; the *Dao*$^{-/-}$ mouse is on a 129Sv/Ev background, while the ddY/*Dao*$^{-}$ is on a ddY background. The ddY strain is albino, and therefore has a radically altered visual system [740], which renders it unsuitable for longitudinal circadian screening, not least because of its increased vulnerability to light-induced retinal degeneration [741].

This problem is compounded by the fact that NMDAR overactivity is excitotoxic and causes retinal apoptosis [583], while levels of D-serine, an NMDAR co-agonist, are increased in the retina of ddY/*Dao*$^{-}$ mice [487]. Indeed, it has been shown that NMDAR-mediated retinal ganglion cell death in rats is exacerbated by D-serine administration, and suppressed by DAO administration [584]. Moreover, elevated D-serine contributes to retinal ganglion cell loss in a rodent model of diabetic retinopathy [742], leading to deficits in both image-forming and non-image-forming visual function [743]. In fact, NMDAR-related neurotoxicity may contribute to a range of retinopathies, including glaucoma and retinal ischaemia [584].

It is therefore possible that the ddY strain's innate vulnerability to retinal degeneration, together with increased retinal D-serine due to the genetic inactivation of DAO, triggers significant retinal degeneration in the inner plexiform layer, which would explain the irregular circadian phenotype of the ddY/*Dao*$^{-}$ mouse. Consistent with this account, light-induced retinal apoptosis is significantly increased in ddY/*Dao*$^{-}$ mice relative to wildtypes [Melanie Sobczyk, *unpublished data*]. To further validate this hypothesis, it would be necessary to quantify retinal cell density in a cohort of ddY/*Dao*$^{-}$ mice and wildtype controls. It would also be useful to confirm that retinal apoptosis and retinal cell density are not as dramatically altered in *Dao*$^{-/-}$ mice. Finally, it would make sense to characterise sleep and circadian rhythms in the *Dao1*^{G181R} mouse, which was created by transferring the point mutation in *Dao* from the ddY/*Dao*$^{-}$ mice to a C57BL/6J background. If circadian disruption in the ddY/*Dao*$^{-}$ mouse reflects an interaction between increased brain D-serine and the model's albinism, one would not expect to observe SCRD in the *Dao1*^{G181R} mouse, which possesses the same point mutation in *Dao* as the ddY/*Dao*$^{-}$ mouse, but is not on an albino background.

Another consideration is that knockout and mutant mice are rarely identical. The circadian gene *Clock* provides a good example of this; the semi-dominant *Clock* mutation lengthens circadian period and abolishes circadian rhythmicity [744], whereas *Clock* knockout mice continue to express robust circadian rhythms [745]. Hence, having a gene which is expressed partially and/or functions abnormally can sometimes have more deleterious effects than a complete knockout. Returning to the models described here, ddY/*Dao*$^{-}$ mutant mice show normal expression of a catalytically inactive DAO enzyme [499, 512, 513], whereas *Dao*$^{-/-}$ mice show no detectable expression or activity of DAO [534]. Hence, *Dao*$^{-/-}$ mice may be more prone to compensatory developmental changes, which 'rescue' their circadian phenotype. For example,

the absence of DAO might lead to a compensatory changes in the expression of the D-serine transporter *Asc-1*, the D-serine synthesising enzyme *Srr*, or the glycine transporter *GlyT1*. The expression of all three genes is unaltered in ddY/*Dao*$^{-}$ mice [499], but has yet to be assessed in *Dao*$^{-/-}$ mice. Contrary to this hypothesis, D-serine levels are elevated in the same brain regions in *Dao*$^{-/-}$ mice as they are in ddY/*Dao*$^{-}$ mice. D-serine concentration is significantly elevated in the cerebellum, hippocampus and hypothalamus of ddY/*Dao*$^{-}$ mice [472, 515-518]. Likewise, increased D-serine is evident in the cerebellum and hippocampus of *Dao*$^{-/-}$ mice [591,Pfizer Inc., *unpublished data*], while D-serine levels have yet to be quantified in the hypothalamus. A similar pattern has been reported in the *Dao1*^{G181R} mouse, although elevated D-serine is also seen in whole cortex (but not prefrontal cortex) [466]. As explained, sleep and circadian rhythms have yet to be characterised in this mouse.

Immobility-determined sleep has also been assessed in ddY/*Dao*$^{-}$ mice, although only for a single 24 h period in a relatively small sample (6 male wildtypes and 5 male mutants) [Melanie Sobczyk, *unpublished data*]. In contrast to their severely altered circadian phenotype, this analysis yielded no evidence of sleep disruption in ddY/*Dao*$^{-}$ mutants; sleep duration and fragmentation were both unaffected by genotype. Hence, the sleep phenotypes of *Dao*$^{-/-}$ and ddY/*Dao*$^{-}$ mice are more consistent than their circadian phenotypes.

Conclusions

We expected to observe significant SCRD in *Dao*$^{-/-}$ mice, given that (a) the glutamatergic system is implicated in sleep and circadian function at multiple levels; (b) NMDAR receptors are expressed in the retina, SCN, and distributed widely throughout the brain; and (c) upregulated NMDAR-mediated neurotransmission has previously been reported in *Dao* mutant mice [499, 501]. However, our results clearly demonstrate that the constitutive genetic ablation

of DAO has no impact on the sleep or rest-activity rhythms of 129Sv/Ev mice. This may reflect the fact that *Dao* is not expressed in brain regions which are critically involved in the regulation of sleep and circadian rhythms (e.g. the SCN, VLPO and PVN), and/or that DAO does not regulate D-serine concentration (and therefore glutamatergic function) in all of the areas in which it is expressed (as is the case in the frontal cortex; see Chapter 1). Another possibility is that the genetic ablation of *Dao* leads to compensatory changes in the expression of other genes, which prevent the excessive accumulation of D-serine in the brains of $Dao^{-/-}$ mice. Either way, the constitutive genetic ablation of *Dao* is clearly not the same as its reversible pharmacological inhibition; the approach that would be taken in schizophrenia patients. Hence, future studies should characterise sleep and circadian rhythms in conditional *Dao* knockout models, or in wildtype rodents subjected to chronic administration of a DAO inhibitor, such as sodium benzoate. The absence of SCRD in these models would tentatively suggest that pharmacological DAO inhibition should not exacerbate SCRD in schizophrenia patients. In the meantime, clinical trials involving DAO inhibitors should include indices of sleep and circadian function as a precautionary measure. Actigraphy and sleep polysomnography are prohibitively expensive, but sleep and activity questionnaires or diaries could easily be implemented at no additional cost.

6. Sleep, circadian and behavioural characterisation of the *Grm2/3*$^{-/-}$ mouse

6.1. Introduction

As outlined in Chapters 1 and 5, sleep and circadian rhythm disruption (SCRD) is common in schizophrenia patients [326]. Some of these abnormalities may be secondary to the disorder and its drug treatment, but the co-morbidity of schizophrenia and SCRD may also stem from dysfunction in common brain mechanisms (e.g. specific neurotransmitter systems) [125, 343]. The glutamate system is one such candidate mechanism, given strong evidence of glutamatergic dysfunction in schizophrenia (see section 1.2.5.) and given that altered glutamatergic neurotransmission could impact on sleep and circadian function at multiple levels (see section 5.1.).

At the receptor level, group II metabotropic glutamate receptors may be particularly relevant to the pathophysiology of schizophrenia (see section 1.10.2.). There is also increasing evidence that implicates group II metabotropic glutamate receptors in sleep and circadian function. Firstly, *Grm2* and *Grm3* are expressed in the SCN [702, 746]. mGlu2 and mGlu3 modulate NMDA-evoked calcium responses in SCN neurons, hinting at a possible role in photic entrainment [747]. Consistent with this, mGlu2/3-modulating drugs influence the magnitude of light-induced phase delays in the rest-activity rhythms of wildtype hamsters [748, 749]. Secondly, the administration of mGlu2/3-modulating drugs profoundly alters sleep structure in wildtype rats; both agonists and antagonists trigger a selective suppression of REM sleep [575-582]. The basal amygdala has been highlighted as a potential mediator of these effects [578]. Thirdly, an mGlu2/3 antagonist and an mGlu2 negative allosteric modulator increase sleep fragmentation in wildtype rats [576]. Finally, mGlu2 and/or mGlu3 may regulate the inhibitory

output of the thalamic reticular nucleus, which forms part of the ascending arousal system [750, 751].

This chapter describes the sleep and circadian characterisation of the *Grm2/3* double knockout (*Grm2/3*$^{-/-}$) mouse. Our aim was to provide additional evidence for the involvement of group II metabotropic glutamate receptors in the regulation of sleep and circadian rhythms. Based on the evidence described above, we predicted that *Grm2/3*$^{-/-}$ mice would demonstrate: (1) a reduction in total sleep duration; (2) increased sleep fragmentation; and (3) heightened sensitivity to the circadian effects of light (e.g. light-induced phase shifts of greater magnitude).

6.2. Methods

6.2.1. Animals

Grm2/3 double knockout (*Grm2/3*$^{-/-}$) mice were obtained from GlaxoSmithKline (Harlow, UK). These mice were generated as described previously [561]. Briefly, *Grm2* knockout mice (*Grm2*$^{-/-}$) [564] were crossed with *Grm3* knockout mice (*Grm3*$^{-/-}$) [752] to generate double heterozygous (*Grm2*$^{+/-}$*Grm3*$^{+/-}$) offspring. (Both single knockout models were on a C57Bl/6 background. GRM2$^{-/-}$ mice had been backcrossed onto the C57Bl/6 line for 21 generations, and GRM3$^{-/-}$ mice backcrossed onto C57Bl/6 for 11 generations). Double heterozygous mice were then crossed to generate 1:16 double knockout mice (*Grm2/3*$^{-/-}$), 1:16 wildtype mice (*Grm2/3*$^{+/+}$), and 14:16 mice that were heterozygous for *Grm2* and/or *Grm3*. Separate lines of *Grm2/3*$^{-/-}$ and *Grm2/3*$^{+/+}$ mice were subsequently established to avoid the prohibitive wastage of animals that would have resulted had all *Grm2/3*$^{+/+}$ and *Grm2/3*$^{-/-}$ mice been derived from double heterozygous crosses. After six generations, the *Grm2/3*$^{-/-}$ line was out-crossed onto C57Bl/6 mice in order to generate more double heterozygous mice. In turn, these mice were inter-crossed to produce new *Grm2/3*$^{+/+}$ and *Grm2/3*$^{-/-}$ lines. The animals used in this thesis were from the F2 - F6 generations of these separate lines. *Grm2/3*$^{-/-}$ mice exhibited normal development and longevity, although females did not breed if they were older than 3 months when first co-housed with a male. A genotyping protocol is included in Appendix 8.7.

Age-matched males were used in all experiments. Mice were at least 2 months old at the onset of sleep and circadian screening and were no older than 9 months upon completion of testing. Only males were tested due to the potentially confounding influence of the oestrus cycle on wheel-running activity [592]. Two cohorts of mice participated in sleep and circadian screening. Cohort 1 consisted of 11 *Grm2/3*$^{+/+}$ mice and 12 *Grm2/3*$^{-/-}$ mice, while cohort 2 was comprised of 12 mice of each genotype. For the experiment involving the administration of the

drug RO4432717 (F.Hoffmann-LaRoche, Basel, Switzerland), a separate cohort of 22 male wildtype C57Bl/6J mice was used (Harlan, UK). Mice were singly-housed throughout testing (as is necessary for sleep and circadian screening), and had access to food and water *ad libitum*. All behavioural procedures were performed in accordance with the United Kingdom Animals (Scientific Procedures) Act of 1986 and the University of Oxford Policy on the Use of Animals in Scientific Research. All experiments were approved by the University of Oxford Animal Welfare and Ethical Review Board, and were conducted under the PPL 30/2812 by PILs ICC0614BD (formerly 30/9339) and 30/8553.

6.2.2. Order of tests

Cohorts 1 and 2 completed an extensive wheel-running (circadian) screen consisting of several standard protocols (full details below). Video-tracking, passive-infrared motion detection and object interaction testing were only performed on cohort 2. The order of these tests was counterbalanced across genotype groups. Half of cohort 2 underwent video-tracking followed by PIR motion detection, then wheel-running, and finally object interaction testing. The other half of cohort 2 were subjected to PIR motion detection followed by video-tracking, then object interaction testing, and finally wheel-running.

6.2.3. Video-tracking (sleep and circadian) analyses

Video-tracking analyses were based on an established protocol [307]. Mice were individually housed in large cages (44 cm long × 26 cm wide × 12 cm high), positioned within light-tight chambers (LTCs), illuminated by an overhead cool white LED light-source. LTCs were maintained at constant temperature (21°C) and humidity (50%). Each LTC contained 6 cages, with 3 mice of each genotype housed in alternating positions. A standard 12:12 h light/dark (12:12 LD) cycle was employed and illuminance was 100 lux at the base of each cage. Three 24 h videos (i.e. 3 separate 12:12 LD cycles) were recorded at weekly intervals, using a near-infrared CCTV camera (Maplin Electronics, Rotherham, UK). All videos were recorded at 3 frames per second, in the AVI file format. An acrylic block was placed under the food hopper to keep the mouse in the recording field at all times.

Video files were stored on a digital hard drive recorder (Samsung, Suwon, South Korea) prior to analysis with ANY-maze 4.5 (Stoelting, Wood Dale, Illinois). Multiple immobility-determined sleep parameters were extracted from the video footage: total sleep time, light and dark phase sleep time, light and dark phase sleep bouts, and light and dark phase sleep bout duration. Sleep was defined as a period of immobility of at least 40 s, a previously established proxy measure of sleep [307]. This measure has an extremely high concordance (>95%) with EEG-based sleep determination [307]. Immobility sensitivity was set at 95% to prevent the detection of movements caused by breathing during sleep. Note that sleep time is expressed as a percentage of recording time.

In addition to the sleep parameters outlined above, four activity parameters were extracted from the video footage using ANY-maze 4.5: total activity, light and dark phase activity (distance travelled in metres), and relative light phase activity (the percentage of total activity occurring

during the light phase). Note that one *Grm2/3*$^{+/+}$ mouse was excluded from all dark phase sleep and activity analyses as it escaped from its cage during dark phase recording.

3-5 days after the third 24 h recording, mice were exposed to a 1 h 100 lux light pulse from zeitgeber time (ZT) 16 to 17. (ZT0 refers to the onset of the light phase, while ZT12 denotes the onset of the dark phase). Negative masking – percent activity suppression induced by the light pulse – was computed to provide an indication of photosensitivity [728]. This parameter was calculated by comparing activity levels during the light pulse with average activity levels during the same time window (ZT16-17) across the previous 3 days.

6.2.4. Passive-infrared (PIR) motion detection (sleep and circadian) analyses

Due to the prohibitive size of the video files, it was impractical to analyse more than 72 h of video data. Passive-infrared (PIR) motion detection provides a less data-heavy alternative, enabling the estimation of sleep over a longer period; in this case, 14 consecutive days of 12:12 LD at 100 lux. It also enables the computation of standard circadian parameters such as period length (see below), which cannot be extracted from isolated 24 h video recordings. Full details of this novel technique, developed in our laboratory, should be published in the near future [304]. Housing conditions for the PIR protocol were identical to that of the video-tracking protocol outlined above. Again, an acrylic block was placed under the food hopper to keep the mouse in the motion detection field at all times. Raw data from the PIR motion sensors took the form of % time active per 10 s epoch, with sensors activated both by gross locomotion and small movements such as turning of the head. Three immobility-determined sleep parameters were extracted from the raw PIR data using Microsoft Excel 2013 (Microsoft, Redmond, USA): total sleep time, light phase sleep time and dark phase sleep time. Note that methods do not yet exist to automatically compute parameters pertaining to the frequency and duration of sleep bouts from PIR data. As with the previously described video-based method of sleep determination [307], sleep was defined as a period of immobility of at least 40 s. We have recently confirmed that this measure has an extremely high concordance (>95%) with both video-based sleep determination and EEG-based sleep determination [304].

In addition to the sleep parameters outlined above, four activity parameters were extracted from the raw PIR data using the ClockLab toolbox (Actimetrics, Illinois, USA) for MatLab (MathWorks, Massachusetts, USA): total activity, light and dark phase activity (expressed in arbitrary units), and relative light phase activity (as above).

Standard circadian parameters were also computed from the raw PIR data using ClockLab; these comprised two measures of circadian rhythm fragmentation (daily activity bouts and daily activity bout duration), two measures of circadian rhythm consistency (chi-square periodogram amplitude and onset tau error), and onset tau (henceforth referred to as period length). Activity bouts were defined using pre-established criteria for ClockLab (maximum gap: 18 min; threshold: 5 %). An additional circadian parameter – interdaily stability – was computed using the software package Actiwatch Activity & Sleep Analysis 7 (Cambridge Neurotechnology, Cambridge, UK). Interdaily stability is a non-parametric measure that quantifies the similarity of activity patterns across multiple days [310].

6.2.5. Wheel-running (circadian) analyses

This screen was based on an established protocol [309, 311, 355]. Housing conditions were identical to that of the video-tracking and PIR protocols described above, except that cages were fitted with running wheels (18 cm diameter). As previously, illuminance was 100 lux at the base of each cage. Mice in both cohorts were exposed to 14 days of 12:12 LD and 11 days of constant dark (DD). In addition, cohort 1 was subjected to 13 days of constant light (LL), and a 6 h phase advance during 12:12 LD.

During 12:12 LD, four activity parameters were extracted from the raw wheel-running data using ClockLab: total activity, light and dark phase activity (wheel rotations), and relative light phase activity (as above). The six circadian parameters computed from the raw PIR data (see above) were also computed from the raw wheel-running data, using ClockLab and Actiwatch Activity & Sleep Analysis 7. Again, activity bouts were defined using pre-established criteria (maximum gap: 18 min; threshold: 5 counts/min). Note that two *Grm2/3*$^{-/-}$ mice were omitted from these activity bout analyses as their activity levels were too low to derive bout data. ClockLab was also used to quantify period length under free-running conditions (i.e. DD and LL), while re-entrainment following the 6 h phase advance was scored manually from individual actograms as the number of days taken to re-entrain.

Both cohorts were subjected to type I and type II phase-shifting light pulses [726] (using previously described protocols [309, 727]) to induce a phase delay in their wheel-running rhythms, providing an indication of circadian photosensitivity. For the type I pulse, mice were exposed to 100 lux light for 15 minutes at circadian time (CT) 16 during DD. The magnitude of the phase delay was quantified by fitting one regression line through 10 consecutive activity onsets preceding the light pulse, and another through 6 consecutive activity onsets following

the pulse. The first 2 activity onsets following the light pulse were disregarded because of possible transition effects [309]. For the type II pulse, mice were exposed to 100 lux light for one hour at ZT16 during a standard 12:12 LD cycle. Following the pulse, mice were released into DD. The magnitude of the phase delay was quantified by fitting one regression line through 6 consecutive activity onsets preceding the light pulse, and another through 6 consecutive activity onsets following the pulse. This time, only one activity onset following the light pulse was disregarded [309]. For both light pulses, the magnitude of the phase delay was calculated as the time difference between the two regression lines on the first day after the light pulse. Negative masking was also computed for the type II pulse, using the same method employed in the video-tracking screen.

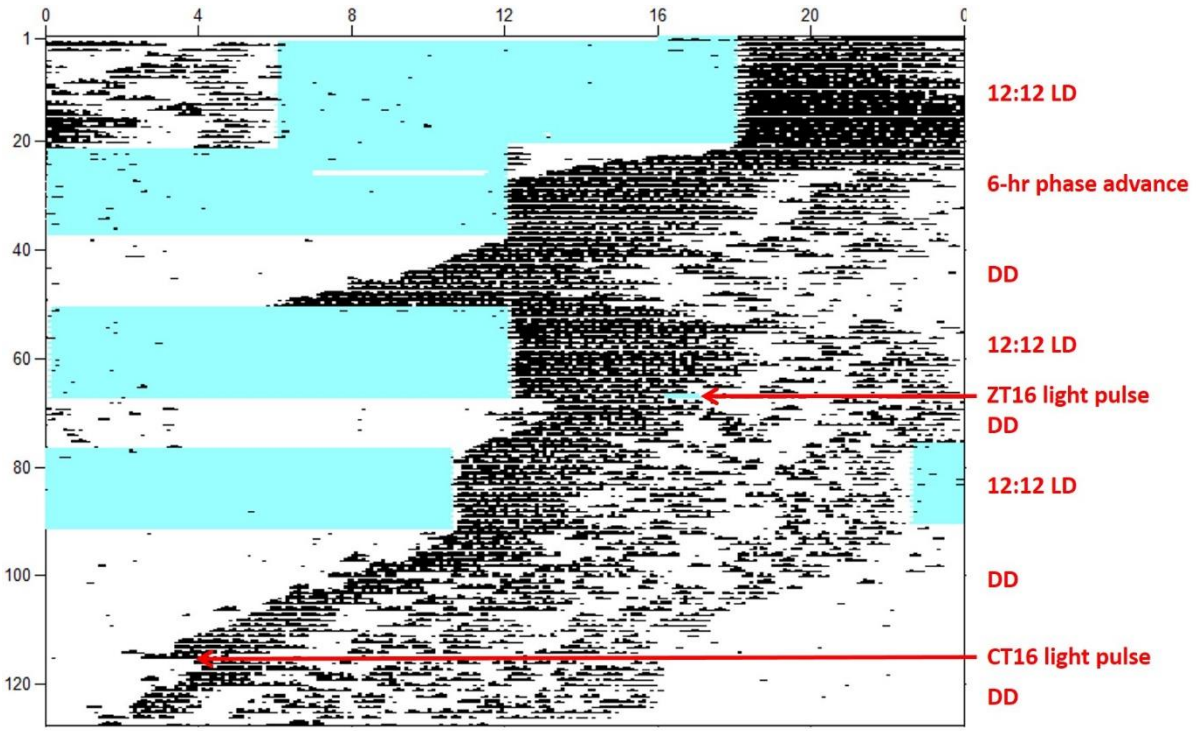

Figure 6.1. Representative wheel-running actogram of a *Grm2/3*$^{-/-}$ mouse progressing through the various light schedules of the wheel-running (circadian) screen. The x-axis denotes clock-time in hours, while the y-axis denotes time in days. The blue and white shading corresponds to periods of light and dark, respectively. The black bars denote periods of wheel-running activity, presented in 6 min epochs. The height of the bars corresponds to the number of wheel rotations within each epoch. Note that mice were only subjected to constant light (LL) at the end of the circadian screen, to avoid light-induced retinal degeneration influencing performance under the other light schedules. Representative wheel-running actograms of LL are depicted in Fig. 6.4.

6.2.6. Administration of an mGlu2/3 negative allosteric modulator to wildtype mice prior to a type I phase-shifting light pulse

To further investigate the hypothesis that group II metabotropic glutamate receptors modulate photic entrainment, the mGlu2/3 negative allosteric modulator RO4432717 was administered to wildtype mice in a standard phase-shifting paradigm. The pharmacology of RO4432717 (previously known as compound 7i) is described elsewhere [753]. 22 male wildtype C57Bl/6J mice (aged 80 days) were individually housed in large cages (44 cm long × 26 cm wide × 12 cm high), fitted with running wheels (18 cm diameter), under a 12:12 LD cycle at 400 lux. All mice were kept under constant dark conditions for 1 day prior to the administration of a 30 min type I phase-shifting light pulse (400 lux) at CT 16. 3 mice underwent no pre-treatment, while 6 mice received an intraperitoneal injection of saline (0.3 ml) at CT 12 on the day of the light pulse. The remaining 13 mice received an intraperitoneal injection of RO4432717 at CT12. Three dosages were used: 3 mg (4 mice), 10 mg (5 mice) and 30 mg (4 mice); injection volumes were kept constant at 0.3 ml. The magnitude of the phase delay was calculated using the method described above. Note that this experiment was performed by Aarti Jagannath.

6.2.7. Home-cage object interaction test

To evaluate whether the altered wheel-running behaviour of *Grm2/3*$^{-/-}$ mice was a consequence of increased object neophobia (toward their running wheels), a simple object interaction task was conducted within the home-cage. At ZT16, a novel object was introduced to the empty home-cages of all 24 mice from cohort 2. The object was an acrylic play-tube measuring 10 cm in length and 5 cm in diameter. The play-tube was secured to the home-cage floor with adhesive putty, in one of three positions; against the left-hand wall, in the centre of the cage, or against the right-hand wall. The location of the play-tube was counterbalanced across genotype groups. The play-tube was transparent, allowing the mice to be tracked even when they were inside it. Object interaction was defined as the amount of time spent in contact with the play-tube (including time spent within it). This parameter was calculated for the first 10 minutes and the first hour following the introduction of the object to the home-cage, as well as the entirety of the subsequent dark (active) phase, using the software package ANY-maze 4.5 (Stoelting, Wood Dale, Illinois).

6.2.8. Statistical analysis

All statistical analyses were performed with SPSS 22.0 (IBM, Armonk, New York). Unless otherwise stated, all reported statistics are the result of analyses of variance (ANOVAs), with genotype included as the independent variable. Differences were considered to be statistically significant at p-values < 0.05. Greenhouse-Geisser corrections were applied where appropriate, but uncorrected degrees of freedom are reported in order to preserve the transparency of the statistical design. For experiments involving multiple cohorts, further ANOVAs were conducted with cohort included as an extra independent variable. No additional effects or interactions were observed, so these data are not shown. In all figures, * indicates a p-value ≤ 0.05, ** indicates a p-value ≤ 0.01, and *** indicates a p-value ≤ 0.001. Error bars depict the standard error of the mean. $\underline{M}$ = mean.

6.3. Results

6.3.1. Grm2/3$^{-/-}$ mice display reduced sleep time and increased sleep fragmentation

Video-tracking sleep analyses

Relative to *Grm2/3*$^{+/+}$ mice, total sleep time was markedly reduced in *Grm2/3*$^{-/-}$ mice ($F_{1,21}$ = 6.456, P = 0.019; Fig. 6.2A). This reduction in sleep time was driven by decreased light phase sleep ($F_{1,22}$ = 18.107, P = <0.001; Fig. 6.2B); on average, *Grm2/3*$^{+/+}$ mice spent 77.0% of the light phase asleep, while *Grm2/3*$^{-/-}$ mice slept for only 71.1% of the light phase. By contrast, dark phase sleep time did not vary according to genotype ($F_{1,21}$ = 1.868, P = 0.186; Fig. 6.2C).

Sleep during the light phase was not only reduced but also more fragmented in *Grm2/3*$^{-/-}$ mice (see Fig. 6.2D); *Grm2/3*$^{-/-}$ mice demonstrated a greater number of light phase sleep bouts ($F_{1,22}$ = 4.664, P = 0.042; Fig. 6.2E) of a shorter average duration ($F_{1,22}$ = 9.315, P = 0.006; Fig. 6.2F). Dark phase sleep bouts were also shorter in *Grm2/3*$^{-/-}$ than *Grm2/3*$^{+/+}$ mice ($F_{1,21}$ = 5.735, P = 0.026), although the total number of dark phase sleep bouts was unaffected by genotype ($F_{1,21}$ = 0.050, P = 0.825). There were no effects or interactions involving recording day for any of these analyses, reflecting the fact that the sleep profiles of *Grm2/3*$^{+/+}$ and *Grm2/3*$^{-/-}$ mice were relatively consistent across the three recording sessions.

PIR sleep analyses

Over 14 days of continuous recording under 12:12 LD, light phase sleep time was reduced in *Grm2/3*$^{-/-}$ mice relative to *Grm2/3*$^{+/+}$ mice ($F_{1,22}$ = 9.037, P = 0.007; Fig. 6.2H). On average, *Grm2/3*$^{+/+}$ mice spent 82.3% of the light phase asleep, while *Grm2/3*$^{-/-}$ mice slept for only 76.6% of the light phase. There was also a trend towards a reduction in total sleep time ($F_{1,22}$

= 3.510, P = 0.074; Fig. 6.2G), but genotype had no effect on dark phase sleep time ($F_{1,22}$ = 0.459, P = 0.505; Fig. 6.2I).

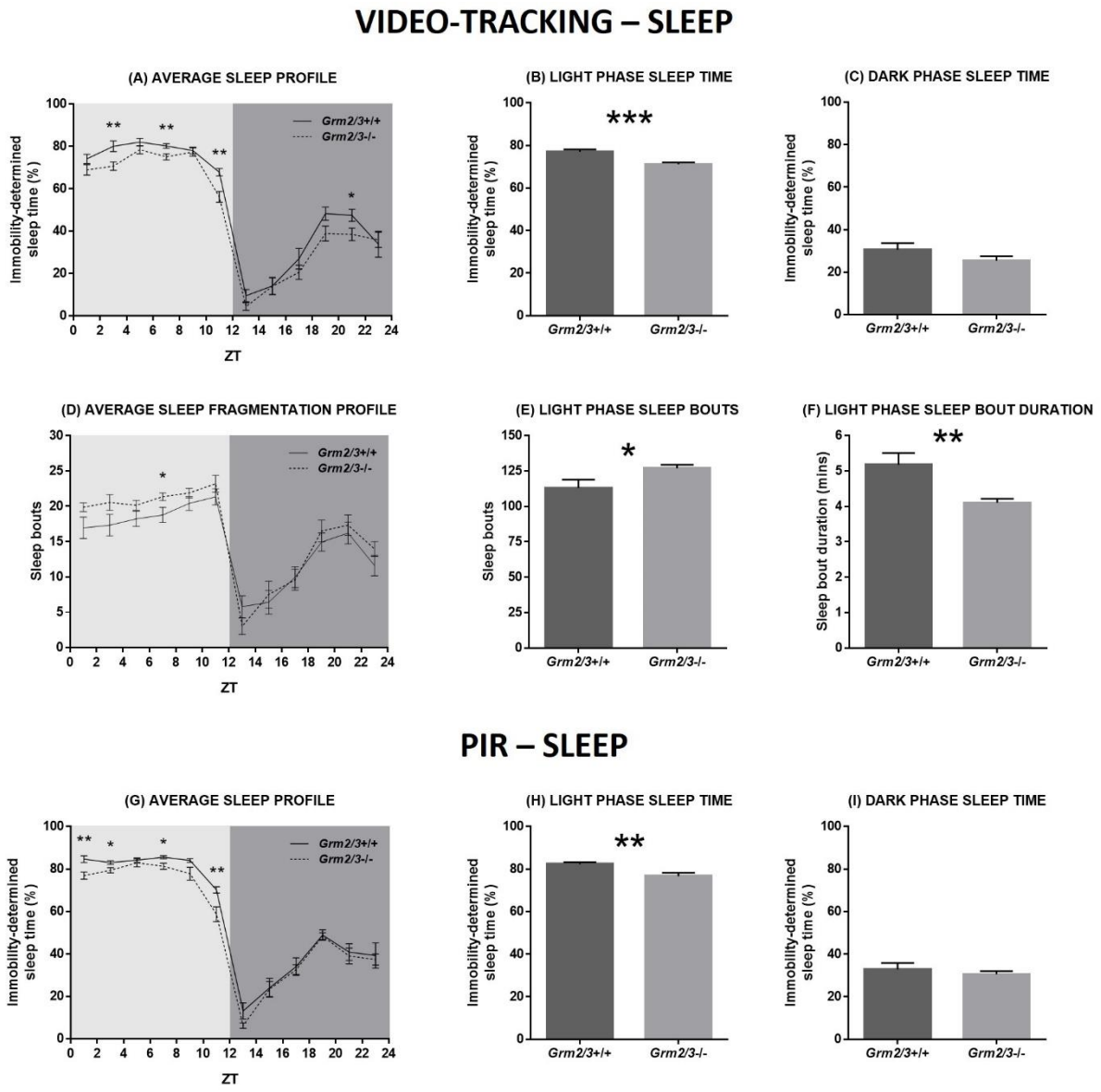

Figure 6.2. Sleep time is reduced and sleep fragmentation is increased in *Grm2/3*$^{-/-}$ mice. Figures 2A-F depict immobility-determined sleep parameters derived from 3 separate days of video-tracking data. Figures 2G-I depict immobility-determined sleep parameters derived from 14 consecutive days of passive-infrared (PIR) data. (A & G) Average sleep profiles, (B & H) light phase sleep time, and (C & I) dark phase sleep time for *Grm2/3*$^{+/+}$ and *Grm2/3*$^{-/-}$ mice during a 12:12 h light/dark (12:12 LD) cycle at 100 lux. (D) Average temporal distribution of sleep bouts, (E) number of light phase sleep bouts, and (F) light phase sleep bout duration in *Grm2/3*$^{+/+}$ and *Grm2/3*$^{-/-}$ mice during 12:12 LD at 100 lux. Sleep was defined as a period of immobility of at least 40 s. Data in figures 2A, D & G are presented in 2 h time bins. ZT = zeitgeber time. Note that methods do not yet exist to automatically compute parameters pertaining to the frequency and duration of sleep bouts from PIR data.

6.3.2. Grm2/3$^{-/-}$ mice are more sensitive to the circadian effects of light

Wheel-running analyses: Period length in constant dark and constant light

Over 11 days of continuous recording under DD, genotype had no effect on free-running period length ($F_{1,45}$ = 1.159, P = 0.287; Fig. 6.3A); average period length was 23.82 h in *Grm2/3*$^{+/+}$ mice and 23.78 h in *Grm2/3*$^{-/-}$ mice. By contrast, period length was considerably longer in *Grm2/3*$^{-/-}$ than *Grm2/3*$^{+/+}$ mice over 13 days of continuous recording under LL ($F_{1,21}$ = 7.242, P = 0.014; Fig. 6.3B); average period length was 24.87 h in *Grm2/3*$^{-/-}$ mice, but only 24.53 h in *Grm2/3*$^{+/+}$ mice. (Representative actograms of DD and LL are depicted in Fig. 6.4A).

Wheel-running analyses: Phase delays induced by nocturnal light pulses

A type I phase-shifting light pulse at CT 16 produced larger phase delays in the rest-activity rhythms of *Grm2/3*$^{-/-}$ than *Grm2/3*$^{+/+}$ mice ($F_{1,44}$ = 5.498, P = 0.024; Fig. 6.3C); the average phase delay was 1.51 h in *Grm2/3*$^{-/-}$ mice, but only 1.16 h in *Grm2/3*$^{+/+}$ mice. A type II phase-shifting light pulse at ZT16 also yielded larger phase delays in the rest-activity rhythms of *Grm2/3*$^{-/-}$ than *Grm2/3*$^{+/+}$ mice ($F_{1,45}$ = 4.736, P = 0.035; Fig. 6.3D); the average phase delay was 1.13 h in *Grm2/3*$^{-/-}$ mice, but only 0.91 h in *Grm2/3*$^{+/+}$ mice. (Representative actograms of type I and type II phase-shifting light pulses are depicted in Fig. 6.4B and 6.4C, respectively).

Wheel-running and video-tracking analyses: Negative masking during nocturnal light pulses

Negative masking was unaffected by genotype, regardless of the method used to assay locomotor activity. Genotype had no effect on the degree of activity suppression induced by a type II light pulse in either the wheel-running screen ($F_{1,45}$ = 0.994, P = 0.324; Fig. 6.3E) or the video-tracking screen ($F_{1,22}$ = 0.111, P = 0.743; Fig. 6.3F).

6.3.3. Wildtype mice are more sensitive to the circadian effects of light following the administration of an mGlu2/3 negative allosteric modulator

To address the possibility that the increased light sensitivity of *Grm2/3*$^{-/-}$ mice is a consequence of altered neurodevelopment or other long-term compensatory changes, we evaluated the impact of the mGlu2/3 negative allosteric modulator RO4432717 on the phase-shifting responses of wildtype C57Bl/6J mice. There was no difference in the magnitude of phase delays (induced by a type I light pulse at CT 16) between untreated wildtype mice and wildtype mice injected with saline at CT 12 ($F_{1,7}$ = 0.096, P = 0.766; Fig. 6.3G). Relative to saline-treated mice, phase delays were greater in mice injected with the RO4432717 at CT12. This difference was statistically significant at the 10 mg dosage ($F_{1,9}$ = 5.406, P = 0.045), but not at the 3 mg dosage ($F_{1,8}$ = 0.724, P = 0.420) or 30 mg dosage ($F_{1,8}$ = 2.194, P = 0.177). The 30 mg dose yielded large, but more variable effects.

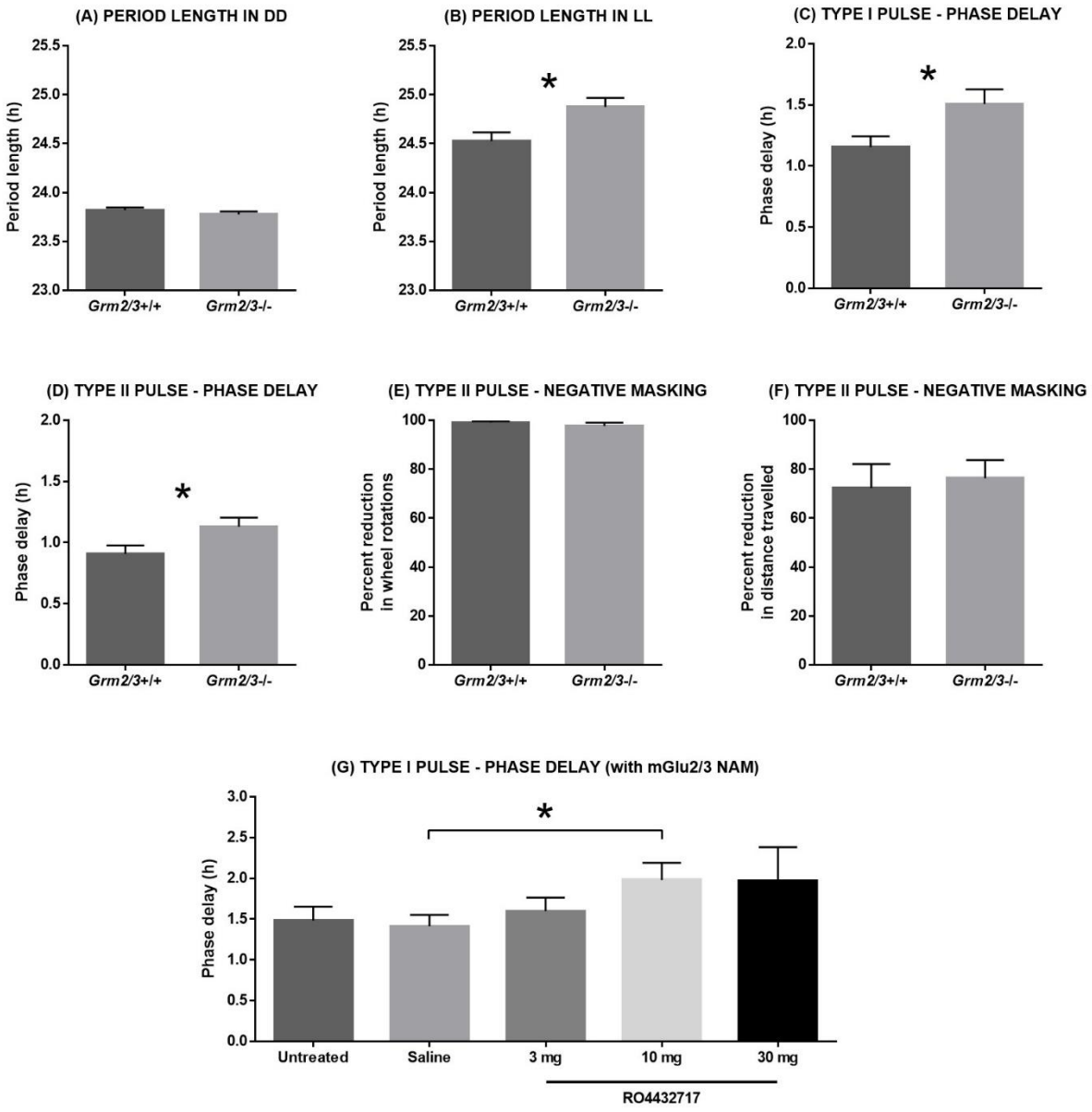

Figure 6.3. Light sensitivity is increased by the genetic ablation and pharmacological inhibition of mGlu2 & 3. All figures depict circadian parameters derived from wheel-running data, with the exception of figure 3F, which is based on video-tracking data. (A) Free-running period length in constant dark (DD) does not differ between *Grm2/3*$^{+/+}$ and *Grm2/3*$^{-/-}$ mice. (B) Free-running period length in constant light (LL) is greater in *Grm2/3*$^{-/-}$ than *Grm2/3*$^{+/+}$ mice. (C & D) Phase delays induced by type I (figure 3C) and type II (figure 3D) phase-shifting light pulses are larger in *Grm2/3*$^{-/-}$ than *Grm2/3*$^{+/+}$ mice. (E & F) *Grm2/3*$^{+/+}$ and *Grm2/3*$^{-/-}$ mice show similar levels of negative masking during a type II light pulse, as assayed by wheel-running (figure 3E) and video-tracking (figure 3F). (G) In wildtype C57Bl/6J mice, phase delays induced by a type I light pulse are enhanced following the administration of the mGlu2/3 negative allosteric modulator (NAM) RO4432717.

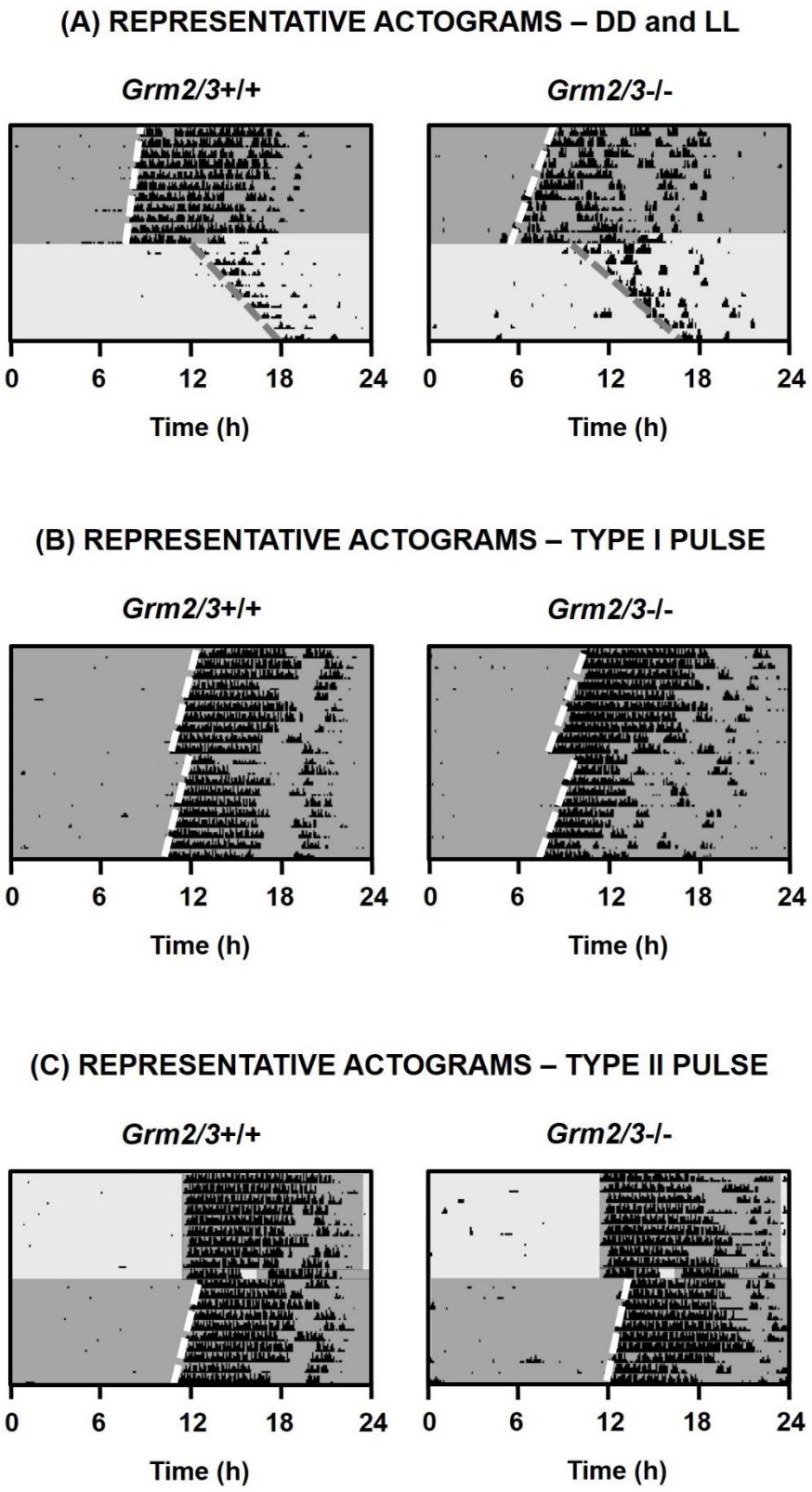

Figure 6.4. Representative wheel-running actograms of *Grm2/3*$^{+/+}$ and *Grm2/3*$^{-/-}$ mice during (A) constant dark and constant light, (B) a type I phase-shifting light pulse at CT 16, and (C) a type II phase-shifting light pulse at ZT 16. Each row depicts a single 24 h period. The light and dark grey shading corresponds to periods of (100 lux) light and dark, respectively. The black bars denote periods of wheel-running activity, binned in 6 min epochs. The height of the bars corresponds to the number of wheel rotations within each epoch.

6.3.4. Apparent circadian disruption in Grm2/3$^{-/-}$ mice is a consequence of the use of running wheels

Wheel-running activity analyses

Over 14 days of continuous recording under 12:12 LD, total wheel-running activity was markedly reduced in *Grm2/3*$^{-/-}$ mice relative to *Grm2/3*$^{+/+}$ mice ($F_{1,45}$ = 8.165, P = 0.006; Fig. 6.5A). This reflects the fact that *Grm2/3*$^{-/-}$ mice were significantly less active than *Grm2/3*$^{+/+}$ mice during the dark phase ($F_{1,45}$ = 8.503, P = 0.006; Fig. 6.5C). By contrast, genotype had no effect on activity during the light phase ($F_{1,45}$ = 1.257, P = 0.268; Fig. 6.5B); indeed, numerically speaking, *Grm2/3*$^{-/-}$ mice were *more* active than *Grm2/3*$^{+/+}$ mice during the light phase. Consequently, the percentage of total daily activity which occurred during the light phase was greater in *Grm2/3*$^{-/-}$ mice than *Grm2/3*$^{+/+}$ mice ($F_{1,45}$ = 7.585, P = 0.008). (Note that mean values for all circadian wheel-running analyses are included in Table 6.1, and representative actograms of 12:12 LD are depicted in Fig. 6.6A).

In addition to this reduction in total activity, the wheel-running rhythms of *Grm2/3*$^{-/-}$ mice were more fragmented than those of *Grm2/3*$^{+/+}$ mice. *Grm2/3*$^{-/-}$ mice engaged in more daily activity bouts ($\underline{M}$ = 4.4) than *Grm2/3*$^{+/+}$ mice ($\underline{M}$ = 3.5), resulting in a main effect of genotype on the number of daily activity bouts ($F_{1,43}$ = 5.071, P = 0.029; Fig. 6.7A). Moreover, the average duration of these bouts was shorter in *Grm2/3*$^{-/-}$ mice ($\underline{M}$ = 114 min) than *Grm2/3*$^{+/+}$ mice ($\underline{M}$ = 175 min). Hence, there was also a main effect of genotype on activity bout duration ($F_{1,43}$ = 9.137, P = 0.004; Fig. 6.7B).

The wheel-running rhythms of *Grm2/3*$^{-/-}$ mice were also less consistent from one day to the next. Interdaily stability was much lower in *Grm2/3*$^{-/-}$ mice than *Grm2/3*$^{+/+}$ mice ($F_{1,45}$ = 10.094, P = 0.003; Fig. 6.7C), while chi-square periodogram amplitude was also reduced in

Grm2/3$^{-/-}$ mice ($F_{1,45}$ = 4.722, P = 0.035; Fig. 6.7D). In addition, onset tau error – the degree of variability in daily activity onset – was greater in *Grm2/3*$^{-/-}$ than *Grm2/3*$^{+/+}$ mice ($F_{1,45}$ = 3.417, P = 0.071).

Period length under 12:12 LD was unaffected by genotype ($F_{1,45}$ = 0.010, P = 0.922). Likewise, *Grm2/3*$^{+/+}$ and *Grm2/3*$^{-/-}$ mice were equally able to adjust to a shift in the light/dark cycle. Following a 6 h phase advance in 12:12 LD, genotype had no effect on the number of days required for re-entrainment ($F_{1,21}$ = 0.494, P = 0.490).

Parameter	*Grm2/3*$^{+/+}$ (mean ± SEM)	*Grm2/3*$^{-/-}$ (mean ± SEM)	p-value
Daily activity (wheel rotations)	12571 ± 898 (*n* = 23)	8914 ± 910 (*n* = 24)	0.006
Dark phase activity (wheel rotations)	12408 ± 890 (*n* = 23)	8682 ± 915 (*n* = 24)	0.006
Light phase activity (wheel rotations)	163 ± 25 (*n* = 23)	232 ± 55 (*n* = 24)	0.268
Relative light phase activity (%)	1.4 ± 0.2 (*n* = 23)	3.6 ± 0.8 (*n* = 24)	0.008
Daily activity bouts	3.5 ± 0.3 (*n* = 23)	4.4 ± 0.3 (*n* = 22)	0.029
Activity bout duration (min)	175 ± 15 (*n* = 23)	114 ± 14 (*n* = 22)	0.004
Interdaily stability (AU)	1.07 ± 0.05 (*n* = 23)	0.81 ± 0.06 (*n* = 24)	0.003
Chi-square periodogram amplitude (AU)	1841 ± 70 (*n* = 23)	1553 ± 111 (*n* = 24)	0.035
Onset tau error (h)	0.16 ± 0.05 (*n* = 23)	0.48 ± 0.16 (*n* = 24)	0.071
Period length (h)	23.99 ± 0.01 (*n* = 23)	23.99 ± 0.02 (*n* = 24)	0.922
Alpha (h)	13.84 ± 1.16 (*n* = 23)	12.82 ± 3.33 (*n* = 24)	0.172

Table 6.1. Descriptive statistics for selected circadian parameters derived from 14 consecutive days of wheel-running data. Mice were housed under a 12:12 h light/dark (12:12 LD) cycle at 100 lux. Units of measurement and sample sizes are indicated in brackets. AU = arbitrary units. SEM = standard error of the mean.

Video-tracking activity analyses

When mice were housed in cages lacking running wheels, and locomotor activity was determined with near-infrared cameras, the rest-activity profiles of *Grm2/3*$^{-/-}$ mice were very different from those derived using running wheels (see Fig. 6.5D). As with running wheels, light phase activity was greater in *Grm2/3*$^{-/-}$ mice than *Grm2/3*$^{+/+}$ mice ($F_{1,22}$ = 6.166, P = 0.021; Fig. 6.5E), although the percentage of total daily activity which occurred during the light phase did not vary according to genotype ($F_{1,21}$ = 0.625, P = 0.438). Crucially, however, genotype

had *no effect* on dark phase activity ($F_{1,21}$ = 0.217, P = 0.646; Fig. 6.5F) or total activity levels ($F_{1,21}$ = 0.395, P = 0.536). There were no effects or interactions involving recording day for any of these analyses, reflecting the fact that the sleep profiles of *Grm2/3*$^{+/+}$ and *Grm2/3*$^{-/-}$ mice were relatively consistent across the three recording sessions. Note that standard circadian parameters such as period length cannot be extracted from isolated 24 h video recordings.

PIR activity analyses

When mice were housed in cages lacking running wheels, and locomotor activity was determined with PIR motion detectors, the rest-activity profiles of *Grm2/3*$^{-/-}$ mice were again very different from those derived using running wheels (see Fig. 6.5G). As with running wheels, light phase activity was greater in *Grm2/3*$^{-/-}$ mice than *Grm2/3*$^{+/+}$ mice ($F_{1,22}$ = 2.551, P = 0.124; Fig. 6.5H), and the percentage of total daily activity which occurred during the light phase was higher in *Grm2/3*$^{-/-}$ mice ($F_{1,22}$ = 3.991, P = 0.058), although neither of these effects reached statistical significance. More importantly, however, genotype had *no effect* on dark phase activity ($F_{1,22}$ = 0.606, P = 0.445; Fig. 6.5I) or total activity levels ($F_{1,22}$ = 0.122, P = 0.730). (Note that mean values for all circadian PIR analyses are included in Table 6.2, and representative actograms of 12:12 LD are depicted in Fig. 6.6B).

Notably, there was no evidence that the rest-activity rhythms of *Grm2/3*$^{-/-}$ mice were less consistent than those of *Grm2/3*$^{-/-}$ mice; chi-square periodogram amplitude ($F_{1,22}$ = 0.034, P = 0.855; Fig. 6.7H) and onset tau error ($F_{1,22}$ = 1.563, P = 0.224) were both unaffected by genotype. Moreover, interdaily stability – which was significantly *reduced* in the wheel-running rhythms of *Grm2/3*$^{-/-}$ mice – was *greater* in *Grm2/3*$^{-/-}$ than *Grm2/3*$^{+/+}$ mice in the PIR-derived dataset ($F_{1,22}$ = 3.248, P = 0.085; Fig. 6.7G). A similar picture emerged for activity fragmentation; whereas the wheel-running activity of *Grm2/3*$^{-/-}$ mice was *more* fragmented

than that of *Grm2/3*$^{+/+}$ mice, home-cage activity fragmentation was *reduced* in *Grm2/3*$^{-/-}$ mice in the PIR-derived dataset. *Grm2/3*$^{-/-}$ mice engaged in fewer activity bouts than *Grm2/3*$^{+/+}$ mice ($F_{1,22}$ = 5.131, P = 0.034; Fig. 6.7E), while average bout duration was longer in *Grm2/3*$^{-/-}$ mice ($F_{1,22}$ = 9.391, P = 0.006; Fig. 6.7F). As in the wheel-running screen, period length was unaffected by genotype ($F_{1,22}$ = 0.832, P = 0.372).

Parameter	*Grm2/3*$^{+/+}$ (mean ± SEM)	*Grm2/3*$^{-/-}$ (mean ± SEM)	p-value
Daily activity (AU)	2563 ± 209 (*n* = 12)	2470 ± 163 (*n* = 12)	0.730
Dark phase activity (AU)	2213 ± 194 (*n* = 12)	2032 ± 128 (*n* = 12)	0.445
Light phase activity (AU)	350 ± 19 (*n* = 12)	438 ± 52 (*n* = 12)	0.124
Relative light phase activity (%)	14.2 ± 0.9 (*n* = 12)	17.4 ± 1.4 (*n* = 12)	0.058
Daily activity bouts	12.6 ± 0.5 (*n* = 12)	11.1 ± 0.4 (*n* = 12)	0.034
Activity bout duration (min)	66 ± 4 (*n* = 12)	86 ± 5 (*n* = 12)	0.006
Interdaily stability (AU)	0.72 ± 0.02 (*n* = 12)	0.77 ± 0.02 (*n* = 12)	0.085
Chi-square periodogram amplitude (AU)	1653 ± 115 (*n* = 12)	1627 ± 83 (*n* = 12)	0.855
Onset tau error (h)	0.49 ± 0.06 (*n* = 12)	0.60 ± 0.07 (*n* = 12)	0.224
Period length (h)	23.95 ± 0.01 (*n* = 12)	23.97 ± 0.02 (*n* = 12)	0.372
Alpha (h)	4.31 ± 2.97 (*n* = 12)	3.85 ± 2.55 (*n* = 12)	0.692

Table 6.2. Descriptive statistics for selected circadian parameters derived from 14 consecutive days of passive-infrared (PIR) data. Mice were housed under a 12:12 h light/dark (12:12 LD) cycle at 100 lux. Units of measurement and sample sizes are indicated in brackets. AU = arbitrary units. SEM = standard error of the mean.

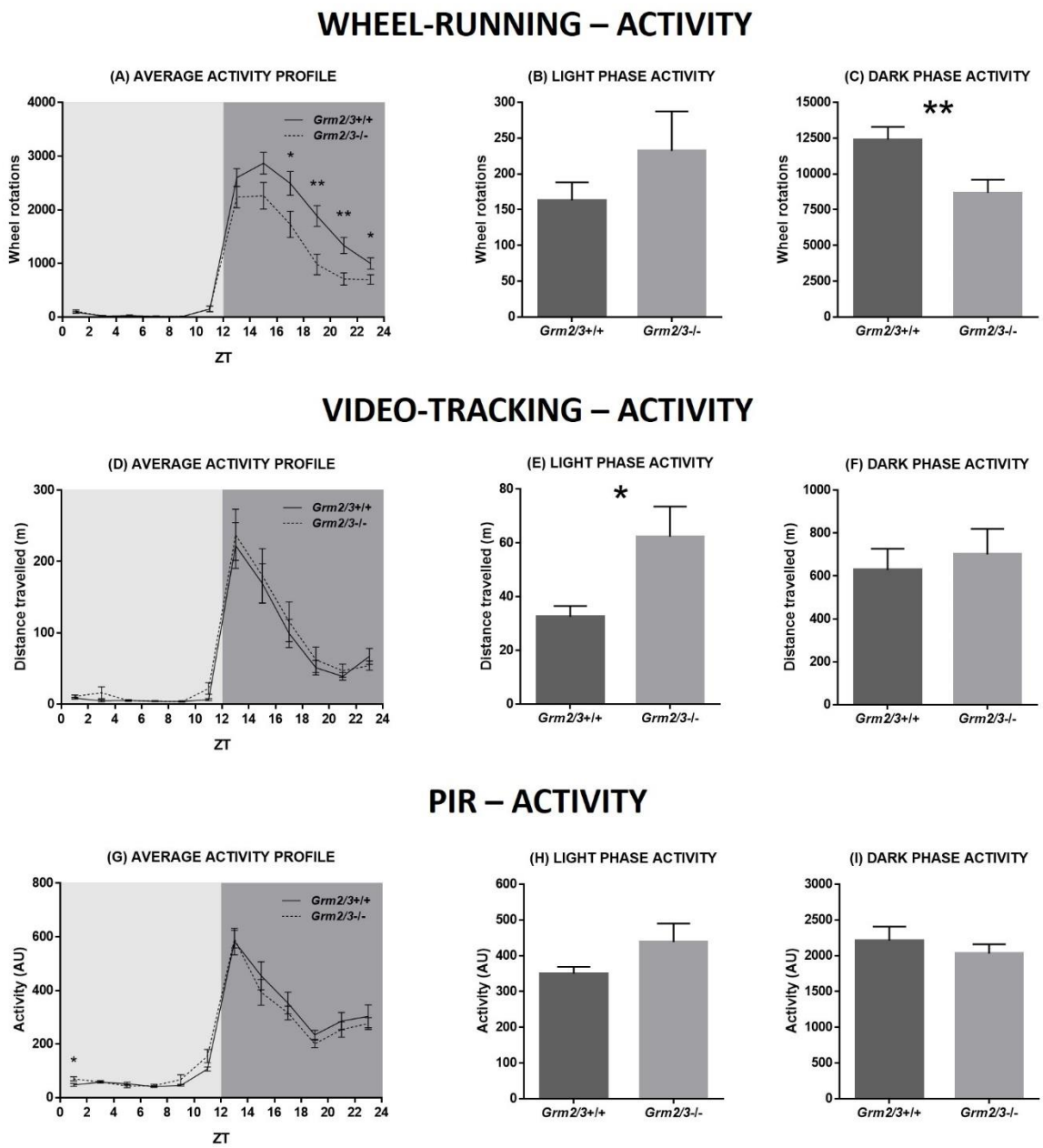

Figure 6.5. Light phase wheel-running activity is reduced in Grm2/3$^{-/-}$ mice, but general home-cage activity is not. Figures 5A-C depict activity parameters derived from 14 consecutive days of wheel-running data. Figures 5D-F depict activity parameters derived from 3 separate days of video-tracking data. Figures 5G-I depict activity parameters derived from 14 consecutive days of passive-infrared (PIR) data. (A, D & G) Average activity profiles, (B, E & H) light phase activity, and (C, F & I) dark phase activity for *Grm2/3*$^{+/+}$ and *Grm2/3*$^{-/-}$ mice during a 12:12 h light/dark (12:12 LD) cycle at 100 lux. Data in figures 5A, D & G are presented in 2 h time bins. ZT = zeitgeber time. AU = arbitrary units.

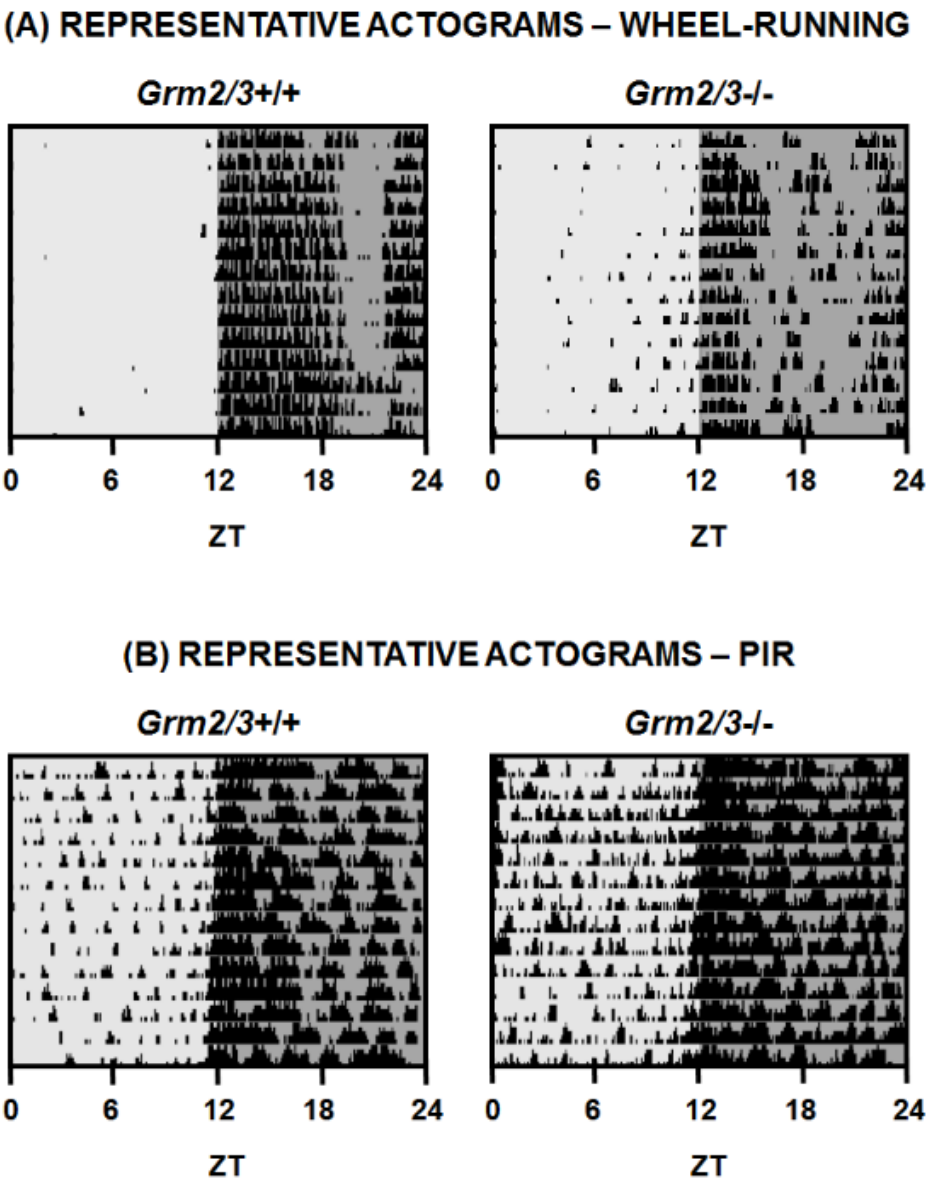

Figure 6.6. Representative actograms of *Grm2/3*$^{+/+}$ and *Grm2/3*$^{-/-}$ mice during a 12:12 h light/dark (12:12 LD) cycle. Each row depicts a single 24 h period. The light and dark grey shading corresponds to periods of (100 lux) light and dark, respectively. (A) Representative wheel-running actograms. The black bars denote periods of wheel-running activity, binned in 6 min epochs. The height of the bars corresponds to the number of wheel rotations within each epoch. (B) Representative passive-infrared (PIR) actograms. The black bars denote periods of home-cage activity, binned in 6 min epochs. The height of the bars corresponds to % time active within each epoch. ZT = zeitgeber time.

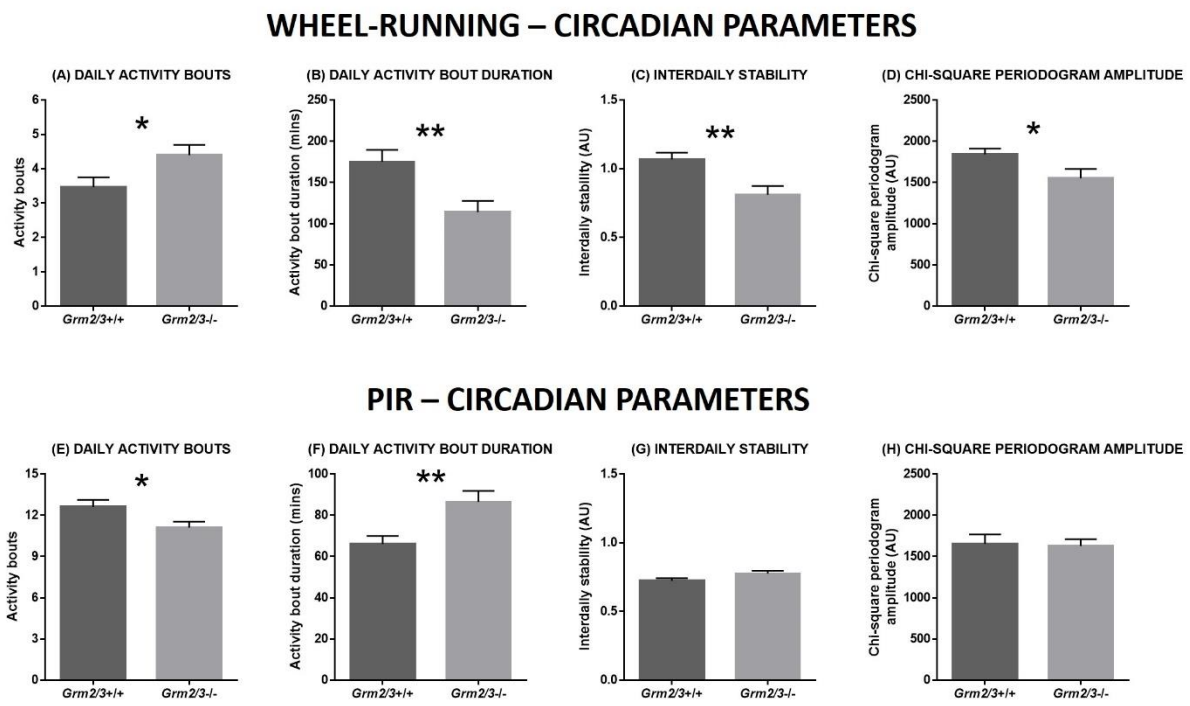

Figure 6.7. The circadian characteristics of *Grm2/3*$^{-/-}$ mice are dependent on the assays used to measure activity. Figures 7A-D depict circadian parameters derived from 14 consecutive days of wheel-running data. Figures 7E-H depict circadian parameters derived from 14 consecutive days of passive-infrared (PIR) data. (A & E) Daily activity bouts, (B & F) daily activity bout duration, (C & G) interdaily stability, and (D & H) chi-square periodogram amplitude in *Grm2/3*$^{+/+}$ and *Grm2/3*$^{-/-}$ mice during a 12:12 h light/dark (12:12 LD) cycle at 100 lux. Activity bouts were defined using pre-established criteria, as described in the materials and methods. AU = arbitrary units.

6.3.5. Home-cage object interaction is unaltered in Grm2/3$^{-/-}$ mice

To explore whether the reduced wheel-running activity of *Grm2/3*$^{-/-}$ mice was a reflection of heightened object neophobia, a simple home-cage object interaction task was conducted. Genotype had no influence on interaction with the play-tube during the first 10 minutes ($F_{1,22}$ = 0.430, P = 0.519; Fig. 6.8A) or the first hour following its introduction to the empty home-cage ($F_{1,22}$ = 0.019, P = 0.892; Fig. 6.8B). Likewise, object interaction did not vary by genotype during the subsequent dark (active) phase ($F_{1,22}$ = 0.004, P = 0.953; Fig. 6.8C). Genotype had no effect on distance travelled during the first 10 minutes ($F_{1,22}$ = 0.023, P = 0.880), the first hour ($F_{1,22}$ = 0.158, P = 0.695), or the subsequent dark phase ($F_{1,22}$ = 0.037, P = 0.849).

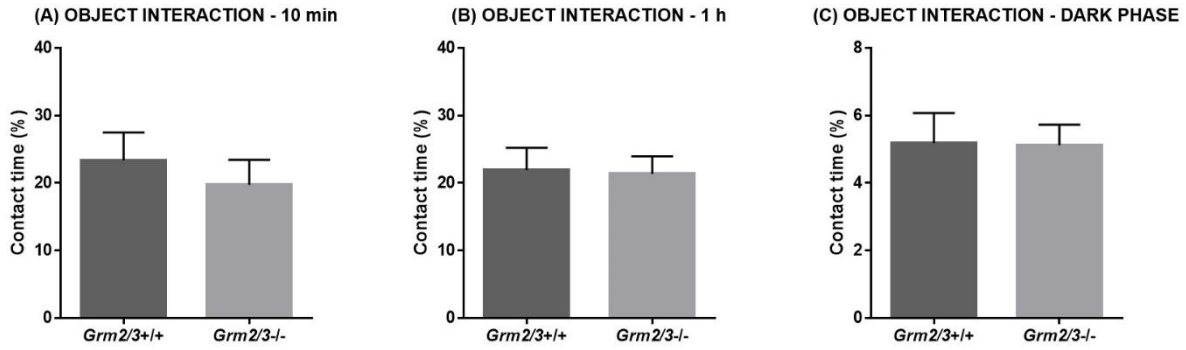

Figure 6.8. Home-cage object interaction is unaltered in *Grm2/3*$^{-/-}$ mice. Genotype has no effect on interaction with a novel object during the first 10 min (A) or first hour (B) after its introduction to the home-cage (at ZT16), or during the entirety of the subsequent dark phase (C). The object was a transparent acrylic play-tube. Object interaction was defined as the amount of time spent in contact with the play-tube (including time spent within it).

6.4. Discussion

The sleep and circadian characterisation of the *Grm2/3* double knockout (*Grm2/3*$^{-/-}$) mouse resulted in three novel findings. Firstly, *Grm2/3*$^{-/-}$ mice displayed a decrease in immobility-determined sleep time and an increase in immobility-determined sleep fragmentation. Secondly, *Grm2/3*$^{-/-}$ mice demonstrated heightened sensitivity to the circadian effects of light, as determined using running wheels. More specifically, they showed increased period lengthening in constant light, and greater phase delays in response to type I and type II phase-shifting light pulses. Thirdly, the wheel-running activity of *Grm2/3*$^{-/-}$ mice was significantly perturbed under a standard 12:12 LD cycle.

Reduced sleep time and increased sleep fragmentation in Grm2/3$^{-/-}$ *mice*

Our observation of reduced sleep time in *Grm2/3*$^{-/-}$ mice is consistent with reports of reduced sleep in wildtype rats following the administration of various mGlu2/3-modulating drugs [575-582]. In these pharmacological models, reduced sleep time typically reflects the selective suppression of REM sleep. Somewhat counter-intuitively, REM sleep is reduced by mGlu2/3 agonists, antagonists, positive allosteric modulators and negative allosteric modulators alike [575-582]. This is suggestive of an inverted U-shaped relationship between presynaptic glutamate release and REM sleep time. Crucially, the mGlu2/3 agonist LY354740 inhibits REM sleep in wildtype mice but not in *Grm2*$^{-/-}$ mice, which strongly implicates mGlu2 in the regulation of REM sleep [575].

In which brain region(s) do group II metabotropic glutamate receptors exert their influence on REM sleep? The amygdala is a promising candidate, since it is known to influence sleep regulation [754-759], and *Grm2* is highly expressed in this region [540, 760, 761]. Indeed, Dong and colleagues observed reduced REM sleep in wildtype rats following microinjection

of the mGlu2/3 agonist LY379268 directly into the basal amygdala [578]. Another region of interest is the thalamic reticular nucleus, which forms part of the ascending arousal system; mGlu2/3 antagonists are known to modulate the inhibitory output of this structure [750, 751].

In addition to reduced sleep time, *Grm2/3*$^{-/-}$ mice exhibited an increase in sleep fragmentation. Consistent with this observation, both the mGlu2/3 antagonist LY341495 and the mGlu2 negative allosteric modulator RO4491533 increase the number of transitions between sleep and wakefulness in wildtype rats [576]. Hence, group II metabotropic glutamate receptors may be involved in the putative 'flip-flop' circuit involving the VLPO that is hypothesised to control sleep onset and offset [295]. This could be a direct effect of altered glutamatergic neurotranmission at synapses between SCN efferents and the VLPO [718-720] and/or the result of changes in thalamic reticular nucleus function [750, 751]. Moreover, the inability of *Grm2/3*$^{-/-}$ mice to remain asleep for sustained periods could explain the overall reduction in their sleep time. It should also be noted that reduced sleep and increased sleep fragmentation are common in schizophrenia patients [327, 328, 335].

mGlu2 and/or mGlu3 modulate the sensitivity of the circadian system to light

Period length in constant light was significantly greater in *Grm2/3*$^{-/-}$ mice than *Grm2/3*$^{+/+}$ mice, despite the fact that period length was unaffected by genotype under constant dark conditions. Moreover, following both type I and type II phase-shifting light pulses, phase delays were greater in *Grm2/3*$^{-/-}$ mice than *Grm2/3*$^{+/+}$ mice. Negative masking during the type II pulse was unaffected by genotype, although this may reflect a ceiling effect, since the suppression of wheel-running activity was almost absolute in mice of both genotypes. Consistent with our observations in *Grm*2/3$^{-/-}$ mice, light-induced phase delays in wildtype C57Bl/6J mice were enhanced by the administration of the mGlu2/3 negative allosteric modulator RO4432717.

While it has previously been reported that mGlu2/3-modulating drugs can influence the magnitude of light-induced phase delays in wildtype hamsters [748, 749], our own data represent the first demonstration of such an effect in wildtype mice. Furthermore, it is significant that we obtained analogous results in a transgenic model and an acute pharmacological model; this suggests that the heightened light sensitivity of the *Grm2/3*$^{-/-}$ mouse does not arise as a consequence of altered neurodevelopment or other long-term compensatory changes.

Collectively, these results demonstrate that mGlu2 and/or mGlu3 can modulate the sensitivity of the circadian system to light, which raises the possibility that mGlu2/3-modulating compounds may be useful for the treatment of circadian rhythm disorders. However, the relevance of these findings to schizophrenia is unclear. In humans, the suppression of nocturnal melatonin secretion by light is the standard measure of circadian photosensitivity; there is some evidence that this response is upregulated in bipolar disorder and seasonal affective disorder [762], but such studies have not been undertaken in individuals with schizophrenia.

It is possible that the enhanced light-induced phase delays shown by *Grm2/3*$^{-/-}$ mice reflect the absence of mGlu2 and/or mGlu3 from RHT-SCN synapses. As outlined in Chapters 1 & 5, photic entrainment cues are transmitted from the eye to the SCN via the axons of intrinsically photosensitive retinal ganglion cells (ipRGCs), which together make up the RHT [186, 187]. While ionotropic glutamate receptors *mediate* the transduction of light information from the retina to the SCN via the RHT [188-193], metabotropic glutamate receptors may play a *modulatory* role at RHT-SCN synapses [747-749]. Consistent with the role of group II metabotropic glutamate receptors as presynaptic inhibitory autoreceptors, mGlu2/3 agonists serve to inhibit NMDA-evoked calcium influx in SCN neurons [747], presumably via a

reduction in presynaptic glutamate release. By the same logic, the antagonism or deletion of group II metabotropic glutamate receptors might be expected to *increase* presynaptic glutamate release at RHT-SCN synapses, explaining the enhanced light-induced phase delays witnessed in *Grm2/3*$^{-/-}$ mice and in wildtype C57Bl/6J mice following the administration of RO4432717. It should also be noted that *Grm2* is expressed in the retina, in cholinergic amacrine cells [541-543], although its role here is not well understood. *Grm3* is not expressed in the mammalian retina [541-543].

The effect of the mGlu2/3 negative allosteric modulator RO4432717 on sleep in wildtype rats

In recent months, sleep has been assessed in adult male Sprague-Dawley rats following the administration of the mGlu2/3 NAM RO4432717 [Silvia Gatti, *unpublished data*], the same compound used in the present manuscript. Various sleep parameters were recorded for 6 h after injections that occurred during the middle of the dark phase (at ZT19). Consistent with the effects of a range of mGlu2/3-modulating drugs (see above), administration of RO4432717 at the highest test concentration (10 mg/kg) produced a significant wake-promoting effect. The latency to both REM and NREM sleep onset was significantly increased after RO4432717 injection relative to vehicle injection (0.3 % Tween in purified water). Administration of RO4432717 at 10 mg/kg was followed by a period of consolidated wake; hence, wake time was significantly increased, and both REM and NREM sleep time were significantly decreased. Wake bout duration was also increased. Finally, locomotor activity was significantly increased following the administration of at RO4432717 at 10 mg/kg, presumably as a consequence of increased wake time. The two lower concentrations of RO4432717 (the lowest being 1 mg/kg) produced little effect on the sleep parameters measured in this study. The effects of RO4432717 administration during the light phase has yet to be tested.

Origins and implications of perturbed wheel-running activity in Grm2/3$^{-/-}$ mice

The 24 h rhythms in the wheel-running behaviour of *Grm2/3*$^{-/-}$ mice were characterised by increased activity fragmentation and reduced consistency, while total activity levels were substantially reduced. Nonetheless, general home-cage activity levels – assessed with both near infrared cameras and PIR motion detectors – were unchanged in *Grm2/3*$^{-/-}$ mice. The consistency of home-cage activity rhythms, as measured with PIR motion detectors, was also unaffected by genotype. This implies that the perturbed wheel-running rhythms of *Grm2/3*$^{-/-}$ mice were a consequence of the use of the wheels themselves, rather than evidence of underlying circadian dysregulation.

It is somewhat more difficult to explain why the PIR-derived activity rhythms of *Grm2/3*$^{-/-}$ mice were *less* fragmented than those of *Grm2/3*$^{+/+}$ mice, when their wheel-running rhythms were *more* fragmented. One possibility is that the activity of *Grm2/3*$^{-/-}$ mice was also more fragmented in the PIR paradigm (see Fig. 6.6), but their activity bouts were so short that many were not registered by ClockLab. Indeed, very short bouts (< 18 min duration) would not have been registered according to the bout recognition criteria that we selected (maximum gap: 18 min; threshold: 5 %). By contrast, *Grm2/3*$^{-/-}$ mice demonstrated greater light phase activity than *Grm2/3*$^{+/+}$ mice in all three assays (wheel-running, PIR and video-tracking). This could be a direct consequence of their reduced light phase sleep time, and so again, need not be the result of an altered circadian system.

There are several possible reasons for the significantly reduced wheel-running activity of *Grm2/3*$^{-/-}$ mice, which are not mutually exclusive. It could reflect heightened object neophobia – a manifestation of increased anxiety – since all mice were housed in empty home-cages prior to the introduction of running wheels. This seems unlikely, however, given that *Grm2/3*$^{+/+}$ and

Grm2/3$^{-/-}$ mice showed equal exploration of another novel object (a transparent play-tube) immediately after its introduction to the home-cage. Moreover, a previous study found no evidence of altered anxiety in *Grm2/3*$^{-/-}$ mice in either the elevated plus maze, open field test, black and white alleys, or novelty-suppressed feeding tasks [574]. A more straightforward explanation is a deficit in motor function. In support of this hypothesis, *Grm2/3*$^{-/-}$ mice demonstrate mild but significant impairments in standard tests of motor coordination; they are impaired at both the accelerating rotarod task and the multiple static rods task [574]. A third possibility is that *Grm2/3*$^{-/-}$ mice are less *motivated* to engage in wheel-running activity; perhaps the physical act of wheel-running is inherently less rewarding for *Grm2/3*$^{-/-}$ than *Grm2/3*$^{+/+}$ mice. Indeed, long-term voluntary wheel-running is known to be rewarding for rodents, and produces plastic changes in mesolimbic dopaminergic reward circuity [763]. Significantly, striatal dopamine is markedly reduced in *Grm2/3*$^{-/-}$ mice, particularly in the nucleus accumbens [676], a brain region involved in reward and motivation [764, 765]. A final possibility is that reduced wheel-running in *Grm2/3*$^{-/-}$ mice reflects a reduction in arousal, which again could be related to the role of mGlu2 and mGlu3 in the reticular thalamic nucleus [750, 751]. Note that reduced arousal has already been proposed as an explanation for their impaired performance in appetitive spatial memory tasks [561].

Interestingly, our results deviate slightly from those of previous experiments that have studied locomotor activity in *Grm2/3*$^{-/-}$ mice. Lyon and colleagues observed that *Grm2/3*$^{-/-}$ mice were less active than *Grm2/3*$^{+/+}$ mice in cages lacking running wheels, particularly in the dark phase [561]. These results should be treated with caution, however, as activity was assessed over a relatively short period (less than 3 light/dark cycles), and recording began immediately after transferring the mice from the familiar home-cage environment to a novel activity-monitoring

cage [561]. Furthermore, mice were group-housed within the home-cage in this study [561], whereas mice were singly-housed during the experiments described in this chapter.

Conclusions

The results described in this chapter add to a considerable body of evidence implicating group II metabotropic glutamate receptors in both sleep and photic entrainment pathways. As predicted, *Grm2/3*$^{-/-}$ mice displayed a reduction in total sleep time and increased sleep fragmentation. This is consistent with the effects of a wide range of mGlu2/3-modulating drugs on sleep duration [575-582] and sleep fragmentation in wildtype rats [576]. In line with our third prediction, the genetic ablation of mGlu2 and mGlu3 heightened the sensitivity of the circadian system to light. *Grm2/3*$^{-/-}$ mice displayed increased period lengthening in constant light, and greater phase delays in response to nocturnal light pulses. Greater light-induced phase delays were also exhibited by wildtype C57Bl/6J mice following administration of the mGlu2/3 NAM RO4432717. These observations build on prior reports that mGlu2/3-modulating drugs can alter the magnitude of light-induced phase delays in wildtype hamsters [748, 749]. As outlined in Chapter 1, there is a robust association between the *Grm3* locus and schizophrenia [60]. Hence, the results of the current chapter tentatively suggest that mGlu3 might contribute to SCRD in schizophrenia. This conclusion is clearly consistent with our hypothesis that SCRD and schizophrenia share common mechanistic origins [125, 343]. Finally, we found that the circadian phenotype of the *Grm2/3*$^{-/-}$ mouse was critically dependent on the method used to assay its locomotor behaviour. This finding speaks to the debate about the suitability of running-wheels as a circadian assay for psychiatrically-relevant mouse models. This theme is discussed in detail in Chapter 7.

7. General discussion

7.1. Behavioural, sleep and circadian characterisation of the *Dao*$^{-/-}$ mouse

7.1.1. Summary of observed phenotype

The majority of the experiments described in this thesis involved the behavioural characterisation of *Dao*$^{-/-}$ mice. The purpose of these experiments was to build on an existing literature concerning the behaviour of *Dao* mutant mice, and the behaviour of wildtype rodents following the administration of D-serine and DAO inhibiting drugs. The ultimate goal of this research was to better understand the contribution of DAO to brain function and behaviour, and to assess the potential therapeutic value of DAO inhibition as a treatment for schizophrenia. The following paragraph provides a brief summary of the behavioural experiments performed with *Dao*$^{-/-}$ mice. A thorough interpretation of these results is provided at the end of Chapters 2 to 5, while common themes and unanswered questions are highlighted in the sections that follow.

Our first aim was to confirm whether anxiety is heightened in *Dao*$^{-/-}$ mice, as it is in ddY/*Dao*$^{-}$ mice, *Dao1*^{G181R} mice, and wildtype mice after D-serine administration [514]. A comprehensive anxiety screen involving five different tests revealed that anxiety was indeed elevated in *Dao*$^{-/-}$ mice relative to *Dao*$^{+/+}$ mice (see Chapter 2).

Our second goal was to determine whether short-term memory performance is enhanced in *Dao*$^{-/-}$ mice. Relative to *Dao*$^{+/+}$ mice, *Dao*$^{-/-}$ mice demonstrated enhanced recognition memory performance, and enhanced spontaneous alternation in the T-maze (see Chapter 2). This finding is novel, as short-term memory performance has yet to be tested in ddY/*Dao*$^{-}$ or *Dao1*^{G181R}

mice, although enhanced rewarded alternation has been observed in wildtype mice after D-serine administration [522].

Our third aim was to establish whether long-term spatial memory acquisition is enhanced in *Dao*$^{-/-}$ mice. This was an important question to address, given that previous studies of *Dao* mutants had yielded conflicting results. We subjected *Dao*$^{+/+}$ and *Dao*$^{-/-}$ mice to three long-term spatial memory tests: the Morris watermaze, appetitive Y-maze and aversive (swim escape) Y-maze. Our results indicate that long-term spatial memory acquisition is unaltered in *Dao*$^{-/-}$ mice, and that previous inconsistency in the *Dao* mutant literature may be explained by key methodological differences between studies. More generally, these data imply that performance in the Morris watermaze may be confounded by anxiety, and we suggest methodological alterations to the paradigm that might overcome this confound (see Chapter 3).

Our fourth goal was to investigate whether prepulse inhibition (PPI) is altered in *Dao*$^{-/-}$ mice. Again, this question was provoked by inconsistency in the *Dao* mutant literature. We observed a highly complex phenotype, wherein PPI was influenced by the genotype, sex and stress levels of the animals being tested (see Chapter 4). Once more, these data speak to the apparently conflicting findings of previous studies with *Dao* mutants, but raise as many questions as they provide answers.

Our fifth and final aim was to determine whether sleep or circadian rhythms are disrupted in *Dao*$^{-/-}$ mice, as they are in ddY/*Dao*$^{-}$ mice [Melanie Sobczyk, *unpublished data*]. Despite their previously characterised anxiety phenotype, we observed no evidence or sleep or circadian rhythm disruption (SCRD) in *Dao*$^{-/-}$ mice. These data and their implications are presented in

Chapter 5. In Section 7.4., they are further discussed in relation to the ‘shared neuropathophysiology’ hypothesis of SCRD in schizophrenia.

7.1.2. Mechanistic basis of altered behaviour in the Dao$^{-/-}$ mouse

At the end of Chapters 2 to 5, specific brain regions were highlighted that might mediate the effect of DAO inactivity on the observed behavioural phenotype of the *Dao*$^{-/-}$ mouse. In Chapter 2, the hippocampus was suggested as a possible mediator of its enhanced short-term memory performance and heightened anxiety, while in Chapter 4, the nucleus accumbens was pinpointed as a potential mediator of its altered PPI phenotype. The following paragraphs consider the proposed contribution of the hippocampus in more detail, and also assess the possible involvement of the cerebellum.

Hippocampal NMDA receptors

Dao expression and DAO activity have been detected in the rodent hippocampus [45]. Consistent with this, D-serine levels are elevated in the hippocampus in both *Dao1*^{G181R} mice [466] and *Dao*$^{-/-}$ mice [Pfizer Inc., *unpublished data*]. Altered hippocampal function provides the most parsimonious explanation of the behavioural phenotype of the *Dao*$^{-/-}$ mouse, since the hippocampus is relevant to anxiety, memory and prepulse inhibition. It is generally accepted that the ventral and dorsal hippocampus make dissociable contributions to anxiety and memory function, respectively [611]. Lesions to the ventral hippocampus reduce anxiety but do not affect memory performance in rodents, whereas lesions to the dorsal hippocampus impair memory performance but have no effect on anxiety [602, 612-619]. It should also be noted that heightened anxiety in *Dao*$^{-/-}$ mice – in which NMDAR activation is likely to be increased – is consistent with the fact that NMDAR antagonists reduce anxiety in both rodents and humans [766]. The genetic ablation of hippocampal NMDARs is also anxiolytic [766, 767].

While the contribution of the hippocampus to spatial recognition memory is uncontested, its involvement in object recognition memory is far from certain. The literature on this subject is

highly contentious and beyond the scope of this thesis, but the general consensus is that object recognition memory is dependent on the entorhinal and perirhinal cortices, but not the hippocampus [768-771]). Consistent with the fact that D-serine is increased in the hippocampus but not the cortex of *Dao*$^{-/-}$ mice, they demonstrated a highly significant enhancement in the spatial recognition memory task, but no significant advantage in the object recognition memory task. The hippocampus is also known to be important for spontaneous alternation – another task in which *Dao*$^{-/-}$ mice demonstrated an enhancement – since performance in this task is impaired by hippocampal lesions [621]. Having said this, odour recognition memory performance is independent of the hippocampus in rodents [772], but was significantly enhanced in *Dao*$^{-/-}$ mice.

In relation to PPI, neonatal excitotoxic lesions to the ventral hippocampus are known to reduce PPI in adult rats [773, 774]. Likewise, PPI is reduced by the infusion of NMDA into the ventral hippocampus [775-779], an effect that is counteracted by the co-infusion of the NMDAR-antagonist AP5 [780]. By contrast, NMDAR infusion, electrolytic lesions and excitotoxic lesions in the dorsal hippocampus have no effect on PPI [777, 781]. Moreover, PPI is reduced by 20 Hz electrical stimulation of the ventral hippocampus, but not by equivalent electrical stimulation of the dorsal hippocampus [782]. The ventral hippocampus is thought to exert its effect on PPI via efferents to the nucleus accumbens [778], which fits neatly with evidence implicating this brain region in the regulation of PPI (see Chapter 4). Nonetheless, this literature does not explain why PPI can be either increased or reduced in *Dao*$^{-/-}$ mice, depending on the sex and stress levels of the mouse being tested. Possible reasons for these effects are explored in Chapter 4.

Based on this accumulated evidence, it seems plausible that heightened hippocampal NMDAR activation could account for both the anxiety and short-term memory phenotypes of the *Dao*$^{-/-}$ mouse, and that it could also contribute to its altered PPI phenotype. While increased NMDAR activation in the dorsal hippocampus could explain their enhanced short-term memory performance, increased NMDAR activation in the ventral hippocampus could contribute to their elevated anxiety and altered prepulse inhibition. In future, one could test these hypotheses directly by injecting D-serine or a DAO inhibitor directly into the dorsal or ventral hippocampus of wildtype rodents. Alternatively, one could downregulate *Dao* expression in the dorsal or ventral hippocampus through lentiviral RNA-interference (RNAi). It would also be useful to confirm that NMDAR-mediated neurotransmission is upregulated in these brain regions in *Dao*$^{-/-}$ mice, using electrophysiological techniques. So far, this has only been confirmed in the dorsal horn of the spinal cord of ddY/*Dao*$^{-}$ mice [501].

How could increased hippocampal NMDAR activation facilitate short-term learning and memory in the *Dao*$^{-/-}$ mouse? Although long-term spatial memory acquisition is widely (although not universally) believed to depend on NMDAR-mediated hippocampal LTP [460, 461], short-term memory performance may depend on a qualitatively different mechanism [783, 784]. In the T-maze spontaneous alternation task, mice typically select the opposite arm to the previous arm that they entered, because of an innate preference for novelty. For the same reason, they generally pay more attention to the novel object, odour or spatial location in the test phase of recognition memory tasks. It has been argued that this novelty preference reflects a process called 'habituation', which is defined *as 'the decline in the tendency to respond to a stimulus following previous exposure'* [464]. Habituation may involve a reduction in activity in the neuronal network that represents the familiar object, odour or spatial location [464]. Since LTP increases the excitability of neurons, it is unlikely to be responsible for this process.

Instead, LTD is more likely to underpin short-term memory performance in both spatial and non-spatial tasks [462-465]. The enhanced short-term memory performance of *Dao*$^{-/-}$ mice could therefore reflect more rapid habituation, as a consequence of enhanced NMDAR-mediated LTD. Indeed, it has already been shown that D-serine facilitates hippocampal LTD in wildtype rodents [523, 533].

Cerebellum

The cerebellum is another brain region that could contribute to the observed behavioural phenotype of the *Dao*$^{-/-}$ mouse. *Dao* is highly expressed in the rodent cerebellum [45, 472], and D-serine and D-alanine levels are significantly elevated in *Dao* mutants [466, 472] and *Dao*$^{-/-}$ mice in this region [591,Pfizer Inc., *unpublished data*]. Although the cerebellum is better known for its role in motor control, it also contributes to cognitive and affective processes [785-788], via its involvement in cortico-thalamic-cerebellar circuits [146, 789, 790]. There is increasing evidence that these circuits may be dysfunctional in schizophrenia [146, 789-793], while functional neuroimaging studies have reported associations between poor cognitive performance and abnormal cerebellar activity in both schizophrenia patients and healthy volunteers [794]. Significantly, cerebellar DAO mRNA is increased in the post-mortem brain tissue of schizophrenia patients [45, 485, 496]. In future, one could assess the cerebellar contribution to the behavioural phenotype of *Dao*$^{-/-}$ mice via the partial downregulation of cerebellar *Dao* expression through lentiviral RNA-interference (RNAi). Cerebellar DAO knockdown has already been optimised in mice, although behavioural tests were not included in this study [795]. It would also be useful to confirm that NMDAR-mediated neurotransmission is upregulated in the cerebellum of *Dao*$^{-/-}$ mice. This could be tested electrophysiologically.

D-alanine

In the brains of *Dao* mutants, increases in D-alanine levels are more widespread than increases in D-serine [472]. In ddY/*Dao*$^{-}$ mice, for example, D-serine concentration is unaltered in the cortex, but cortical D-alanine concentration is dramatically increased [472]. To date, D-alanine levels have not been assessed in the brains of *Dao*$^{-/-}$ mice. Like D-serine, D-alanine is a potent NMDAR co-agonist that is degraded by DAO [488-490], although the enzyme that catalyses its synthesis is currently unknown. Hence, it is conceivable that D-alanine could contribute to the behavioural phenotypes of *Dao*$^{-/-}$ mice and *Dao* mutants. In future, one could explore this hypothesis by administering D-alanine to wildtype rodents. At present, very little is known about the effects of D-alanine on any schizophrenia-relevant behaviours, although it does reverse PCP-induced hyperlocomotion in wildtype rats [490]. In addition, there is unpublished data which shows that in wildtype rats, D-alanine administration improves performance in an attentional set-shifting task [Phil Burnet, *unpublished data*]. This is significant, since attentional set-shifting is impaired in schizophrenia patients [796]. Moreover, improvements have been observed in the cognitive symptoms of schizophrenia patients following the the co-administration of D-alanine and antipsychotic medication [797].

Sex differences

Sex differences were a common theme in the behavioural phenotype of *Dao*$^{-/-}$ mice. Firstly, novelty-suppressed feeding was significantly increased in female *Dao*$^{-/-}$ mice, but no such change was evident in male *Dao*$^{-/-}$ mice. This is consistent with the fact that the anxiety phenotypes of both ddY/*Dao*$^{-}$ mice and *Dao1*^{G181R} mice are more pronounced in females than males [514]. Conversely, the effect of radial platform distance on Morris watermaze performance was greater in male *Dao*$^{-/-}$ mice than female *Dao*$^{-/-}$ mice. The contribution of sex to PPI was even more complex: in the absence of injection stress, PPI was reduced in male

Dao$^{-/-}$ mice relative to male *Dao*$^{+/+}$ mice, but increased in female *Dao*$^{-/-}$ mice relative to female *Dao*$^{+/+}$ mice. Following injection stress, these contingencies were reversed. The ovarian steroid hormone oestrogen is a likely to contribute these genotype-by-sex interactions. Females may be more sensitive to the effects of increased brain D-serine, since oestrogen is known to upregulate NMDAR function within the brain [798]. In particular, oestrogen increases the expression of the NMDAR subunit GluN1 in the hippocampus and the NMDAR subunits GluN2A and GluN2B in the hypothalamus [798, 799]. Oestrogen also promotes dendritic spine formation and synaptogenesis in the hippocampus and hypothalamus, both during development and adulthood, via its interaction with NMDARs [800-802]. As mentioned in Chapter 4, the striatum is as a possible mediator of the effect of sex on PPI in *Dao*$^{-/-}$ mice, given that oestrogen influences dopaminergic activity in the striatum and NAc [681]. Despite this assorted evidence, we are some way from providing a satisfactory account of how oestrogen interacts with *Dao* inactivity to produce the distinct behavioural alterations of *Dao*$^{-/-}$ mice in different behavioural tasks. More generally, the observation of significant sex differences in the behaviour of *Dao*$^{-/-}$ mice emphasises the importance of testing both males and females when characterising the behaviour of transgenic models.

7.1.3. Future directions

Tasks relevant to the positive and negative symptoms of schizophrenia

In the experiments described in this thesis, we characterised the performance of *Dao*$^{-/-}$ mice in a variety of memory tests. By contrast, we have yet to subject *Dao*$^{-/-}$ mice to any tests that are relevant to the positive or negative symptoms of schizophrenia. Previous studies involving the administration of D-serine or DAO inhibitors to wildtype rodents (see Table 1.5) suggest that behavioural alterations might also be witnessed in these tasks.

Tasks relevant to the cognitive symptoms of schizophrenia

Memory impairments are not the only cognitive deficits witnessed in schizophrenia patients; impaired cognitive flexibility is also common [803, 804]. Reversal learning in the Morris watermaze is one means of assessing cognitive flexibility. *Dao1*^{G181R} mice demonstrate enhanced Morris watermaze reversal learning [466], as do wildtype mice after D-serine administration [523]. As outlined in Chapter 3, we did not observe enhanced reversal learning in *Dao*$^{-/-}$ mice in the Morris watermaze. As mentioned, it would be useful to test reversal learning in *Dao*$^{-/-}$ mice in the radial arm maze or Barnes maze. This would establish whether reversal learning is genuinely unaltered in *Dao*$^{-/-}$ mice, or whether our negative findings in the Morris watermaze were the result of methodological differences between our study and previous studies [466, 523].

The interaction between Dao inactivity and the stress response

There are possible parallels between our PPI findings and our observations in the Morris watermaze. In the same way that PPI in *Dao*$^{-/-}$ mice was reduced under certain conditions but increased under others, the Morris watermaze performance of *Dao*$^{+/+}$ mice was facilitated on certain trials but impaired on others. It is possible that both findings reflect an interaction

between DAO inactivity and the stress response; intraperitoneal injections evoke a mild stress response, while there may be a progressive increase in stress across consecutive watermaze trials. Testing this hypothesis would be difficult, since it is hard to quantify the stress responses of mice on a minute-by-minute basis. Plasma corticosterone is often used as an index of the stress, and it is known that corticosterone levels rise following restraint and/or injection stress [805], along with heart rate and body temperature [806]. Moreover, plasma corticosterone levels are significantly elevated 30 minutes after the completion of 6 consecutive 1 minute trials in the Morris watermaze [807]. However, no study has profiled changes in corticosterone across successive watermaze trials. Such an experiment may not be informative, since there is a delay of up to 5 minutes between the initial exposure to a stressor and the onset of a detectable corticosterone response in rodents [603]. Hence, corticosterone measurements could not serve as a proxy for subjective stress levels in individual trials. Heart rate can also be discounted since it will be increased by experimenter handling and the vigorous exercise of swimming in the watermaze, while body temperature would be reduced by the exposure to cold water. A better alternative might be to monitor EEG correlates of stress throughout behavioural testing using a telemetry system [808]. However, it would be difficult to combine telemetry with watermaze testing, as mice need to be close to the receiver at all times. Likewise, tethered EEG would be complicated by the large size of the test arena. In sum, there are many technical challenges associated with measuring the stress response of rodents during behavioural testing. At present, no satisfactory biomarkers exist for this type of experiment.

7.1.4. Potential weaknesses of the Dao$^{-/-}$ mouse model

There are several limitations inherent to the *Dao*$^{-/-}$ model, which are important to acknowledge. Firstly, DAO activity may be modulated by the protein D-amino acid oxidase activator (DAOA) in the human brain, but DAOA has no known orthologue in rodents [44]. Although it is unclear whether DAOA facilitates or inhibits DAO activity [44, 491], the possibility exists that D-serine metabolism is regulated in a fundamentally different manner in humans and rodents. Moreover, overall levels of DAO activity are generally higher in humans than they are in mice [486]. In particular, DAO activity is apparent in frontal brain regions in humans, but is almost undetectable in frontal areas in mice [486]. This is despite the fact that DAO mRNA is found in the forebrain of both humans and rodents [45].

Another weakness of the model is that, as a constitutive knockout, the observed behavioural phenotype could be due to altered neurodevelopment or compensatory changes in gene expression. Consistent with this suggestion, there is evidence which implicates DAO in neurodevelopmental processes [472]. Having said this, NMDAR subunit expression is unaltered in the brains of ddY/*Dao*$^{-}$ mice [472] and cerebellar DAO knockdown mice [795]. Moreover, the behavioural effects of D-serine on anxiety in wildtype rodents closely parallel the behavioural effects of the genetic ablation of DAO.

The fact that some cohorts of *Dao*$^{-/-}$ mice were singly-housed may also have been a confound; since single housing is be stressful, the observed behavioural alterations could reflect an interaction between *Dao* inactivity and this additional stressor. However, this seems unlikely given that heightened anxiety was observed in both singly- and group-housed *Dao*$^{-/-}$ mice.

Another important point is that the behavioural alterations of *Dao* mutants and *Dao*$^{-/-}$ mice – and indeed the behavioural alterations of wildtype rodents after the administration of D-serine or DAO inhibitors – are thought to reflect the elevation of brain D-serine concentration *above* normal levels. In schizophrenia patients, the aim is to *reverse* cognitive impairments by *restoring* D-serine concentration to normal levels. Hence, a better approach might be to create a *Dao* overexpressing mouse (which would be more representative of individuals with schizophrenia), and then administer D-serine or DAO inhibitors in order to reverse their cognitive impairments (should they exist). This approach may be worth pursuing in the future.

7.1.5. Clinical implications

There is moderate evidence that *Dao* is a susceptibility gene for schizophrenia [44, 480-482], while *Dao* expression and DAO activity are elevated in the brains of schizophrenia patients [485, 494-498]. Conversely, D-serine concentration is reduced in patients' serum and cerebrospinal fluid [475-479]. Given that D-serine is an NMDAR co-agonist, the overactivity of DAO – and resulting insufficiency of D-serine – could contribute to the NMDAR hypofunction proposed to exist in schizophrenia [45, 97-100, 493]. Consequently, the administration of D-serine [504-507] and DAO inhibiting drugs [684-686] have both been suggested as potential treatments for schizophrenia. Our data add to a growing body of preclinical evidence which suggests that these approaches could ameliorate the memory deficits of schizophrenia patients, although these effects may not extend to long-term associative memory. In addition, these benefits could come at the cost of heightened anxiety. Our data also imply that these treatments could have different effects in male and female patients. Nonetheless, they are worthy of further investigation, especially given the success of a recent clinical trial involving the administration of the DAO inhibitor sodium benzoate to schizophrenia patients [502].

7.2. Sleep, circadian rhythms and schizophrenia-relevant behavioural abnormalities in the *Grm2/3*$^{-/-}$ mouse

7.2.1. SCRD in the Grm2/3$^{-/-}$ *mouse*

Sleep and circadian characterisation of the *Grm2/3*$^{-/-}$ mouse was performed in order to test the 'shared neuropathophysiology' hypothesis of schizophrenia. This theory posits that the co-morbidity of schizophrenia and SCRD stems from dysfunction in common brain mechanisms (e.g. specific neurotransmitter systems) [125, 343]. According to this hypothesis, one might predict that the manipulation of schizophrenia-relevant genes in mice should result in simultaneous SCRD and schizophrenia-relevant behavioural abnormalities (e.g. impaired memory or reduced prepulse inhibition). We expected to observe SCRD in the *Grm2/3*$^{-/-}$ mouse, given evidence that:

1) There is glutamatergic dysfunction in schizophrenia (see section 1.2.5.).
2) Glutamatergic neurotransmission contributes to sleep and circadian function at multiple levels (see section 5.1.).
3) Group II mGlus may be particularly relevant to the pathophysiology of schizophrenia (see section 1.10.2.)
4) Group II mGlus are implicated in sleep and circadian function at multiple levels (see Section 6.1).

Consistent with our hypothesis, significant SCRD was observed in *Grm2/3*$^{-/-}$ mice (see Chapter 6). More specifically, they demonstrated increased sleep fragmentation, and reduced sleep time, particularly in the light (inactive) phase. They also displayed increased sensitivity to the

circadian effects of light, manifested as increased period lengthening in constant light, and greater phase delays in response to type I and type II phase-shifting light pulses.

7.2.2. Relevance of the observed SCRD phenotype to schizophrenia

The observation of significant sleep disruption in the *Grm2/3*$^{-/-}$ mouse provides clear support for the 'shared neuropathophysiology' hypothesis of SCRD in schizophrenia. Further support is provided by the fact that its sleep phenotype is reminiscent of the sleep phenotype of many schizophrenia patients; reduced sleep duration and increased sleep fragmentation are both common in individuals with schizophrenia [327, 328, 333-335]. In future, one should establish whether the reduced sleep in *Grm2/3*$^{-/-}$ mice reflects an equal reduction in REM or NREM sleep, or a selective reduction of one or the other. This question could easily be addressed with EEG-based sleep analysis. One would expect to observe a selective reduction in REM sleep, given that REM sleep is reduced by mGlu2/3 agonists, antagonists, positive allosteric modulators and negative allosteric modulators alike [575-582]. Although reduced REM sleep duration is seen in some schizophrenia patients, reduced REM sleep latency is more common, together with reductions in slow-wave sleep (i.e. NREM stage 3) duration [327, 328, 333-335]. Moreover, REM sleep latency is significantly associated with the negative symptoms of schizophrenia, as well as attentional set-shifting performance [401, 412-414]. However, this does not invalidate the *Grm2/3*$^{-/-}$ model, as sleep disruption in schizophrenia is highly heterogeneous; the exact nature of SCRD varies from patient to patient [327, 328, 333-335], in much the same way that the exact combination of behavioural symptoms varies between patients [146]. Based on this knowledge, and based on the fact that REM sleep disruption has been observed in other psychiatric disorders [809], reduced REM sleep could be conceptualised as a neuropsychiatric endophenotype [147]. Significantly, *Grm3* is also associated with bipolar disorder [550, 551], and, in contrast to schizophrenia, reduced REM sleep is very common in this condition [809].

By contrast, it is currently unclear whether the increased photosensitivity of the *Grm2/3*$^{-/-}$ mouse is relevant to schizophrenia. In humans, circadian photosensitivity is typically assessed by quantifying the light-induced suppression of nocturnal melatonin secretion. This response has yet to be assessed in schizophrenia patients, an issue which should be assessed in the future. However, the light-induced suppression of nocturnal melatonin secretion *is* increased in patients with bipolar disorder and seasonal affective disorder [762]. This suggests that the *Grm2/3*$^{-/-}$ mouse may be as relevant to bipolar disorder as it is to schizophrenia. Again, this is consistent with the fact that *Grm3* variants have been significantly associated with bipolar disorder [550, 551].

Finally, *Grm2/3*$^{-/-}$ mice demonstrated significantly perturbed wheel-running activity under a 12:12 LD cycle. Their wheel-running behaviour was characterised by increased activity fragmentation and reduced consistency, while total activity levels were substantially reduced. Interestingly, the wheel-running activity profiles of *Grm2/3*$^{-/-}$ mice bear a close resemblance to the inconsistent and fragmented activity profiles of schizophrenia patients, as assessed by actigraphy in a recent study [349]. However, as described in Chapter 6, the activity profiles of *Grm2/3*$^{+/+}$ and *Grm2/3*$^{-/-}$ mice were virtually identical when homecage activity was assessed with NIR cameras or PIR motion detectors. This suggests that the altered wheel-running behaviour of *Grm2/3*$^{-/-}$ mice was an artefact of the use of the running wheels, rather than evidence of underlying circadian dysregulation. This conclusion has important implications for the use of running wheels in circadian research, as discussed in Section 7.7.

7.2.3. Future directions

Further circadian phenotyping

Due to time constraints, phase delays were only quantified after a type I phase-shifting light pulse at CT 16 and a type II phase-shifting light pulse at ZT 16. In future, light pulses should be administered at a range of other timepoints in order to generate phase-response curves (PRCs) for *Grm2/3*$^{+/+}$ and *Grm2/3*$^{-/-}$ mice. With just a single timepoint, one cannot be absolutely certain that *Grm2/3*$^{-/-}$ mice are more sensitive to phase-shifting light pulses. Instead, their PRC may simply be shifted relative to *Grm2/3*$^{+/+}$ mice.

Further sleep phenotyping

As mentioned above, it would be useful to establish the observed reduction in sleep duration reflects a reduction in REM sleep, NREM sleep, or both. Besides this, other important questions remain unanswered. For example, does sleep disruption in *Grm2/3*$^{-/-}$ mice reflect the absence of mGlu2, mGlu3, or both from the brain? To address this question, one could characterise sleep in *Grm2*$^{-/-}$ and *Grm3*$^{-/-}$ mice. This approach might not be revealing, given that the behavioural phenotypes of both models is mild in comparison to that of the *Grm2/3*$^{-/-}$ mouse [561, 562]. As explained in Section 1.10.3., this may reflect the compensatory upregulation of *Grm3* expression in *Grm2*$^{-/-}$ mice, and the compensatory upregulation of *Grm2* expression in *Grm3*$^{-/-}$ mice [560]. Assuming that there is degree of functional redundancy in the roles of mGlu2 and mGlu3, one might not expect to observe sleep disruption in either model. Clearly, such a result would not indicate that mGlu2 and mGlu3 are uninvolved in sleep regulation.

In this context, a better alternative might be to target mGlu2 and mGlu3 separately using selective pharmacological agents. Until very recently, there were few pharmacological

compounds that discriminated between mGlu2 and mGlu3 [43, 810], so this approach was not possible. Hence, to date, almost all of the sleep research involving the administration of mGlu2/3 modulating drugs to wildtype rodents has employed compounds that target both mGlu2 and mGlu3 [575-582]. More selective compounds are becoming increasingly available, so the consequences of mGlu2 and mGlu3 modulation can now be evaluated separately.

Even in the absence of selective pharmacological agents, the respective roles of mGlu2 and mGlu3 could be tested pharmacologically by administering mGlu2/3 modulating drugs to *Grm2*$^{-/-}$ and *Grm3*$^{-/-}$ mice. This approach has already been taken in a study by Ahnaou and colleagues, who administered the non-selective mGlu2/3 agonist LY354740 to wildtype mice and *Grm2*$^{-/-}$ mice [575]. Significantly, LY354740 inhibited REM sleep in wildtype mice but not in *Grm2*$^{-/-}$ mice. This tentatively suggests that REM sleep is regulated by mGlu2 and not mGlu3. To further validate this hypothesis, one would need to confirm that LY354740 can suppress REM sleep in *Grm3*$^{-/-}$ mice. Without this evidence, it is possible that the negative result in *Grm2*$^{-/-}$ mice was due to a reduction in total number of group II mGlus within the brain, rather than the selective loss of mGlu2. If mGlu3 is uninvolved in REM sleep regulation this would have important implications for the 'shared neuropathophysiology' hypothesis, since there is no evidence of an association between *Grm2* and schizophrenia. It also remains to be seen whether mGlu2 or mGlu3 (or both) modulate sensitivity to the circadian effects of light. Two studies have demonstrated that the magnitude of light-induced phase shifts are altered following the administration of mGlu2/3 modulating drugs, but neither used drugs that were specific to mGlu2 or mGlu3 [748, 749]. A further alternative would be to generate conditional *Grm2*$^{-/-}$ or *Grm3*$^{-/-}$ mice. As with the pharmacological approach, this would eliminate the possibility of long-term compensatory changes in gene expression. It would also avoid the confounding influence of injection stress (unless pharmacological agents were

administered by minipump), which has been shown to have opposite behavioural effects in *Grm2/3*$^{+/+}$ and *Grm2/3*$^{-/-}$ mice.

It is also unclear as to which brain region or regions are responsible for the altered sleep phenotype of the *Grm2/3*$^{-/-}$ mouse. The amygdala is a promising candidate, given that REM sleep is suppressed in wildtype rats by the microinjection of an mGlu2/3 agonist directly into the basal amygdala [578]. Further suggestions are provided in Section 6.4. In future, the involvement of these brain regions could be investigated with local microinjections.

Investigating the relationship between sleep disruption and the schizophrenia-like behavioural symptoms of the Grm2/3$^{-/-}$ *mouse*

The phenotype of the *Grm2/3*$^{-/-}$ mouse is consistent with the 'shared neuropathophysiology' hypothesis of SCRD in schizophrenia in that it demonstrates concurrent sleep disruption and schizophrenia-like working memory and long-term memory deficits. However, the relationship between the model's sleep phenotype and its memory phenotype is currently unknown. Intuitively, it seems unlikely that impaired memory function could directly disrupt sleep. Hence, three possible explanations exist (see Fig. 7.1).

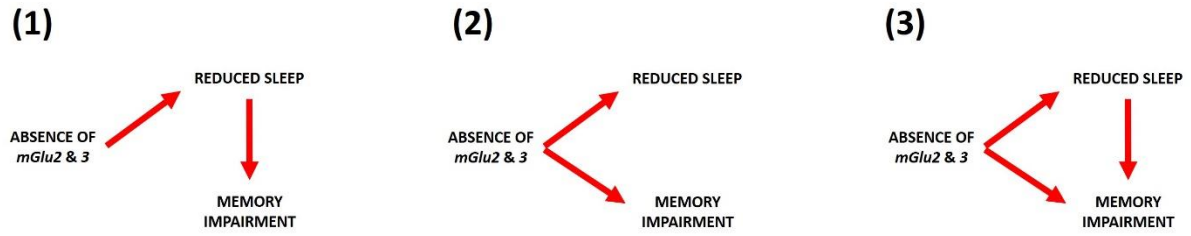

Fig. 7.1. Possible relationships between reduced sleep and memory impairment in the *Grm2/3-/-* mouse. (1) The absence of mGlu2 and mGlu3 causes sleep loss in *Grm2/3*$^{-/-}$ mice, which is *entirely* responsible for their impaired memory performance. (2) The absence of mGlu2 and mGlu3 causes sleep loss *and* memory deficits by *separate* pathways. (3) The absence of mGlu2 and mGlu3 causes sleep loss *and* memory deficits by *separate* pathways, but sleep disturbance serves to *exacerbate* the memory impairments of *Grm2/3*$^{-/-}$ mice.

Explanation 1 seems highly improbable, given that rodent memory performance can be altered by the acute administration of mGlu2/3 modulating drugs (see Section 1.10.4). Since the animals do not sleep in the intervening period between drug administration and the onset of the memory test, sleep disruption cannot mediate the effect of the drug on test performance. Thus, only two possible explanations remain. If explanation 2 is correct, then an intervention that reverses sleep loss should have no impact on the memory performance of *Grm2/3*$^{-/-}$ mice. However, if explanation 3 is correct, then such an intervention should result in a partial but incomplete reversal of their impaired memory performance.

From a clinical perspective, this issue is important to resolve. If option 3 is correct, and sleep disruption makes a *causal contribution* to the cognitive phenotype of the *Grm2/3*$^{-/-}$ mouse, then the same could be true of schizophrenia patients. In turn, this would imply that the targeted treatment of sleep disruption might improve the cognitive symptoms of individuals with schizophrenia. To falsify this hypothesis (in rodents at least), one could identify a behavioural or pharmacological intervention that increases sleep time in *Grm2/3*$^{-/-}$ mice, and assess their memory performance both with and without this intervention. Proof-of-principle for such an experiment is provided by the work of Morton and colleagues, who employed this approach with the R6/2 transgenic mouse model of Huntington's disease. In this model, which demonstrates significant SCRD, light phase administration of the sedative drug Alprazolam had the dual effect of improving behavioural rhythmicity and improving cognitive performance in a simple two-choice swim task [453, 454]. This work tentatively suggests that SCRD makes a causal contribution to cognitive dysfunction in Huntington's disease. In future, one could apply the same intervention in *Grm2/3*$^{-/-}$ mice, and assess its impact on light phase sleep time, sleep fragmentation and memory performance.

It is highly conceivable that sleep loss contributes to the memory deficits of *Grm2/3*$^{-/-}$ mice, given that experimental sleep deprivation elicits a wide range of cognitive impairments in wildtype rodents. These include object recognition memory deficits [424, 425], spatial recognition memory deficits [426, 427], long-term spatial memory deficits in the Morris water maze [428-432] and radial arm maze [433], and attentional impairments in the 5-choice serial reaction time task [434].

Exactly how could sleep loss impair the memory performance of *Grm2/3*$^{-/-}$ mice? Sleep is believed to be important for long-term memory consolidation [207], so it could be suggested that their memory is impaired via interference with this process. However, as explained in Section 1.10.3., *Grm2/3*$^{-/-}$ mice display deficits in three different memory tasks: the rewarded Y-maze task, the T-maze rewarded alternation task, and the Y-maze spatial novelty preference task [561]. Of these the tasks, only the rewarded Y-maze task is a long-term memory task. Hence, the impairment of overnight memory consolidation cannot explain the observed deficits in the other two tasks. Moreover, *Grm2/3*$^{-/-}$ mice show no impairment in the aversive (swim escape) Y-maze task or the aversively-motivated Morris watermaze task [561], both of which are long-term memory tasks. This also suggests that memory consolidation is unimpaired in *Grm2/3*$^{-/-}$ mice, and, furthermore, that their altered memory performance is in some way related to the arousal-inducing properties of the various tasks.

Lyon and colleagues have themselves suggested that *arousal* may be *reduced* in *Grm2/3*$^{-/-}$ mice [561]. This could explain their poor performance in appetitive memory tasks, given the proposed inverted U-shaped relationship between arousal and cognitive performance, as described by the Yerkes-Dodson Law [811] (see Fig. 7.2A). When arousal is increased in aversive, water-based memory tasks, *Grm2/3*$^{-/-}$ mice are no longer at a disadvantage relative to

Grm2/3$^{+/+}$ mice (see Fig. 7.2B). Then, when arousal is increased still further by a stressful injection, *Grm2/3*$^{-/-}$ mice might be expected to outperform *Grm2/3*$^{+/+}$ mice (see Fig. 7.2C), as they do in the T-maze rewarded alternation task following an intraperitoneal saline injection [561]. This explanation can now be extended to include the hypothesis that chronic partial sleep loss is at least partially responsible for the reduced arousal phenotype of the *Grm2/3*$^{-/-}$ mouse. In support of this claim, it has consistently been shown that sleep deprivation reduces waking arousal in humans [812-815]. Having said this, it is also possible that the reduced arousal phenotype of the *Grm2/3*$^{-/-}$ mouse is a *direct* consequence of changes in the ascending arousal system, which result in reduced arousal during periods of wakefulness. Of course, these two theories are not mutually exclusive.

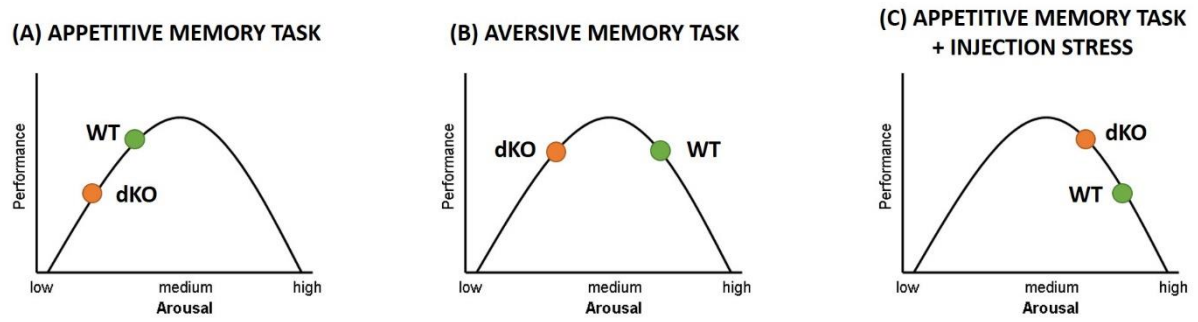

Figure 7.2. Using the Yerkes-Dodson curve to explain the spatial memory performance of *Grm2/3*$^{+/+}$ (WT) and *Grm2/3*$^{-/-}$ (dKO) mice. (A) In appetitive memory tasks, WT mice outperform dKO mice. (B) In aversive memory tasks, dKO mice are no longer at a disadvantage relative to WT mice. (C). In an appetitive memory task preceded by a stressful intraperitoneal saline injection, dKO mice outperform WT mice.

Further behavioural phenotyping

In Chapter 6, it was proposed that the reduced wheel-running activity of *Grm2/3*$^{-/-}$ mice might be a reflection of changes in mesolimbic dopaminergic reward circuitry. Certainly, there is good evidence that long-term voluntary wheel-running is rewarding for rodents, and that it produces plastic changes in mesolimbic dopaminergic reward circuity [763]. Significantly, striatal dopamine is markedly reduced in *Grm2/3*$^{-/-}$ mice, particularly in the nucleus accumbens

[676], a brain region involved in reward and motivation [764, 765]. If this theory is correct, then the *Grm2/3*$^{-/-}$ mouse may eventually be considered a better model of the negative symptoms of schizophrenia (and possibly bipolar disorder) than of the cognitive symptoms. Hence, it will be especially important to subject *Grm2/3*$^{-/-}$ mice to a battery of tests relevant to the negative symptoms of schizophrenia. These could include tests of social interaction, behavioural despair (e.g. tail suspension test or Porsolt forced swim test) or anhedonia (sucrose preference test or intracranial self-stimulation). There is good reason to believe that sucrose preference might be reduced, as a trend-level decrease has already been observed in *Grm2/3*$^{-/-}$ mice in a relatively small sample [Louisa Lyon, *unpublished data*].

Aside from the spatial memory tests mentioned in the preceding paragraphs, no other schizophrenia-relevant behaviours have been assessed in *Grm2/3*$^{-/-}$ mice. Future studies should address this knowledge gap. After assessing a range of negative symptom-like behaviours, it would be useful to establish whether *Grm2/3*$^{-/-}$ mice are impaired at non-spatial memory tasks, such as the object recognition memory task, as there is evidence of object recognition memory deficits in schizophrenia patients [133]. Secondly, one could assess PPI in *Grm2/3*$^{-/-}$ mice, given that PPI deficits have been widely reported in schizophrenia [137-141]. Lastly, one could test behaviours relevant to the positive symptoms of schizophrenia, such as NMDAR-induced hyperlocomotion.

Given preliminary evidence that *Grm3* expression might be reduced in the brains of schizophrenia patients [552], one might expect any additional behavioural alterations, if observed, to be in the same direction as in schizophrenia. Hence, short-term memory performance may be impaired, PPI and social interaction might be reduced, and behavioural despair, anhedonia and NMDAR-induced hyperlocomotion may be increased. Having said this,

one would not expect to observe *all* of these behavioural alterations, given that schizophrenia is a complex multi-gene disorder, and no transgenic model is likely to recapitulate the full range of symptoms observed in a schizophrenia patient (see Section 1.3.). However, the identification of any additional schizophrenia-relevant behavioural alterations would afford further opportunities to investigate the relationship between schizophrenia-relevant behaviour and sleep disruption. For example, if reduced PPI is observed in *Grm2/3*$^{-/-}$ mice, is this effect ameliorated by an intervention that reverses sleep loss? There is some reason to believe that it might, given that sleep deprivation reduces PPI in wildtype rats [435-437]. By the same token, NMDAR antagonist-induced hyperlocomotion is greater after sleep deprivation in wildtype rats [423], and object recognition memory is impaired by sleep deprivation in wildtype mice and hamsters [424, 425].

7.2.4. Potential Weaknesses of the Grm2/3$^{-/-}$ mouse model

A weakness of the *Grm2/3*$^{-/-}$ model is that *Grm2/3*$^{+/+}$ and *Grm2/3*$^{-/-}$ mice were maintained as separate lines. This decision was taken in order to avoid the prohibitive wastage of animals that would have resulted had all *Grm2/3*$^{+/+}$ and *Grm2/3*$^{-/-}$ mice been derived from double heterozygous crosses. Using this approach, 14 out of every 16 mice would have been heterozygous for *Grm2* and/or *Grm3,* and would not have been used for sleep and circadian screening. Hence, the possibility exists that the observed behavioural differences between the lines were the product of genetic drift caused by *de novo* mutations. To minimise this risk of this, the *Grm2/3*$^{+/+}$ and *Grm2/3*$^{-/-}$ lines were renewed after six generations by out-crossing the *Grm2/3*$^{-/-}$ line onto C57Bl/6 mice (see Section 6.2.). It should also be noted that the reduced sleep and altered phase-shifting phenotypes of the *Grm2/3*$^{-/-}$ mouse closely paralleled the effects of mGlu2/3 antagonists on the behaviour of wildtype rats and mice.

The second key limitation of the model is that it is impossible to determine whether the absence of mGlu2 or mGlu3 (or both) are responsible for the observed SCRD phenotype. This is important to establish, given that *Grm2* is not associated with schizophrenia.

Another important point is that mice were singly-housed throughout sleep and circadian screening. By contrast, mice were group-housed in previous experiments in which schizophrenia-relevant behaviours were assessed [561, 562]. Hence, comparisons cannot be drawn between the two datasets with complete confidence. In future, one would need to demonstrate simultaneous SCRD and impaired memory performance in *Grm2/3*$^{-/-}$ mice housed under identical conditions.

7.2.5. Direct clinical implications of the involvement of group II mGlus in sleep regulation

As well as speaking to the 'shared neuropathophysiology' hypothesis of SCRD in schizophrenia, our data has more direct clinical implications. The use of both mGlu2/3 agonists and antagonists have been suggested as potential treatments for schizophrenia [43], while the use of mGlu2/3 antagonists has been proposed as a possible treatment for depression [816]. The fact that mGlu2/3 agonists, antagonists, positive and negative allosteric modulators all reduce REM sleep in wildtype rats [575-582] – together with the observation of reduced sleep in *Grm2/3*$^{-/-}$ mice – suggests that there is a genuine risk that sleep loss could result from treatment with these compounds. Future clinical trials involving mGlu2/3 modulating drugs should therefore include measures of sleep quality. Additionally, light-induced melatonin suppression could be used to assess the sensitivity of the circadian system to light.

7.3. Investigating the 'shared neuropathophysiology' hypothesis in other genetic mouse models

Since the *Grm2/3*$^{-/-}$ mouse demonstrates concurrent SCRD and schizophrenia-relevant behaviours, it is clearly consistent with the 'shared neuropathophysiology' hypothesis of SCRD in schizophrenia. It therefore joins the *Bdr* mutant model, which has been shown to do the same. In the paragraphs that follow, we pinpoint eight further genes that might contribute to the co-morbidity of SCRD and schizophrenia. Future studies could characterise sleep, circadian rhythms and schizophrenia-relevant behaviours in mice in which these genes have been manipulated. However, it should be noted that the ultimate goal of the 'shared neuropathophysiology' hypothesis is not to identify as many models as possible with simultaneous deficits. Instead it should be to investigate the nature of the relationship between SCRD and schizophrenia-relevant behaviours in the models in which they co-occur.

ErbB4

NRG1 (see Section 1.7.3) acts through the same family of tyrosine kinase receptors as TGF-a, a putative inhibitory output signal of the SCN [197]. TGF-a acts on ERBB1 receptors, whilst NRG1 acts on ERBB4 receptors. ERBB1 receptors have a known role in locomotor activity and sleep; mice with reduced ERBB1 receptor activity show reduced negative masking by light [197]. Future studies should address whether ERBB4 receptors play a similar role. Polymorphisms in *ErbB4* have previously been associated with schizophrenia [38].

Gsk3b

Dysregulation of the serine/threonine protein kinase GSK3 has been implicated in schizophrenia and bipolar disorder [51]. GSK3 activity is inhibited by the proteins encoded by the putative schizophrenia risk genes *Disc1* and *Akt1* [51, 817]. Significantly, the GSK3

inhibitor TDZD-8 ameliorates hyperactivity and PPI deficits in the *Disc1-L100P* mutant, a schizophrenia-relevant mouse model [51]. In a second model, the *Disc1-Q31L* mutant mouse, TDZD-8 corrects a PPI deficit, reduces immobility in the forced swim test, and increases social interaction [51]. Interestingly, clinicians often prescribe the mood stabiliser lithium (a GSK3 inhibitor) to schizophrenia patients to augment their antipsychotic medication, although the efficacy of this strategy is unclear [818]. GSK3b has a known role in circadian function; it phosphorylates clock proteins and regulates several components of the transcriptional–translational feedback loop that generates circadian rhythms [819-822]. GSK3b also inhibits CREB DNA-binding activity [823], which is involved in circadian signal transduction [824].

Pde4d

PDE4 is a phosphodiesterase that been associated with schizophrenia in a number of studies [52-54]. Like GSK3, PDE4 activity is inhibited by the protein encoded by the putative schizophrenia risk gene *Disc1* [51, 817]. Crucially, the PDE4 inhibitor Rolipram acts as a cognitive enhancer, facilitating LTP, memory performance and latent inhibition in wildtype rodents [825-827], and attenuating PPI deficits in the *Disc1-L100P* mutant mouse [51]. In addition, Rolipram has antidepressant-like properties; it reduces immobility in the forced swim test in wildtype rats [827]. From a circadian perspective, PDE4 regulates cAMP signalling, which is involved in circadian signal transduction [828]. Intriguingly, a polymorphism in *Pde4d* has been associated with sleepiness in healthy individuals [829].

Tcf4

Several large GWAS studies have identified the basic helix-loop-helix transcription factor TCF4 as one of the most significant schizophrenia susceptibility genes [55]. The protein encoded by this gene resembles ID (inhibitor of DNA-binding) proteins, which act as negative

regulators of the TTFL that generates intracellular circadian rhythms [830]. To date, at least eight different *Tcf4* mutants have been produced by ENU mutagenesis, but their circadian profiles have yet to be characterised.

Comt

Catechol-*O*-methyltransferase (COMT) is an enzyme which degrades catecholamines such as dopamine, a neurotransmitter which is strongly implicated in schizophrenia [46]. There is mixed evidence from genetic linkage and association studies that *Comt* is a susceptibility gene for schizophrenia [46], while the *Comt* gene is also relevant to the disorder by virtue of its location on chromosome 22, band q11.2 [831], since microdeletions in this region are associated with a 20 to 30-fold increased risk of schizophrenia [832]. In healthy humans, *Comt* genotype is associated with alterations in executive function, working memory performance and PPI [46, 833], while transgenic mouse models demonstrate comparable phenotypes [834, 835]. Sleep and circadian function has yet to be investigated in these mice, but there is good evidence that COMT is relevant to sleep regulation, since mutations in *Comt* are associated with sleep disturbances during adolescence [836]. *Comt* polymorphisms have also been implicated in sleep disturbances in children with attention deficit hyperactivity disorder [837], as well as healthy young men [838]. *Comt* genotype has a significant impact on the efficacy on the wake-promoting drug modafinil [839], while the COMT inhibitor tolcapone is known to increase sleep quality and reduce daytime sleepiness in advanced Parkinson's disease patients [840].

Nos

Nitric oxide synthases (NOS) are a family of enzymes that catalyse the synthesis of nitric oxide (NO) from L-arginine. NO is a second messenger of the NMDAR, and also interacts with the

serotonergic and dopaminergic neurotransmitter systems. Non-coding variants of the *Nos1* gene have been associated with schizophrenia [841, 842]. They are also associated with altered prefrontal cortical function and performance in prefrontal cortex-dependent tasks, such as the go/no-go task [843]. *Nos* expression may be altered in the brains of schizophrenia patients [844], while plasma and serum levels of NO are increased in schizophrenia patients that have undergone antipsychotic treatment [845]. Sodium nitroprusside, a nitric oxide donor, has also been suggested as a potential treatment for the disorder [846]. From a circadian perspective, NO and NOS are clearly implicated in the light-input pathway and photic entrainment [847]. *Nos* is expressed in the SCN of rats and hamsters [848], as well as guinea pigs [849], while NO immunoreactivity has been detected in the SCN of hamsters and rats [848, 850-852]. Significantly, NOS inhibitors block light-induced glutamate release from the terminals of retinal ganglion cells in the SCN [853, 854], and attenuate both NMDA- and light-induced phase shifts in the rest-activity rhythms of rodents [855, 856]. NOS inhibitors also impair entrainment to T23 cycles and inhibit light-evoked *Per1* expression in the SCN [857]. REM sleep is substantially reduced in $Nos^{-/-}$ mice [858]. Likewise, NOS inhibitors and NO scavengers reduce sleep time in rats, while NO donors increase sleep time [859]. Interestingly, the total number of *Nos*-expressing SCN neurons is reduced in schizophrenia patients [860].

A_1R

The adenosine system represents a promising avenue for future research into the relationship between schizophrenia and disturbed sleep. As outlined in Section 1.5.3., the neuromodulator adenosine may be the biological substrate of homeostatic drive for sleep, since it accumulates in the brain during wakefulness [298], and the administration of adenosine or adenosine receptor agonists promotes sleep in rats and cats [299, 300]. Recently, the ‘adenosine hypothesis of schizophrenia’ was proposed by Boison and colleagues, which argues that

adenosinergic dysfunction is involved in the pathophysiology of schizophrenia [861]. There are various lines of evidence that support this hypothesis [861]. Expression of the adenosine receptor $A_{2A}R$ is increased in the striatum of schizophrenia patients [862], while the expression of specific adenosine deaminases may be decreased [863]. Polymorphisms in *A_1R*, the gene that encodes the A_1R adenosine receptor have also been associated with schizophrenia [864]. There is no evidence of an association between *$A_{2A}R$* and schizophrenia, although the $A_{2A}R$-coupling G-protein *G_{olf}* may be associated the disorder [865, 866]. In rodents, adenosine receptor antagonists can reverse the positive symptom-like behaviours of rodents induced by dopamine receptor agonists and NMDAR antagonists. By contrast, adenosine receptor agonists *impair* learning and memory, as do manipulations that downregulate adenosine receptor function. Conversely, adenosine receptor antagonists *enhance* cognitive performance in rodents [861].

Drd2

The 'dopamine hypothesis' is the oldest and best-known neurotransmitter-based hypothesis of schizophrenia. The evidence for this hypothesis is outlined in Section 1.2.5. The D_2 dopamine receptor – encoded by the gene *Drd2* – is central to the hypothesis, given that antipsychotic drugs act on D_2 dopamine receptors [88], and their therapeutic efficacy is associated with their D_2 receptor binding affinity [89, 90]. Likewise, there is evidence from post-mortem studies of increased striatal D_2 receptor binding in the brains of schizophrenia patients [91]. Early reports of a significant association between *Drd2* and schizophrenia were refuted and then dismissed [867], until recently, a significant association was reported in the biggest meta-analysis of GWAS studies to date [60]. Crucially, *$Drd2^{-/-}$* mice demonstrate impaired negative masking, which implicates D_2 receptors in circadian function [868]. By contrast, their rest-activity rhythms are normal [868].

7.4. Does the absence of SCRD in *Dao*$^{-/-}$ mice invalidate the 'shared neuropathophysiology' hypothesis?

Although significant SCRD was observed in the *Grm2/3*$^{-/-}$ mouse, we found no evidence of altered sleep or circadian rhythms in the *Dao*$^{-/-}$ mouse (see Chapter 5). This is in stark contrast to the ddY/*Dao*$^{-}$ mouse, which demonstrates severe circadian disruption (at least in its wheel-running rhythms), but no sign of sleep disturbance [Melanie Sobczyk, *unpublished data*]. The mechanistic basis of circadian disruption in ddY/*Dao*$^{-}$ mice is currently unknown, although it may reflect an interaction between the absence of DAO activity and the albinism of the ddY strain, which renders it more vulnerable to retinal degeneration. This hypothesis is discussed in more detail in Chapter 5.

Does the absence of SCRD in *Dao*$^{-/-}$ mice invalidate the 'shared neuropathophysiology' hypothesis, which suggests that the manipulation of schizophrenia-relevant genes should result in both SCRD and schizophrenia-relevant behavioural deficits? The answer to this question is no, as this hypothesis does not suggest that there is complete overlap between the mechanisms responsible for SCRD and the mechanisms responsible for schizophrenia-relevant behaviours. If there was 100% overlap between these mechanisms, then SCRD would be witnessed in 100% of schizophrenia patients, which clearly is not the case. (The actual figure is somewhere between 30% and 80% [328]). Likewise, schizophrenia-relevant behaviours would be witnessed in 100% of individuals who are afflicted by SCRD. Again, although schizophrenia-relevant behaviours are often preceded by – or co-occur with – sleep disturbances (see Section 1.8.2.), the degree of co-morbidity is clearly not 100%. Hence, all that can be concluded from the *Dao*$^{-/-}$ mouse is that in rodents, SCRD is not an inevitable consequence of the genetic manipulation of neurotransmitter systems implicated in schizophrenia.

Another relevant point is that in schizophrenia, there is evidence that *Dao* expression and DAO activity are increased, rather than decreased [485, 494-498]. Therefore, the direction of the manipulation employed in the *Dao*$^{-/-}$ model (i.e. genetic ablation of *Dao*) is the exact opposite of that seen in schizophrenia. Arguably, therefore, the *Dao*$^{-/-}$ mouse is not a model of the schizophrenia disease process in the same way that the *Grm2/3*$^{-/-}$ mouse is, given preliminary evidence that *Grm3* expression may be *reduced* in schizophrenia [552]. From this perspective, one might expect to observe SCRD in a *Dao* overexpressing mice, but not in the *Dao*$^{-/-}$ model. This simplistic hypothesis is logical, but the reality is often more complicated. To give an example, the *Vipr2*$^{-/-}$ mouse displays significant circadian disruption, despite the fact that schizophrenia is associated with *Vipr2* microduplication [49].

Although the lack of SCRD in the *Dao*$^{-/-}$ mouse does not invalidate the 'shared neuropathophysiology' hypothesis, it highlights a possible weakness in it. Mouse models that demonstrate simultaneous SCRD and schizophrenia-relevant behaviours are interpreted as evidence that support the hypothesis, but models that do not cannot be interpreted as counter-evidence. This makes the hypothesis very difficult to falsify. Should SCRD be observed in 25% of schizophrenia-relevant mouse models? 50%? Or 75%? In many ways, this point is moot, since the ultimate goal of the hypothesis is not to identify as many models as possible with simultaneous deficits. Instead, once several such models have been identified, the immediate priority should be to determine whether SCRD makes a *causal contribution* to each model's schizophrenia-relevant behaviours. If it does, this will have important therapeutic implications. If not, then the 'shared neuropathophysiology' hypothesis will have little impact on the way that schizophrenia is treated. In this case, SCRD should simply be considered an additional schizophrenia-relevant behaviour, which – like cognitive impairment, reduced PPI or MK801–induced hyperlocomotion – would increase the validity of the models in which it is observed.

7.5. Generalisation of the 'shared neuropathophysiology' hypothesis to other animal models

For the sake of brevity, this thesis has focused on schizophrenia-relevant *transgenic* mouse models. However, the 'shared neuropathophysiology' hypothesis could equally be tested in other types of schizophrenia-relevant rodent model. These include lesion-based models, pharmacological models, environmental models and 'gene-by-environment' models, as introduced in Section 1.3. Hence, the MAM E17 rat can be added to the list of schizophrenia-relevant rodent models that support the 'shared neuropathophysiology' hypothesis. This neurodevelopmental model is created by exposing pregnant dams to the toxin methylazoxymethanol acetate (MAM) on the gestational day 17 [154]. The offspring of these dams demonstrate a range of schizophrenia-relevant behavioural abnormalities in adulthood, including impaired spatial working memory, attentional set-shifting and reversal learning, and reduced PPI [154, 869]. Crucially, they also display significant SCRD, in the form of fragmented NREM sleep and impaired slow wave sleep propagation [870].

In future, the same principles could even be applied to schizophrenia-relevant non-human primate (NHP) models, which are a new addition to the literature [871]. The single biggest advantage of this approach is that the prefrontal cortex is far more developed in NHPs than rodents [872], and schizophrenia is believed to involve prefrontal cortex dysfunction. At the other end of the scale, sleep has even been studied in drosophila models in which the schizophrenia-associated gene *Disc1* has been manipulated [873]), although it is questionable whether schizophrenia-relevant behaviours could ever be assessed in drosophila [874].

7.6. Generalisation of the 'shared neuropathophysiology' hypothesis to other neuropsychiatric and neurodegenerative disorders

Although schizophrenia has provided the focus of this thesis, the principles of the 'shared neuropathophysiology' hypothesis could be generalised to any brain-based disorder in which SCRD is observed. Indeed, significant SCRD is prevalent in a wide range of neuropsychiatric and neurodegenerative conditions, including Huntington's disease, Parkinson's disease, Alzheimer's disease, major depression, bipolar disorder and a range of anxiety disorders [125, 875-879]. In the same way that SCRD may exacerbate the behavioural symptoms of schizophrenia, the same could be said of the negative and cognitive symptoms of major depression and bipolar disorder, mania in bipolar disorder, or the cognitive impairments seen in all of the aforementioned neurodegenerative disorders. Likewise, SCRD might contribute to episodes of psychosis in any psychiatric disorder. Just as we have advocated the use of rodent models to test the specific predictions of the 'shared neuropathophysiology' hypothesis in relation to schizophrenia, they could equally be tested in rodent models relevant to any other disorder. For example, simultaneous sleep, circadian and behavioural deficits have already been reported in the R6/2 transgenic mouse model of Huntington's disease [449], while a causal contribution of SCRD to memory impairments has also been demonstrated in this model [453, 454]. SCRD has also been observed in rodent models of Alzheimer's disease [880], Parkinson's disease [881, 882], anxiety [691, 692], depression [883, 884] and mania [885;Hugh Piggins, *unpublished data*]. It should also be noted that many environmental risk factors and susceptibility genes are shared between multiple neuropsychiatric disorders. Conclusions drawn from rodent models of these genes and these risk factors would therefore be applicable to a range of different conditions. Finally, to echo the sentiments of the previous section, the

‘shared neuropathophysiology’ hypothesis can equally be tested in non-rodent animal models. Indeed, rest-activity rhythms and cognitive performance are currently under investigation in a transgenic sheep model of Huntington’s disease [886].

7.7. Methodological insights

Besides addressing specific predictions about the sleep, circadian and behavioural phenotypes of *Dao*$^{-/-}$ and *Grm2/3*$^{-/-}$ mice, this thesis has yielded several important methodological insights, regarding the use of running wheels and passive infrared (PIR) motion detectors to assess the circadian locomotor behaviour of mice, and the use of the Morris watermaze to assess long-term spatial memory. These topics are discussed below.

Wheel-running as a circadian assay

Wheel-running behaviour is a robust and affordable method for measuring circadian locomotor activity. However, there are limitations associated with this approach, which are important to acknowledge. Although recent research suggests that wheel-running is a natural and elective behaviour rather than a stereotypic behaviour [319], wheel-running activity both influences – and is influenced by – the function of a wide range of brain regions.

To begin with, wheel-running activity is an index of voluntary exercise, rather than spontaneous movement. Therefore, wheel-running behaviour may be subject to multiple influences including arousal, motivation, anxiety, and sensitivity to reward [320, 321]. For this reason, abnormalities in the brain circuitry that underlies any of these psychological constructs – for example mesolimbic dopaminergic reward circuitry – is likely to influence wheel-running behaviour. Hence, wheel-running activity could be perturbed in animals in which the circadian system is perfectly intact, as is possibly the case with the *Grm2/3*$^{-/-}$ mouse (see Chapter 6). In addition, wheel-running activity requires a degree of motor coordination, so is likely to be reduced in mice with motor deficits. This could also explain the altered wheel-running phenotype of the *Grm2/3*$^{-/-}$ mouse, which demonstrates subtle but significant impairments in the accelerating rotarod task and multiple static rods task [574]. Given that most

psychiatrically-relevant mouse models display alterations in a wide range of behaviours and brain circuits, wheel-running may not be the most appropriate method to assess the rest-activity rhythms of these models.

While both circadian and non-circadian brain circuitry can influence wheel-running activity, the opposite is also true. For example, long-term voluntary wheel-running produces plastic changes in mesolimbic dopaminergic reward circuity in rats [763]. Likewise, mice selectively bred for high voluntary wheel-running activity showed elevated dopamine levels in the dorsal striatum and nucleus accumbens, as well as changes in D1 and D2 dopamine receptor signalling pathways [887, 888]. It has also been demonstrated that wheel running enhances neurogenesis, cell proliferation and long-term potentiation in the dentate gyrus of the hippocampus, together with long-term spatial memory performance in the Morris watermaze [889, 890]. In addition, wheel running reduces learned helplessness in rodents, a behavioural test relevant to depression [891, 892]. Exercise has been shown to slow the onset or progression of disease in mouse models of stress, depression and aging [893, 894].

Interestingly, there is also evidence that running wheel activity can alter circadian function [895]. The phase-shifting capacity of mice under long days (18 h day: 6 h night) is greater in the presence of running wheels [896], while access to running wheels has been shown to accelerate the re-entrainment of peripheral clocks [897]. Indeed, even the size of the running wheel can influence both the period length and the phase-shifting capacity of the circadian clock [898]. Exercise must feed back to the animal's internal clock, as scheduled voluntary exercise is sufficient to entrain the circadian clock and prevent free-running activity under constant conditions [899]. Scheduled voluntary exercise also improves behavioural and molecular indices of circadian rhythmicity in disease-relevant models, such as the

schizophrenia-relevant *Vipr2*$^{-/-}$ mouse and the R6/2 transgenic mouse model of Huntington's disease [450, 900]. Taken together, these data suggest that rather than simply providing a means of assessing rest-activity rhythms of mice, running wheels can actually influence the phenotypes of the mice being characterised. Therefore, video-tracking or PIR motion detection may be preferable to the use of running wheels for the circadian screening of psychiatrically-relevant mouse models. Having said this, the involvement of dopaminergic reward circuitry in wheel-running behaviour means that it may be a suitable assay for use in addiction research [879].

Passive infrared motion detection as a circadian assay

The experiments described in Chapter 6 were the first to use PIR motion detectors to simultaneously assess sleep and circadian function in a transgenic mouse. The similarity of the PIR-derived and video-derived sleep data presented here serves as further validation of this novel technique. PIR assays offer several key advantages over video-tracking assays. Firstly, they enable the estimation of sleep over a longer period of time, providing a more representative view of an animal's sleep profile. Secondly, they enable the computation of standard circadian parameters such as period length, which cannot be extracted from isolated 24 h video recordings. This enables sleep and circadian rhythms to be characterised simultaneously, in a manner that is impossible with running wheels or NIR cameras. Thirdly, the PIR system is small, relatively cheap and portable, and can therefore be installed in virtually any laboratory. This eradicates the expense and labour that is currently required to perform a preliminary circadian screen of a transgenic mouse, as the mice no longer need to be shipped from the host laboratory to a specialist sleep and circadian laboratory. Finally, PIR data can be analysed using existing software such as ClockLab (Actimetrics, Illinois, USA). At present, there is no specialist software available for the extraction of circadian parameters from video data.

Recommendations for the Morris watermaze paradigm

The experiments described in Chapter 3 clearly demonstrate that Morris watermaze performance can be influenced by the radial distance of the hidden platform from the side-wall. At the very least, this highlights the need to use platforms at multiple radial distances, and to counterbalance radial platform distance across genotype groups. At the most, it suggests that altered Morris watermaze performance in countless studies may have been misattributed to memory enhancements or impairments, when in fact they were the product of altered anxiety, or some combination of altered anxiety and altered memory. The data from Chapter 3 also highlight the need to analyse Morris watermaze data on a trial-by-trial basis. We would argue not only that trial-by-genotype interactions should be reported, but that they are a phenomenon worthy of investigation in and of themselves (see Section 3.4. & 7.1.3.).

The aversive (swim escape) Y-maze task should not be considered a direct replacement for the Morris watermaze task

In the Morris watermaze, *Dao*$^{-/-}$ mice outperformed *Dao*$^{+/+}$ mice in the peripheral platform condition, but were outperformed by *Dao*$^{+/+}$ mice in the central platform condition. We have argued that this is because the centre of the arena is more exposed than the periphery, and therefore more anxiogenic. By contrast, the three arms of the Y-maze are physically identical, so each arm should be equally anxiogenic. On this basis, it could be argued that the Y-maze is a better test of long-term spatial memory than the MWM, since it is less confounded by anxiety. However, this simplistic conclusion overlooks the fact that the MWM and Y-maze assess different psychological constructs, which may rely on different underlying mechanisms. Both tests involve spatial navigation using distal extra-maze cues, but in the Y-maze, animals face a choice between a limited number of discrete options (i.e. the goal and non-goal arms). In the MWM, no such choice is presented. Consequently, Y-maze performance may involve a

'behavioural inhibition' component which the MWM lacks; mice must refrain from entering the non-goal arm, even though it bears a strong physical resemblance to the goal arm [620]. This difference may explain why the ablation of hippocampal NMDARs inhibits performance in the the radial arm maze, but not in the standard version of the MWM [620]. Consistent with this argument, mice lacking hippocampal NMDARs *are* impaired at a modified version of the MWM in which the platform location and a 'distractor' location are denoted by identical visual cues, forcing the animal to choose between the two [620]. Due to this fundamental difference in the nature of the tasks, the aversive (swim escape) Y-maze cannot be considered a direct alternative to the MWM.

7.8. Conclusion

The 'shared neuropathophysiology' hypothesis argues that although some of the sleep and circadian abnormalities in schizophrenia may be secondary to the disorder and its drug treatment, the co-morbidity of schizophrenia and SCRD may also stem from dysfunction in common brain mechanisms. According to this hypothesis, simultaneous SCRD and schizophrenia-relevant behavioural deficits should be observed in some (although not necessarily all) transgenic mouse models in which schizophrenia-associated genes have been manipulated. Based on the results described in this thesis, the *Grm2/3*$^{-/-}$ mouse joins the *Bdr* mutant mouse as the second genetic mouse model to fulfil these criteria. *Vipr2*$^{-/-}$, *Cckar*$^{-/-}$ and *Nrg1* mutant mice also demonstrate SCRD, so can be added to this list if they are shown to display schizophrenia-relevant behavioural abnormalities. To the best of our knowledge, no other schizophrenia-relevant model exists that has been subjected to sleep, circadian *and* behavioural assessment; at least no other *transgenic* mouse model. In Section 7.3, we highlight a number of additional models which we would expect to demonstrate both SCRD and schizophrenia-relevant behavioural deficits.

However, even if it is correct, the 'shared neuropathophysiology' hypothesis has limited clinical relevance unless SCRD is shown to make a causal contribution to the schizophrenia-like behaviours witnessed in these models. Experiments which address this issue should therefore be made a priority in future research, and the *Grm2/3*$^{-/-}$ mouse is one model that could be used in such experiments. It SCRD does *not* make a causal contribution to schizophrenia-like behaviours, it may best be conceptualised as a 'biomarker' of impaired neurotransmission or synaptic connectivity across distributed brain networks; the type of dysfunction that is believed to exist in schizophrenia. If it *does* make a causal contribution, this would have potentially important implications for the way schizophrenia is treated. More specifically, it

would infer that the targeted treatment of SCRD would lead to improvements in the behavioural symptoms of schizophrenia patients. This would be hugely significant, since the treatment of schizophrenia has barely changed since the introduction of antipsychotic drugs in the 1950s, drugs which have little impact on the negative and cognitive symptoms of the disorder.

Of course, demonstrating that an SCRD-targeting intervention improves schizophrenia-like behaviours in a transgenic mouse would be no substitute for a successful clinical trial demonstrating that an SCRD-targeting intervention improves the symptoms of schizophrenia patients. However, a randomised controlled trial of this nature has yet to be conducted. Given the associated expense, preclinical evidence of the effectiveness of such an intervention would likely be needed before such a trial is undertaken. Additionally, the mechanistic basis of SCRD can be probed in mouse models in a way that is not possible in patients. Hence, mouse models may yield insights into which SCRD-targeting interventions are most likely to be effective, a field of research which is already underway with the R6/2 transgenic mouse model of Huntington's disease. This final point highlights the greatest potential strength of SCRD-targeting interventions; they may be applicable to a wide range of neuropsychiatric and neurodegenerative disorders beyond schizophrenia.

8. Appendices

8.1. Publications arising from this thesis

The work described in this thesis yielded the following data papers and reviews:

Harrison PJ, Pritchett D, Stumpenhorst K, Betts JF, Nissen W, et al. (2012) Genetic mouse models relevant to schizophrenia: taking stock and looking forward. Neuropharmacology 62: 1164-1167.

Pritchett D, Wulff K, Oliver PL, Bannerman DM, Davies KE, et al. (2012) Evaluating the links between schizophrenia and sleep and circadian rhythm disruption. J Neural Transm 119: 1061-1075.

Frank E, Benabou M, Bentzley B, Bianchi M, Goldstein T, Pritchett D, et al. (2014) Influencing circadian and sleep-wake regulation for prevention and intervention in mood and anxiety disorders: what makes a good homeostat? Ann N Y Acad Sci 1334: 1-25.

Pritchett D, Hasan S, Tam SKE, Engle SJ, Brandon NJ, et al. (2015) D-amino acid oxidase knockout (Dao-/-) mice show enhanced short-term memory performance and heightened anxiety, but no sleep or circadian rhythm disruption. European Journal of Neuroscience 41(9): 1167-79

Tam SKE, Pritchett D, Brown LA, Foster RG, Bannerman DM, Peirson SN. (2015) Sleep and circadian rhythm disruption and recognition memory in schizophrenia. Methods in Enzymology 552: 325-49

Pritchett D, Jagannath A, Brown LA, Tam SKE, Hasan S, et al. (2015) Deletion of metabotropic glutamate receptors 2 and 3 (mGlu2 & mGlu3) in mice disrupts sleep and wheel-running activity, and increases the sensitivity of the circadian system to light. PLoS One 10(5):e0125523

Pritchett D, Taylor AM, Engle SJ, Brandon NJ, Sharp T, et al. (*in preparation*) Morris watermaze performance in D-amino acid oxidase knockout (Dao-/-) mice is critically dependent on the radial distance of the hidden platform from the side-wall.

8.2. Additional information from Chapter 3

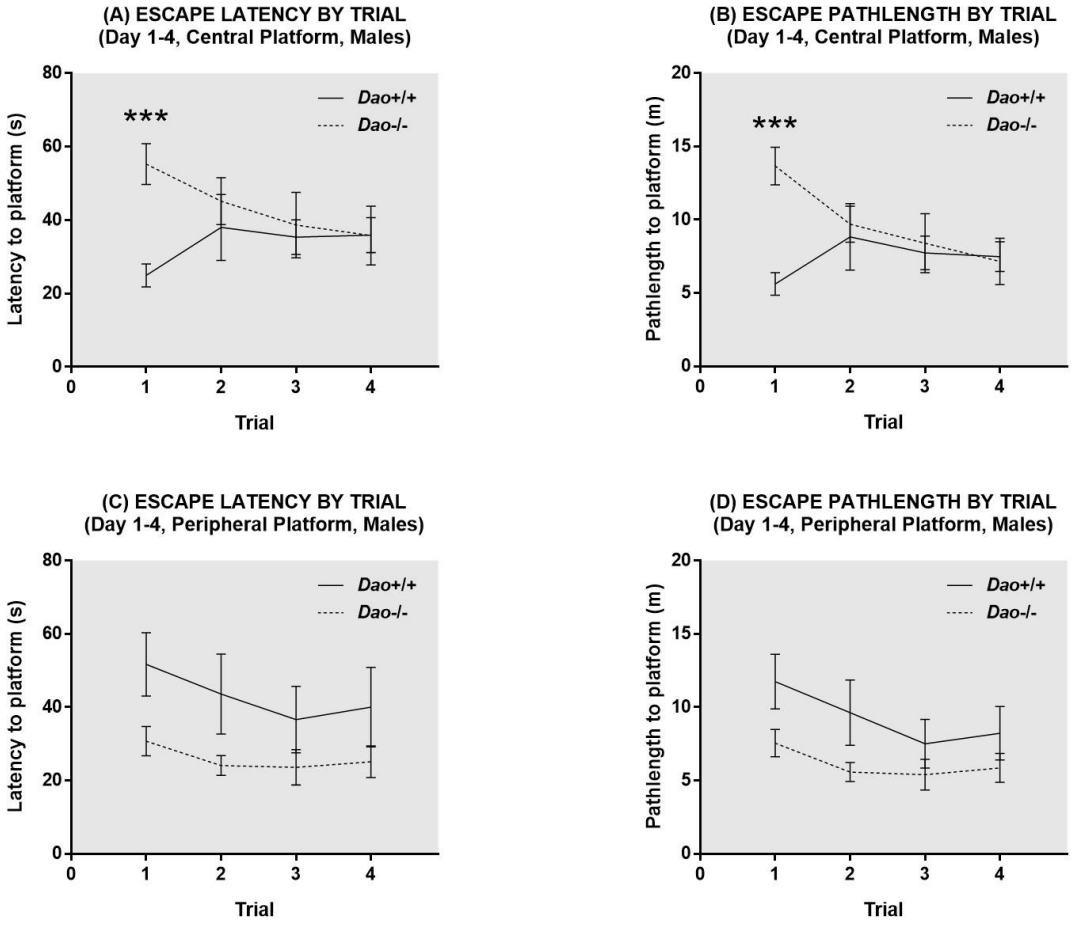

Figure 8.1. Morris watermaze performance in control (*Dao*$^{+/+}$) and knockout (*Dao*$^{-/-}$) mice in *Experiment 2* in males only (*n*=11 animals per genotype). (A-B) Across the four days of acquisition training, male *Dao*$^{+/+}$ mice in the central platform condition significantly outperformed *Dao*$^{-/-}$ mice on trial 1, but not on the subsequent three trials. (C-D) In the peripheral platform condition, male *Dao*$^{-/-}$ mice outperformed *Dao*$^{+/+}$ mice on all 4 trials, although this advantage was not statistically significant for any trial.

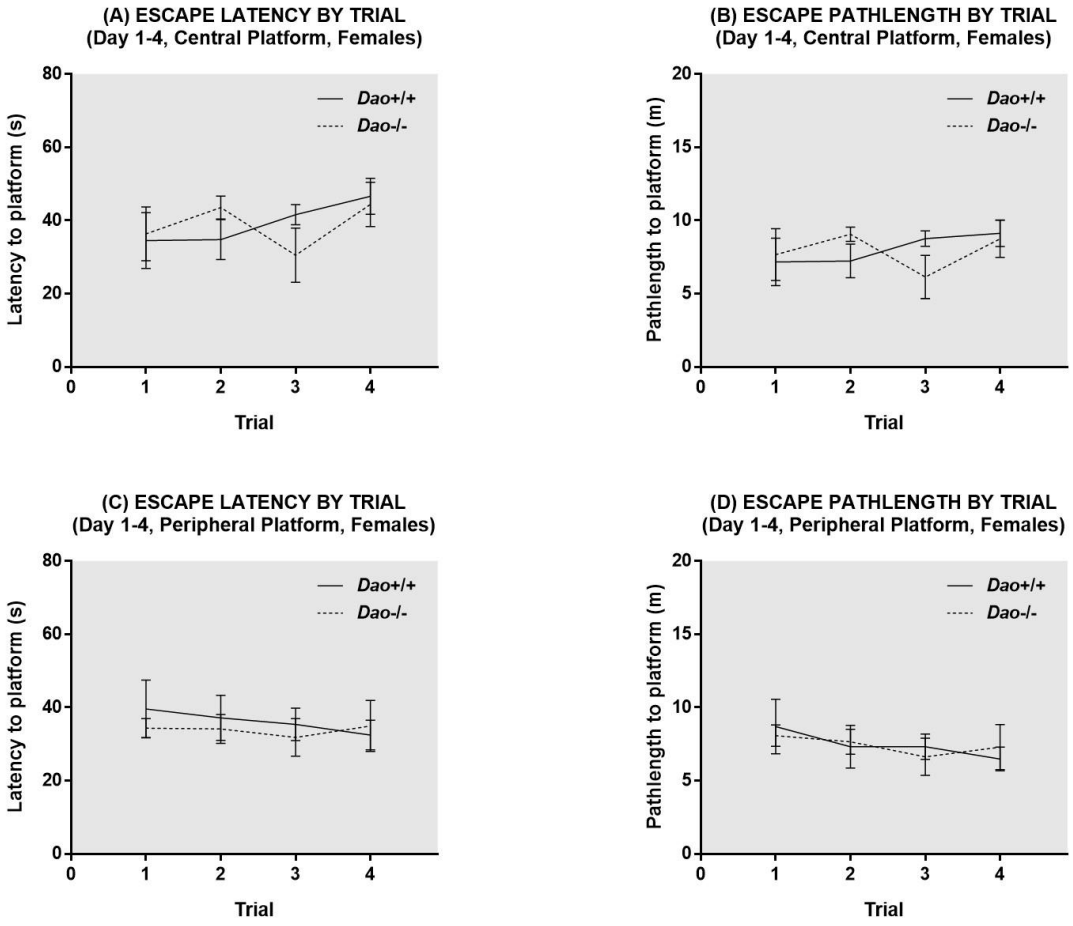

Figure 8.2 Morris watermaze performance in control (*Dao*$^{+/+}$) and knockout (*Dao*$^{-/-}$) mice in *Experiment 2* in females only (*n*=12 animals per genotype). (A-D) Across the four days of acquisition training, genotype had no effect on the performance of female mice on any trial. This was true of both the central platform condition (Fig. 9.2A & 9.2B) and the peripheral platform condition (Fig. 9.2C & 9.2D).

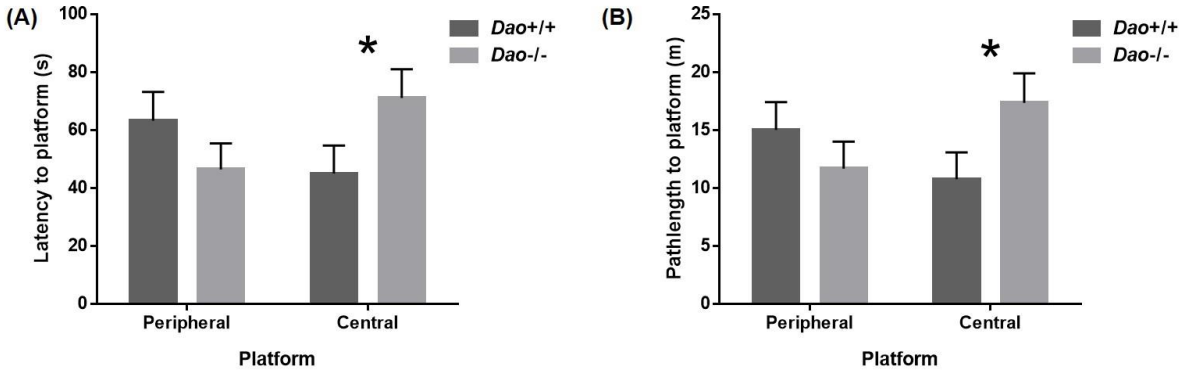

Figure 8.3. Morris watermaze performance in control (*Dao*$^{+/+}$) and knockout (*Dao*$^{-/-}$) mice (*n*=11 males; *n*=12 females per genotype) on the first trial of the first acquisition session of *Experiment 2*. (A-B) *Dao*$^{-/-}$ mice outperformed *Dao*$^{+/+}$ mice in the peripheral platform condition, but were outperformed by *Dao*$^{+/+}$ mice in the central platform condition. This was true of both the escape latency data (Fig. 9.3A) and the pathlength data (Fig. 9.3B).

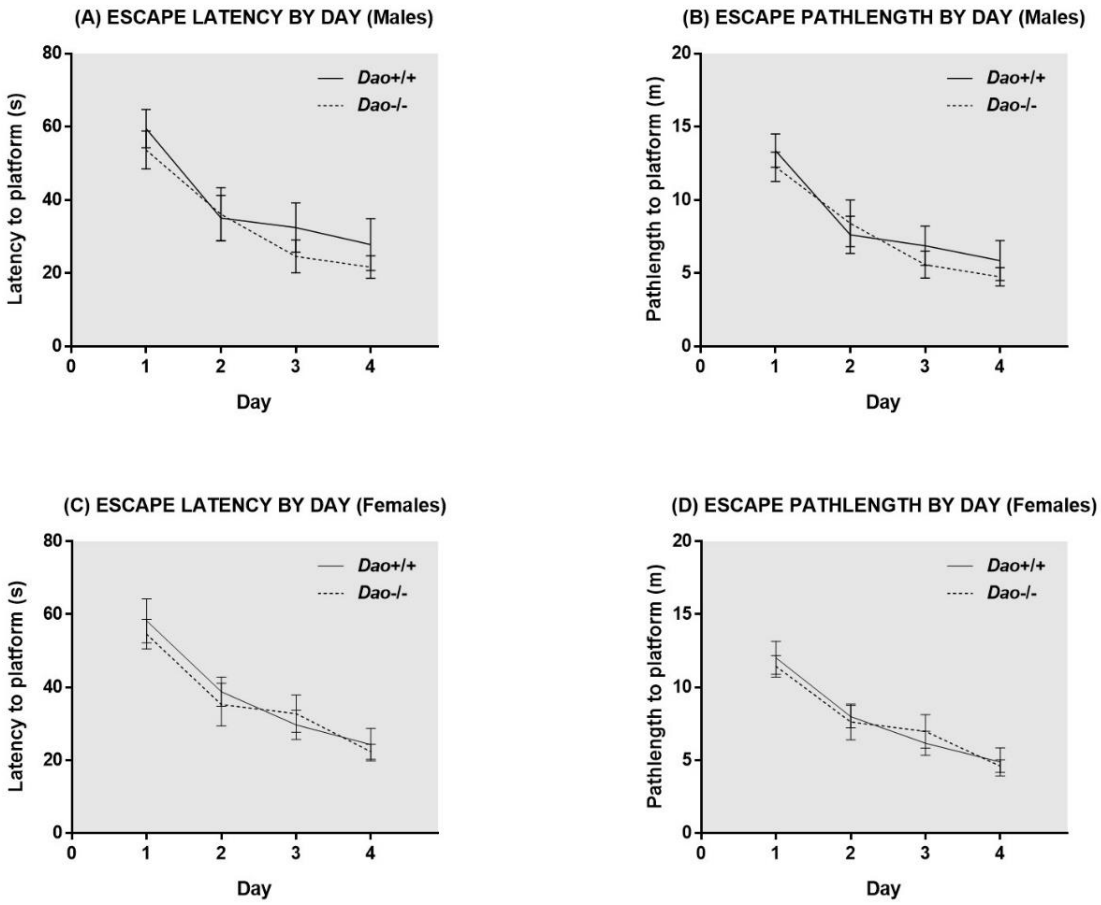

Figure 8.4. Morris watermaze performance in control (*Dao*$^{+/+}$) and knockout (*Dao*$^{-/-}$) mice (*n*=11 males; *n*=12 females per genotype; *Experiment 2*). (A-D) With data collapsed across the four trials of each training session, genotype had no apparent impact on the watermaze performance of male mice (Fig. 9.4A & 9.4B) or female mice (Fig. 9.4C & 9.4D) during the acquisition phase.

In *Experiment 2*, the probe trial performance of mice in the peripheral platform condition was superior to that of mice in the central platform condition; they spent more time in the platform quadrant ($F_{1,38}$ = 8.035, P = 0.007; Supplementary Fig. 9.5), and made more platform crosses ($F_{1,38}$ = 3.082, P = 0.087). This result was unexpected given that mice in the two conditions performed similarly during the four-day acquisition phase; radial platform distance had no effect on either escape latency or pathlength, and there were no interactions between day and radial platform distance or trial number and radial platform distance (Ps = ≥ 0.245). It therefore seems likely that mice in the central platform condition were solving the watermaze task using a strategy that did not involve knowledge of which quadrant the platform was located in. Given the smaller surface area of the central platform zone relative to the peripheral platform zone, it is easy to see why this information would be less important to mice in the central platform condition.

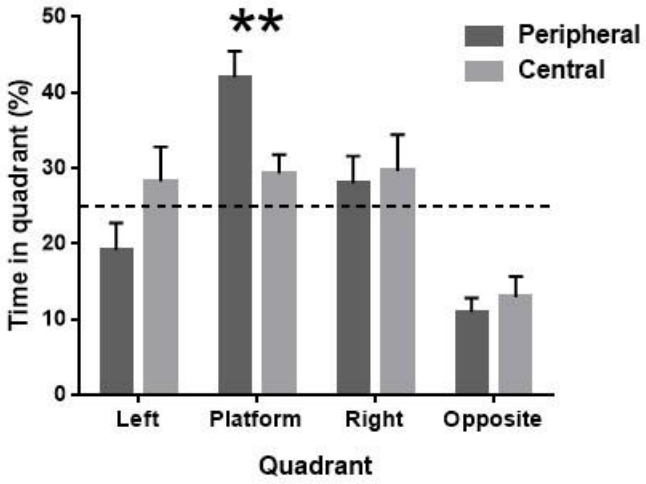

Figure 8.5. Radial platform distance had a significant influence on probe trial performance in *Experiment 2*. Only mice in the peripheral platform condition demonstrated a clear preference for the platform quadrant; time spent in this quadrant exceeded chance level (25%) in the peripheral platform condition (Student's *t*-test, t_{23} = 4.934, P = <0.001, $\underline{M}$ = 42.0%) but not in the central platform condition (Student's *t*-test, t_{21} = 1.720, P = 0.100, $\underline{M}$ = 29.3%).

Interestingly, there was main effect of trial number on percent time spent in the peripheral zone during the acquisition phase of *Experiment 2* ($F_{3,114}$ = 5.703, P = 0.001; Supplementary Fig. 9.6A). Post-hoc analyses revealed a significant increase in time spent in the peripheral zone between trials 1 and 2 ($F_{1,38}$ = 16.958, P = <0.001), but no change between trials 2 and 3, or trials 3 and 4 (Ps = ≥ 0.374). This increase in peripheral zone swimming occurred regardless of genotype or sex, so there were no interactions between trial number and genotype or trial number and sex (Ps = ≥ 0.445; Supplementary Fig. 9.6B & 9.6C). More surprisingly, there was no interaction between trial number and radial platform distance ($F_{3,114}$ = 0.848, P = 0.470; Supplementary Fig. 9.6D); even mice in the central platform condition demonstrated an increase in peripheral zone swimming between trials 1 and 2. To the best of our knowledge, we are the first to report this phenomenon.

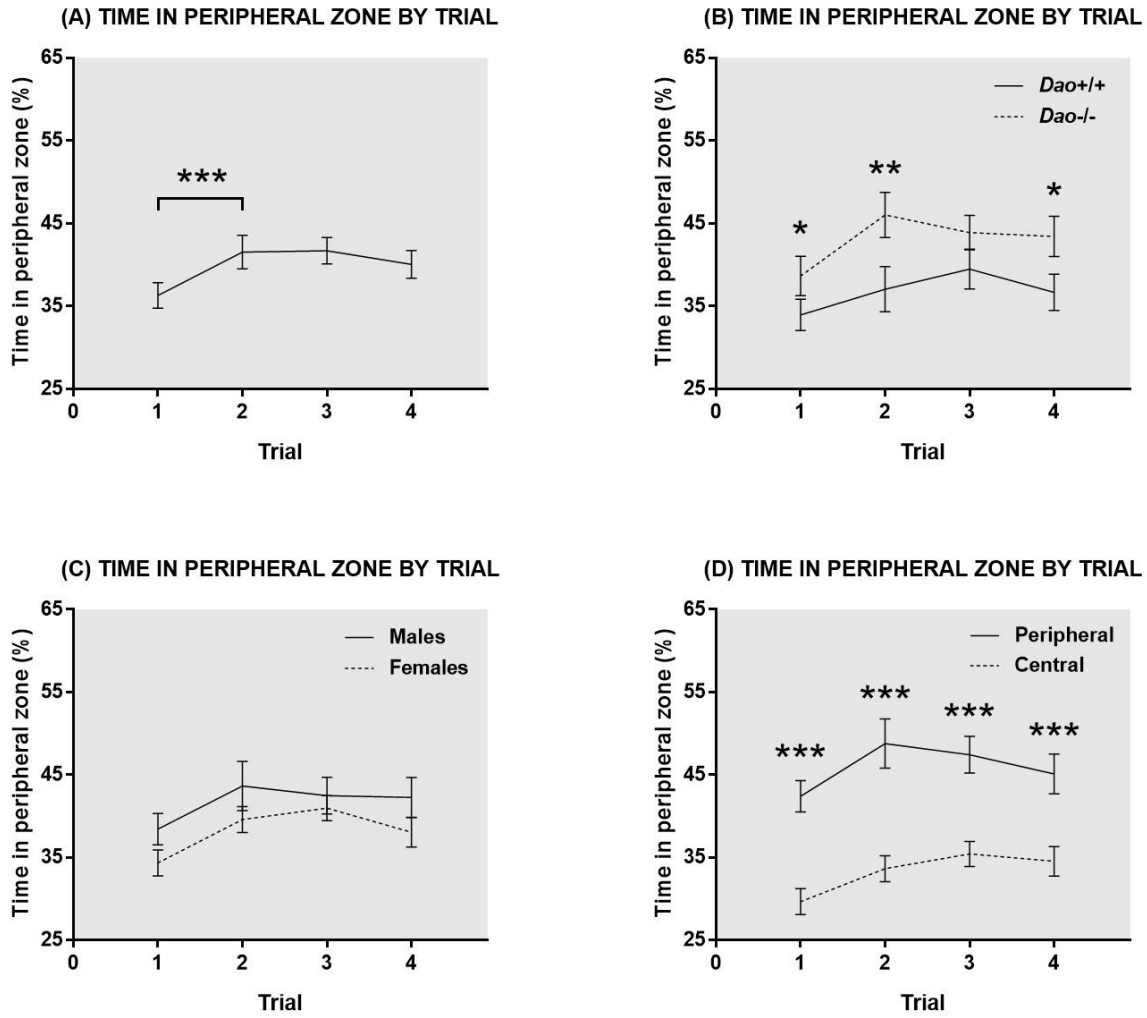

Figure 8.6. Spatial analyses of swimming behaviour during the acquisition phase of *Experiment 2*. (A) Percent time spent in the peripheral zone increased significantly between trials 1 and 2, but did not change between trials 2 and 3, or trials 3 and 4. (B-D) This increase in peripheral zone swimming occurred regardless of genotype, sex, or radial platform distance. Predictably, mice in the peripheral platform condition spent more time in the peripheral zone than mice in the central platform condition ($F_{1,38}$ = 32.922, P = <0.001; Fig. 9.6D). All figures are based on all 16 trials (i.e. 4 trials per day for 4 days) of the acquisition phase.

Why would peripheral zone swimming increase between trials 1 and 2, regardless of the location of the hidden platform? It is possible that this behaviour reflects an increase in anxiety across trials. An alternative explanation is that on trial 1, when the position of the platform is unclear, mice place relatively few restrictions on their swimming behaviour. By trial 4, when the platform's position is better established, mice may circle the maze in the periphery while orientating themselves relative to the distal extra-maze cues, before swimming directly the platform by the shortest possible route.

8.3. Morris watermaze performance of D-cycloserine-treated wildtype rats

This unpublished dataset was provided for re-analysis by David Bannerman. Age-matched adult male rats were tested. 22 rats were given an intraperitoneal injection of sterile saline solution 30 minutes prior to Morris watermaze testing, and 22 rats were given an intraperitoneal injection of D-cycloserine 30 minutes prior to testing. D-cycloserine was injected at 10 ml/kg, resulting in a dose of 6 mg/kg. The acquisition phase consisted of a single training session on day 1 and a single training session on day 2. There were three trials per session.

With data collapsed across the three trials of each three-trial acquisition session, treatment had no effect on either escape latency ($F_{1,42}$ = 2.062, P = 0.158) or pathlength ($F_{1,42}$ = 0.708, P = 0.405), and there were no interactions between day and treatment (escape latency: $F_{1,42}$ = 0.080, P = 779; pathlength: $F_{1,42}$ = 0.015, P = 0.904). There was a main effect of day on escape latency ($F_{1,42}$ = 117.202, P = <0.001) and pathlength ($F_{1,42}$ = 126.022, P = <0.001), reflecting the steady decline in these variables across consecutive days. There was also a main effect of trial number on escape latency ($F_{2,84}$ = 33.374, P = <0.001) and pathlength ($F_{2,84}$ = 40.981, P = <0.001), reflecting the gradual decrease in these variables across consecutive trials.

Crucially, there was a borderline significant treatment-by-trial number interaction for both escape latency ($F_{2,84}$ = 3.005, P = 0.055) and pathlength ($F_{2,84}$ = 3.059, P = 0.052). These interactions reflect the fact that D-cycloserine treated rats outperformed vehicle treated rats on trial 1 of each acquisition session, but were outperformed by vehicle-treated rats on trials 2 and 3. Post-hoc analyses revealed that the performance advantage of vehicle-treated rats on trial 3 was significant for escape latency ($F_{1,42}$ = 8.384, P = 0.006) and pathlength ($F_{1,42}$ = 5.105, P = 0.029).

Treatment had no effect on swim speed ($F_{1,42}$ = <0.001, P = 0.985). There was a main effect of trial number on swim speed ($F_{2,84}$ = 4.232, P = 0.018), and a main effect of day on swim speed ($F_{1,42}$ = 4.964, P = 0.031), reflecting the steady decline in this variable across consecutive days and trials. There was no interaction between treatment and trial number or treatment and day (Ps = >0.190). Thigmotaxis data were unavailable for this Morris watermaze dataset. No other measures of spatial swimming preferences were recorded in this study.

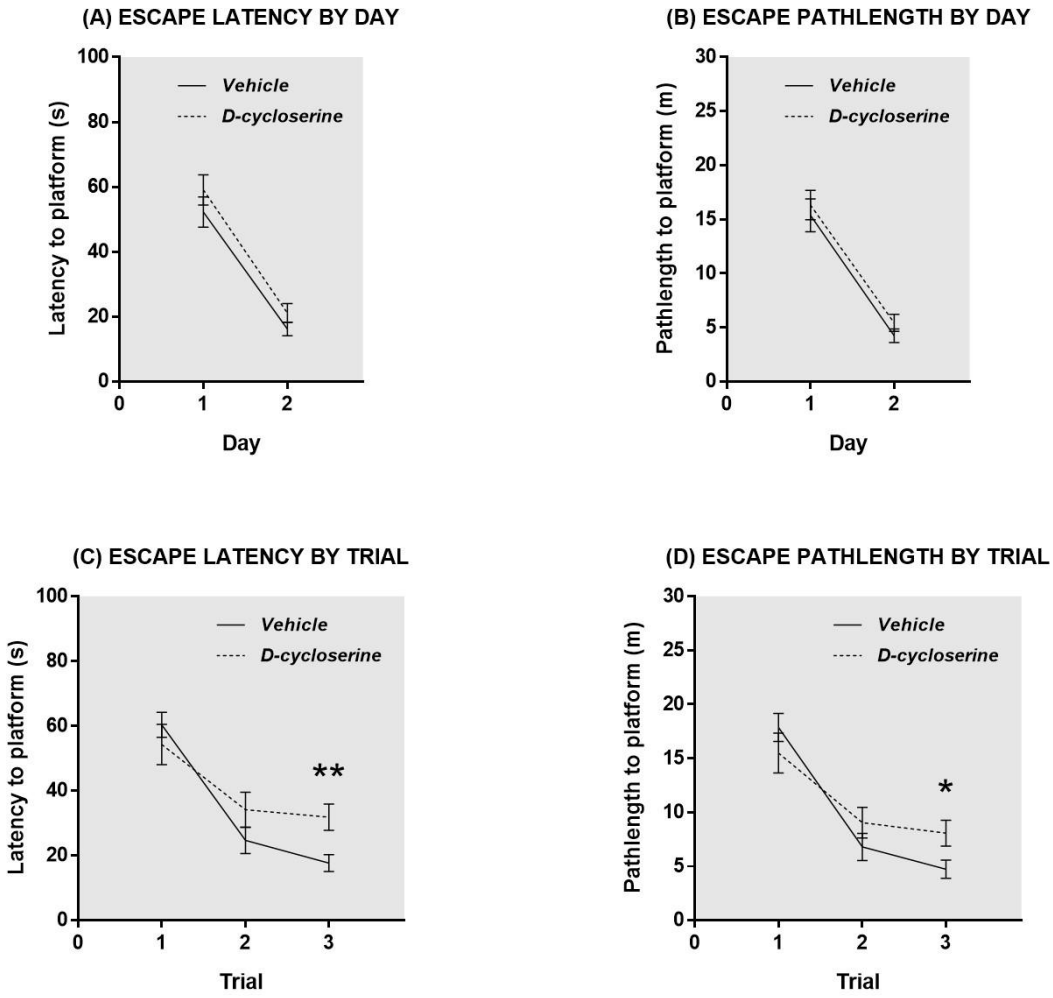

Figure 8.7. Morris watermaze performance in D-cycloserine-treated wildtype rats and vehicle-treated wildtype rats (*n*=22 males per group). Acquisition training took place across two days, with three successive trials performed on each day. (A-B) With data collapsed across the three trials of each training session, treatment had no apparent impact on watermaze performance during the two-day acquisition phase. (C-D) Across the first two days of acquisition training, D-cycloserine-treated rats outperformed vehicle-treated rats on the first trial of each day, but not on the subsequent two trials. Indeed, on the third trial, the performance of vehicle-treated rats was significantly superior to that of D-cycloserine-treated rats, in terms of both escape latency ($F_{1,42}$ = 8.384, P = 0.006) and pathlength ($F_{1,42}$ = 5.105, P = 0.029).

8.4. Additional information from Chapter 4

Baseline movement within the PPI paradigm

Average baseline movement values for each mouse were entered into an ANOVA, with genotype and sex as between-subjects variables, and injection stress as a within-subjects variable. Average baseline movement was unaffected by genotype ($F_{1,42}$ = 0.068, P = 0.795; Fig. 9.7A), sex ($F_{1,42}$ = 0.349, P = 0.558; Fig. 9.7B), and injection stress ($F_{1,42}$ = 0.167, P = 0.685; Fig. 9.7C). There were no significant interactions between any of the variables (Ps = >0.315). There is little consensus about the meaning of baseline movement in PPI protocols, although reduced baseline movement may be indicative of increased anxiety [Tomasz Schneider, *personal communication*].

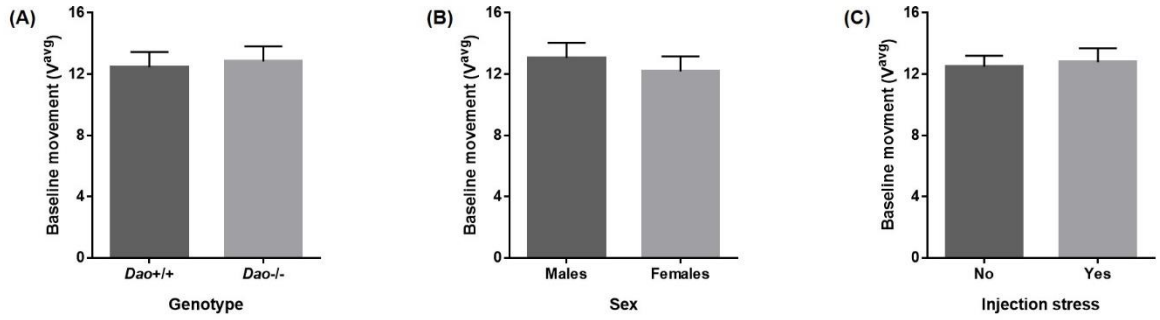

Figure 8.8. Baseline movement within the PPI paradigm. (A) Baseline movement did not differ between *Dao*$^{+/+}$ and *Dao*$^{-/-}$ mice. (B) Baseline movement did not differ between male and female mice. (C) Injection stress had no impact on baseline movement.

Baseline movement within the acoustic startle habituation protocol

Across the 21 'silent' trials included in the startle habituation protocol, there was a borderline-significant effect of genotype on baseline movement, which was lower in *Dao*$^{-/-}$ mice than *Dao*$^{+/+}$ mice ($F_{1,18}$ = 4.387, P = 0.051; Fig. 9.8A). By contrast, there was no main effect of sex on baseline movement ($F_{1,18}$ = 0.383, P = 0.544; Fig. 9.8B), and no interaction between genotype and sex ($F_{1,18}$ = 1.009, P = 0.329). The observation of reduced baseline movement in *Dao*$^{-/-}$ mice is consistent with their heightened anxiety phenotype, as described in Chapter 2.

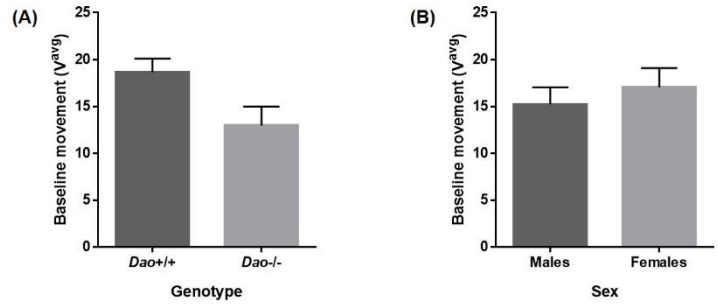

Figure 8.9. Baseline movement within the acoustic startle habituation protocol. (A) Baseline movement was significantly reduced in *Dao*$^{-/-}$ mice relative to *Dao*$^{+/+}$ mice. (B) Baseline movement did not differ between male and female mice.

8.5. Genotyping protocol for *Dao*$^{-/-}$ mice

The following genotyping protocol was provided by Judith Schweimer [534].

1) Extract the DNA of each individual mouse from ear clips with a Qiagen DNeasy Blood and Tissue kit (#69504).
2) Prepare 1.5% Agarose gel (1.5g Agarose in 100ml TAE buffer, plus 10µl Ethidium bromide).

Dao PCR setup:

WT	KO
H_2O (12.2ml)	H_2O (12.2ml)
Buffer (2ml)	Buffer (2ml)
dNTPs (0.7ml)	dNTPs (0.7ml)
G3 10 mM (0.7ml)	dNeo2 10 mM (0.7ml)
G4 10 mM (0.7ml)	G4 10 mM (0.7ml)
$MgCl_2$ (0.7 µl)	$MgCl_2$ (0.7 µl)
DNA (2 ml)	DNA (2 ml)
Taq Polymerase (0.5 ml)	Taq Polymerase (0.5 ml)
Total Volume (19.5 ml)	Total Volume (19.5ml)
240 bp	~700 bp

G3 (Forward, WT only): CAGGGCAAAGGGACTGAATA
G4 (Reverse, KO & WT): CACTCCACCACCATCGATTA
dNEO2 (Forward, KO only): ACATAGCGTTGGCTACCCGTGATA

MAGIC57 PCR Conditions: 95ºC, 4 min → 57ºC, 30 sec → 72ºC, 60 sec → 94ºC, 30 sec → Go to step 2, 35X → 59ºC, 30 sec → 72ºC, 5 min → 4ºC, forever

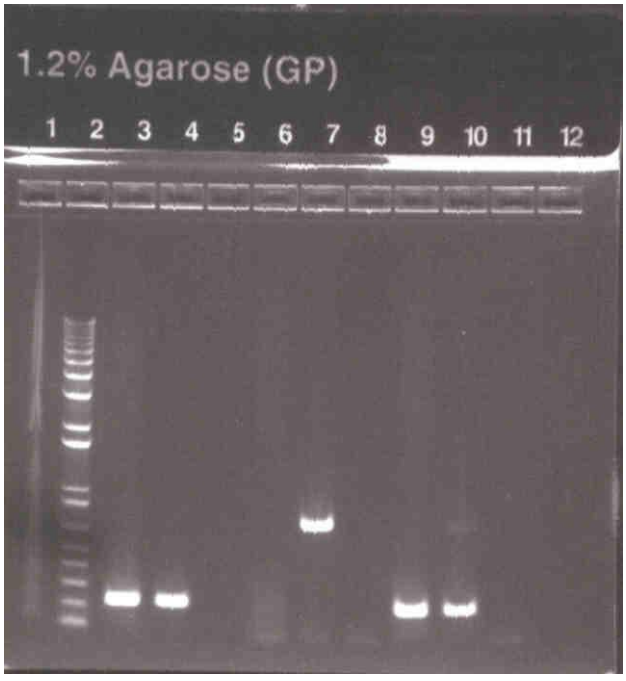

1. Blank
2. 1 Kb Plus Marker
3. g3/g4 WT
4. g3/g4 HET
5. g3/g4 H2O
6. dNEO2/g4 WT
7. dNEO2/g4 HET
8. dNEO2/g4 H2O
9. g3/g4/dNEO2 WT
10. g3/g4/dNEO2 KO
11. g3/g4/dNEO2 H2O

Note: This does not work as a 3-primer reaction. The wild-type fragment competes out the KO fragment.

8.6. DAO coding sequence and protein sequence in mice

Mus musculus D-amino acid oxidase (Dao), coding sequence (NCBI Ref: NM_010018.2)

ATTCCTGGCTGGTGGGCAGAGGGCTGAAGTCAACACAGCCCAGAGAGTCAGGAGCAGTCCTGCTGGAACCTGCAC
CCCAGGTTATTTTTCTCCCGACACCTGGCACCAGTGGCTGCTGTGATGCGCGTGGCCGTGATCGGAGCAGGAGTC
ATTGGGCTCTCCACAGCCCTCTGCATTCATGAGCGTTACCACCCAACACAGCCACTGCACATGAAGATCTATGCA
GATCGATTCACCCCGTTCACCACGAGCGATGTGGCCGCCGGCCTCTGGCAGCCTTATCTCTCTGACCCCAGCAAC
CCTCAGGAGGCGGAGTGGAGCCAGCAAACGTTTGATTACCTGCTGAGCTGCCTCCATTCTCCAAACGCTGAAAAA
ATGGGCCTGGCCCTAATCTCAGGCTACAACCTCTTCCGAGATGAAGTTCCGGACCCTTTCTGGAAAAACGCAGTT
CTGGGATTCCGGAAGCTGACCCCCAGTGAGATGGACCTGTTCCCTGATTATGGCTACGGCTGGTTCAATACAAGC
CTCCTTCTAGAGGGGAAGAGCTACCTGCCATGGCTAACTGAGAGGTTAACTGAGAGGGGAGTGAAGCTTATCCAT
CGGAAGGTGGAGTCTCTCGAAGAGGTGGCAAGAGGAGTGGATGTGATTATCAACTGCACCGGGGTGTGGGCCGGG
GCCCTGCAAGCAGATGCCTCCCTGCAGCCAGGCCGGGGCCAGATCATCCAGGTGGAGGCCCCTTGGATTAAACAC
TTCATCCTCACCCATGATCCTAGCCTTGGTATCTACAACTCTCCGTACATCATCCCAGGTTCCAAGACAGTTACG
CTCGGGGGTATATTCCAGCTGGGGAACTGGAGCGGGTTAAACAGCGTCCGTGACCACAATACCATTTGGAAGAGC
TGCTGTAAACTGGAGCCCACCCTGAAGAATGCAAGAATTGTGGGTGAACTCACTGGCTTCCGGCCAGTCCGGCCT
CAGGTCCGGCTAGAAAGAGAATGGCTTCATTTTGGATCTTCAAGTGCAGAGGTCATCCACAACTATGGTCATGGA
GGTTACGGGCTCACAATCCACTGGGGTTGTGCAATGGAGGCGGCCAACCTCTTCGGGAAAATTCTAGAGGAAAAG
AAGTTGTCCAGGTTGCCTCCCTCCCACCTCTGAGGACTCTAGTGATCACCGTGTGCCCCAAGACGACACCCCCCC
TTCGGCCAATGATATGTGATGCTCCTGGATGATGCTCTCTCCCCAGCCCCACCCCCAGCCACTCCCCAACCCACC
CCGACCACTCCCCCAGCCCCGCCGGCCACTCCCCCAGCCCCACCCCTGGCTTCCTCTGGCAAAGGCATGAAGGGA
GGAAATCTTGCTGCTCCTGCCACTCATCCACTGCTGCCTGGTCCTTCCAGTGCAGTGATTCTTGCTGGTCCTAAC
CAAGGCTTGGGTGAGATAGGCTGCGTGGTGCAATTCTTCTCAAGCCGTAGTGACTGTACTGAGGCTGGTGGTACC
GGGTGGCAGGACCTGCGTTCAGACCTATAAGGAGTGGTCTGGATCTTTTGCTTAGAACTCTGACGAATGGTTCAC
AACACACTCCATGCGTATCTGTAGTGATGGGAGGAGGGGGTTAGGAGCAGGACGTTGGGGAGAGGAGGAGGAGTT
GGAGGAGGAGCACTCCACTGGTCAACATTATTAAAACACTGGATATCCAAACTCTTCAGGAT

Mus musculus D-amino acid oxidase (Dao), protein sequence (NCBI Ref: NP_034148.2)

MRVAVIGAGVIGLSTALCIHERYHPTQPLHMKIYADRFTPFTTSDVAAGLWQPYLSDPSNPQEAEWSQQTFDYLL
SCLHSPNAEKMGLALISGYNLFRDEVPDPFWKNAVLGFRKLTPSEMDLFPDYGYGWFNTSLLLEGKSYLPWLTER
LTERGVKLIHRKVESLEEVARGVDVIINCTGVWAGALQADASLQPGRGQIIQVEAPWIKHFILTHDPSLGIYNSP
YIIPGSKTVTLGGIFQLGNWSGLNSVRDHNTIWKSCCKLEPTLKNARIVGELTGFRPVRPQVRLEREWLHFGSSS
AEVIHNYGHGGYGLTIHWGCAMEAANLFGKILEEKKLSRLPPSHL

Key: Black = Coding sequence
Grey = Non-coding sequence
Red = Sequence deleted in the *Dao*$^{-/-}$ mouse
Yellow background = Essential amino acid residues of the enzyme's active site

8.7. Genotyping protocol for *Grm2/3*$^{-/-}$ mice

The following genotyping protocol was provided by Louisa Lyon [561]. The absence of GRM2 mRNA in founding members of the GRM2$^{-/-}$ population was confirmed by the use of *in situ* hybridisation histochemistry (Yokoi et al., 1996), as was the absence of GRM3 mRNA in the founding members of the GRM3$^{-/-}$ population (Corti et al., 2007a). Genotypes of all animals were confirmed by the "Mouse genotyping group" at GSK, Harlow, using separate PCRs for GRM2 and GRM3 mRNA.

GRM2 fragments were amplified using forward oligonucleotide primers (CTG TCT CTC TAT CTC TCT GC) and reverse primers (TGT GTG TGT GTA ACA TGA TGG). PCRs were performed with a denaturing step at 95 °C (15 mins) then 94 °C (30 s), followed by annealing at 60 °C (90 s) and extension at 72 °C (1 min). After 35 cycles, the reaction was maintained at 72 °C for a further 10 mins. PCR product was then resolved onto a 2% agarose gel. The wildtype product was a single 900 bp band, and the ko product a 450 bp band.

GRM3 genotyping yielded a wildtype product that was 2 kbp long, and a knockout product that was 500 bp. The large disparity in size prevented the two fragments from being amplified in a single multiplex PCR. Two separate PCRs were therefore conducted, one for the wildtype product (forward primer: GTT TCT AGG ACT TCC TAT GG; reverse primer: AAC GAT GCT CTG ACA AAC TCC) and a second for the knockout product (forward primer: CGT ACG TCG GTT GCT ATG G; reverse primer: GTC AGA TAT AGT GAG AGC AGG). Both PCRs were performed with a denaturing step at 95 °C (15 mins) then 94 °C (30 s), followed by annealing at 56 °C (90 s) and extension at 72 °C (150 s). After 35 cycles, the reaction was maintained at 72 °C for 10 mins. PCR product was resolved onto a 2% agarose gel.

9. References

1. van Os J, Kapur S. Schizophrenia. The Lancet. 2009;374(9690):635-45.
2. Marwaha S, Johnson S, Bebbington P, Stafford M, Angermeyer MC, Brugha T, et al. Rates and correlates of employment in people with schizophrenia in the UK, France and Germany. Br J Psychiatry. 2007;191:30-7.
3. Picchioni MM, Murray RM. Schizophrenia. Bmj. 2007;335(7610):91-5.
4. Hoang U, Stewart R, Goldacre MJ. Mortality after hospital discharge for people with schizophrenia or bipolar disorder: retrospective study of linked English hospital episode statistics, 1999-2006. Bmj. 2011;343:d5422.
5. Crump C, Winkleby MA, Sundquist K, Sundquist J. Comorbidities and mortality in persons with schizophrenia: a Swedish national cohort study. Am J Psychiatry. 2013;170(3):324-33.
6. Crump C, Sundquist K, Winkleby MA, Sundquist J. Mental disorders and risk of accidental death. Br J Psychiatry. 2013;203(3):297-302.
7. Crump C, Sundquist K, Winkleby MA, Sundquist J. Mental disorders and vulnerability to homicidal death: Swedish nationwide cohort study. Bmj. 2013;346:f557.
8. Buckley PF, Miller BJ, Lehrer DS, Castle DJ. Psychiatric comorbidities and schizophrenia. Schizophr Bull. 2009;35(2):383-402.
9. McGrath J, Saha S, Welham J, El Saadi O, MacCauley C, Chant D. A systematic review of the incidence of schizophrenia: the distribution of rates and the influence of sex, urbanicity, migrant status and methodology. BMC medicine. 2004;2:13.
10. McGrath JJ. Myths and plain truths about schizophrenia epidemiology--the NAPE lecture 2004. Acta psychiatrica Scandinavica. 2005;111(1):4-11.
11. Messias EL, Chen CY, Eaton WW. Epidemiology of schizophrenia: review of findings and myths. The Psychiatric clinics of North America. 2007;30(3):323-38.
12. Castle D, Wessely S, Der G, Murray RM. The incidence of operationally defined schizophrenia in Camberwell, 1965-84. Br J Psychiatry. 1991;159:790-4.
13. Hassett A. Psychosis in the elderly. London: Taylor and Francis; 2005.
14. Kumra S, Shaw M, Merka P, Nakayama E, Augustin R. Childhood-onset schizophrenia: research update. Canadian journal of psychiatry Revue canadienne de psychiatrie. 2001;46(10):923-30.
15. McGrath J. Hypothesis: Is low prenatal vitamin D a risk-modifying factor for schizophrenia? Schizophrenia Research. 1999;40(3):173-7.
16. Jablensky A, Sartorius N, Ernberg G, Anker M, Korten A, Cooper JE, et al. Schizophrenia: manifestations, incidence and course in different cultures. A World Health Organization ten-country study. Psychological medicine Monograph supplement. 1992;20:1-97.
17. Kirkbride JB, Fearon P, Morgan C, Dazzan P, Morgan K, Murray RM, et al. Neighbourhood variation in the incidence of psychotic disorders in Southeast London. Social psychiatry and psychiatric epidemiology. 2007;42(6):438-45.
18. Kirkbride JB, Fearon P, Morgan C, Dazzan P, Morgan K, Tarrant J, et al. Heterogeneity in incidence rates of schizophrenia and other psychotic syndromes: findings from the 3-center AeSOP study. Arch Gen Psychiatry. 2006;63(3):250-8.
19. Andreasen NC. Symptoms, signs, and diagnosis of schizophrenia. Lancet. 1995;346(8973):477-81.
20. Fioravanti M, Bianchi V, Cinti M. Cognitive deficits in schizophrenia: an updated metanalysis of the scientific evidence. BMC Psychiatry. 2012;12(1):1-20.
21. Nuechterlein KH, Barch DM, Gold JM, Goldberg TE, Green MF, Heaton RK. Identification of separable cognitive factors in schizophrenia. Schizophr Res. 2004;72(1):29-39.
22. Bowie CR, Harvey PD. Cognitive deficits and functional outcome in schizophrenia. Neuropsychiatric disease and treatment. 2006;2(4):531-6.
23. Aleman A, Hijman R, de Haan EH, Kahn RS. Memory impairment in schizophrenia: a meta-analysis. Am J Psychiatry. 1999;156(9):1358-66.
24. Forbes NF, Carrick LA, McIntosh AM, Lawrie SM. Working memory in schizophrenia: a meta-analysis. Psychological medicine. 2009;39(6):889-905.
25. Rushe TM, Woodruff PW, Murray RM, Morris RG. Episodic memory and learning in patients with chronic schizophrenia. Schizophr Res. 1999;35(1):85-96.

26. Fatouros-Bergman H, Cervenka S, Flyckt L, Edman G, Farde L. Meta-analysis of cognitive performance in drug-naïve patients with schizophrenia. Schizophrenia Research. 2014;158(1–3):156-62.
27. Goldberg TE, Weinberger DR. Effects of neuroleptic medications on the cognition of patients with schizophrenia: a review of recent studies. The Journal of clinical psychiatry. 1996;57 Suppl 9:62-5.
28. Hoff AL, Riordan H, O'Donnell DW, Morris L, DeLisi LE. Neuropsychological functioning of first-episode schizophreniform patients. Am J Psychiatry. 1992;149(7):898-903.
29. Landro NI. Memory function in schizophrenia. Acta psychiatrica Scandinavica Supplementum. 1994;384:87-94.
30. Meltzer HY, Matsubara S, Lee JC. Classification of typical and atypical antipsychotic drugs on the basis of dopamine D-1, D-2 and serotonin2 pKi values. J Pharmacol Exp Ther. 1989;251(1):238-46.
31. Leucht S, Tardy M, Komossa K, Heres S, Kissling W, Davis JM. Maintenance treatment with antipsychotic drugs for schizophrenia. Cochrane Database Syst Rev. 2012;5:Cd008016.
32. Tyrer P, Kendall T. The spurious advance of antipsychotic drug therapy. The Lancet. 2009;373(9657):4-5.
33. Novick D, Haro JM, Suarez D, Vieta E, Naber D. Recovery in the outpatient setting: 36-month results from the Schizophrenia Outpatients Health Outcomes (SOHO) study. Schizophr Res. 2009;108(1-3):223-30.
34. Geyer M, Tamminga C. Measurement and treatment research to improve cognition in schizophrenia: neuropharmacological aspects. Psychopharmacology. 2004;174(1):1-2.
35. Cardno AG, Gottesman, II. Twin studies of schizophrenia: from bow-and-arrow concordances to star wars Mx and functional genomics. American journal of medical genetics. 2000;97(1):12-7.
36. Sullivan PF, Kendler KS, Neale MC. Schizophrenia as a complex trait: evidence from a meta-analysis of twin studies. Arch Gen Psychiatry. 2003;60(12):1187-92.
37. Harrison PJ, Law AJ. Neuregulin 1 and schizophrenia: genetics, gene expression, and neurobiology. Biol Psychiatry. 2006;60(2):132-40.
38. Mei L, Xiong W-C. Neuregulin 1 in neural development, synaptic plasticity and schizophrenia. Nat Rev Neurosci. 2008;9(6):437-52.
39. Stefansson H, Sigurdsson E, Steinthorsdottir V, Bjornsdottir S, Sigmundsson T, Ghosh S, et al. Neuregulin 1 and susceptibility to schizophrenia. American journal of human genetics. 2002;71(4):877-92.
40. Arguello PA, Gogos JA. A signaling pathway AKTing up in schizophrenia. The Journal of Clinical Investigation. 2008;118(6):2018-21.
41. Brandon NJ, Sawa A. Linking neurodevelopmental and synaptic theories of mental illness through DISC1. Nat Rev Neurosci. 2011;12(12):707-22.
42. Johnstone M, Thomson PA, Hall J, McIntosh AM, Lawrie SM, Porteous DJ. DISC1 in schizophrenia: genetic mouse models and human genomic imaging. Schizophr Bull. 2011;37(1):14-20.
43. Harrison PJ, Lyon L, Sartorius LJ, Burnet PW, Lane TA. The group II metabotropic glutamate receptor 3 (mGluR3, mGlu3, GRM3): expression, function and involvement in schizophrenia. J Psychopharmacol. 2008;22(3):308-22.
44. Chumakov I, Blumenfeld M, Guerassimenko O, Cavarec L, Palicio M, Abderrahim H, et al. Genetic and physiological data implicating the new human gene G72 and the gene for D-amino acid oxidase in schizophrenia. Proc Natl Acad Sci U S A. 2002;99(21):13675-80.
45. Verrall L, Burnet PW, Betts JF, Harrison PJ. The neurobiology of D-amino acid oxidase and its involvement in schizophrenia. Mol Psychiatry. 2010;15(2):122-37.
46. Tunbridge EM, Weinberger DR, Harrison PJ. A novel protein isoform of catechol O-methyltransferase (COMT): brain expression analysis in schizophrenia and bipolar disorder and effect of Val158Met genotype. Mol Psychiatry. 2006;11(2):116-7.
47. Williams NM, O'Donovan MC, Owen MJ. Is the dysbindin gene (DTNBP1) a susceptibility gene for schizophrenia? Schizophr Bull. 2005;31(4):800-5.
48. Corradini I, Verderio C, Sala M, Wilson MC, Matteoli M. SNAP-25 in neuropsychiatric disorders. Annals of the New York Academy of Sciences. 2009;1152:93-9.
49. Vacic V, McCarthy S, Malhotra D, Murray F, Chou H-H, Peoples A, et al. Duplications of the neuropeptide receptor gene VIPR2 confer significant risk for schizophrenia. Nature. 2011;471(7339):499-503.

50. Koefoed P, Hansen TV, Woldbye DP, Werge T, Mors O, Hansen T, et al. An intron 1 polymorphism in the cholecystokinin-A receptor gene associated with schizophrenia in males. Acta psychiatrica Scandinavica. 2009;120(4):281-7.
51. Lipina TV, Wang M, Liu F, Roder JC. Synergistic interactions between PDE4B and GSK-3: DISC1 mutant mice. Neuropharmacology. 2012;62(3):1252-62.
52. Fatemi SH, King DP, Reutiman TJ, Folsom TD, Laurence JA, Lee S, et al. PDE4B polymorphisms and decreased PDE4B expression are associated with schizophrenia. Schizophr Res. 2008;101(1-3):36-49.
53. Numata S, Ueno S, Iga J, Song H, Nakataki M, Tayoshi S, et al. Positive association of the PDE4B (phosphodiesterase 4B) gene with schizophrenia in the Japanese population. J Psychiatr Res. 2008;43(1):7-12.
54. Tomppo L, Hennah W, Lahermo P, Loukola A, Tuulio-Henriksson A, Suvisaari J, et al. Association between genes of Disrupted in schizophrenia 1 (DISC1) interactors and schizophrenia supports the role of the DISC1 pathway in the etiology of major mental illnesses. Biol Psychiatry. 2009;65(12):1055-62.
55. Brzozka MM, Radyushkin K, Wichert SP, Ehrenreich H, Rossner MJ. Cognitive and sensorimotor gating impairments in transgenic mice overexpressing the schizophrenia susceptibility gene Tcf4 in the brain. Biol Psychiatry. 2010;68(1):33-40.
56. Schizophrenia Working Group of the Psychiatric Genomics C. Genome-wide association study identifies five new schizophrenia loci. Nature genetics. 2011;43(10):969-76.
57. O'Donovan MC, Craddock N, Norton N, Williams H, Peirce T, Moskvina V, et al. Identification of loci associated with schizophrenia by genome-wide association and follow-up. Nature genetics. 2008;40(9):1053-5.
58. Crow TJ. The emperors of the schizophrenia polygene have no clothes. Psychological medicine. 2008;38(12):1681-5.
59. Chakravarti A. Population genetics--making sense out of sequence. Nature genetics. 1999;21(1 Suppl):56-60.
60. Schizophrenia Working Group of the Psychiatric Genomics C. Biological insights from 108 schizophrenia-associated genetic loci. Nature. 2014;511(7510):421-7.
61. Stankiewicz P, Lupski JR. Structural variation in the human genome and its role in disease. Annual review of medicine. 2010;61:437-55.
62. Bassett AS, Scherer SW, Brzustowicz LM. Copy Number Variations in Schizophrenia: Critical Review and New Perspectives on Concepts of Genetics and Disease. The American Journal of Psychiatry. 2010;167(8):899-914.
63. Cook EH, Jr., Scherer SW. Copy-number variations associated with neuropsychiatric conditions. Nature. 2008;455(7215):919-23.
64. St Clair D. Copy Number Variation and Schizophrenia. Schizophrenia Bulletin. 2009;35(1):9-12.
65. St Clair D. Structural and copy number variants in the human genome: implications for psychiatry. Br J Psychiatry. 2013;202(1):5-6.
66. Bassett AS, Chow EWC. Schizophrenia and 22q11.2 Deletion Syndrome. Current psychiatry reports. 2008;10(2):148-57.
67. Monks S, Niarchou M, Davies AR, Walters JT, Williams N, Owen MJ, et al. Further evidence for high rates of schizophrenia in 22q11.2 deletion syndrome. Schizophr Res. 2014;153(1-3):231-6.
68. Georgieva L, Rees E, Moran JL, Chambert KD, Milanova V, Craddock N, et al. De novo CNVs in bipolar affective disorder and schizophrenia. Hum Mol Genet. 2014;23(24):6677-83.
69. Xu B, Roos JL, Levy S, van Rensburg EJ, Gogos JA, Karayiorgou M. Strong association of de novo copy number mutations with sporadic schizophrenia. Nature genetics. 2008;40(7):880-5.
70. McDonald C, Murray RM. Early and late environmental risk factors for schizophrenia. Brain research Brain research reviews. 2000;31(2-3):130-7.
71. Torrey EF, Miller J, Rawlings R, Yolken RH. Seasonality of births in schizophrenia and bipolar disorder: a review of the literature. Schizophr Res. 1997;28(1):1-38.
72. Brown AS, Susser ES. Prenatal nutritional deficiency and risk of adult schizophrenia. Schizophr Bull. 2008;34(6):1054-63.
73. Cannon M, Jones PB, Murray RM. Obstetric complications and schizophrenia: historical and meta-analytic review. Am J Psychiatry. 2002;159(7):1080-92.
74. Dalman C, Thomas HV, David AS, Gentz J, Lewis G, Allebeck P. Signs of asphyxia at birth and risk of schizophrenia. Population-based case-control study. Br J Psychiatry. 2001;179:403-8.

75. McNeil TF, Cantor-Graae E, Weinberger DR. Relationship of obstetric complications and differences in size of brain structures in monozygotic twin pairs discordant for schizophrenia. Am J Psychiatry. 2000;157(2):203-12.
76. Fatemi SH, Folsom TD. The neurodevelopmental hypothesis of schizophrenia, revisited. Schizophr Bull. 2009;35(3):528-48.
77. Weinberger DR. On the plausibility of "the neurodevelopmental hypothesis" of schizophrenia. Neuropsychopharmacology. 1996;14(3 Suppl):1s-11s.
78. Harrison PJ, Weinberger DR. Schizophrenia genes, gene expression, and neuropathology: on the matter of their convergence. Mol Psychiatry. 2005;10(1):40-68; image 5.
79. Glantz LA, Lewis DA. Decreased dendritic spine density on prefrontal cortical pyramidal neurons in schizophrenia. Arch Gen Psychiatry. 2000;57(1):65-73.
80. Harrison PJ. The neuropathology of schizophrenia. A critical review of the data and their interpretation. Brain : a journal of neurology. 1999;122 (Pt 4):593-624.
81. Sweet RA, Henteleff RA, Zhang W, Sampson AR, Lewis DA. Reduced dendritic spine density in auditory cortex of subjects with schizophrenia. Neuropsychopharmacology. 2009;34(2):374-89.
82. Walker EF, Grimes KE, Davis DM, Smith AJ. Childhood precursors of schizophrenia: facial expressions of emotion. Am J Psychiatry. 1993;150(11):1654-60.
83. Walker EF, Savoie T, Davis D. Neuromotor precursors of schizophrenia. Schizophr Bull. 1994;20(3):441-51.
84. Keshavan MS. Development, disease and degeneration in schizophrenia: a unitary pathophysiological model. J Psychiatr Res. 1999;33(6):513-21.
85. Meltzer HY, Stahl SM. The dopamine hypothesis of schizophrenia: a review. Schizophr Bull. 1976;2(1):19-76.
86. Curran C, Byrappa N, McBride A. Stimulant psychosis: systematic review. Br J Psychiatry. 2004;185:196-204.
87. Lieberman JA, Kane JM, Alvir J. Provocative tests with psychostimulant drugs in schizophrenia. Psychopharmacology (Berl). 1987;91(4):415-33.
88. Talbot PS, Laruelle M. The role of in vivo molecular imaging with PET and SPECT in the elucidation of psychiatric drug action and new drug development. Eur Neuropsychopharmacol. 2002;12(6):503-11.
89. Creese I, Burt DR, Snyder SH. Dopamine receptor binding predicts clinical and pharmacological potencies of antischizophrenic drugs. Science. 1976;192(4238):481-3.
90. Seeman P, Lee T. Antipsychotic drugs: direct correlation between clinical potency and presynaptic action on dopamine neurons. Science. 1975;188(4194):1217-9.
91. Harrison PJ. Postmortem studies in schizophrenia. Dialogues in Clinical Neuroscience. 2000;2(4):349-57.
92. Laruelle M, Abi-Dargham A, Gil R, Kegeles L, Innis R. Increased dopamine transmission in schizophrenia: relationship to illness phases. Biol Psychiatry. 1999;46(1):56-72.
93. Knable MB, Weinberger DR. Dopamine, the prefrontal cortex and schizophrenia. J Psychopharmacol. 1997;11(2):123-31.
94. Goldman-Rakic PS, Muly EC, 3rd, Williams GV. D(1) receptors in prefrontal cells and circuits. Brain research Brain research reviews. 2000;31(2-3):295-301.
95. Davis KL, Kahn RS, Ko G, Davidson M. Dopamine in schizophrenia: a review and reconceptualization. Am J Psychiatry. 1991;148(11):1474-86.
96. Weinberger DR. Implications of normal brain development for the pathogenesis of schizophrenia. Arch Gen Psychiatry. 1987;44(7):660-9.
97. Coyle JT. NMDA receptor and schizophrenia: a brief history. Schizophr Bull. 2012;38(5):920-6.
98. Kantrowitz JT, Javitt DC. N-methyl-d-aspartate (NMDA) receptor dysfunction or dysregulation: the final common pathway on the road to schizophrenia? Brain Res Bull. 2010;83(3-4):108-21.
99. Marek GJ, Behl B, Bespalov AY, Gross G, Lee Y, Schoemaker H. Glutamatergic (N-methyl-D-aspartate receptor) hypofrontality in schizophrenia: too little juice or a miswired brain? Molecular pharmacology. 2010;77(3):317-26.
100. Olney JW, Newcomer JW, Farber NB. NMDA receptor hypofunction model of schizophrenia. J Psychiatr Res. 1999;33(6):523-33.
101. Zito K, Scheuss V. NMDA Receptor Function and Physiological Modulation. In: Squire LR, editor. Encyclopedia of Neuroscience Oxford: Academic Press; 2009. p. 1157-64.

102. Javitt DC, Zukin SR. Recent advances in the phencyclidine model of schizophrenia. Am J Psychiatry. 1991;148(10):1301-8.
103. Krystal JH, Karper LP, Seibyl JP, Freeman GK, Delaney R, Bremner JD, et al. Subanesthetic effects of the noncompetitive NMDA antagonist, ketamine, in humans. Psychotomimetic, perceptual, cognitive, and neuroendocrine responses. Arch Gen Psychiatry. 1994;51(3):199-214.
104. Lahti AC, Koffel B, LaPorte D, Tamminga CA. Subanesthetic doses of ketamine stimulate psychosis in schizophrenia. Neuropsychopharmacology. 1995;13(1):9-19.
105. Shim SS, Hammonds MD, Kee BS. Potentiation of the NMDA receptor in the treatment of schizophrenia: focused on the glycine site. European archives of psychiatry and clinical neuroscience. 2008;258(1):16-27.
106. Clinton SM, Meador-Woodruff JH. Abnormalities of the NMDA Receptor and Associated Intracellular Molecules in the Thalamus in Schizophrenia and Bipolar Disorder. Neuropsychopharmacology. 2004;29(7):1353-62.
107. Pilowsky LS, Bressan RA, Stone JM, Erlandsson K, Mulligan RS, Krystal JH, et al. First in vivo evidence of an NMDA receptor deficit in medication-free schizophrenic patients. Mol Psychiatry. 2006;11(2):118-9.
108. Glennon RA. Do classical hallucinogens act as 5-HT2 agonists or antagonists? Neuropsychopharmacology. 1990;3(5-6):509-17.
109. Iqbal N, van Praag HM. The role of serotonin in schizophrenia. Eur Neuropsychopharmacol. 1995;5 Suppl:11-23.
110. Burnet PW, Eastwood SL, Harrison PJ. 5-HT1A and 5-HT2A receptor mRNAs and binding site densities are differentially altered in schizophrenia. Neuropsychopharmacology. 1996;15(5):442-55.
111. Erdmann J, Shimron-Abarbanell D, Rietschel M, Albus M, Maier W, Korner J, et al. Systematic screening for mutations in the human serotonin-2A (5-HT2A) receptor gene: identification of two naturally occurring receptor variants and association analysis in schizophrenia. Human genetics. 1996;97(5):614-9.
112. Inayama Y, Yoneda H, Sakai T, Ishida T, Nonomura Y, Kono Y, et al. Positive association between a DNA sequence variant in the serotonin 2A receptor gene and schizophrenia. American journal of medical genetics. 1996;67(1):103-5.
113. Williams J, Spurlock G, McGuffin P, Mallet J, Nothen MM, Gill M, et al. Association between schizophrenia and T102C polymorphism of the 5-hydroxytryptamine type 2a-receptor gene. European Multicentre Association Study of Schizophrenia (EMASS) Group. Lancet. 1996;347(9011):1294-6.
114. Carlsson A, Waters N, Holm-Waters S, Tedroff J, Nilsson M, Carlsson ML. Interactions between monoamines, glutamate, and GABA in schizophrenia: new evidence. Annual review of pharmacology and toxicology. 2001;41:237-60.
115. Bruton CJ, Crow TJ, Frith CD, Johnstone EC, Owens DG, Roberts GW. Schizophrenia and the brain: a prospective clinico-neuropathological study. Psychological medicine. 1990;20(2):285-304.
116. Weinberger DR. From neuropathology to neurodevelopment. The Lancet. 1995;346(8974):552-7.
117. Weinberger DR, DeLisi LE, Perman GP, Targum S, Wyatt RJ. Computed tomography in schizophreniform disorder and other acute psychiatric disorders. Arch Gen Psychiatry. 1982;39(7):778-83.
118. Lawrie SM, Whalley H, Byrne M, Miller P, Best JJK, Johnstone EC. Brain structure change and psychopathology in subjects at high risk of schizophrenia. Schizophrenia Research. 2000;41(1):11.
119. Pantellis C, Velakoulis D, Suckling J. Left medial temporal lobe reduction occurs during the transition from high risk to first episode psychosis. Schizophrenia Research. 2000;41:1-35.
120. Lippmann S, Manshadi M, Baldwin H, Drasin G, Rice J, Alrajeh S. Cerebellar vermis dimensions on computerized tomographic scans of schizophrenic and bipolar patients. Am J Psychiatry. 1982;139(5):667-8.
121. Weinberger DR, Kleinman JE, Luchins DJ, Bigelow LB, Wyatt RJ. Cerebellar pathology in schizophrenia: a controlled postmortem study. Am J Psychiatry. 1980;137(3):359-61.
122. McGlashan TH, Hoffman RE. Schizophrenia as a disorder of developmentally reduced synaptic connectivity. Arch Gen Psychiatry. 2000;57(7):637-48.
123. Schmitt A, Hasan A, Gruber O, Falkai P. Schizophrenia as a disorder of disconnectivity. European archives of psychiatry and clinical neuroscience. 2011;261(Suppl 2):150-4.
124. Harrison PJ, Pritchett D, Stumpenhorst K, Betts JF, Nissen W, Schweimer J, et al. Genetic mouse models relevant to schizophrenia: taking stock and looking forward. Neuropharmacology. 2012;62(3):1164-7.

125. Pritchett D, Wulff K, Oliver PL, Bannerman DM, Davies KE, Harrison PJ, et al. Evaluating the links between schizophrenia and sleep and circadian rhythm disruption. J Neural Transm. 2012;119(10):1061-75.
126. Nilsson M, Carlsson A, Carlsson ML. Glycine and D-serine decrease MK-801-induced hyperactivity in mice. J Neural Transm. 1997;104(11-12):1195-205.
127. Sams-Dodd F. Phencyclidine-induced stereotyped behaviour and social isolation in rats: a possible animal model of schizophrenia. Behavioural pharmacology. 1996;7(1):3-23.
128. Lee PR, Brady DL, Shapiro RA, Dorsa DM, Koenig JI. Social interaction deficits caused by chronic phencyclidine administration are reversed by oxytocin. Neuropsychopharmacology. 2005;30(10):1883-94.
129. Castagne V, Moser P, Roux S, Porsolt RD. Rodent models of depression: forced swim and tail suspension behavioral despair tests in rats and mice. Current protocols in neuroscience / editorial board, Jacqueline N Crawley [et al]. 2011;Chapter 8:Unit 8.10A.
130. Moreau J-L. Simulating the anhedonia symptom of depression in animals. Dialogues in Clinical Neuroscience. 2002;4(4):351-60.
131. McHugh SB, Bannerman DM. Cognition: Learning and Memory: Spatial. In: Koob GF, Moal ML, Thompson RF, editors. Encyclopedia of Behavioral Neuroscience. Oxford: Academic Press; 2010. p. 279-87.
132. Lyon L, Saksida LM, Bussey TJ. Spontaneous object recognition and its relevance to schizophrenia: a review of findings from pharmacological, genetic, lesion and developmental rodent models. Psychopharmacology (Berl). 2012;220(4):647-72.
133. Danion JM, Rizzo L, Bruant A. Functional mechanisms underlying impaired recognition memory and conscious awareness in patients with schizophrenia. Arch Gen Psychiatry. 1999;56(7):639-44.
134. Bissonette GB, Powell EM. Reversal learning and attentional set-shifting in mice. Neuropharmacology. 2012;62(3):1168-74.
135. Garner JP, Thogerson CM, Wurbel H, Murray JD, Mench JA. Animal neuropsychology: validation of the Intra-Dimensional Extra-Dimensional set shifting task for mice. Behav Brain Res. 2006;173(1):53-61.
136. Amitai N, Markou A. Disruption of performance in the five-choice serial reaction time task induced by administration of N-methyl-D-aspartate receptor antagonists: relevance to cognitive dysfunction in schizophrenia. Biol Psychiatry. 2010;68(1):5-16.
137. Swerdlow NR, Weber M, Qu Y, Light GA, Braff DL. Realistic expectations of prepulse inhibition in translational models for schizophrenia research. Psychopharmacology (Berl). 2008;199(3):331-88.
138. Braff DL, Geyer MA, Swerdlow NR. Human studies of prepulse inhibition of startle: normal subjects, patient groups, and pharmacological studies. Psychopharmacology (Berl). 2001;156(2-3):234-58.
139. Kumari V, Fannon D, Geyer MA, Premkumar P, Antonova E, Simmons A, et al. Cortical grey matter volume and sensorimotor gating in schizophrenia. Cortex; a journal devoted to the study of the nervous system and behavior. 2008;44(9):1206-14.
140. Ludewig K, Geyer MA, Vollenweider FX. Deficits in prepulse inhibition and habituation in never-medicated, first-episode schizophrenia. Biol Psychiatry. 2003;54(2):121-8.
141. Mackeprang T, Kristiansen KT, Glenthoj BY. Effects of antipsychotics on prepulse inhibition of the startle response in drug-naive schizophrenic patients. Biol Psychiatry. 2002;52(9):863-73.
142. Arguello PA, Gogos JA. Cognition in mouse models of schizophrenia susceptibility genes. Schizophr Bull. 2010;36(2):289-300.
143. Nestler EJ, Hyman SE. Animal models of neuropsychiatric disorders. Nat Neurosci. 2010;13(10):1161-9.
144. Papaleo F, Lipska BK, Weinberger DR. Mouse models of genetic effects on cognition: relevance to schizophrenia. Neuropharmacology. 2012;62(3):1204-20.
145. Ellison-Wright I, Glahn DC, Laird AR, Thelen SM, Bullmore E. The anatomy of first-episode and chronic schizophrenia: an anatomical likelihood estimation meta-analysis. Am J Psychiatry. 2008;165(8):1015-23.
146. Andreasen NC. A unitary model of schizophrenia: Bleuler's "fragmented phrene" as schizencephaly. Arch Gen Psychiatry. 1999;56(9):781-7.
147. Kaffman A, Krystal JH. New frontiers in animal research of psychiatric illness. Methods in molecular biology (Clifton, NJ). 2012;829:3-30.

148. Tseng KY, Chambers RA, Lipska BK. The neonatal ventral hippocampal lesion as a heuristic neurodevelopmental model of schizophrenia. Behavioural brain research. 2009;204(2):295-305.
149. Chen J, Lipska BK, Weinberger DR. Genetic Mouse Models of Schizophrenia: From Hypothesis-Based To Susceptibility Gene-Based Models. Biological Psychiatry. 2006;59(12):1180-8.
150. Palmer AA, Brown AS, Keegan D, Siska LD, Susser E, Rotrosen J, et al. Prenatal protein deprivation alters dopamine-mediated behaviors and dopaminergic and glutamatergic receptor binding. Brain Res. 2008;1237:62-74.
151. Palmer AA, Printz DJ, Butler PD, Dulawa SC, Printz MP. Prenatal protein deprivation in rats induces changes in prepulse inhibition and NMDA receptor binding. Brain Res. 2004;996(2):193-201.
152. Fendt M, Lex A, Falkai P, Henn FA, Schmitt A. Behavioural alterations in rats following neonatal hypoxia and effects of clozapine: implications for schizophrenia. Pharmacopsychiatry. 2008;41(4):138-45.
153. Schmitt A, Fendt M, Zink M, Ebert U, Starke M, Berthold M, et al. Altered NMDA receptor expression and behavior following postnatal hypoxia: potential relevance to schizophrenia. J Neural Transm. 2007;114(2):239-48.
154. Lodge DJ, Grace AA. Gestational methylazoxymethanol acetate administration: a developmental disruption model of schizophrenia. Behav Brain Res. 2009;204(2):306-12.
155. Meyer U, Feldon J. To poly(I:C) or not to poly(I:C): advancing preclinical schizophrenia research through the use of prenatal immune activation models. Neuropharmacology. 2012;62(3):1308-21.
156. Kannan G, Sawa A, Pletnikov MV. Mouse models of gene-environment interactions in schizophrenia. Neurobiol Dis. 2013;57:5-11.
157. Johnson CH, Elliott JA, Foster R, Honma K, Kronauer RE. Fundamental Properties of Circadian Rhythms. In: Dunlap JC, Loros JJ, DeCoursey PJ, editors. Chronobiology: biological timekeeping. Sunderland: Sinauer Associates; 2004. p. 67-106.
158. Benloucif S, Guico MJ, Reid KJ, Wolfe LF, L'Hermite-Baleriaux M, Zee PC. Stability of melatonin and temperature as circadian phase markers and their relation to sleep times in humans. J Biol Rhythms. 2005;20(2):178-88.
159. Hastings MH. Circadian clocks. Current Biology. 1997;7(11):R670-R2.
160. Lavery DJ, Schibler U. Circadian transcription of the cholesterol 7 alpha hydroxylase gene may involve the liver-enriched bZIP protein DBP. Genes & development. 1993;7(10):1871-84.
161. Portaluppi F, Vergnani L, Manfredini R, Fersini C. Endocrine mechanisms of blood pressure rhythms. Annals of the New York Academy of Sciences. 1996;783:113-31.
162. Rabinowitz L. Aldosterone and potassium homeostasis. Kidney international. 1996;49(6):1738-42.
163. Bell-Pedersen D, Cassone VM, Earnest DJ, Golden SS, Hardin PE, Thomas TL, et al. Circadian rhythms from multiple oscillators: lessons from diverse organisms. Nature reviews Genetics. 2005;6(7):544-56.
164. Beaver LM, Gvakharia BO, Vollintine TS, Hege DM, Stanewsky R, Giebultowicz JM. Loss of circadian clock function decreases reproductive fitness in males of Drosophila melanogaster. Proceedings of the National Academy of Sciences of the United States of America. 2002;99(4):2134-9.
165. DeCoursey PJ, Krulas JR, Mele G, Holley DC. Circadian performance of suprachiasmatic nuclei (SCN)-lesioned antelope ground squirrels in a desert enclosure. Physiology & behavior. 1997;62(5):1099-108.
166. DeCoursey PJ, Walker JK, Smith SA. A circadian pacemaker in free-living chipmunks: essential for survival? J Comp Physiol A. 2000;186(2):169-80.
167. Dodd AN, Salathia N, Hall A, Kevei E, Toth R, Nagy F, et al. Plant circadian clocks increase photosynthesis, growth, survival, and competitive advantage. Science. 2005;309(5734):630-3.
168. Green RM, Tingay S, Wang Z-Y, Tobin EM. Circadian Rhythms Confer a Higher Level of Fitness to Arabidopsis Plants. Plant Physiology. 2002;129(2):576-84.
169. Ouyang Y, Andersson CR, Kondo T, Golden SS, Johnson CH. Resonating circadian clocks enhance fitness in cyanobacteria. Proc Natl Acad Sci U S A. 1998;95(15):8660-4.
170. Welsh DK, Logothetis DE, Meister M, Reppert SM. Individual neurons dissociated from rat suprachiasmatic nucleus express independently phased circadian firing rhythms. Neuron. 1995;14(4):697-706.
171. Moore RY, Eichler VB. Loss of a circadian adrenal corticosterone rhythm following suprachiasmatic lesions in the rat. Brain Res. 1972;42(1):201-6.
172. Stephan FK, Zucker I. Circadian rhythms in drinking behavior and locomotor activity of rats are eliminated by hypothalamic lesions. Proc Natl Acad Sci U S A. 1972;69(6):1583-6.

173. DeCoursey PJ, Buggy J. Circadian rhythmicity after neural transplant to hamster third ventricle: specificity of suprachiasmatic nuclei. Brain Res. 1989;500(1-2):263-75.
174. Ralph MR, Foster RG, Davis FC, Menaker M. Transplanted suprachiasmatic nucleus determines circadian period. Science. 1990;247(4945):975-8.
175. Hastings M. The brain, circadian rhythms, and clock genes. BMJ : British Medical Journal. 1998;317(7174):1704-7.
176. Inouye ST, Kawamura H. Persistence of circadian rhythmicity in a mammalian hypothalamic "island" containing the suprachiasmatic nucleus. Proc Natl Acad Sci U S A. 1979;76(11):5962-6.
177. Schwartz WJ, Gainer H. Suprachiasmatic nucleus: use of 14C-labeled deoxyglucose uptake as a functional marker. Science. 1977;197(4308):1089-91.
178. Gillette MU. The suprachiasmatic nuclei: circadian phase-shifts induced at the time of hypothalamic slice preparation are preserved in vitro. Brain Res. 1986;379(1):176-81.
179. Edgar RS, Green EW, Zhao Y, van Ooijen G, Olmedo M, Qin X, et al. Peroxiredoxins are conserved markers of circadian rhythms. Nature. 2012;485(7399):459-64.
180. Reppert SM, Weaver DR. Coordination of circadian timing in mammals. Nature. 2002;418(6901):935-41.
181. Stangherlin A, Reddy AB. Regulation of Circadian Clocks by Redox Homeostasis. The Journal of Biological Chemistry. 2013;288(37):26505-11.
182. Ralph MR, Menaker M. A mutation of the circadian system in golden hamsters. Science. 1988;241(4870):1225-7.
183. Lowrey PL, Shimomura K, Antoch MP, Yamazaki S, Zemenides PD, Ralph MR, et al. Positional syntenic cloning and functional characterization of the mammalian circadian mutation tau. Science. 2000;288(5465):483-92.
184. Preitner N, Damiola F, Lopez-Molina L, Zakany J, Duboule D, Albrecht U, et al. The orphan nuclear receptor REV-ERBalpha controls circadian transcription within the positive limb of the mammalian circadian oscillator. Cell. 2002;110(2):251-60.
185. Guler AD, Ecker JL, Lall GS, Haq S, Altimus CM, Liao HW, et al. Melanopsin cells are the principal conduits for rod-cone input to non-image-forming vision. Nature. 2008;453(7191):102-5.
186. Hattar S, Kumar M, Park A, Tong P, Tung J, Yau KW, et al. Central projections of melanopsin-expressing retinal ganglion cells in the mouse. J Comp Neurol. 2006;497(3):326-49.
187. Provencio I, Cooper HM, Foster RG. Retinal projections in mice with inherited retinal degeneration: implications for circadian photoentrainment. J Comp Neurol. 1998;395(4):417-39.
188. Abe H, Rusak B, Robertson HA. Photic induction of Fos protein in the suprachiasmatic nucleus is inhibited by the NMDA receptor antagonist MK-801. Neuroscience Letters. 1991;127(1):9-12.
189. Colwell CS, Foster RG, Menaker M. NMDA receptor antagonists block the effects of light on circadian behavior in the mouse. Brain Res. 1991;554(1-2):105-10.
190. Kornhauser JM, Nelson DE, Mayo KE, Takahashi JS. Photic and circadian regulation of c-fos gene expression in the hamster suprachiasmatic nucleus. Neuron. 1990;5(2):127-34.
191. Liou SY, Shibata S, Iwasaki K, Ueki S. Optic nerve stimulation-induced increase of release of 3H-glutamate and 3H-aspartate but not 3H-GABA from the suprachiasmatic nucleus in slices of rat hypothalamus. Brain Res Bull. 1986;16(4):527-31.
192. Mikkelsen JD, Larsen PJ, Mick G, Vrang N, Ebling FJ, Maywood ES, et al. Gating of retinal inputs through the suprachiasmatic nucleus: role of excitatory neurotransmission. Neurochemistry international. 1995;27(3):263-72.
193. Tominaga K, Geusz ME, Michel S, Inouye ST. Calcium imaging in organotypic cultures of the rat suprachiasmatic nucleus. Neuroreport. 1994;5(15):1901-5.
194. Hastings MH, Maywood ES, Reddy AB. Two decades of circadian time. Journal of neuroendocrinology. 2008;20(6):812-9.
195. Colwell CS. Linking neural activity and molecular oscillations in the SCN. Nat Rev Neurosci. 2011;12(10):553-69.
196. Silver R, LeSauter J, Tresco PA, Lehman MN. A diffusible coupling signal from the transplanted suprachiasmatic nucleus controlling circadian locomotor rhythms. Nature. 1996;382(6594):810-3.
197. Kramer A, Yang FC, Snodgrass P, Li X, Scammell TE, Davis FC, et al. Regulation of daily locomotor activity and sleep by hypothalamic EGF receptor signaling. Science. 2001;294(5551):2511-5.

198. Guilding C, Piggins HD. Challenging the omnipotence of the suprachiasmatic timekeeper: are circadian oscillators present throughout the mammalian brain? Eur J Neurosci. 2007;25(11):3195-216.
199. Balsalobre A, Damiola F, Schibler U. A serum shock induces circadian gene expression in mammalian tissue culture cells. Cell. 1998;93(6):929-37.
200. Yoo SH, Yamazaki S, Lowrey PL, Shimomura K, Ko CH, Buhr ED, et al. PERIOD2::LUCIFERASE real-time reporting of circadian dynamics reveals persistent circadian oscillations in mouse peripheral tissues. Proc Natl Acad Sci U S A. 2004;101(15):5339-46.
201. Duffield GE. DNA microarray analyses of circadian timing: the genomic basis of biological time. Journal of neuroendocrinology. 2003;15(10):991-1002.
202. O'Neill JS, Reddy AB. Circadian clocks in human red blood cells. Nature. 2011;469(7331):498-503.
203. O'Neill JS, van Ooijen G, Dixon LE, Troein C, Corellou F, Bouget FY, et al. Circadian rhythms persist without transcription in a eukaryote. Nature. 2011;469(7331):554-8.
204. Zepelin H, Siegel JM, Tobler I. Mammalian sleep. In: Kryger MH, Roth T, Dement WC, editors. Principles and practices of sleep medicine. New York: Saunders; 2005.
205. Bryant PA, Trinder J, Curtis N. Sick and tired: does sleep have a vital role in the immune system? Nat Rev Immunol. 2004;4(6):457-67.
206. Inoué S, Honda K, Komoda Y. Sleep as neuronal detoxification and restitution. Behavioural Brain Research. 1995;69(1–2):91-6.
207. Stickgold R. Sleep-dependent memory consolidation. Nature. 2005;437(7063):1272-8.
208. Tononi G, Cirelli C. Sleep function and synaptic homeostasis. Sleep medicine reviews. 2006;10(1):49-62.
209. Banks S, Dinges DF. Behavioral and physiological consequences of sleep restriction. Journal of clinical sleep medicine : JCSM : official publication of the American Academy of Sleep Medicine. 2007;3(5):519-28.
210. Oginska H, Pokorski J. Fatigue and mood correlates of sleep length in three age-social groups: School children, students, and employees. Chronobiology international. 2006;23(6):1317-28.
211. Scott JP, McNaughton LR, Polman RC. Effects of sleep deprivation and exercise on cognitive, motor performance and mood. Physiology & behavior. 2006;87(2):396-408.
212. Selvi Y, Gulec M, Agargun MY, Besiroglu L. Mood changes after sleep deprivation in morningness-eveningness chronotypes in healthy individuals. Journal of sleep research. 2007;16(3):241-4.
213. Johnson EO, Roth T, Breslau N. The association of insomnia with anxiety disorders and depression: exploration of the direction of risk. J Psychiatr Res. 2006;40(8):700-8.
214. Kahn-Greene ET, Killgore DB, Kamimori GH, Balkin TJ, Killgore WD. The effects of sleep deprivation on symptoms of psychopathology in healthy adults. Sleep medicine. 2007;8(3):215-21.
215. Riemann D, Voderholzer U. Primary insomnia: a risk factor to develop depression? J Affect Disord. 2003;76(1-3):255-9.
216. Sharma V, Mazmanian D. Sleep loss and postpartum psychosis. Bipolar Disord. 2003;5(2):98-105.
217. Dahl RE, Lewin DS. Pathways to adolescent health sleep regulation and behavior. The Journal of adolescent health : official publication of the Society for Adolescent Medicine. 2002;31(6 Suppl):175-84.
218. Kelman BB. The sleep needs of adolescents. The Journal of school nursing : the official publication of the National Association of School Nurses. 1999;15(3):14-9.
219. Muecke S. Effects of rotating night shifts: literature review. Journal of advanced nursing. 2005;50(4):433-9.
220. Acheson A, Richards JB, de Wit H. Effects of sleep deprivation on impulsive behaviors in men and women. Physiology & behavior. 2007;91(5):579-87.
221. McKenna BS, Dickinson DL, Orff HJ, Drummond SP. The effects of one night of sleep deprivation on known-risk and ambiguous-risk decisions. Journal of sleep research. 2007;16(3):245-52.
222. O'Brien EM, Mindell JA. Sleep and risk-taking behavior in adolescents. Behavioral sleep medicine. 2005;3(3):113-33.
223. Venkatraman V, Chuah YM, Huettel SA, Chee MW. Sleep deprivation elevates expectation of gains and attenuates response to losses following risky decisions. Sleep. 2007;30(5):603-9.
224. Baranski JV, Pigeau RA. Self-monitoring cognitive performance during sleep deprivation: effects of modafinil, d-amphetamine and placebo. Journal of sleep research. 1997;6(2):84-91.

225. Boivin DB, Tremblay GM, James FO. Working on atypical schedules. Sleep medicine. 2007;8(6):578-89.
226. Killgore WD, McBride SA, Killgore DB, Balkin TJ. The effects of caffeine, dextroamphetamine, and modafinil on humor appreciation during sleep deprivation. Sleep. 2006;29(6):841-7.
227. Roehrs T, Roth T. Sleep, sleepiness, sleep disorders and alcohol use and abuse. Sleep medicine reviews. 2001;5(4):287-97.
228. Roehrs T, Roth T. Sleep, sleepiness, and alcohol use. Alcohol research & health : the journal of the National Institute on Alcohol Abuse and Alcoholism. 2001;25(2):101-9.
229. Dinges DF, Pack F, Williams K, Gillen KA, Powell JW, Ott GE, et al. Cumulative sleepiness, mood disturbance, and psychomotor vigilance performance decrements during a week of sleep restricted to 4-5 hours per night. Sleep. 1997;20(4):267-77.
230. Lamond N, Jay SM, Dorrian J, Ferguson SA, Jones C, Dawson D. The dynamics of neurobehavioural recovery following sleep loss. Journal of sleep research. 2007;16(1):33-41.
231. Pilcher JJ, Huffcutt AI. Effects of sleep deprivation on performance: a meta-analysis. Sleep. 1996;19(4):318-26.
232. Chee MW, Chuah LY. Functional neuroimaging insights into how sleep and sleep deprivation affect memory and cognition. Current opinion in neurology. 2008;21(4):417-23.
233. Dworak M, Schierl T, Bruns T, Struder HK. Impact of singular excessive computer game and television exposure on sleep patterns and memory performance of school-aged children. Pediatrics. 2007;120(5):978-85.
234. Goder R, Scharffetter F, Aldenhoff JB, Fritzer G. Visual declarative memory is associated with non-rapid eye movement sleep and sleep cycles in patients with chronic non-restorative sleep. Sleep medicine. 2007;8(5):503-8.
235. Oken BS, Salinsky MC, Elsas SM. Vigilance, alertness, or sustained attention: physiological basis and measurement. Clin Neurophysiol. 2006;117(9):1885-901.
236. Baranski JV, Thompson MM, Lichacz FM, McCann C, Gil V, Pasto L, et al. Effects of sleep loss on team decision making: motivational loss or motivational gain? Human factors. 2007;49(4):646-60.
237. Harrison Y, Horne JA. The impact of sleep deprivation on decision making: a review. Journal of experimental psychology Applied. 2000;6(3):236-49.
238. Killgore WD, Balkin TJ, Wesensten NJ. Impaired decision making following 49 h of sleep deprivation. Journal of sleep research. 2006;15(1):7-13.
239. Killgore WD, Killgore DB, Day LM, Li C, Kamimori GH, Balkin TJ. The effects of 53 hours of sleep deprivation on moral judgment. Sleep. 2007;30(3):345-52.
240. Lucidi F, Russo PM, Mallia L, Devoto A, Lauriola M, Violani C. Sleep-related car crashes: risk perception and decision-making processes in young drivers. Accident; analysis and prevention. 2006;38(2):302-9.
241. Horne JA. Sleep loss and "divergent" thinking ability. Sleep. 1988;11(6):528-36.
242. Jones K, Harrison Y. Frontal lobe function, sleep loss and fragmented sleep. Sleep medicine reviews. 2001;5(6):463-75.
243. Killgore WD, Kahn-Greene ET, Lipizzi EL, Newman RA, Kamimori GH, Balkin TJ. Sleep deprivation reduces perceived emotional intelligence and constructive thinking skills. Sleep medicine. 2008;9(5):517-26.
244. Randazzo AC, Muehlbach MJ, Schweitzer PK, Walsh JK. Cognitive function following acute sleep restriction in children ages 10-14. Sleep. 1998;21(8):861-8.
245. van der Kloet D, Giesbrecht T, Lynn SJ, Merckelbach H, de Zutter A. Sleep normalization and decrease in dissociative experiences: evaluation in an inpatient sample. Journal of abnormal psychology. 2012;121(1):140-50.
246. Basner M, Glatz C, Griefahn B, Penzel T, Samel A. Aircraft noise: effects on macro- and microstructure of sleep. Sleep medicine. 2008;9(4):382-7.
247. Basner M, Muller U, Elmenhorst EM, Kluge G, Griefahn B. Aircraft noise effects on sleep: a systematic comparison of EEG awakenings and automatically detected cardiac activations. Physiological measurement. 2008;29(9):1089-103.
248. Philip P, Akerstedt T. Transport and industrial safety, how are they affected by sleepiness and sleep restriction? Sleep medicine reviews. 2006;10(5):347-56.

249. Pilcher JJ, Lambert BJ, Huffcutt AI. Differential effects of permanent and rotating shifts on self-report sleep length: a meta-analytic review. Sleep. 2000;23(2):155-63.
250. Scott LD, Hwang WT, Rogers AE, Nysse T, Dean GE, Dinges DF. The relationship between nurse work schedules, sleep duration, and drowsy driving. Sleep. 2007;30(12):1801-7.
251. Kundermann B, Krieg JC, Schreiber W, Lautenbacher S. The effect of sleep deprivation on pain. Pain research & management : the journal of the Canadian Pain Society = journal de la societe canadienne pour le traitement de la douleur. 2004;9(1):25-32.
252. Landis CA, Savage MV, Lentz MJ, Brengelmann GL. Sleep deprivation alters body temperature dynamics to mild cooling and heating not sweating threshold in women. Sleep. 1998;21(1):101-8.
253. Roehrs T, Hyde M, Blaisdell B, Greenwald M, Roth T. Sleep loss and REM sleep loss are hyperalgesic. Sleep. 2006;29(2):145-51.
254. Davis S, Mirick DK. Circadian disruption, shift work and the risk of cancer: a summary of the evidence and studies in Seattle. Cancer causes & control : CCC. 2006;17(4):539-45.
255. Hansen J. Risk of breast cancer after night- and shift work: current evidence and ongoing studies in Denmark. Cancer causes & control : CCC. 2006;17(4):531-7.
256. Gangwisch JE, Malaspina D, Boden-Albala B, Heymsfield SB. Inadequate sleep as a risk factor for obesity: analyses of the NHANES I. Sleep. 2005;28(10):1289-96.
257. Knutson KL, Spiegel K, Penev P, Van Cauter E. The metabolic consequences of sleep deprivation. Sleep medicine reviews. 2007;11(3):163-78.
258. Laposky AD, Bass J, Kohsaka A, Turek FW. Sleep and circadian rhythms: key components in the regulation of energy metabolism. FEBS letters. 2008;582(1):142-51.
259. Maemura K, Takeda N, Nagai R. Circadian rhythms in the CNS and peripheral clock disorders: role of the biological clock in cardiovascular diseases. Journal of pharmacological sciences. 2007;103(2):134-8.
260. Yang C, Winkelman JW. Clinical significance of sleep EEG abnormalities in chronic schizophrenia. Schizophr Res. 2006;82(2-3):251-60.
261. Young ME, Bray MS. Potential role for peripheral circadian clock dyssynchrony in the pathogenesis of cardiovascular dysfunction. Sleep medicine. 2007;8(6):656-67.
262. Irwin M. Effects of sleep and sleep loss on immunity and cytokines. Brain, behavior, and immunity. 2002;16(5):503-12.
263. Lorton D, Lubahn CL, Estus C, Millar BA, Carter JL, Wood CA, et al. Bidirectional communication between the brain and the immune system: implications for physiological sleep and disorders with disrupted sleep. Neuroimmunomodulation. 2006;13(5-6):357-74.
264. Kahol K, Leyba MJ, Deka M, Deka V, Mayes S, Smith M, et al. Effect of fatigue on psychomotor and cognitive skills. American journal of surgery. 2008;195(2):195-204.
265. Meerlo P, Sgoifo A, Suchecki D. Restricted and disrupted sleep: effects on autonomic function, neuroendocrine stress systems and stress responsivity. Sleep medicine reviews. 2008;12(3):197-210.
266. Colten HR, Altevogt BM. Sleep Physiology. Sleep Disorders and Sleep Deprivation: An Unmet Public Health Problem. Washington DC: National Academies Press; 2006.
267. Schulz H. Rethinking Sleep Analysis: Comment on the AASM Manual for the Scoring of Sleep and Associated Events. Journal of clinical sleep medicine : JCSM : official publication of the American Academy of Sleep Medicine. 2008;4(2):99-103.
268. Silber MH, Ancoli-Israel S, Bonnet MH, Chokroverty S, Grigg-Damberger MM, Hirshkowitz M, et al. The visual scoring of sleep in adults. Journal of clinical sleep medicine : JCSM : official publication of the American Academy of Sleep Medicine. 2007;3(2):121-31.
269. Aserinsky E, Kleitman N. Regularly occurring periods of eye motility, and concomitant phenomena, during sleep. Science. 1953;118(3062):273-4.
270. Schwartz JRL, Roth T. Neurophysiology of Sleep and Wakefulness: Basic Science and Clinical Implications. Current neuropharmacology. 2008;6(4):367-78.
271. Fuller PM, Gooley JJ, Saper CB. Neurobiology of the sleep-wake cycle: sleep architecture, circadian regulation, and regulatory feedback. J Biol Rhythms. 2006;21(6):482-93.
272. Moruzzi G, Magoun HW. Brain stem reticular formation and activation of the EEG. Electroencephalography and clinical neurophysiology. 1949;1(4):455-73.
273. Starzl TE, Taylor CW, Magoun HW. Ascending conduction in reticular activating system, with special reference to the diencephalon. Journal of neurophysiology. 1951;14(6):461-77.

274. Saper CB, Chou TC, Scammell TE. The sleep switch: hypothalamic control of sleep and wakefulness. Trends in neurosciences. 2001;24(12):726-31.
275. Hallanger AE, Levey AI, Lee HJ, Rye DB, Wainer BH. The origins of cholinergic and other subcortical afferents to the thalamus in the rat. J Comp Neurol. 1987;262(1):105-24.
276. Saper CB, Scammell TE, Lu J. Hypothalamic regulation of sleep and circadian rhythms. Nature. 2005;437(7063):1257-63.
277. McCormick DA. Cholinergic and noradrenergic modulation of thalamocortical processing. Trends in neurosciences. 1989;12(6):215-21.
278. Jones BE. Arousal systems. Frontiers in bioscience : a journal and virtual library. 2003;8:s438-51.
279. Saper CB. Organization of cerebral cortical afferent systems in the rat. II. Hypothalamocortical projections. J Comp Neurol. 1985;237(1):21-46.
280. Aston-Jones G, Bloom FE. Activity of norepinephrine-containing locus coeruleus neurons in behaving rats anticipates fluctuations in the sleep-waking cycle. J Neurosci. 1981;1(8):876-86.
281. Estabrooke IV, McCarthy MT, Ko E, Chou TC, Chemelli RM, Yanagisawa M, et al. Fos expression in orexin neurons varies with behavioral state. J Neurosci. 2001;21(5):1656-62.
282. Mileykovskiy BY, Kiyashchenko LI, Siegel JM. Behavioral correlates of activity in identified hypocretin/orexin neurons. Neuron. 2005;46(5):787-98.
283. Steininger TL, Alam MN, Gong H, Szymusiak R, McGinty D. Sleep-waking discharge of neurons in the posterior lateral hypothalamus of the albino rat. Brain Res. 1999;840(1-2):138-47.
284. Verret L, Goutagny R, Fort P, Cagnon L, Salvert D, Leger L, et al. A role of melanin-concentrating hormone producing neurons in the central regulation of paradoxical sleep. BMC neuroscience. 2003;4:19.
285. Lee MG, Hassani OK, Alonso A, Jones BE. Cholinergic basal forebrain neurons burst with theta during waking and paradoxical sleep. J Neurosci. 2005;25(17):4365-9.
286. Gerashchenko D, Blanco-Centurion C, Greco MA, Shiromani PJ. Effects of lateral hypothalamic lesion with the neurotoxin hypocretin-2-saporin on sleep in Long-Evans rats. Neuroscience. 2003;116(1):223-35.
287. Sherin JE, Shiromani PJ, McCarley RW, Saper CB. Activation of ventrolateral preoptic neurons during sleep. Science. 1996;271(5246):216-9.
288. Gaus SE, Strecker RE, Tate BA, Parker RA, Saper CB. Ventrolateral preoptic nucleus contains sleep-active, galaninergic neurons in multiple mammalian species. Neuroscience. 2002;115(1):285-94.
289. Sherin JE, Elmquist JK, Torrealba F, Saper CB. Innervation of histaminergic tuberomammillary neurons by GABAergic and galaninergic neurons in the ventrolateral preoptic nucleus of the rat. J Neurosci. 1998;18(12):4705-21.
290. Lu J, Greco MA, Shiromani P, Saper CB. Effect of lesions of the ventrolateral preoptic nucleus on NREM and REM sleep. J Neurosci. 2000;20(10):3830-42.
291. Chamberlin NL, Arrigoni E, Chou TC, Scammell TE, Greene RW, Saper CB. Effects of adenosine on gabaergic synaptic inputs to identified ventrolateral preoptic neurons. Neuroscience. 2003;119(4):913-8.
292. Chou TC, Bjorkum AA, Gaus SE, Lu J, Scammell TE, Saper CB. Afferents to the ventrolateral preoptic nucleus. J Neurosci. 2002;22(3):977-90.
293. Gallopin T, Fort P, Eggermann E, Cauli B, Luppi PH, Rossier J, et al. Identification of sleep-promoting neurons in vitro. Nature. 2000;404(6781):992-5.
294. Kohler C, Ericson H, Watanabe T, Polak J, Palay SL, Palay V, et al. Galanin immunoreactivity in hypothalamic neurons: further evidence for multiple chemical messengers in the tuberomammillary nucleus. J Comp Neurol. 1986;250(1):58-64.
295. Schwartz JR, Roth T. Neurophysiology of sleep and wakefulness: basic science and clinical implications. Current neuropharmacology. 2008;6(4):367-78.
296. Achermann P, Borbely AA. Mathematical models of sleep regulation. Frontiers in bioscience : a journal and virtual library. 2003;8:s683-93.
297. Borbely AA, Tobler I. Homeostatic and circadian principles in sleep regulation in the rat. In: McGinty D, editor. Brain mechanisms of sleep. New York: Raven Press; 1985. p. 35-44.
298. Benington JH, Kodali SK, Heller HC. Stimulation of A1 adenosine receptors mimics the electroencephalographic effects of sleep deprivation. Brain Res. 1995;692(1-2):79-85.

299. Scammell TE, Estabrooke IV, McCarthy MT, Chemelli RM, Yanagisawa M, Miller MS, et al. Hypothalamic arousal regions are activated during modafinil-induced wakefulness. J Neurosci. 2000;20(22):8620-8.
300. Strecker RE, Morairty S, Thakkar MM, Porkka-Heiskanen T, Basheer R, Dauphin LJ, et al. Adenosinergic modulation of basal forebrain and preoptic/anterior hypothalamic neuronal activity in the control of behavioral state. Behav Brain Res. 2000;115(2):183-204.
301. Hines DJ, Schmitt LI, Hines RM, Moss SJ, Haydon PG. Antidepressant effects of sleep deprivation require astrocyte-dependent adenosine mediated signaling. Translational psychiatry. 2013;3:e212.
302. Edgar DM, Dement WC, Fuller CA. Effect of SCN lesions on sleep in squirrel monkeys: evidence for opponent processes in sleep-wake regulation. J Neurosci. 1993;13(3):1065-79.
303. Chou TC, Scammell TE, Gooley JJ, Gaus SE, Saper CB, Lu J. Critical role of dorsomedial hypothalamic nucleus in a wide range of behavioral circadian rhythms. J Neurosci. 2003;23(33):10691-702.
304. Dijk DJ, Czeisler CA. Contribution of the circadian pacemaker and the sleep homeostat to sleep propensity, sleep structure, electroencephalographic slow waves, and sleep spindle activity in humans. J Neurosci. 1995;15(5 Pt 1):3526-38.
305. Brown LA, Hasan S, Foster RG, Peirson SN. COMPASS: Continuous Open Mouse Phenotyping of Activity and Sleep Status.
306. Donohue KD, Medonza DC, Crane ER, O'Hara BF. Assessment of a non-invasive high-throughput classifier for behaviours associated with sleep and wake in mice. Biomedical engineering online. 2008;7:14.
307. Fisher SP, Godinho SI, Pothecary CA, Hankins MW, Foster RG, Peirson SN. Rapid assessment of sleep-wake behavior in mice. J Biol Rhythms. 2012;27(1):48-58.
308. Pack AI, Galante RJ, Maislin G, Cater J, Metaxas D, Lu S, et al. Novel method for high-throughput phenotyping of sleep in mice. Physiological genomics. 2007;28(2):232-8.
309. Jud C, Schmutz I, Hampp G, Oster H, Albrecht U. A guideline for analyzing circadian wheel-running behavior in rodents under different lighting conditions. Biological procedures online. 2005;7:101-16.
310. Van Someren EJ, Swaab DF, Colenda CC, Cohen W, McCall WV, Rosenquist PB. Bright light therapy: improved sensitivity to its effects on rest-activity rhythms in Alzheimer patients by application of nonparametric methods. Chronobiology international. 1999;16(4):505-18.
311. Albrecht U, Foster RG. Placing ocular mutants into a functional context: a chronobiological approach. Methods (San Diego, Calif). 2002;28(4):465-77.
312. Savelyev SA, Larsson KC, Johansson AS, Lundkvist GB. Slice preparation, organotypic tissue culturing and luciferase recording of clock gene activity in the suprachiasmatic nucleus. Journal of visualized experiments : JoVE. 2011;(48).
313. Abraham D, Dallmann R, Steinlechner S, Albrecht U, Eichele G, Oster H. Restoration of circadian rhythmicity in circadian clock-deficient mice in constant light. J Biol Rhythms. 2006;21(3):169-76.
314. Qian X, Droste SK, Lightman SL, Reul JM, Linthorst AC. Circadian and ultradian rhythms of free glucocorticoid hormone are highly synchronized between the blood, the subcutaneous tissue, and the brain. Endocrinology. 2012;153(9):4346-53.
315. Franken P, Malafosse A, Tafti M. Genetic variation in EEG activity during sleep in inbred mice. Am J Physiol. 1998;275(4 Pt 2):R1127-37.
316. McShane BB, Galante RJ, Biber M, Jensen ST, Wyner AJ, Pack AI. Assessing REM Sleep in Mice Using Video Data. Sleep. 2012;35(3):433-42.
317. Gonder JC, Laber K. A renewed look at laboratory rodent housing and management. ILAR journal / National Research Council, Institute of Laboratory Animal Resources. 2007;48(1):29-36.
318. Voikar V, Polus A, Vasar E, Rauvala H. Long-term individual housing in C57BL/6J and DBA/2 mice: assessment of behavioral consequences. Genes Brain Behav. 2005;4(4):240-52.
319. Meijer JH, Robbers Y. Wheel running in the wild. Proceedings Biological sciences / The Royal Society. 2014;281(1786).
320. Novak CM, Burghardt PR, Levine JA. The use of a running wheel to measure activity in rodents: relationship to energy balance, general activity, and reward. Neurosci Biobehav Rev. 2012;36(3):1001-14.
321. Sherwin CM. Voluntary wheel running: a review and novel interpretation. Animal behaviour. 1998;56(1):11-27.

322. Tam SK, Pritchett D, Brown LA, Foster RG, Bannerman DM, Peirson SN. Sleep and circadian rhythm disruption and recognition memory in schizophrenia. Methods Enzymol. 2015;552:325-49.
323. Foster RG, Helfrich-Forster C. The regulation of circadian clocks by light in fruitflies and mice. Philos Trans R Soc Lond B Biol Sci. 2001;356(1415):1779-89.
324. Hossain SM, Wong BK, Simpson EM. The dark phase improves genetic discrimination for some high throughput mouse behavioral phenotyping. Genes Brain Behav. 2004;3(3):167-77.
325. Ebihara S, Marks T, Hudson DJ, Menaker M. Genetic control of melatonin synthesis in the pineal gland of the mouse. Science. 1986;231(4737):491-3.
326. Goto M, Oshima I, Tomita T, Ebihara S. Melatonin content of the pineal gland in different mouse strains. Journal of pineal research. 1989;7(2):195-204.
327. Manoach DS, Stickgold R. Does abnormal sleep impair memory consolidation in schizophrenia? Frontiers in human neuroscience. 2009;3:21.
328. Cohrs S. Sleep disturbances in patients with schizophrenia : impact and effect of antipsychotics. CNS drugs. 2008;22(11):939-62.
329. Afonso P, Brissos S, Figueira ML, Paiva T. Schizophrenia patients with predominantly positive symptoms have more disturbed sleep-wake cycles measured by actigraphy. Psychiatry Res. 2011;189(1):62-6.
330. Bromundt V, Koster M, Georgiev-Kill A, Opwis K, Wirz-Justice A, Stoppe G, et al. Sleep-wake cycles and cognitive functioning in schizophrenia. Br J Psychiatry. 2011;198(4):269-76.
331. Myers E, Startup H, Freeman D. Cognitive behavioural treatment of insomnia in individuals with persistent persecutory delusions: a pilot trial. Journal of behavior therapy and experimental psychiatry. 2011;42(3):330-6.
332. Waters F, Sinclair C, Rock D, Jablensky A, Foster RG, Wulff K. Daily variations in sleep-wake patterns and severity of psychopathology: a pilot study in community-dwelling individuals with chronic schizophrenia. Psychiatry Res. 2011;187(1-2):304-6.
333. Benca RM, Obermeyer WH, Thisted RA, Gillin J. Sleep and psychiatric disorders: A meta-analysis. Archives of General Psychiatry. 1992;49(8):651-68.
334. Keshavan MS, Reynolds CF, Kupfer DJ. Electroencephalographic sleep in schizophrenia: A critical review. Comprehensive Psychiatry. 1990;31(1):34-47.
335. Monti JM, BaHammam AS, Pandi-Perumal SR, Bromundt V, Spence DW, Cardinali DP, et al. Sleep and circadian rhythm dysregulation in schizophrenia. Prog Neuropsychopharmacol Biol Psychiatry. 2013;43:209-16.
336. Martin J, Jeste DV, Caliguiri MP, Patterson T, Heaton R, Ancoli-Israel S. Actigraphic estimates of circadian rhythms and sleep/wake in older schizophrenia patients. Schizophr Res. 2001;47(1):77-86.
337. Martin JL, Jeste DV, Ancoli-Israel S. Older schizophrenia patients have more disrupted sleep and circadian rhythms than age-matched comparison subjects. J Psychiatr Res. 2005;39(3):251-9.
338. Wulff K, Joyce E, Middleton B, Dijk DJ, Foster RG. The suitability of actigraphy, diary data, and urinary melatonin profiles for quantitative assessment of sleep disturbances in schizophrenia: a case report. Chronobiology international. 2006;23(1-2):485-95.
339. Wulff K, Porcheret K, Cussans E, Foster RG. Sleep and circadian rhythm disturbances: multiple genes and multiple phenotypes. Current opinion in genetics & development. 2009;19(3):237-46.
340. Goldman M, Tandon R, DeQuardo JR, Taylor SF, Goodson J, McGrath M. Biological predictors of 1-year outcome in schizophrenia in males and females. Schizophr Res. 1996;21(2):65-73.
341. Hofstetter JR, Lysaker PH, Mayeda AR. Quality of sleep in patients with schizophrenia is associated with quality of life and coping. BMC Psychiatry. 2005;5:13.
342. Auslander LA, Jeste DV. Perceptions of problems and needs for service among middle-aged and elderly outpatients with schizophrenia and related psychotic disorders. Community Ment Health J. 2002;38(5):391-402.
343. Wulff K, Gatti S, Wettstein JG, Foster RG. Sleep and circadian rhythm disruption in psychiatric and neurodegenerative disease. Nat Rev Neurosci. 2010;11(8):589-99.
344. Krystal AD, Thakur M, Roth T. Sleep disturbance in psychiatric disorders: effects on function and quality of life in mood disorders, alcoholism, and schizophrenia. Annals of clinical psychiatry : official journal of the American Academy of Clinical Psychiatrists. 2008;20(1):39-46.

345. Ruhrmann S, Schultze-Lutter F, Salokangas RK, Heinimaa M, Linszen D, Dingemans P, et al. Prediction of psychosis in adolescents and young adults at high risk: results from the prospective European prediction of psychosis study. Arch Gen Psychiatry. 2010;67(3):241-51.
346. Monti JM, Monti D. Sleep in schizophrenia patients and the effects of antipsychotic drugs. Sleep medicine reviews. 2004;8(2):133-48.
347. Miller DD. Atypical antipsychotics: sleep, sedation, and efficacy. Primary care companion to the Journal of clinical psychiatry. 2004;6(Suppl 2):3-7.
348. Yamashita H, Mori K, Nagao M, Okamoto Y, Morinobu S, Yamawaki S. Effects of changing from typical to atypical antipsychotic drugs on subjective sleep quality in patients with schizophrenia in a Japanese population. The Journal of clinical psychiatry. 2004;65(11):1525-30.
349. Wulff K, Dijk DJ, Middleton B, Foster RG, Joyce EM. Sleep and circadian rhythm disruption in schizophrenia. Br J Psychiatry. 2012;200(4):308-16.
350. Weinberger DR, Harrison PJ. Schizophrenia. 3rd ed. Oxford: Wiley-Blackwell; 2011.
351. Jeans AF, Oliver PL, Johnson R, Capogna M, Vikman J, Molnar Z, et al. A dominant mutation in Snap25 causes impaired vesicle trafficking, sensorimotor gating, and ataxia in the blind-drunk mouse. Proc Natl Acad Sci U S A. 2007;104(7):2431-6.
352. Oliver PL, Davies KE. Interaction between environmental and genetic factors modulates schizophrenic endophenotypes in the Snap-25 mouse mutant blind-drunk. Hum Mol Genet. 2009;18(23):4576-89.
353. Kumari V, Soni W, Sharma T. Normalization of information processing deficits in schizophrenia with clozapine. Am J Psychiatry. 1999;156(7):1046-51.
354. Oranje B, Van Oel CJ, Gispen-De Wied CC, Verbaten MN, Kahn RS. Effects of typical and atypical antipsychotics on the prepulse inhibition of the startle reflex in patients with schizophrenia. Journal of clinical psychopharmacology. 2002;22(4):359-65.
355. Oliver PL, Sobczyk MV, Maywood ES, Edwards B, Lee S, Livieratos A, et al. Disrupted circadian rhythms in a mouse model of schizophrenia. Current biology : CB. 2012;22(4):314-9.
356. Piggins HD, Cutler DJ. The roles of vasoactive intestinal polypeptide in the mammalian circadian clock. The Journal of endocrinology. 2003;177(1):7-15.
357. Cutler DJ, Haraura M, Reed HE, Shen S, Sheward WJ, Morrison CF, et al. The mouse VPAC2 receptor confers suprachiasmatic nuclei cellular rhythmicity and responsiveness to vasoactive intestinal polypeptide in vitro. Eur J Neurosci. 2003;17(2):197-204.
358. Kallo I, Kalamatianos T, Wiltshire N, Shen S, Sheward WJ, Harmar AJ, et al. Transgenic approach reveals expression of the VPAC2 receptor in phenotypically defined neurons in the mouse suprachiasmatic nucleus and in its efferent target sites. Eur J Neurosci. 2004;19(8):2201-11.
359. Maywood ES, Reddy AB, Wong GK, O'Neill JS, O'Brien JA, McMahon DG, et al. Synchronization and maintenance of timekeeping in suprachiasmatic circadian clock cells by neuropeptidergic signaling. Current biology : CB. 2006;16(6):599-605.
360. Hughes AT, Fahey B, Cutler DJ, Coogan AN, Piggins HD. Aberrant gating of photic input to the suprachiasmatic circadian pacemaker of mice lacking the VPAC2 receptor. J Neurosci. 2004;24(14):3522-6.
361. Hughes AT, Piggins HD. Behavioral responses of Vipr2-/- mice to light. J Biol Rhythms. 2008;23(3):211-9.
362. Chaudhury D, Loh DH, Dragich JM, Hagopian A, Colwell CS. Select cognitive deficits in vasoactive intestinal peptide deficient mice. BMC neuroscience. 2008;9:63.
363. Achim AM, Lefebvre AA, Cellard C, Bouchard RH, Roy MA, Tremblay S. The role of recollection in source memory: an examination of schizophrenia patients and their first-degree relatives. Brain and cognition. 2011;75(2):147-53.
364. Danion JM, Kazes M, Huron C, Karchouni N. Do patients with schizophrenia consciously recollect emotional events better than neutral events? Am J Psychiatry. 2003;160(10):1879-81.
365. Yang K, Trepanier CH, Li H, Beazely MA, Lerner EA, Jackson MF, et al. Vasoactive intestinal peptide acts via multiple signal pathways to regulate hippocampal NMDA receptors and synaptic transmission. Hippocampus. 2009;19(9):779-89.
366. Stefansson H, Sarginson J, Kong A, Yates P, Steinthorsdottir V, Gudfinnsson E, et al. Association of neuregulin 1 with schizophrenia confirmed in a Scottish population. American journal of human genetics. 2003;72(1):83-7.
367. Lin HF, Liu YL, Liu CM, Hung SI, Hwu HG, Chen WJ. Neuregulin 1 gene and variations in perceptual aberration of schizotypal personality in adolescents. Psychological medicine. 2005;35(11):1589-98.

368. Hashimoto R, Straub RE, Weickert CS, Hyde TM, Kleinman JE, Weinberger DR. Expression analysis of neuregulin-1 in the dorsolateral prefrontal cortex in schizophrenia. Mol Psychiatry. 2004;9(3):299-307.
369. Duffy L, Cappas E, Lai D, Boucher AA, Karl T. Cognition in transmembrane domain neuregulin 1 mutant mice. Neuroscience. 2010;170(3):800-7.
370. Pei JC, Liu CM, Lai WS. Distinct phenotypes of new transmembrane-domain neuregulin 1 mutant mice and the rescue effects of valproate on the observed schizophrenia-related cognitive deficits. Front Behav Neurosci. 2014;8:126.
371. Deakin IH, Law AJ, Oliver PL, Schwab MH, Nave KA, Harrison PJ, et al. Behavioural characterization of neuregulin 1 type I overexpressing transgenic mice. Neuroreport. 2009;20(17):1523-8.
372. Deakin IH, Nissen W, Law AJ, Lane T, Kanso R, Schwab MH, et al. Transgenic overexpression of the type I isoform of neuregulin 1 affects working memory and hippocampal oscillations but not long-term potentiation. Cerebral cortex (New York, NY : 1991). 2012;22(7):1520-9.
373. Johnson MA, Devay P, Role LW. The cystine-rich domain of the neuregulin-1 gene (crd-NRG-1) is required for survival of a subset of neurons in the suprachiasmatic nucleus (SCN). Society for Neuroscience; Washington DC2002.
374. Snodgrass-Belt P, Gilbert JL, Davis FC. Central administration of transforming growth factor-alpha and neuregulin-1 suppress active behaviors and cause weight loss in hamsters. Brain Res. 2005;1038(2):171-82.
375. Bernstein HG, Lendeckel U, Bertram I, Bukowska A, Kanakis D, Dobrowolny H, et al. Localization of neuregulin-1alpha (heregulin-alpha) and one of its receptors, ErbB-4 tyrosine kinase, in developing and adult human brain. Brain Res Bull. 2006;69(5):546-59.
376. Sharif A, Duhem-Tonnelle V, Allet C, Baroncini M, Loyens A, Kerr-Conte J, et al. Differential erbB signaling in astrocytes from the cerebral cortex and the hypothalamus of the human brain. Glia. 2009;57(4):362-79.
377. Noble F, Wank SA, Crawley JN, Bradwejn J, Seroogy KB, Hamon M, et al. International Union of Pharmacology. XXI. Structure, distribution, and functions of cholecystokinin receptors. Pharmacological reviews. 1999;51(4):745-81.
378. Bachus SE, Hyde TM, Herman MM, Egan MF, Kleinman JE. Abnormal cholecystokinin mRNA levels in entorhinal cortex of schizophrenics. J Psychiatr Res. 1997;31(2):233-56.
379. Zachrisson O, de Belleroche J, Wendt KR, Hirsch S, Lindefors N. Cholecystokinin CCK(B) receptor mRNA isoforms: expression in schizophrenic brains. Neuroreport. 1999;10(16):3265-8.
380. Tachikawa H, Harada S, Kawanishi Y, Okubo T, Shiraishi H. Novel polymorphisms of the human cholecystokinin A receptor gene: an association analysis with schizophrenia. American journal of medical genetics. 2000;96(2):141-5.
381. Tachikawa H, Harada S, Kawanishi Y, Okubo T, Suzuki T. Linked polymorphisms (-333G>T and -286A>G) in the promoter region of the CCK-A receptor gene may be associated with schizophrenia. Psychiatry Res. 2001;103(2-3):147-55.
382. Toirac I, Sanjuan J, Aguilar EJ, Gonzalez JC, Artigas F, Rivero O, et al. Association between CCK-AR gene and schizophrenia with auditory hallucinations. Psychiatric genetics. 2007;17(2):47-53.
383. Wei J, Hemmings GP. The CCK-A receptor gene possibly associated with auditory hallucinations in schizophrenia. European psychiatry : the journal of the Association of European Psychiatrists. 1999;14(2):67-70.
384. Marshall FH, Barnes S, Hughes J, Woodruff GN, Hunter JC. Cholecystokinin modulates the release of dopamine from the anterior and posterior nucleus accumbens by two different mechanisms. J Neurochem. 1991;56(3):917-22.
385. Kapas L, Obal F, Jr., Alfoldi P, Rubicsek G, Penke B, Obal F. Effects of nocturnal intraperitoneal administration of cholecystokinin in rats: simultaneous increase in sleep, increase in EEG slow-wave activity, reduction of motor activity, suppression of eating, and decrease in brain temperature. Brain Res. 1988;438(1-2):155-64.
386. Tsujino N, Yamanaka A, Ichiki K, Muraki Y, Kilduff TS, Yagami K, et al. Cholecystokinin activates orexin/hypocretin neurons through the cholecystokinin A receptor. J Neurosci. 2005;25(32):7459-69.
387. Shimazoe T, Morita M, Ogiwara S, Kojiya T, Goto J, Kamakura M, et al. Cholecystokinin-A receptors regulate photic input pathways to the circadian clock. Faseb j. 2008;22(5):1479-90.
388. Alhola P, Polo-Kantola P. Sleep deprivation: Impact on cognitive performance. Neuropsychiatric disease and treatment. 2007;3(5):553-67.

389. Horne JA. Human sleep, sleep loss and behaviour. Implications for the prefrontal cortex and psychiatric disorder. Br J Psychiatry. 1993;162:413-9.
390. Petrovsky N, Ettinger U, Hill A, Frenzel L, Meyhofer I, Wagner M, et al. Sleep deprivation disrupts prepulse inhibition and induces psychosis-like symptoms in healthy humans. J Neurosci. 2014;34(27):9134-40.
391. Ratcliff R, Van Dongen HP. Sleep deprivation affects multiple distinct cognitive processes. Psychonomic bulletin & review. 2009;16(4):742-51.
392. Van Dongen HP, Maislin G, Mullington JM, Dinges DF. The cumulative cost of additional wakefulness: dose-response effects on neurobehavioral functions and sleep physiology from chronic sleep restriction and total sleep deprivation. Sleep. 2003;26(2):117-26.
393. Kyriacou CP, Hastings MH. Circadian clocks: genes, sleep, and cognition. Trends in cognitive sciences. 2010;14(6):259-67.
394. Forest G, Poulin J, Daoust A-M, Lussier I, Stip E, Godbout R. Attention and non-REM sleep in neuroleptic-naive persons with schizophrenia and control participants. Psychiatry Research. 2007;149(1–3):33-40.
395. Goder R, Boigs M, Braun S, Friege L, Fritzer G, Aldenhoff JB, et al. Impairment of visuospatial memory is associated with decreased slow wave sleep in schizophrenia. J Psychiatr Res. 2004;38(6):591-9.
396. Goder R, Fritzer G, Gottwald B, Lippmann B, Seeck-Hirschner M, Serafin I, et al. Effects of olanzapine on slow wave sleep, sleep spindles and sleep-related memory consolidation in schizophrenia. Pharmacopsychiatry. 2008;41(3):92-9.
397. Manoach DS, Thakkar KN, Stroynowski E, Ely A, McKinley SK, Wamsley E, et al. Reduced overnight consolidation of procedural learning in chronic medicated schizophrenia is related to specific sleep stages. J Psychiatr Res. 2010;44(2):112-20.
398. Wamsley EJ, Shinn AK, Tucker MA, Ono KE, McKinley SK, Ely AV, et al. The effects of eszopiclone on sleep spindles and memory consolidation in schizophrenia: a randomized placebo-controlled trial. Sleep. 2013;36(9):1369-76.
399. Wamsley EJ, Tucker MA, Shinn AK, Ono KE, McKinley SK, Ely AV, et al. Reduced sleep spindles and spindle coherence in schizophrenia: mechanisms of impaired memory consolidation? Biol Psychiatry. 2012;71(2):154-61.
400. Wulff K, Joyce E. Circadian rhythms and cognition in schizophrenia. Br J Psychiatry. 2011;198(4):250-2.
401. Das M, Das R, Khastgir U, Goswami U. REM sleep latency and neurocognitive dysfunction in schizophrenia. Indian Journal of Psychiatry. 2005;47(3):133-8.
402. Mander BA, Reid KJ, Baron KG, Tjoa T, Parrish TB, Paller KA, et al. EEG measures index neural and cognitive recovery from sleep deprivation. J Neurosci. 2010;30(7):2686-93.
403. Manoach DS, Cain MS, Vangel MG, Khurana A, Goff DC, Stickgold R. A failure of sleep-dependent procedural learning in chronic, medicated schizophrenia. Biol Psychiatry. 2004;56(12):951-6.
404. Ferrarelli F, Huber R, Peterson MJ, Massimini M, Murphy M, Riedner BA, et al. Reduced sleep spindle activity in schizophrenia patients. Am J Psychiatry. 2007;164(3):483-92.
405. Babkoff H, Sing HC, Thorne DR, Genser SG, Hegge FW. Perceptual distortions and hallucinations reported during the course of sleep deprivation. Perceptual and motor skills. 1989;68(3 Pt 1):787-98.
406. Petrovsky N, Ettinger U. Sleep deprivation disrupts prepulse inhibition and induces psychosis-like symptoms in healthy humans. 2014;34(27):9134-40.
407. Freeman D, Pugh K, Vorontsova N, Southgate L. Insomnia and paranoia. Schizophr Res. 2009;108(1-3):280-4.
408. Birchwood M, Smith J, Macmillan F, Hogg B, Prasad R, Harvey C, et al. Predicting relapse in schizophrenia: the development and implementation of an early signs monitoring system using patients and families as observers, a preliminary investigation. Psychological medicine. 1989;19(3):649-56.
409. Freeman D, Stahl D, McManus S, Meltzer H, Brugha T, Wiles N, et al. Insomnia, worry, anxiety and depression as predictors of the occurrence and persistence of paranoid thinking. Social psychiatry and psychiatric epidemiology. 2012;47(8):1195-203.
410. Tekell JL, Hoffmann R, Hendrickse W, Greene RW, Rush AJ, Armitage R. High frequency EEG activity during sleep: characteristics in schizophrenia and depression. Clinical EEG and neuroscience. 2005;36(1):25-35.
411. Murray G, Harvey A. Circadian rhythms and sleep in bipolar disorder. Bipolar Disord. 2010;12(5):459-72.

412. Ganguli R, Reynolds CF, 3rd, Kupfer DJ. Electroencephalographic sleep in young, never-medicated schizophrenics. A comparison with delusional and nondelusional depressives and with healthy controls. Arch Gen Psychiatry. 1987;44(1):36-44.
413. Kato M, Kajimura N, Okuma T, Sekimoto M, Watanabe T, Yamadera H, et al. Association between delta waves during sleep and negative symptoms in schizophrenia. Pharmaco-eeg studies by using structurally different hypnotics. Neuropsychobiology. 1999;39(3):165-72.
414. van Kammen DP, van Kammen WB, Peters J, Goetz K, Neylan T. Decreased slow-wave sleep and enlarged lateral ventricles in schizophrenia. Neuropsychopharmacology. 1988;1(4):265-71.
415. Lunsford-Avery JR, Orr JM, Gupta T, Pelletier-Baldelli A, Dean DJ, Smith Watts AK, et al. Sleep dysfunction and thalamic abnormalities in adolescents at ultra high-risk for psychosis. Schizophr Res. 2013;151(1-3):148-53.
416. Gillin JC, Buchsbaum M, Wu J, Clark C, Bunney W, Jr. Sleep deprivation as a model experimental antidepressant treatment: findings from functional brain imaging. Depression and anxiety. 2001;14(1):37-49.
417. Hemmeter UM, Hemmeter-Spernal J, Krieg JC. Sleep deprivation in depression. Expert review of neurotherapeutics. 2010;10(7):1101-15.
418. Wirz-Justice A, Benedetti F, Berger M, Lam RW, Martiny K, Terman M, et al. Chronotherapeutics (light and wake therapy) in affective disorders. Psychological medicine. 2005;35(7):939-44.
419. Wirz-Justice A, Van den Hoofdakker RH. Sleep deprivation in depression: what do we know, where do we go? Biol Psychiatry. 1999;46(4):445-53.
420. Gujar N, Yoo SS, Hu P, Walker MP. Sleep deprivation amplifies reactivity of brain reward networks, biasing the appraisal of positive emotional experiences. J Neurosci. 2011;31(12):4466-74.
421. Bliss EL, Clark LD, West CD. Studies of sleep deprivation-relationship to schizophrenia. AMA archives of neurology and psychiatry. 1959;81(3):348-59.
422. Dahl RE. The regulation of sleep and arousal: Development and psychopathology. Development and psychopathology. 1996;8(01):3-27.
423. Dubiela FP, Messias MF, Moreira KD, Zanlorenci LH, Grassl C, Filho RF, et al. Reciprocal interactions between MK-801, sleep deprivation and recovery in modulating rat behaviour. Behav Brain Res. 2011;216(1):180-5.
424. Palchykova S, Crestani F, Meerlo P, Tobler I. Sleep deprivation and daily torpor impair object recognition in Djungarian hamsters. Physiology & behavior. 2006;87(1):144-53.
425. Palchykova S, Winsky-Sommerer R, Meerlo P, Durr R, Tobler I. Sleep deprivation impairs object recognition in mice. Neurobiol Learn Mem. 2006;85(3):263-71.
426. Binder S, Baier PC, Molle M, Inostroza M, Born J, Marshall L. Sleep enhances memory consolidation in the hippocampus-dependent object-place recognition task in rats. Neurobiol Learn Mem. 2012;97(2):213-9.
427. Inostroza M, Binder S, Born J. Sleep-dependency of episodic-like memory consolidation in rats. Behav Brain Res. 2013;237:15-22.
428. Hajali V, Sheibani V, Esmaeili-Mahani S, Shabani M. Female rats are more susceptible to the deleterious effects of paradoxical sleep deprivation on cognitive performance. Behav Brain Res. 2012;228(2):311-8.
429. Smith C, Rose GM. Evidence for a paradoxical sleep window for place learning in the Morris water maze. Physiology & behavior. 1996;59(1):93-7.
430. Yang RH, Hu SJ, Wang Y, Zhang WB, Luo WJ, Chen JY. Paradoxical sleep deprivation impairs spatial learning and affects membrane excitability and mitochondrial protein in the hippocampus. Brain Res. 2008;1230:224-32.
431. Youngblood BD, Smagin GN, Elkins PD, Ryan DH, Harris RB. The effects of paradoxical sleep deprivation and valine on spatial learning and brain 5-HT metabolism. Physiology & behavior. 1999;67(5):643-9.
432. Youngblood BD, Zhou J, Smagin GN, Ryan DH, Harris RB. Sleep deprivation by the "flower pot" technique and spatial reference memory. Physiology & behavior. 1997;61(2):249-56.
433. Smith CT, Conway JM, Rose GM. Brief paradoxical sleep deprivation impairs reference, but not working, memory in the radial arm maze task. Neurobiol Learn Mem. 1998;69(2):211-7.
434. Cordova CA, Said BO, McCarley RW, Baxter MG, Chiba AA, Strecker RE. Sleep deprivation in rats produces attentional impairments on a 5-choice serial reaction time task. Sleep. 2006;29(1):69-76.

435. Chang HA, Liu YP, Tung CS, Chang CC, Tzeng NS, Huang SY. Effects of REM sleep deprivation on sensorimotor gating and startle habituation in rats: role of social isolation in early development. Neurosci Lett. 2014;575:63-7.
436. Frau R, Orru M, Puligheddu M, Gessa GL, Mereu G, Marrosu F, et al. Sleep deprivation disrupts prepulse inhibition of the startle reflex: reversal by antipsychotic drugs. The international journal of neuropsychopharmacology / official scientific journal of the Collegium Internationale Neuropsychopharmacologicum (CINP). 2008;11(7):947-55.
437. Liu YP, Tung CS, Chuang CH, Lo SM, Ku YC. Tail-pinch stress and REM sleep deprivation differentially affect sensorimotor gating function in modafinil-treated rats. Behav Brain Res. 2011;219(1):98-104.
438. Lopez-Rodriguez F, Kim J, Poland RE. Total sleep deprivation decreases immobility in the forced-swim test. Neuropsychopharmacology. 2004;29(6):1105-11.
439. Porsolt RD, Anton G, Blavet N, Jalfre M. Behavioural despair in rats: a new model sensitive to antidepressant treatments. Eur J Pharmacol. 1978;47(4):379-91.
440. Ruby NF, Fernandez F, Garrett A, Klima J, Zhang P, Sapolsky R, et al. Spatial memory and long-term object recognition are impaired by circadian arrhythmia and restored by the GABAAAntagonist pentylenetetrazole. PLoS One. 2013;8(8):e72433.
441. Ruby NF, Hwang CE, Wessells C, Fernandez F, Zhang P, Sapolsky R, et al. Hippocampal-dependent learning requires a functional circadian system. Proc Natl Acad Sci U S A. 2008;105(40):15593-8.
442. LeGates TA, Altimus CM, Wang H, Lee HK, Yang S, Zhao H, et al. Aberrant light directly impairs mood and learning through melanopsin-expressing neurons. Nature. 2012;491(7425):594-8.
443. Altimus CM, Guler AD, Villa KL, McNeill DS, Legates TA, Hattar S. Rods-cones and melanopsin detect light and dark to modulate sleep independent of image formation. Proc Natl Acad Sci U S A. 2008;105(50):19998-20003.
444. van der Horst GT, Muijtjens M, Kobayashi K, Takano R, Kanno S, Takao M, et al. Mammalian Cry1 and Cry2 are essential for maintenance of circadian rhythms. Nature. 1999;398(6728):627-30.
445. Vitaterna MH, Selby CP, Todo T, Niwa H, Thompson C, Fruechte EM, et al. Differential regulation of mammalian Period genes and circadian rhythmicity by cryptochromes 1 and 2. Proceedings of the National Academy of Sciences of the United States of America. 1999;96(21):12114-9.
446. De Bundel D, Gangarossa G, Biever A, Bonnefont X, Valjent E. Cognitive dysfunction, elevated anxiety, and reduced cocaine response in circadian clock-deficient cryptochrome knockout mice. Frontiers in Behavioral Neuroscience. 2013;7:152.
447. Kantrowitz JT, Oakman E, Bickel S, Citrome L, Spielman A, Silipo G, et al. The importance of a good night's sleep: an open-label trial of the sodium salt of gamma-hydroxybutyric acid in insomnia associated with schizophrenia. Schizophr Res. 2010;120(1-3):225-6.
448. Freeman D, Startup H, Myers E, Harvey A, Geddes J, Yu LM, et al. The effects of using cognitive behavioural therapy to improve sleep for patients with delusions and hallucinations (the BEST study): study protocol for a randomized controlled trial. Trials. 2013;14:214.
449. Morton AJ, Wood NI, Hastings MH, Hurelbrink C, Barker RA, Maywood ES. Disintegration of the sleep-wake cycle and circadian timing in Huntington's disease. J Neurosci. 2005;25(1):157-63.
450. Cuesta M, Aungier J, Morton AJ. Behavioral therapy reverses circadian deficits in a transgenic mouse model of Huntington's disease. Neurobiol Dis. 2014;63:85-91.
451. Maywood ES, Fraenkel E, McAllister CJ, Wood N, Reddy AB, Hastings MH, et al. Disruption of peripheral circadian timekeeping in a mouse model of Huntington's disease and its restoration by temporally scheduled feeding. J Neurosci. 2010;30(30):10199-204.
452. Skillings EA, Wood NI, Morton AJ. Beneficial effects of environmental enrichment and food entrainment in the R6/2 mouse model of Huntington's disease. Brain and behavior. 2014;4(5):675-86.
453. Pallier PN, Maywood ES, Zheng Z, Chesham JE, Inyushkin AN, Dyball R, et al. Pharmacological imposition of sleep slows cognitive decline and reverses dysregulation of circadian gene expression in a transgenic mouse model of Huntington's disease. J Neurosci. 2007;27(29):7869-78.
454. Pallier PN, Morton AJ. Management of sleep/wake cycles improves cognitive function in a transgenic mouse model of Huntington's disease. Brain Res. 2009;1279:90-8.
455. Cull-Candy S, Brickley S, Farrant M. NMDA receptor subunits: diversity, development and disease. Current opinion in neurobiology. 2001;11(3):327-35.
456. Dumas TC. Developmental regulation of cognitive abilities: modified composition of a molecular switch turns on associative learning. Progress in neurobiology. 2005;76(3):189-211.

457. Monyer H, Burnashev N, Laurie DJ, Sakmann B, Seeburg PH. Developmental and regional expression in the rat brain and functional properties of four NMDA receptors. Neuron. 1994;12(3):529-40.
458. Dingledine R, Borges K, Bowie D, Traynelis SF. The glutamate receptor ion channels. Pharmacological reviews. 1999;51(1):7-61.
459. Llansola M, Sanchez-Perez A, Cauli O, Felipo V. Modulation of NMDA receptors in the cerebellum. 1. Properties of the NMDA receptor that modulate its function. Cerebellum (London, England). 2005;4(3):154-61.
460. Martin SJ, Grimwood PD, Morris RG. Synaptic plasticity and memory: an evaluation of the hypothesis. Annual review of neuroscience. 2000;23:649-711.
461. Silva AJ. Molecular and cellular cognitive studies of the role of synaptic plasticity in memory. Journal of neurobiology. 2003;54(1):224-37.
462. Brown MW, Bashir ZI. Evidence concerning how neurons of the perirhinal cortex may effect familiarity discrimination. Philos Trans R Soc Lond B Biol Sci. 2002;357(1424):1083-95.
463. Griffiths S, Scott H, Glover C, Bienemann A, Ghorbel MT, Uney J, et al. Expression of long-term depression underlies visual recognition memory. Neuron. 2008;58(2):186-94.
464. Sanderson DJ, McHugh SB, Good MA, Sprengel R, Seeburg PH, Rawlins JNP, et al. Spatial working memory deficits in GluA1 AMPA receptor subunit knockout mice reflect impaired short-term habituation: Evidence for Wagner's dual-process memory model. Neuropsychologia. 2010;48(8):2303-15.
465. Warburton EC, Koder T, Cho K, Massey PV, Duguid G, Barker GR, et al. Cholinergic neurotransmission is essential for perirhinal cortical plasticity and recognition memory. Neuron. 2003;38(6):987-96.
466. Labrie V, Duffy S, Wang W, Barger SW, Baker GB, Roder JC. Genetic inactivation of D-amino acid oxidase enhances extinction and reversal learning in mice. Learn Mem. 2009;16(1):28-37.
467. Mothet JP, Parent AT, Wolosker H, Brady RO, Jr., Linden DJ, Ferris CD, et al. D-serine is an endogenous ligand for the glycine site of the N-methyl-D-aspartate receptor. Proc Natl Acad Sci U S A. 2000;97(9):4926-31.
468. Oliet SH, Mothet JP. Regulation of N-methyl-D-aspartate receptors by astrocytic D-serine. Neuroscience. 2009;158(1):275-83.
469. Papouin T, Ladepeche L, Ruel J, Sacchi S, Labasque M, Hanini M, et al. Synaptic and extrasynaptic NMDA receptors are gated by different endogenous coagonists. Cell. 2012;150(3):633-46.
470. Schell MJ, Molliver ME, Snyder SH. D-serine, an endogenous synaptic modulator: localization to astrocytes and glutamate-stimulated release. Proc Natl Acad Sci U S A. 1995;92(9):3948-52.
471. Hashimoto A, Nishikawa T, Oka T, Takahashi K. Endogenous D-serine in rat brain: N-methyl-D-aspartate receptor-related distribution and aging. J Neurochem. 1993;60(2):783-6.
472. Yamanaka M, Miyoshi Y, Ohide H, Hamase K, Konno R. D-Amino acids in the brain and mutant rodents lacking D-amino-acid oxidase activity. Amino Acids. 2012;43(5):1811-21.
473. Schell MJ, Brady RO, Jr., Molliver ME, Snyder SH. D-serine as a neuromodulator: regional and developmental localizations in rat brain glia resemble NMDA receptors. J Neurosci. 1997;17(5):1604-15.
474. Hashimoto A, Kumashiro S, Nishikawa T, Oka T, Takahashi K, Mito T, et al. Embryonic development and postnatal changes in free D-aspartate and D-serine in the human prefrontal cortex. J Neurochem. 1993;61(1):348-51.
475. Bendikov I, Nadri C, Amar S, Panizzutti R, De Miranda J, Wolosker H, et al. A CSF and postmortem brain study of D-serine metabolic parameters in schizophrenia. Schizophr Res. 2007;90(1-3):41-51.
476. Brouwer A, Luykx JJ, van Boxmeer L, Bakker SC, Kahn RS. NMDA-receptor coagonists in serum, plasma, and cerebrospinal fluid of schizophrenia patients: a meta-analysis of case-control studies. Neurosci Biobehav Rev. 2013;37(8):1587-96.
477. Hashimoto K, Engberg G, Shimizu E, Nordin C, Lindstrom LH, Iyo M. Reduced D-serine to total serine ratio in the cerebrospinal fluid of drug naive schizophrenic patients. Prog Neuropsychopharmacol Biol Psychiatry. 2005;29(5):767-9.
478. Hashimoto K, Fukushima T, Shimizu E, Komatsu N, Watanabe H, Shinoda N, et al. Decreased serum levels of D-serine in patients with schizophrenia: evidence in support of the N-methyl-D-aspartate receptor hypofunction hypothesis of schizophrenia. Arch Gen Psychiatry. 2003;60(6):572-6.
479. Yamada K, Ohnishi T, Hashimoto K, Ohba H, Iwayama-Shigeno Y, Toyoshima M, et al. Identification of multiple serine racemase (SRR) mRNA isoforms and genetic analyses of SRR and DAO in schizophrenia and D-serine levels. Biol Psychiatry. 2005;57(12):1493-503.

480. Allen NC, Bagade S, McQueen MB, Ioannidis JP, Kavvoura FK, Khoury MJ, et al. Systematic meta-analyses and field synopsis of genetic association studies in schizophrenia: the SzGene database. Nature genetics. 2008;40(7):827-34.
481. Shi J, Gershon ES, Liu C. Genetic associations with schizophrenia: meta-analyses of 12 candidate genes. Schizophr Res. 2008;104(1-3):96-107.
482. Sun J, Kuo PH, Riley BP, Kendler KS, Zhao Z. Candidate genes for schizophrenia: a survey of association studies and gene ranking. American journal of medical genetics Part B, Neuropsychiatric genetics : the official publication of the International Society of Psychiatric Genetics. 2008;147b(7):1173-81.
483. Roussos P, Giakoumaki SG, Adamaki E, Georgakopoulos A, Robakis NK, Bitsios P. The association of schizophrenia risk D-amino acid oxidase polymorphisms with sensorimotor gating, working memory and personality in healthy males. Neuropsychopharmacology. 2011;36(8):1677-88.
484. Pollegioni L, Piubelli L, Sacchi S, Pilone MS, Molla G. Physiological functions of D-amino acid oxidases: from yeast to humans. Cellular and molecular life sciences : CMLS. 2007;64(11):1373-94.
485. Verrall L, Walker M, Rawlings N, Benzel I, Kew JN, Harrison PJ, et al. d-Amino acid oxidase and serine racemase in human brain: normal distribution and altered expression in schizophrenia. Eur J Neurosci. 2007;26(6):1657-69.
486. Sasabe J, Miyoshi Y, Suzuki M, Mita M, Konno R, Matsuoka M, et al. D-amino acid oxidase controls motoneuron degeneration through D-serine. Proc Natl Acad Sci U S A. 2012;109(2):627-32.
487. Gustafson EC, Morgans CW, Tekmen M, Sullivan SJ, Esguerra M, Konno R, et al. Retinal NMDA receptor function and expression are altered in a mouse lacking D-amino acid oxidase. Journal of neurophysiology. 2013;110(12):2718-26.
488. McBain CJ, Kleckner NW, Wyrick S, Dingledine R. Structural requirements for activation of the glycine coagonist site of N-methyl-D-aspartate receptors expressed in Xenopus oocytes. Molecular pharmacology. 1989;36(4):556-65.
489. Sakata K, Fukushima T, Minje L, Ogurusu T, Taira H, Mishina M, et al. Modulation by L- and D-isoforms of amino acids of the L-glutamate response of N-methyl-D-aspartate receptors. Biochemistry. 1999;38(31):10099-106.
490. Tanii Y, Nishikawa T, Hashimoto A, Takahashi K. Stereoselective antagonism by enantiomers of alanine and serine of phencyclidine-induced hyperactivity, stereotypy and ataxia in the rat. J Pharmacol Exp Ther. 1994;269(3):1040-8.
491. Sacchi S, Bernasconi M, Martineau M, Mothet JP, Ruzzene M, Pilone MS, et al. pLG72 modulates intracellular D-serine levels through its interaction with D-amino acid oxidase: effect on schizophrenia susceptibility. J Biol Chem. 2008;283(32):22244-56.
492. Kvajo M, Dhilla A, Swor DE, Karayiorgou M, Gogos JA. Evidence implicating the candidate schizophrenia/bipolar disorder susceptibility gene G72 in mitochondrial function. Mol Psychiatry. 2008;13(7):685-96.
493. Labrie V, Wong AH, Roder JC. Contributions of the D-serine pathway to schizophrenia. Neuropharmacology. 2012;62(3):1484-503.
494. Burnet PW, Eastwood SL, Bristow GC, Godlewska BR, Sikka P, Walker M, et al. D-amino acid oxidase activity and expression are increased in schizophrenia. Mol Psychiatry. 2008;13(7):658-60.
495. Habl G, Zink M, Petroianu G, Bauer M, Schneider-Axmann T, von Wilmsdorff M, et al. Increased D-amino acid oxidase expression in the bilateral hippocampal CA4 of schizophrenic patients: a post-mortem study. J Neural Transm. 2009;116(12):1657-65.
496. Kapoor R, Lim KSY, Cheng A, Garrick T, Kapoor V. Preliminary evidence for a link between schizophrenia and NMDA–glycine site receptor ligand metabolic enzymes, d-amino acid oxidase (DAAO) and kynurenine aminotransferase-1 (KAT-1). Brain Research. 2006;1106(1):205-10.
497. Madeira C, Freitas ME, Vargas-Lopes C, Wolosker H, Panizzutti R. Increased brain d-amino acid oxidase (DAAO) activity in schizophrenia. Schizophrenia Research. 2008;101(1–3):76-83.
498. Ono K, Shishido Y, Park H, Kawazoe T, Iwana S, Chung S, et al. Potential pathophysiological role of d-amino acid oxidase in schizophrenia: immunohistochemical and in situ hybridization study of the expression in human and rat brain. J Neural Transm. 2009;116(10):1335-47.
499. Almond SL, Fradley RL, Armstrong EJ, Heavens RB, Rutter AR, Newman RJ, et al. Behavioral and biochemical characterization of a mutant mouse strain lacking D-amino acid oxidase activity and its implications for schizophrenia. Mol Cell Neurosci. 2006;32(4):324-34.

500. Panatier A, Theodosis DT, Mothet JP, Touquet B, Pollegioni L, Poulain DA, et al. Glia-derived D-serine controls NMDA receptor activity and synaptic memory. Cell. 2006;125(4):775-84.
501. Wake K, Yamazaki H, Hanzawa S, Konno R, Sakio H, Niwa A, et al. Exaggerated responses to chronic nociceptive stimuli and enhancement of N-methyl-D-aspartate receptor-mediated synaptic transmission in mutant mice lacking D-amino-acid oxidase. Neurosci Lett. 2001;297(1):25-8.
502. Lane HY, Lin CH, Green MF, Hellemann G, Huang CC, Chen PW, et al. Add-on treatment of benzoate for schizophrenia: a randomized, double-blind, placebo-controlled trial of D-amino acid oxidase inhibitor. JAMA Psychiatry. 2013;70(12):1267-75.
503. Lin CH, Chen PK, Chang YC, Chuo LJ, Chen YS, Tsai GE, et al. Benzoate, a D-Amino Acid Oxidase Inhibitor, for the Treatment of Early-Phase Alzheimer Disease: A Randomized, Double-Blind, Placebo-Controlled Trial. Biol Psychiatry. 2013.
504. Heresco-Levy U, Javitt DC, Ebstein R, Vass A, Lichtenberg P, Bar G, et al. D-serine efficacy as add-on pharmacotherapy to risperidone and olanzapine for treatment-refractory schizophrenia. Biol Psychiatry. 2005;57(6):577-85.
505. Kantrowitz JT, Malhotra AK, Cornblatt B, Silipo G, Balla A, Suckow RF, et al. High dose D-serine in the treatment of schizophrenia. Schizophr Res. 2010;121(1-3):125-30.
506. Tsai G, Yang P, Chung LC, Lange N, Coyle JT. D-serine added to antipsychotics for the treatment of schizophrenia. Biol Psychiatry. 1998;44(11):1081-9.
507. Tsai GE, Lin PY. Strategies to enhance N-methyl-D-aspartate receptor-mediated neurotransmission in schizophrenia, a critical review and meta-analysis. Curr Pharm Des. 2010;16(5):522-37.
508. Hashimoto K, Fujita Y, Horio M, Kunitachi S, Iyo M, Ferraris D, et al. Co-administration of a D-amino acid oxidase inhibitor potentiates the efficacy of D-serine in attenuating prepulse inhibition deficits after administration of dizocilpine. Biol Psychiatry. 2009;65(12):1103-6.
509. Carone FA, Ganote CE. D-serine nephrotoxicity. The nature of proteinuria, glucosuria, and aminoaciduria in acute tubular necrosis. Archives of pathology. 1975;99(12):658-62.
510. Ganote CE, Peterson DR, Carone FA. The nature of D-serine--induced nephrotoxicity. Am J Pathol. 1974;77(2):269-82.
511. Morehead RP, Fishman WH, Artom C. The Nephrotoxic Action of DL-Serine as Related to Certain Dietary Factors. The American Journal of Pathology. 1946;22(2):385-93.
512. Konno R, Yamamoto K, Niwa A, Yasumura Y. Presence of D-amino-acid oxidase protein in mutant mice lacking D-amino-acid oxidase activity. The International journal of biochemistry. 1991;23(11):1301-5.
513. Konno R, Yasumura Y. Mouse mutant deficient in D-amino acid oxidase activity. Genetics. 1983;103(2):277-85.
514. Labrie V, Clapcote SJ, Roder JC. Mutant mice with reduced NMDA-NR1 glycine affinity or lack of D-amino acid oxidase function exhibit altered anxiety-like behaviors. Pharmacol Biochem Behav. 2009;91(4):610-20.
515. Hamase K, Konno R, Morikawa A, Zaitsu K. Sensitive determination of D-amino acids in mammals and the effect of D-amino-acid oxidase activity on their amounts. Biological & pharmaceutical bulletin. 2005;28(9):1578-84.
516. Hashimoto A, Nishikawa T, Konno R, Niwa A, Yasumura Y, Oka T, et al. Free D-serine, D-aspartate and D-alanine in central nervous system and serum in mutant mice lacking D-amino acid oxidase. Neurosci Lett. 1993;152(1-2):33-6.
517. Miyoshi Y, Hamase K, Tojo Y, Mita M, Konno R, Zaitsu K. Determination of D-serine and D-alanine in the tissues and physiological fluids of mice with various D-amino-acid oxidase activities using two-dimensional high-performance liquid chromatography with fluorescence detection. Journal of chromatography B, Analytical technologies in the biomedical and life sciences. 2009;877(24):2506-12.
518. Morikawa A, Hamase K, Inoue T, Konno R, Niwa A, Zaitsu K. Determination of free d-aspartic acid, d-serine and d-alanine in the brain of mutant mice lacking d-amino-acid oxidase activity. Journal of Chromatography B: Biomedical Sciences and Applications. 2001;757(1):119-25.
519. Hashimoto A, Yoshikawa M, Niwa A, Konno R. Mice lacking D-amino acid oxidase activity display marked attenuation of stereotypy and ataxia induced by MK-801. Brain Res. 2005;1033(2):210-5.
520. Zhang M, Ballard ME, Basso AM, Bratcher N, Browman KE, Curzon P, et al. Behavioral characterization of a mutant mouse strain lacking D-amino acid oxidase activity. Behav Brain Res. 2011;217(1):81-7.

521. Maekawa M, Watanabe M, Yamaguchi S, Konno R, Hori Y. Spatial learning and long-term potentiation of mutant mice lacking D-amino-acid oxidase. Neurosci Res. 2005;53(1):34-8.
522. Bado P, Madeira C, Vargas-Lopes C, Moulin TC, Wasilewska-Sampaio AP, Maretti L, et al. Effects of low-dose D-serine on recognition and working memory in mice. Psychopharmacology (Berl). 2011;218(3):461-70.
523. Duffy S, Labrie V, Roder JC. D-serine augments NMDA-NR2B receptor-dependent hippocampal long-term depression and spatial reversal learning. Neuropsychopharmacology. 2008;33(5):1004-18.
524. Shimazaki T, Kaku A, Chaki S. D-Serine and a glycine transporter-1 inhibitor enhance social memory in rats. Psychopharmacology (Berl). 2010;209(3):263-70.
525. Hopkins SC, Campbell UC, Heffernan MLR, Spear KL, Jeggo RD, Spanswick DC, et al. Effects of D-amino acid oxidase inhibition on memory performance and long-term potentiation in vivo. Pharmacology Research & Perspectives. 2013;1(1):n/a-n/a.
526. Smith SM, Uslaner JM, Yao L, Mullins CM, Surles NO, Huszar SL, et al. The behavioral and neurochemical effects of a novel D-amino acid oxidase inhibitor compound 8 [4H-thieno [3,2-b]pyrrole-5-carboxylic acid] and D-serine. J Pharmacol Exp Ther. 2009;328(3):921-30.
527. Hashimoto K, Fujita Y, Ishima T, Chaki S, Iyo M. Phencyclidine-induced cognitive deficits in mice are improved by subsequent subchronic administration of the glycine transporter-1 inhibitor NFPS and D-serine. Eur Neuropsychopharmacol. 2008;18(6):414-21.
528. Karasawa J, Hashimoto K, Chaki S. D-Serine and a glycine transporter inhibitor improve MK-801-induced cognitive deficits in a novel object recognition test in rats. Behav Brain Res. 2008;186(1):78-83.
529. Vardigan JD, Huszar SL, McNaughton CH, Hutson PH, Uslaner JM. MK-801 produces a deficit in sucrose preference that is reversed by clozapine, D-serine, and the metabotropic glutamate 5 receptor positive allosteric modulator CDPPB: relevance to negative symptoms associated with schizophrenia? Pharmacol Biochem Behav. 2010;95(2):223-9.
530. Adage T, Trillat AC, Quattropani A, Perrin D, Cavarec L, Shaw J, et al. In vitro and in vivo pharmacological profile of AS057278, a selective d-amino acid oxidase inhibitor with potential anti-psychotic properties. Eur Neuropsychopharmacol. 2008;18(3):200-14.
531. Lipina T, Labrie V, Weiner I, Roder J. Modulators of the glycine site on NMDA receptors, D-serine and ALX 5407, display similar beneficial effects to clozapine in mouse models of schizophrenia. Psychopharmacology (Berl). 2005;179(1):54-67.
532. Kanahara N, Shimizu E, Ohgake S, Fujita Y, Kohno M, Hashimoto T, et al. Glycine and D: -serine, but not D: -cycloserine, attenuate prepulse inhibition deficits induced by NMDA receptor antagonist MK-801. Psychopharmacology (Berl). 2008;198(3):363-74.
533. Zhang Z, Gong N, Wang W, Xu L, Xu TL. Bell-shaped D-serine actions on hippocampal long-term depression and spatial memory retrieval. Cerebral cortex (New York, NY : 1991). 2008;18(10):2391-401.
534. Schweimer JV, Coullon GS, Betts JF, Burnet PW, Engle SJ, Brandon NJ, et al. Increased burst-firing of ventral tegmental area dopaminergic neurons in D-amino acid oxidase knockout mice in vivo. Eur J Neurosci. 2014;40(7):2999-3009.
535. Conn PJ, Pin JP. Pharmacology and functions of metabotropic glutamate receptors. Annual review of pharmacology and toxicology. 1997;37:205-37.
536. Cartmell J, Schoepp DD. Regulation of neurotransmitter release by metabotropic glutamate receptors. J Neurochem. 2000;75(3):889-907.
537. Lovinger DM, McCool BA. Metabotropic glutamate receptor-mediated presynaptic depression at corticostriatal synapses involves mGLuR2 or 3. Journal of neurophysiology. 1995;73(3):1076-83.
538. Winder DG, Conn PJ. Roles of metabotropic glutamate receptors in glial function and glial-neuronal communication. Journal of neuroscience research. 1996;46(2):131-7.
539. Anwyl R. Metabotropic glutamate receptors: electrophysiological properties and role in plasticity. Brain research Brain research reviews. 1999;29(1):83-120.
540. Ohishi H, Shigemoto R, Nakanishi S, Mizuno N. Distribution of the mRNA for a metabotropic glutamate receptor (mGluR3) in the rat brain: an in situ hybridization study. J Comp Neurol. 1993;335(2):252-66.
541. Brandstätter JH, Koulen P, Wässle H. Diversity of glutamate receptors in the mammalian retina. Vision Research. 1998;38(10):1385-97.

542. Hartveit E, Brandstatter JH, Enz R, Wassle H. Expression of the mRNA of seven metabotropic glutamate receptors (mGluR1 to 7) in the rat retina. An in situ hybridization study on tissue sections and isolated cells. Eur J Neurosci. 1995;7(7):1472-83.
543. Koulen P, Malitschek B, Kuhn R, Wassle H, Brandstatter JH. Group II and group III metabotropic glutamate receptors in the rat retina: distributions and developmental expression patterns. Eur J Neurosci. 1996;8(10):2177-87.
544. Makoff A, Volpe F, Lelchuk R, Harrington K, Emson P. Molecular characterization and localization of human metabotropic glutamate receptor type 3. Brain research Molecular brain research. 1996;40(1):55-63.
545. Ohnuma T, Augood SJ, Arai H, McKenna PJ, Emson PC. Expression of the human excitatory amino acid transporter 2 and metabotropic glutamate receptors 3 and 5 in the prefrontal cortex from normal individuals and patients with schizophrenia. Brain research Molecular brain research. 1998;56(1-2):207-17.
546. Moghaddam B, Adams BW. Reversal of phencyclidine effects by a group II metabotropic glutamate receptor agonist in rats. Science. 1998;281(5381):1349-52.
547. Krystal JH, Abi-Saab W, Perry E, D'Souza DC, Liu N, Gueorguieva R, et al. Preliminary evidence of attenuation of the disruptive effects of the NMDA glutamate receptor antagonist, ketamine, on working memory by pretreatment with the group II metabotropic glutamate receptor agonist, LY354740, in healthy human subjects. Psychopharmacology (Berl). 2005;179(1):303-9.
548. de Quervain DJ, Papassotiropoulos A. Identification of a genetic cluster influencing memory performance and hippocampal activity in humans. Proc Natl Acad Sci U S A. 2006;103(11):4270-4.
549. Egan MF, Straub RE, Goldberg TE, Yakub I, Callicott JH, Hariri AR, et al. Variation in GRM3 affects cognition, prefrontal glutamate, and risk for schizophrenia. Proc Natl Acad Sci U S A. 2004;101(34):12604-9.
550. Fallin M D, Lasseter Virginia K, Avramopoulos D, Nicodemus Kristin K, Wolyniec Paula S, McGrath John A, et al. Bipolar I Disorder and Schizophrenia: A 440–Single-Nucleotide Polymorphism Screen of 64 Candidate Genes among Ashkenazi Jewish Case-Parent Trios. American journal of human genetics. 2005;77(6):918-36.
551. Green E, Grozeva D, Norton N, Jones I, Jones L, O'Donovan MC, et al. Variation at GRM3 influences susceptibility to psychotic bipolar disorder. American journal of human genetics. 2006;141:697.
552. Corti C, Crepaldi L, Mion S, Roth AL, Xuereb JH, Ferraguti F. Altered dimerization of metabotropic glutamate receptor 3 in schizophrenia. Biol Psychiatry. 2007;62(7):747-55.
553. Bulenger S, Marullo S, Bouvier M. Emerging role of homo- and heterodimerization in G-protein-coupled receptor biosynthesis and maturation. Trends in pharmacological sciences. 2005;26(3):131-7.
554. Milligan G. G protein-coupled receptor dimerization: function and ligand pharmacology. Molecular pharmacology. 2004;66(1):1-7.
555. Minneman KP. Heterodimerization and surface localization of G protein coupled receptors. Biochemical pharmacology. 2007;73(8):1043-50.
556. Prinster SC, Hague C, Hall RA. Heterodimerization of g protein-coupled receptors: specificity and functional significance. Pharmacological reviews. 2005;57(3):289-98.
557. Patil ST, Zhang L, Martenyi F, Lowe SL, Jackson KA, Andreev BV, et al. Activation of mGlu2/3 receptors as a new approach to treat schizophrenia: a randomized Phase 2 clinical trial. Nature medicine. 2007;13(9):1102-7.
558. Chaki S. Group II metabotropic glutamate receptor agonists as a potential drug for schizophrenia. European Journal of Pharmacology. 2010;639(1–3):59-66.
559. Harrison PJ. Metabotropic glutamate receptor agonists for schizophrenia. Br J Psychiatry. 2008;192(2):86-7.
560. Lyon L, Kew JN, Corti C, Harrison PJ, Burnet PW. Altered hippocampal expression of glutamate receptors and transporters in GRM2 and GRM3 knockout mice. Synapse. 2008;62(11):842-50.
561. Lyon L, Burnet PW, Kew JN, Corti C, Rawlins JN, Lane T, et al. Fractionation of spatial memory in GRM2/3 (mGlu2/mGlu3) double knockout mice reveals a role for group II metabotropic glutamate receptors at the interface between arousal and cognition. Neuropsychopharmacology. 2011;36(13):2616-28.
562. De Filippis B, Lyon L, Taylor A, Lane T, Burnet PW, Harrison PJ, et al. The role of group II metabotropic glutamate receptors in cognition and anxiety: Comparative studies in GRM2, GRM3 and GRM2/3 knockout mice. Neuropharmacology. 2014;89c:19-32.

563. Morishima Y, Miyakawa T, Furuyashiki T, Tanaka Y, Mizuma H, Nakanishi S. Enhanced cocaine responsiveness and impaired motor coordination in metabotropic glutamate receptor subtype 2 knockout mice. Proc Natl Acad Sci U S A. 2005;102(11):4170-5.
564. Yokoi M, Kobayashi K, Manabe T, Takahashi T, Sakaguchi I, Katsuura G, et al. Impairment of hippocampal mossy fiber LTD in mice lacking mGluR2. Science. 1996;273(5275):645-7.
565. Linden AM, Shannon H, Baez M, Yu JL, Koester A, Schoepp DD. Anxiolytic-like activity of the mGLU2/3 receptor agonist LY354740 in the elevated plus maze test is disrupted in metabotropic glutamate receptor 2 and 3 knock-out mice. Psychopharmacology (Berl). 2005;179(1):284-91.
566. Lyon L, Borel M, Carrion M, Kew JN, Corti C, Harrison PJ, et al. Hippocampal mossy fiber long-term depression in Grm2/3 double knockout mice. Synapse. 2011;65(9):945-54.
567. Aultman JM, Moghaddam B. Distinct contributions of glutamate and dopamine receptors to temporal aspects of rodent working memory using a clinically relevant task. Psychopharmacology (Berl). 2001;153(3):353-64.
568. Higgins GA, Ballard TM, Kew JN, Richards JG, Kemp JA, Adam G, et al. Pharmacological manipulation of mGlu2 receptors influences cognitive performance in the rodent. Neuropharmacology. 2004;46(7):907-17.
569. Spinelli S, Ballard T, Gatti-McArthur S, Richards GJ, Kapps M, Woltering T, et al. Effects of the mGluR2/3 agonist LY354740 on computerized tasks of attention and working memory in marmoset monkeys. Psychopharmacology (Berl). 2005;179(1):292-302.
570. Lorrain DS, Baccei CS, Bristow LJ, Anderson JJ, Varney MA. Effects of ketamine and n-methyl-d-aspartate on glutamate and dopamine release in the rat prefrontal cortex: modulation by a group II selective metabotropic glutamate receptor agonist LY379268. Neuroscience. 2003;117(3):697-706.
571. Moghaddam B, Adams B, Verma A, Daly D. Activation of glutamatergic neurotransmission by ketamine: a novel step in the pathway from NMDA receptor blockade to dopaminergic and cognitive disruptions associated with the prefrontal cortex. J Neurosci. 1997;17(8):2921-7.
572. Fell MJ, McKinzie DL, Monn JA, Svensson KA. Group II metabotropic glutamate receptor agonists and positive allosteric modulators as novel treatments for schizophrenia. Neuropharmacology. 2012;62(3):1473-83.
573. Moghaddam B. Targeting metabotropic glutamate receptors for treatment of the cognitive symptoms of schizophrenia. Psychopharmacology. 2004;174(1):39-44.
574. De Filippis B, Lyon L, Taylor A, Lane T, Burnet PW, Harrison PJ, et al. The role of group II metabotropic glutamate receptors in cognition and anxiety: Comparative studies in GRM2-/-, GRM3-/- and GRM2/3-/- knockout mice. Neuropharmacology. 2015;89:19-32.
575. Ahnaou A, Dautzenberg FM, Geys H, Imogai H, Gibelin A, Moechars D, et al. Modulation of group II metabotropic glutamate receptor (mGlu2) elicits common changes in rat and mice sleep-wake architecture. Eur J Pharmacol. 2009;603(1-3):62-72.
576. Ahnaou A, Ver Donck L, Drinkenburg WH. Blockade of the metabotropic glutamate (mGluR2) modulates arousal through vigilance states transitions: evidence from sleep-wake EEG in rodents. Behav Brain Res. 2014;270:56-67.
577. Cid JM, Tresadern G, Vega JA, de Lucas AI, Matesanz E, Iturrino L, et al. Discovery of 3-cyclopropylmethyl-7-(4-phenylpiperidin-1-yl)-8-trifluoromethyl[1,2,4]triazolo[4 ,3-a]pyridine (JNJ-42153605): a positive allosteric modulator of the metabotropic glutamate 2 receptor. J Med Chem. 2012;55(20):8770-89.
578. Dong E, Wellman LL, Yang L, Sanford LD. Effects of microinjections of Group II metabotropic glutamate agents into the amygdala on sleep. Brain Res. 2012;1452:85-95.
579. Feinberg I, Campbell IG, Schoepp DD, Anderson K. The selective group mGlu2/3 receptor agonist LY379268 suppresses REM sleep and fast EEG in the rat. Pharmacol Biochem Behav. 2002;73(2):467-74.
580. Feinberg I, Schoepp DD, Hsieh KC, Darchia N, Campbell IG. The metabotropic glutamate (mGLU)2/3 receptor antagonist LY341495 [2S-2-amino-2-(1S,2S-2-carboxycyclopropyl-1-yl)-3-(xanth-9-yl)propanoic acid] stimulates waking and fast electroencephalogram power and blocks the effects of the mGLU2/3 receptor agonist ly379268 [(-)-2-oxa-4-aminobicyclo[3.1.0]hexane-4,6-dicarboxylate] in rats. J Pharmacol Exp Ther. 2005;312(2):826-33.
581. Fell MJ, Witkin JM, Falcone JF, Katner JS, Perry KW, Hart J, et al. N-(4-((2-(trifluoromethyl)-3-hydroxy-4-(isobutyryl)phenoxy)methyl)benzyl)-1-methy l-1H-imidazole-4-carboxamide (THIIC), a novel metabotropic glutamate 2 potentiator with potential anxiolytic/antidepressant properties: in vivo

profiling suggests a link between behavioral and central nervous system neurochemical changes. J Pharmacol Exp Ther. 2011;336(1):165-77.

582. Lavreysen H, Langlois X, Ahnaou A, Drinkenburg W, te Riele P, Biesmans I, et al. Pharmacological characterization of JNJ-40068782, a new potent, selective, and systemically active positive allosteric modulator of the mGlu2 receptor and its radioligand [3H]JNJ-40068782. J Pharmacol Exp Ther. 2013;346(3):514-27.

583. Lam TT, Abler AS, Kwong JM, Tso MO. N-methyl-D-aspartate (NMDA)--induced apoptosis in rat retina. Investigative ophthalmology & visual science. 1999;40(10):2391-7.

584. Hama Y, Katsuki H, Tochikawa Y, Suminaka C, Kume T, Akaike A. Contribution of endogenous glycine site NMDA agonists to excitotoxic retinal damage in vivo. Neurosci Res. 2006;56(3):279-85.

585. Gray JA, McNaughton N. The Neuropsychology of Anxiety: An Enquiry into the Functions of the Septohippocampal System. Oxford: Oxford University Press; 2000.

586. Bannerman DM, Rawlins JN, McHugh SB, Deacon RM, Yee BK, Bast T, et al. Regional dissociations within the hippocampus--memory and anxiety. Neurosci Biobehav Rev. 2004;28(3):273-83.

587. Bach DR, Guitart-Masip M, Packard PA, Miro J, Falip M, Fuentemilla L, et al. Human hippocampus arbitrates approach-avoidance conflict. Current biology : CB. 2014;24(5):541-7.

588. Bailey KR, Crawley JN. Anxiety-Related Behaviors in Mice. In: Buccafusco JJ, editor. Methods of Behavior Analysis in Neuroscience. 2nd ed2009.

589. O'Connor TM, O'Halloran DJ, Shanahan F. The stress response and the hypothalamic-pituitary-adrenal axis: from molecule to melancholia. QJM : monthly journal of the Association of Physicians. 2000;93(6):323-33.

590. Vreeburg SA, Zitman FG, van Pelt J, Derijk RH, Verhagen JC, van Dyck R, et al. Salivary cortisol levels in persons with and without different anxiety disorders. Psychosomatic medicine. 2010;72(4):340-7.

591. Rais R, Thomas AG, Wozniak K, Wu Y, Jaaro-Peled H, Sawa A, et al. Pharmacokinetics of oral D-serine in D-amino acid oxidase knockout mice. Drug Metab Dispos. 2012;40(11):2067-73.

592. Pilorz V, Steinlechner S, Oster H. Age and oestrus cycle-related changes in glucocorticoid excretion and wheel-running activity in female mice carrying mutations in the circadian clock genes Per1 and Per2. Physiology & behavior. 2009;96(1):57-63.

593. Gibson EJ, Walk RD. The "visual cliff". Scientific American. 1960;202:64-71.

594. Routtenberg A, Glickman SE. Visual Cliff Behavior in Undomesticated Rodents, Land and Aquatic Turtles, and Cats (Panthera). Journal of comparative and physiological psychology. 1964;58:143-6.

595. Routtenberg A, Glickman SE. Visual Cliff Behavior in Albino and Hooded Rats. Journal of comparative and physiological psychology. 1964;58:140-2.

596. Sloane SA, Shea SL, Procter MM, Dewsbury DA. Visual cliff performance in 10 species of muroid rodents. Animal learning & behavior. 1978;6(2):244-8.

597. Walk RD, Gibson EJ, Tighe TJ. Behavior of light- and dark-reared rats on a visual cliff. Science. 1957;126(3263):80-1.

598. Cahill H, Nathans J. The optokinetic reflex as a tool for quantitative analyses of nervous system function in mice: application to genetic and drug-induced variation. PLoS One. 2008;3(4):e2055.

599. Douglas RM, Alam NM, Silver BD, McGill TJ, Tschetter WW, Prusky GT. Independent visual threshold measurements in the two eyes of freely moving rats and mice using a virtual-reality optokinetic system. Visual neuroscience. 2005;22(5):677-84.

600. Deacon RM. The successive alleys test of anxiety in mice and rats. Journal of visualized experiments : JoVE. 2013;(76).

601. Line SJ, Barkus C, Coyle C, Jennings KA, Deacon RM, Lesch KP, et al. Opposing alterations in anxiety and species-typical behaviours in serotonin transporter overexpressor and knockout mice. Eur Neuropsychopharmacol. 2011;21(1):108-16.

602. McHugh SB, Deacon RM, Rawlins JN, Bannerman DM. Amygdala and ventral hippocampus contribute differentially to mechanisms of fear and anxiety. Behav Neurosci. 2004;118(1):63-78.

603. Romero LM, Reed JM. Collecting baseline corticosterone samples in the field: is under 3 min good enough? Comparative Biochemistry and Physiology Part A: Molecular & Integrative Physiology. 2005;140(1):73-9.

604. Prusky GT, West PW, Douglas RM. Behavioral assessment of visual acuity in mice and rats. Vision Res. 2000;40(16):2201-9.

605. Brooks SP, Pask T, Jones L, Dunnett SB. Behavioural profiles of inbred mouse strains used as transgenic backgrounds. II: cognitive tests. Genes Brain Behav. 2005;4(5):307-17.
606. Koike H, Arguello PA, Kvajo M, Karayiorgou M, Gogos JA. Disc1 is mutated in the 129S6/SvEv strain and modulates working memory in mice. Proc Natl Acad Sci U S A. 2006;103(10):3693-7.
607. Molenhuis RT, de Visser L, Bruining H, Kas MJ. Enhancing the value of psychiatric mouse models; differential expression of developmental behavioral and cognitive profiles in four inbred strains of mice. Eur Neuropsychopharmacol. 2014;24(6):945-54.
608. Rodgers RJ, Boullier E, Chatzimichalaki P, Cooper GD, Shorten A. Contrasting phenotypes of C57BL/6JOlaHsd, 129S2/SvHsd and 129/SvEv mice in two exploration-based tests of anxiety-related behaviour. Physiology & behavior. 2002;77(2-3):301-10.
609. Voikar V, Koks S, Vasar E, Rauvala H. Strain and gender differences in the behavior of mouse lines commonly used in transgenic studies. Physiology & behavior. 2001;72(1-2):271-81.
610. Horiike K, Tojo H, Arai R, Nozaki M, Maeda T. D-amino-acid oxidase is confined to the lower brain stem and cerebellum in rat brain: regional differentiation of astrocytes. Brain Res. 1994;652(2):297-303.
611. Bannerman DM, Sprengel R, Sanderson DJ, McHugh SB, Rawlins JN, Monyer H, et al. Hippocampal synaptic plasticity, spatial memory and anxiety. Nat Rev Neurosci. 2014;15(3):181-92.
612. Bannerman DM, Deacon RMJ, Offen S, Friswell J, Grubb M, Rawlins JNP. Double dissociation of function within the hippocampus: Spatial memory and hyponeophagia. Behavioral Neuroscience. 2002;116(5):884-901.
613. Bannerman DM, Grubb M, Deacon RMJ, Yee BK, Feldon J, Rawlins JNP. Ventral hippocampal lesions affect anxiety but not spatial learning. Behavioural Brain Research. 2003;139(1–2):197-213.
614. Bannerman DM, Yee BK, Good MA, Heupel MJ, Iversen SD, Rawlins JNP. Double dissociation of function within the hippocampus: A comparison of dorsal, ventral, and complete hippocampal cytotoxic lesions. Behavioral Neuroscience. 1999;113(6):1170-88.
615. Hock BJ, Bunsey MD. Differential Effects of Dorsal and Ventral Hippocampal Lesions. The Journal of Neuroscience. 1998;18(17):7027-32.
616. Kjelstrup KG, Tuvnes FA, Steffenach H-A, Murison R, Moser EI, Moser M-B. Reduced fear expression after lesions of the ventral hippocampus. Proceedings of the National Academy of Sciences of the United States of America. 2002;99(16):10825-30.
617. Moser E, Moser MB, Andersen P. Spatial learning impairment parallels the magnitude of dorsal hippocampal lesions, but is hardly present following ventral lesions. J Neurosci. 1993;13(9):3916-25.
618. Moser MB, Moser EI, Forrest E, Andersen P, Morris RG. Spatial learning with a minislab in the dorsal hippocampus. Proceedings of the National Academy of Sciences of the United States of America. 1995;92(21):9697-701.
619. Pothuizen HHJ, Zhang W-N, Jongen-Rêlo AL, Feldon J, Yee BK. Dissociation of function between the dorsal and the ventral hippocampus in spatial learning abilities of the rat: a within-subject, within-task comparison of reference and working spatial memory. European Journal of Neuroscience. 2004;19(3):705-12.
620. Bannerman DM, Bus T, Taylor A, Sanderson DJ, Schwarz I, Jensen V, et al. Dissecting spatial knowledge from spatial choice by hippocampal NMDA receptor deletion. Nat Neurosci. 2012;15(8):1153-9.
621. Deacon RM, Bannerman DM, Kirby BP, Croucher A, Rawlins JN. Effects of cytotoxic hippocampal lesions in mice on a cognitive test battery. Behav Brain Res. 2002;133(1):57-68.
622. Reisel D, Bannerman DM, Schmitt WB, Deacon RM, Flint J, Borchardt T, et al. Spatial memory dissociations in mice lacking GluR1. Nat Neurosci. 2002;5(9):868-73.
623. Prut L, Belzung C. The open field as a paradigm to measure the effects of drugs on anxiety-like behaviors: a review. Eur J Pharmacol. 2003;463(1-3):3-33.
624. Roof RL, Stein DG. Gender differences in Morris water maze performance depend on task parameters. Physiology & behavior. 1999;68(1-2):81-6.
625. Morris RGM. Spatial localization does not require the presence of local cues. Learning and Motivation. 1981;12(2):239-60.
626. Swerdlow NR, Geyer MA, Braff DL. Neural circuit regulation of prepulse inhibition of startle in the rat: current knowledge and future challenges. Psychopharmacology (Berl). 2001;156(2-3):194-215.
627. Campbell LE, Hughes M, Budd TW, Cooper G, Fulham WR, Karayanidis F, et al. Primary and secondary neural networks of auditory prepulse inhibition: a functional magnetic resonance imaging study of sensorimotor gating of the human acoustic startle response. Eur J Neurosci. 2007;26(8):2327-33.

628. Kumari V, Antonova E, Geyer MA, Ffytche D, Williams SC, Sharma T. A fMRI investigation of startle gating deficits in schizophrenia patients treated with typical or atypical antipsychotics. The international journal of neuropsychopharmacology / official scientific journal of the Collegium Internationale Neuropsychopharmacologicum (CINP). 2007;10(4):463-77.
629. Kumari V, Antonova E, Zachariah E, Galea A, Aasen I, Ettinger U, et al. Structural brain correlates of prepulse inhibition of the acoustic startle response in healthy humans. Neuroimage. 2005;26(4):1052-8.
630. Kumari V, Gray JA, Geyer MA, ffytche D, Soni W, Mitterschiffthaler MT, et al. Neural correlates of tactile prepulse inhibition: a functional MRI study in normal and schizophrenic subjects. Psychiatry Res. 2003;122(2):99-113.
631. Postma P, Gray JA, Sharma T, Geyer M, Mehrotra R, Das M, et al. A behavioural and functional neuroimaging investigation into the effects of nicotine on sensorimotor gating in healthy subjects and persons with schizophrenia. Psychopharmacology (Berl). 2006;184(3-4):589-99.
632. Powell SB, Zhou X, Geyer MA. Prepulse inhibition and genetic mouse models of schizophrenia. Behav Brain Res. 2009;204(2):282-94.
633. Cadenhead KS, Geyer MA, Braff DL. Impaired startle prepulse inhibition and habituation in patients with schizotypal personality disorder. Am J Psychiatry. 1993;150(12):1862-7.
634. Cadenhead KS, Swerdlow NR, Shafer KM, Diaz M, Braff DL. Modulation of the startle response and startle laterality in relatives of schizophrenic patients and in subjects with schizotypal personality disorder: evidence of inhibitory deficits. Am J Psychiatry. 2000;157(10):1660-8.
635. Quednow BB, Frommann I, Berning J, Kuhn KU, Maier W, Wagner M. Impaired sensorimotor gating of the acoustic startle response in the prodrome of schizophrenia. Biol Psychiatry. 2008;64(9):766-73.
636. Ziermans TB, Schothorst PF, Sprong M, Magnee MJ, van Engeland H, Kemner C. Reduced prepulse inhibition as an early vulnerability marker of the psychosis prodrome in adolescence. Schizophr Res. 2012;134(1):10-5.
637. Thaker GK. Schizophrenia endophenotypes as treatment targets. Expert opinion on therapeutic targets. 2007;11(9):1189-206.
638. Geyer MA, Krebs-Thomson K, Braff DL, Swerdlow NR. Pharmacological studies of prepulse inhibition models of sensorimotor gating deficits in schizophrenia: a decade in review. Psychopharmacology (Berl). 2001;156(2-3):117-54.
639. Olivier B, Leahy C, Mullen T, Paylor R, Groppi VE, Sarnyai Z, et al. The DBA/2J strain and prepulse inhibition of startle: a model system to test antipsychotics? Psychopharmacology (Berl). 2001;156(2-3):284-90.
640. Ouagazzal AM, Jenck F, Moreau JL. Drug-induced potentiation of prepulse inhibition of acoustic startle reflex in mice: a model for detecting antipsychotic activity? Psychopharmacology (Berl). 2001;156(2-3):273-83.
641. Swerdlow NR, Light GA, Cadenhead KS, Sprock J, Hsieh MH, Braff DL. Startle gating deficits in a large cohort of patients with schizophrenia: relationship to medications, symptoms, neurocognition, and level of function. Arch Gen Psychiatry. 2006;63(12):1325-35.
642. Bitsios P, Giakoumaki SG. Relationship of prepulse inhibition of the startle reflex to attentional and executive mechanisms in man. International journal of psychophysiology : official journal of the International Organization of Psychophysiology. 2005;55(2):229-41.
643. Bitsios P, Giakoumaki SG, Theou K, Frangou S. Increased prepulse inhibition of the acoustic startle response is associated with better strategy formation and execution times in healthy males. Neuropsychologia. 2006;44(12):2494-9.
644. Giakoumaki SG, Bitsios P, Frangou S. The level of prepulse inhibition in healthy individuals may index cortical modulation of early information processing. Brain Res. 2006;1078(1):168-70.
645. Karper LP, Freeman GK, Grillon C, Morgan CA, 3rd, Charney DS, Krystal JH. Preliminary evidence of an association between sensorimotor gating and distractibility in psychosis. J Neuropsychiatry Clin Neurosci. 1996;8(1):60-6.
646. Meincke U, Morth D, Voss T, Thelen B, Geyer MA, Gouzoulis-Mayfrank E. Prepulse inhibition of the acoustically evoked startle reflex in patients with an acute schizophrenic psychosis--a longitudinal study. European archives of psychiatry and clinical neuroscience. 2004;254(6):415-21.
647. Perry W, Braff DL. Information-processing deficits and thought disorder in schizophrenia. Am J Psychiatry. 1994;151(3):363-7.
648. Perry W, Geyer MA, Braff DL. Sensorimotor gating and thought disturbance measured in close temporal proximity in schizophrenic patients. Arch Gen Psychiatry. 1999;56(3):277-81.

649. Green MF, Butler PD, Chen Y, Geyer MA, Silverstein S, Wynn JK, et al. Perception measurement in clinical trials of schizophrenia: promising paradigms from CNTRICS. Schizophr Bull. 2009;35(1):163-81.
650. Labrie V, Fukumura R, Rastogi A, Fick LJ, Wang W, Boutros PC, et al. Serine racemase is associated with schizophrenia susceptibility in humans and in a mouse model. Hum Mol Genet. 2009;18(17):3227-43.
651. Quednow BB, Wagner M, Westheide J, Beckmann K, Bliesener N, Maier W, et al. Sensorimotor Gating and Habituation of the Startle Response in Schizophrenic Patients Randomly Treated With Amisulpride or Olanzapine. Biological Psychiatry. 2005;59(6):536-45.
652. Akdag SJ, Nestor PG, O'Donnell BF, Niznikiewicz MA, Shenton ME, McCarley RW. The startle reflex in schizophrenia: habituation and personality correlates. Schizophr Res. 2003;64(2-3):165-73.
653. Braff DL, Grillon C, Geyer MA. Gating and habituation of the startle reflex in schizophrenic patients. Arch Gen Psychiatry. 1992;49(3):206-15.
654. Ufartes R, Schneider T, Mortensen LS, de Juan Romero C, Hentrich K, Knoetgen H, et al. Behavioural and functional characterization of Kv10.1 (Eag1) knockout mice. Hum Mol Genet. 2013;22(11):2247-62.
655. Dulawa SC, Geyer MA. Effects of strain and serotonergic agents on prepulse inhibition and habituation in mice. Neuropharmacology. 2000;39(11):2170-9.
656. Aasen I, Kolli L, Kumari V. Sex effects in prepulse inhibition and facilitation of the acoustic startle response: implications for pharmacological and treatment studies. J Psychopharmacol. 2005;19(1):39-45.
657. Lehmann J, Pryce CR, Feldon J. Sex differences in the acoustic startle response and prepulse inhibition in Wistar rats. Behav Brain Res. 1999;104(1-2):113-7.
658. Csomor PA, Yee BK, Vollenweider FX, Feldon J, Nicolet T, Quednow BB. On the influence of baseline startle reactivity on the indexation of prepulse inhibition. Behav Neurosci. 2008;122(4):885-900.
659. Turner KM, Burne TH. Comprehensive behavioural analysis of Long Evans and Sprague-Dawley rats reveals differential effects of housing conditions on tests relevant to neuropsychiatric disorders. PLoS One. 2014;9(3):e93411.
660. Gogos A, van den Buuse M, Rossell S. Gender differences in prepulse inhibition (PPI) in bipolar disorder: men have reduced PPI, women have increased PPI. The international journal of neuropsychopharmacology / official scientific journal of the Collegium Internationale Neuropsychopharmacologicum (CINP). 2009;12(9):1249-59.
661. Kim B, Kim H, Joo YH, Lim J, Kim CY, Song K. Sex-different association of DAO with schizophrenia in Koreans. Psychiatry Res. 2010;179(2):121-5.
662. Mansbach RS, Geyer MA, Braff DL. Dopaminergic stimulation disrupts sensorimotor gating in the rat. Psychopharmacology (Berl). 1988;94(4):507-14.
663. Swerdlow NR, Braff DL, Masten VL, Geyer MA. Schizophrenic-like sensorimotor gating abnormalities in rats following dopamine infusion into the nucleus accumbens. Psychopharmacology (Berl). 1990;101(3):414-20.
664. Swerdlow NR, Shoemaker JM, Bongiovanni MJ, Neary AC, Tochen LS, Saint Marie RL. Strain differences in the disruption of prepulse inhibition of startle after systemic and intra-accumbens amphetamine administration. Pharmacol Biochem Behav. 2007;87(1):1-10.
665. Swerdlow NR, Stephany N, Shoemaker JM, Ross L, Wasserman LC, Talledo J, et al. Effects of amantadine and bromocriptine on startle and sensorimotor gating: parametric studies and cross-species comparisons. Psychopharmacology (Berl). 2002;164(1):82-92.
666. Swerdlow NR, Stephany N, Wasserman LC, Talledo J, Shoemaker J, Auerbach PP. Amphetamine effects on prepulse inhibition across-species: replication and parametric extension. Neuropsychopharmacology. 2003;28(4):640-50.
667. Zavitsanou K, Cranney J, Richardson R. Dopamine antagonists in the orbital prefrontal cortex reduce prepulse inhibition of the acoustic startle reflex in the rat. Pharmacol Biochem Behav. 1999;63(1):55-61.
668. De Koning MB, Bloemen OJ, Van Duin ED, Booij J, Abel KM, De Haan L, et al. Pre-pulse inhibition and striatal dopamine in subjects at an ultra-high risk for psychosis. J Psychopharmacol. 2014;28(6):553-60.
669. Curzon P, Decker MW. Effects of phencyclidine (PCP) and (+)MK-801 on sensorimotor gating in CD-1 mice. Prog Neuropsychopharmacol Biol Psychiatry. 1998;22(1):129-46.

670. Depoortere R, Perrault G, Sanger DJ. Prepulse inhibition of the startle reflex in rats: effects of compounds acting at various sites on the NMDA receptor complex. Behavioural pharmacology. 1999;10(1):51-62.
671. Yee BK, Chang DL, Feldon J. The Effects of dizocilpine and phencyclidine on prepulse inhibition of the acoustic startle reflex and on prepulse-elicited reactivity in C57BL6 mice. Neuropsychopharmacology. 2004;29(10):1865-77.
672. Bakshi VP, Swerdlow NR, Geyer MA. Clozapine antagonizes phencyclidine-induced deficits in sensorimotor gating of the startle response. J Pharmacol Exp Ther. 1994;271(2):787-94.
673. Keith VA, Mansbach RS, Geyer MA. Failure of haloperidol to block the effects of phencyclidine and dizocilpine on prepulse inhibition of startle. Biol Psychiatry. 1991;30(6):557-66.
674. Yamada S, Harano M, Annoh N, Nakamura K, Tanaka M. Involvement of serotonin 2A receptors in phencyclidine-induced disruption of prepulse inhibition of the acoustic startle in rats. Biol Psychiatry. 1999;46(6):832-8.
675. Abi-Dargham A, Rodenhiser J, Printz D, Zea-Ponce Y, Gil R, Kegeles LS, et al. Increased baseline occupancy of D2 receptors by dopamine in schizophrenia. Proc Natl Acad Sci U S A. 2000;97(14):8104-9.
676. Lane TA, Boerner T, Bannerman DM, Kew JN, Tunbridge EM, Sharp T, et al. Decreased striatal dopamine in group II metabotropic glutamate receptor (mGlu2/mGlu3) double knockout mice. BMC neuroscience. 2013;14:102.
677. Adler CM, Elman I, Weisenfeld N, Kestler L, Pickar D, Breier A. Effects of acute metabolic stress on striatal dopamine release in healthy volunteers. Neuropsychopharmacology. 2000;22(5):545-50.
678. Koepp MJ, Gunn RN, Lawrence AD, Cunningham VJ, Dagher A, Jones T, et al. Evidence for striatal dopamine release during a video game. Nature. 1998;393(6682):266-8.
679. Pruessner JC, Champagne F, Meaney MJ, Dagher A. Dopamine release in response to a psychological stress in humans and its relationship to early life maternal care: a positron emission tomography study using [11C]raclopride. J Neurosci. 2004;24(11):2825-31.
680. Graf EN, Wheeler RA, Baker DA, Ebben AL, Hill JE, McReynolds JR, et al. Corticosterone acts in the nucleus accumbens to enhance dopamine signaling and potentiate reinstatement of cocaine seeking. J Neurosci. 2013;33(29):11800-10.
681. Hu M, Becker JB. Effects of sex and estrogen on behavioral sensitization to cocaine in rats. J Neurosci. 2003;23(2):693-9.
682. Betts JF, Schweimer JV, Burnham KE, Burnet PW, Sharp T, Harrison PJ. D-amino acid oxidase is expressed in the ventral tegmental area and modulates cortical dopamine. Frontiers in synaptic neuroscience. 2014;6:11.
683. Orellana G, Slachevsky A. Executive functioning in schizophrenia. Frontiers in psychiatry. 2013;4:35.
684. Ferraris DV, Tsukamoto T. Recent advances in the discovery of D-amino acid oxidase inhibitors and their therapeutic utility in schizophrenia. Curr Pharm Des. 2011;17(2):103-11.
685. Sacchi S, Rosini E, Pollegioni L, Molla G. D-amino acid oxidase inhibitors as a novel class of drugs for schizophrenia therapy. Curr Pharm Des. 2013;19(14):2499-511.
686. Smith SM, Uslaner JM, Hutson PH. The Therapeutic Potential of D-Amino Acid Oxidase (DAAO) Inhibitors. Open Med Chem J. 2010;4:3-9.
687. Silva RH, Kameda SR, Carvalho RC, Takatsu-Coleman AL, Niigaki ST, Abilio VC, et al. Anxiogenic effect of sleep deprivation in the elevated plus-maze test in mice. Psychopharmacology (Berl). 2004;176(2):115-22.
688. Koehl M, Battle S, Meerlo P. Sex differences in sleep: the response to sleep deprivation and restraint stress in mice. Sleep. 2006;29(9):1224-31.
689. Pawlyk AC, Morrison AR, Ross RJ, Brennan FX. Stress-induced changes in sleep in rodents: models and mechanisms. Neurosci Biobehav Rev. 2008;32(1):99-117.
690. Tang X, Yang L, Sanford LD. Interactions between brief restraint, novelty and footshock stress on subsequent sleep and EEG power in rats. Brain Res. 2007;1142:110-8.
691. Jakubcakova V, Flachskamm C, Landgraf R, Kimura M. Sleep phenotyping in a mouse model of extreme trait anxiety. PLoS One. 2012;7(7):e40625.
692. Griesauer I, Diao W, Ronovsky M, Elbau I, Sartori S, Singewald N, et al. Circadian abnormalities in a mouse model of high trait anxiety and depression. Annals of medicine. 2014;46(3):148-54.

693. Fenzl T, Touma C, Romanowski CP, Ruschel J, Holsboer F, Landgraf R, et al. Sleep disturbances in highly stress reactive mice: modeling endophenotypes of major depression. BMC neuroscience. 2011;12:29.
694. Touma C, Fenzl T, Ruschel J, Palme R, Holsboer F, Kimura M, et al. Rhythmicity in mice selected for extremes in stress reactivity: behavioural, endocrine and sleep changes resembling endophenotypes of major depression. PLoS One. 2009;4(1):e4325.
695. Yang X-L. Characterization of receptors for glutamate and GABA in retinal neurons. Progress in neurobiology. 2004;73(2):127-50.
696. Gustafson EC, Stevens ER, Wolosker H, Miller RF. Endogenous D-serine contributes to NMDA-receptor-mediated light-evoked responses in the vertebrate retina. Journal of neurophysiology. 2007;98(1):122-30.
697. Stevens ER, Esguerra M, Kim PM, Newman EA, Snyder SH, Zahs KR, et al. D-serine and serine racemase are present in the vertebrate retina and contribute to the physiological activation of NMDA receptors. Proc Natl Acad Sci U S A. 2003;100(11):6789-94.
698. Stevens ER, Gustafson EC, Sullivan SJ, Esguerra M, Miller RF. Light-evoked NMDA receptor-mediated currents are reduced by blocking D-serine synthesis in the salamander retina. Neuroreport. 2010;21(4):239-44.
699. Daniels BA, Baldridge WH. d-Serine enhancement of NMDA receptor-mediated calcium increases in rat retinal ganglion cells. J Neurochem. 2010;112(5):1180-9.
700. Beard ME, Davies T, Holloway M, Holtzman E. Peroxisomes in pigment epithelium and Muller cells of amphibian retina possess D-amino acid oxidase as well as catalase. Experimental eye research. 1988;47(6):795-806.
701. St Jules R, Kennard J, Setlik W, Holtzman E. Frog cones as well as Muller cells have peroxisomes. Experimental eye research. 1992;54(1):1-8.
702. Ebling FJ. The role of glutamate in the photic regulation of the suprachiasmatic nucleus. Progress in neurobiology. 1996;50(2-3):109-32.
703. Golombek DA, Rosenstein RE. Physiology of circadian entrainment. Physiological reviews. 2010;90(3):1063-102.
704. Reppert SM, Weaver DR. Molecular analysis of mammalian circadian rhythms. Annual review of physiology. 2001;63:647-76.
705. Colwell CS, Menaker M. NMDA as well as non-NMDA receptor antagonists can prevent the phase-shifting effects of light on the circadian system of the golden hamster. J Biol Rhythms. 1992;7(2):125-36.
706. Abe H, Rusak B, Robertson HA. NMDA and non-NMDA receptor antagonists inhibit photic induction of Fos protein in the hamster suprachiasmatic nucleus. Brain Res Bull. 1992;28(5):831-5.
707. Gompf HS, Fuller PM, Hattar S, Saper CB, Lu J. Impaired Circadian Photosensitivity in Mice Lacking Glutamate Transmission from Retinal Melanopsin Cells. J Biol Rhythms. 2014.
708. Purrier N, Engeland WC, Kofuji P. Mice deficient of glutamatergic signaling from intrinsically photosensitive retinal ganglion cells exhibit abnormal circadian photoentrainment. PLoS One. 2014;9(10):e111449.
709. Abrahamson EE, Moore RY. Suprachiasmatic nucleus in the mouse: retinal innervation, intrinsic organization and efferent projections. Brain Res. 2001;916(1-2):172-91.
710. van den Pol AN. Glutamate and GABA presence and action in the suprachiasmatic nucleus. J Biol Rhythms. 1993;8 Suppl:S11-5.
711. Michel S, Marek R, Vanderleest HT, Vansteensel MJ, Schwartz WJ, Colwell CS, et al. Mechanism of bilateral communication in the suprachiasmatic nucleus. Eur J Neurosci. 2013;37(6):964-71.
712. Csaki A, Kocsis K, Halasz B, Kiss J. Localization of glutamatergic/aspartatergic neurons projecting to the hypothalamic paraventricular nucleus studied by retrograde transport of [3H]D-aspartate autoradiography. Neuroscience. 2000;101(3):637-55.
713. Cui LN, Coderre E, Renaud LP. Glutamate and GABA mediate suprachiasmatic nucleus inputs to spinal-projecting paraventricular neurons. American journal of physiology Regulatory, integrative and comparative physiology. 2001;281(4):R1283-9.
714. Hermes ML, Coderre EM, Buijs RM, Renaud LP. GABA and glutamate mediate rapid neurotransmission from suprachiasmatic nucleus to hypothalamic paraventricular nucleus in rat. The Journal of physiology. 1996;496 (Pt 3):749-57.

715. Perreau-Lenz S, Kalsbeek A, Pevet P, Buijs RM. Glutamatergic clock output stimulates melatonin synthesis at night. Eur J Neurosci. 2004;19(2):318-24.
716. Zhang L, Kolaj M, Renaud LP. Suprachiasmatic nucleus communicates with anterior thalamic paraventricular nucleus neurons via rapid glutamatergic and gabaergic neurotransmission: state-dependent response patterns observed in vitro. Neuroscience. 2006;141(4):2059-66.
717. Vuillez P, Jacob N, Teclemariam-Mesbah R, Van Rossum A, Vivien-Roels B, Pevet P. Effect of NMDA receptor antagonist MK-801 on light-induced Fos expression in the suprachiasmatic nuclei and on melatonin production in the Syrian hamster. Journal of neuroendocrinology. 1998;10(9):671-7.
718. Saint-Mleux B, Bayer L, Eggermann E, Jones BE, Muhlethaler M, Serafin M. Suprachiasmatic modulation of noradrenaline release in the ventrolateral preoptic nucleus. J Neurosci. 2007;27(24):6412-6.
719. Sun X, Rusak B, Semba K. Electrophysiology and pharmacology of projections from the suprachiasmatic nucleus to the ventromedial preoptic area in rat. Neuroscience. 2000;98(4):715-28.
720. Sun X, Whitefield S, Rusak B, Semba K. Electrophysiological analysis of suprachiasmatic nucleus projections to the ventrolateral preoptic area in the rat. Eur J Neurosci. 2001;14(8):1257-74.
721. Lupi D, Oster H, Thompson S, Foster RG. The acute light-induction of sleep is mediated by OPN4-based photoreception. Nat Neurosci. 2008;11(9):1068-73.
722. Tsai JW, Hannibal J, Hagiwara G, Colas D, Ruppert E, Ruby NF, et al. Melanopsin as a sleep modulator: circadian gating of the direct effects of light on sleep and altered sleep homeostasis in Opn4(-/-) mice. PLoS biology. 2009;7(6):e1000125.
723. Kodama T, Lai YY, Siegel JM. Enhanced glutamate release during REM sleep in the rostromedial medulla as measured by in vivo microdialysis. Brain Res. 1998;780(1):178-81.
724. Lopez-Rodriguez F, Medina-Ceja L, Wilson CL, Jhung D, Morales-Villagran A. Changes in extracellular glutamate levels in rat orbitofrontal cortex during sleep and wakefulness. Archives of medical research. 2007;38(1):52-5.
725. Naylor E, Aillon DV, Gabbert S, Harmon H, Johnson DA, Wilson GS, et al. Simultaneous real-time measurement of EEG/EMG and l-glutamate in mice: A biosensor study of neuronal activity during sleep. Journal of Electroanalytical Chemistry. 2011;656(1–2):106-13.
726. Aschoff J. Circadian rhythms in man. Science. 1965;148(3676):1427-32.
727. Albrecht U, Zheng B, Larkin D, Sun ZS, Lee CC. MPer1 and mper2 are essential for normal resetting of the circadian clock. J Biol Rhythms. 2001;16(2):100-4.
728. Mrosovsky N. Masking: history, definitions, and measurement. Chronobiology international. 1999;16(4):415-29.
729. Sokolove PG, Bushell WN. The chi square periodogram: its utility for analysis of circadian rhythms. Journal of theoretical biology. 1978;72(1):131-60.
730. Hasan S, van der Veen DR, Winsky-Sommerer R, Hogben A, Laing EE, Koentgen F, et al. A human sleep homeostasis phenotype in mice expressing a primate-specific PER3 variable-number tandem-repeat coding-region polymorphism. FASEB J. 2014;28(6):2441-54.
731. Fang G, Xia Y, Zhang C, Liu T, Yao D. Optimized single electroencephalogram channel sleep staging in rats. Laboratory animals. 2010;44(4):312-22.
732. Freedman MS, Lucas RJ, Soni B, von Schantz M, Munoz M, David-Gray Z, et al. Regulation of mammalian circadian behavior by non-rod, non-cone, ocular photoreceptors. Science. 1999;284(5413):502-4.
733. Goebel DJ, Aurelia JL, Tai Q, Jojich L, Poosch MS. Immunocytochemical localization of the NMDA-R2A receptor subunit in the cat retina. Brain Res. 1998;808(2):141-54.
734. Fletcher EL, Hack I, Brandstatter JH, Wassle H. Synaptic localization of NMDA receptor subunits in the rat retina. J Comp Neurol. 2000;420(1):98-112.
735. Kalloniatis M, Sun D, Foster L, Haverkamp S, Wassle H. Localization of NMDA receptor subunits and mapping NMDA drive within the mammalian retina. Visual neuroscience. 2004;21(4):587-97.
736. Hughes TE. Are there ionotropic glutamate receptors on the rod bipolar cell of the mouse retina? Visual neuroscience. 1997;14(1):103-9.
737. Lo W, Molloy R, Hughes TE. Ionotropic glutamate receptors in the retina: moving from molecules to circuits. Vision Res. 1998;38(10):1399-410.
738. Muller F, Greferath U, Wassle H, Wisden W, Seeburg P. Glutamate receptor expression in the rat retina. Neurosci Lett. 1992;138(1):179-82.

739. Volpe JJ, Lee G, Laster L, Robinson JC. Regional distribution of isozymes of D-amino-acid oxidase and acetylesterase in developing primate brain. Experimental neurology. 1970;28(1):76-87.
740. Jeffery G. The albino retina: an abnormality that provides insight into normal retinal development. Trends in neurosciences. 1997;20(4):165-9.
741. De Vera Mudry MC, Kronenberg S, Komatsu S, Aguirre GD. Blinded by the light: retinal phototoxicity in the context of safety studies. Toxicologic pathology. 2013;41(6):813-25.
742. Jiang H, Fang J, Wu B, Yin G, Sun L, Qu J, et al. Overexpression of serine racemase in retina and overproduction of D-serine in eyes of streptozotocin-induced diabetic retinopathy. Journal of neuroinflammation. 2011;8:119.
743. Fernandez DC, Sande PH, de Zavalia N, Belforte N, Dorfman D, Casiraghi LP, et al. Effect of experimental diabetic retinopathy on the non-image-forming visual system. Chronobiology international. 2013;30(4):583-97.
744. Vitaterna MH, King DP, Chang AM, Kornhauser JM, Lowrey PL, McDonald JD, et al. Mutagenesis and mapping of a mouse gene, Clock, essential for circadian behavior. Science. 1994;264(5159):719-25.
745. Debruyne JP, Noton E, Lambert CM, Maywood ES, Weaver DR, Reppert SM. A clock shock: mouse CLOCK is not required for circadian oscillator function. Neuron. 2006;50(3):465-77.
746. Ghosh PK, Baskaran N, van den Pol AN. Developmentally regulated gene expression of all eight metabotropic glutamate receptors in hypothalamic suprachiasmatic and arcuate nuclei--a PCR analysis. Brain research Developmental brain research. 1997;102(1):1-12.
747. Haak LL. Metabotropic glutamate receptor modulation of glutamate responses in the suprachiasmatic nucleus. Journal of neurophysiology. 1999;81(3):1308-17.
748. Gannon RL, Millan MJ. Positive and negative modulation of circadian activity rhythms by mGluR5 and mGluR2/3 metabotropic glutamate receptors. Neuropharmacology. 2011;60(2-3):209-15.
749. Haak LL, Albers HE, Mintz EM. Modulation of photic response by the metabotropic glutamate receptor agonist t-ACPD. Brain Res Bull. 2006;71(1-3):97-100.
750. Salt TE, Turner JP. Modulation of sensory inhibition in the ventrobasal thalamus via activation of group II metabotropic glutamate receptors by 2R,4R-aminopyrrolidine-2,4-dicarboxylate. Experimental brain research. 1998;121(2):181-5.
751. Turner JP, Salt TE. Group II and III metabotropic glutamate receptors and the control of the nucleus reticularis thalami input to rat thalamocortical neurones in vitro. Neuroscience. 2003;122(2):459-69.
752. Corti C, Battaglia G, Molinaro G, Riozzi B, Pittaluga A, Corsi M, et al. The use of knock-out mice unravels distinct roles for mGlu2 and mGlu3 metabotropic glutamate receptors in mechanisms of neurodegeneration/neuroprotection. J Neurosci. 2007;27(31):8297-308.
753. Woltering TJ, Wichmann J, Goetschi E, Knoflach F, Ballard TM, Huwyler J, et al. Synthesis and characterization of 1,3-dihydro-benzo[b][1,4]diazepin-2-one derivatives: Part 4. In vivo active potent and selective non-competitive metabotropic glutamate receptor 2/3 antagonists. Bioorg Med Chem Lett. 2010;20(23):6969-74.
754. Jha SK, Ross RJ, Morrison AR. Sleep-related neurons in the central nucleus of the amygdala of rats and their modulation by the dorsal raphe nucleus. Physiology & behavior. 2005;86(4):415-26.
755. Morrison AR, Sanford LD, Ross RJ. The amygdala: a critical modulator of sensory influence on sleep. Biological signals and receptors. 2000;9(6):283-96.
756. Sanford LD, Nassar P, Ross RJ, Schulkin J, Morrison AR. Prolactin microinjections into the amygdalar central nucleus lead to decreased NREM sleep. Sleep research online : SRO. 1998;1(3):109-13.
757. Sanford LD, Parris B, Tang X. GABAergic regulation of the central nucleus of the amygdala: implications for sleep control. Brain Res. 2002;956(2):276-84.
758. Sanford LD, Yang L, Tang X, Dong E, Ross RJ, Morrison AR. Cholinergic regulation of the central nucleus of the amygdala in rats: effects of local microinjections of cholinomimetics and cholinergic antagonists on arousal and sleep. Neuroscience. 2006;141(4):2167-76.
759. Tang X, Yang L, Liu X, Sanford LD. Influence of tetrodotoxin inactivation of the central nucleus of the amygdala on sleep and arousal. Sleep. 2005;28(8):923-30.
760. Gu G, Lorrain DS, Wei H, Cole RL, Zhang X, Daggett LP, et al. Distribution of metabotropic glutamate 2 and 3 receptors in the rat forebrain: Implication in emotional responses and central disinhibition. Brain Res. 2008;1197:47-62.
761. Tamaru Y, Nomura S, Mizuno N, Shigemoto R. Distribution of metabotropic glutamate receptor mGluR3 in the mouse CNS: differential location relative to pre- and postsynaptic sites. Neuroscience. 2001;106(3):481-503.

762. Nathan PJ, Burrows GD, Norman TR. Melatonin sensitivity to dim white light in affective disorders. Neuropsychopharmacology. 1999;21(3):408-13.
763. Greenwood BN, Foley TE, Le TV, Strong PV, Loughridge AB, Day HE, et al. Long-term voluntary wheel running is rewarding and produces plasticity in the mesolimbic reward pathway. Behav Brain Res. 2011;217(2):354-62.
764. Ikemoto S. Dopamine reward circuitry: two projection systems from the ventral midbrain to the nucleus accumbens-olfactory tubercle complex. Brain research reviews. 2007;56(1):27-78.
765. Lammel S, Lim BK, Ran C, Huang KW, Betley MJ, Tye KM, et al. Input-specific control of reward and aversion in the ventral tegmental area. Nature. 2012;491(7423):212-7.
766. Barkus C, McHugh SB, Sprengel R, Seeburg PH, Rawlins JN, Bannerman DM. Hippocampal NMDA receptors and anxiety: at the interface between cognition and emotion. Eur J Pharmacol. 2010;626(1):49-56.
767. Niewoehner B, Single FN, Hvalby O, Jensen V, Meyer zum Alten Borgloh S, Seeburg PH, et al. Impaired spatial working memory but spared spatial reference memory following functional loss of NMDA receptors in the dentate gyrus. Eur J Neurosci. 2007;25(3):837-46.
768. Aggleton JP. Looking beyond the hippocampus: old and new neurological targets for understanding memory disorders. Proceedings Biological sciences / The Royal Society. 2014;281(1786).
769. Aggleton JP, Brown MW. Episodic memory, amnesia, and the hippocampal-anterior thalamic axis. The Behavioral and brain sciences. 1999;22(3):425-44; discussion 44-89.
770. Aggleton JP, Brown MW. Interleaving brain systems for episodic and recognition memory. Trends in cognitive sciences. 2006;10(10):455-63.
771. Aggleton JP, O'Mara SM, Vann SD, Wright NF, Tsanov M, Erichsen JT. Hippocampal-anterior thalamic pathways for memory: uncovering a network of direct and indirect actions. Eur J Neurosci. 2010;31(12):2292-307.
772. Scott GA, Mtetwa M, Lehmann H. Novel odour recognition memory is independent of the hippocampus in rats. Experimental brain research. 2013;224(2):199-209.
773. Lipska BK, Swerdlow NR, Geyer MA, Jaskiw GE, Braff DL, Weinberger DR. Neonatal excitotoxic hippocampal damage in rats causes post-pubertal changes in prepulse inhibition of startle and its disruption by apomorphine. Psychopharmacology (Berl). 1995;122(1):35-43.
774. Swerdlow NR, Light GA, Breier MR, Shoemaker JM, Saint Marie RL, Neary AC, et al. Sensory and sensorimotor gating deficits after neonatal ventral hippocampal lesions in rats. Developmental neuroscience. 2012;34(2-3):240-9.
775. Bast T, Zhang WN, Heidbreder C, Feldon J. Hyperactivity and disruption of prepulse inhibition induced by N-methyl-D-aspartate stimulation of the ventral hippocampus and the effects of pretreatment with haloperidol and clozapine. Neuroscience. 2001;103(2):325-35.
776. Klarner A, Koch M, Schnitzler HU. Induction of Fos-protein in the forebrain and disruption of sensorimotor gating following N-methyl-D-aspartate infusion into the ventral hippocampus of the rat. Neuroscience. 1998;84(2):443-52.
777. Swerdlow NR, Hanlon FM, Henning L, Kim YK, Gaudet I, Halim ND. Regulation of sensorimotor gating in rats by hippocampal NMDA: anatomical localization. Brain Res. 2001;898(2):195-203.
778. Swerdlow NR, Shoemaker JM, Noh HR, Ma L, Gaudet I, Munson M, et al. The ventral hippocampal regulation of prepulse inhibition and its disruption by apomorphine in rats are not mediated via the fornix. Neuroscience. 2004;123(3):675-85.
779. Zhang W, Pouzet B, Jongen-Relo AL, Weiner I, Feldon J. Disruption of prepulse inhibition following N-methyl-D-aspartate infusion into the ventral hippocampus is antagonized by clozapine but not by haloperidol: a possible model for the screening of atypical antipsychotics. Neuroreport. 1999;10(12):2533-8.
780. Wan FJ, Caine SB, Swerdlow NR. The ventral subiculum modulation of prepulse inhibition is not mediated via dopamine D2 or nucleus accumbens non-NMDA glutamate receptor activity. Eur J Pharmacol. 1996;314(1-2):9-18.
781. Pouzet B, Feldon J, Veenman CL, Yee BK, Richmond M, Nicholas J, et al. The effects of hippocampal and fimbria-fornix lesions on prepulse inhibition. Behav Neurosci. 1999;113(5):968-81.
782. Howland JG, MacKenzie EM, Yim TT, Taepavarapruk P, Phillips AG. Electrical stimulation of the hippocampus disrupts prepulse inhibition in rats: frequency- and site-dependent effects. Behav Brain Res. 2004;152(2):187-97.

783. Wagner AR. Priming in STM: An information processing mechanism for self-generated or retrieval-generated depression in performance. In: Tighe TJ, Leaton RN, editors. Habituation: Perspectives from child development, animal behavior, and neurophysiology. Hillsdale, NJ: Lawrence Erlbaum Associates; 1976. p. 95-128.
784. Wagner AR. SOP: A model of automatic memory processing in animal behavior. . In: Spear NE, Miller RR, editors. Information processing in animals: Memory mechanisms Hillsdale, NJ: Lawrence Erlbaum Associates; 1981. p. 5-47.
785. Desmond JE, Fiez JA. Neuroimaging studies of the cerebellum: language, learning and memory. Trends in cognitive sciences. 1998;2(9):355-62.
786. Leiner HC, Leiner AL, Dow RS. Cognitive and language functions of the human cerebellum. Trends in neurosciences. 1993;16(11):444-7.
787. Schmahmann JD, Sherman JC. The cerebellar cognitive affective syndrome. Brain : a journal of neurology. 1998;121 (Pt 4):561-79.
788. Watson PJ. Nonmotor functions of the cerebellum. Psychological bulletin. 1978;85(5):944-67.
789. Andreasen NC, O'Leary DS, Cizadlo T, Arndt S, Rezai K, Ponto LL, et al. Schizophrenia and cognitive dysmetria: a positron-emission tomography study of dysfunctional prefrontal-thalamic-cerebellar circuitry. Proc Natl Acad Sci U S A. 1996;93(18):9985-90.
790. Andreasen NC, Paradiso S, O'Leary DS. "Cognitive dysmetria" as an integrative theory of schizophrenia: a dysfunction in cortical-subcortical-cerebellar circuitry? Schizophr Bull. 1998;24(2):203-18.
791. Eastwood SL, Law AJ, Everall IP, Harrison PJ. The axonal chemorepellant semaphorin 3A is increased in the cerebellum in schizophrenia and may contribute to its synaptic pathology. Mol Psychiatry. 2003;8(2):148-55.
792. Katsetos CD, Hyde TM, Herman MM. Neuropathology of the cerebellum in schizophrenia--an update: 1996 and future directions. Biol Psychiatry. 1997;42(3):213-24.
793. Konarski JZ, McIntyre RS, Grupp LA, Kennedy SH. Is the cerebellum relevant in the circuitry of neuropsychiatric disorders? Journal of Psychiatry and Neuroscience. 2005;30(3):178-86.
794. Picard H, Amado I, Mouchet-Mages S, Olie JP, Krebs MO. The role of the cerebellum in schizophrenia: an update of clinical, cognitive, and functional evidences. Schizophr Bull. 2008;34(1):155-72.
795. Burnet PW, Anderson PN, Chen L, Nikiforova N, Harrison PJ, Wood MJ. D-amino acid oxidase knockdown in the mouse cerebellum reduces NR2A mRNA. Mol Cell Neurosci. 2011;46(1):167-75.
796. Pantelis C, Wood SJ, Proffitt TM, Testa R, Mahony K, Brewer WJ, et al. Attentional set-shifting ability in first-episode and established schizophrenia: Relationship to working memory. Schizophrenia Research. 2009;112(1–3):104-13.
797. Tsai GE, Yang P, Chang Y-C, Chong M-Y. D-Alanine Added to Antipsychotics for the Treatment of Schizophrenia. Biological Psychiatry. 2006;59(3):230-4.
798. Gazzaley AH, Weiland NG, McEwen BS, Morrison JH. Differential regulation of NMDAR1 mRNA and protein by estradiol in the rat hippocampus. J Neurosci. 1996;16(21):6830-8.
799. Gore AC. Gonadotropin-releasing hormone neurons, NMDA receptors, and their regulation by steroid hormones across the reproductive life cycle. Brain research Brain research reviews. 2001;37(1-3):235-48.
800. Gould E, Woolley CS, Frankfurt M, McEwen BS. Gonadal steroids regulate dendritic spine density in hippocampal pyramidal cells in adulthood. J Neurosci. 1990;10(4):1286-91.
801. Schwarz JM, Liang SL, Thompson SM, McCarthy MM. Estradiol induces hypothalamic dendritic spines by enhancing glutamate release: a mechanism for organizational sex differences. Neuron. 2008;58(4):584-98.
802. Woolley CS, McEwen BS. Estradiol regulates hippocampal dendritic spine density via an N-methyl-D-aspartate receptor-dependent mechanism. J Neurosci. 1994;14(12):7680-7.
803. Orellana G, Slachevsky A. Executive Functioning in Schizophrenia. Frontiers in psychiatry. 2013;4:35.
804. Wobrock T, Ecker UK, Scherk H, Schneider-Axmann T, Falkai P, Gruber O. Cognitive impairment of executive function as a core symptom of schizophrenia. The world journal of biological psychiatry : the official journal of the World Federation of Societies of Biological Psychiatry. 2009;10(4 Pt 2):442-51.
805. Balcombe JP, Barnard ND, Sandusky C. Laboratory routines cause animal stress. Contemporary topics in laboratory animal science / American Association for Laboratory Animal Science. 2004;43(6):42-51.
806. Meijer MK, Spruijt BM, van Zutphen LF, Baumans V. Effect of restraint and injection methods on heart rate and body temperature in mice. Laboratory animals. 2006;40(4):382-91.

807. Harrison FE, Hosseini AH, McDonald MP. Endogenous anxiety and stress responses in water maze and Barnes maze spatial memory tasks. Behav Brain Res. 2009;198(1):247-51.
808. Sanford LD, Yang L, Wellman LL. Telemetry in mice: applications in studies of stress and anxiety disorders. In: Gould TD, editor. Mood and Anxiety Related Phenotypes in Mice. Neuromethods: Human Press, New York; 2011. p. 43-60.
809. Harvey AG, Talbot LS, Gershon A. Sleep Disturbance in Bipolar Disorder Across the Lifespan. Clinical psychology : a publication of the Division of Clinical Psychology of the American Psychological Association. 2009;16(2):256-77.
810. Kew JN, Kemp JA. Ionotropic and metabotropic glutamate receptor structure and pharmacology. Psychopharmacology (Berl). 2005;179(1):4-29.
811. Cohen RA. Yerkes–Dodson Law. In: Kreutzer J, DeLuca J, Caplan B, editors. Encyclopedia of Clinical Neuropsychology. New York: Springer; 2011. p. 2737-8.
812. Bohlin G, Kjellberg A. Self-reported arousal during sleep deprivation and its relation to performance and physiological variables. Scandinavian Journal of Psychology. 1973;14(1):78-86.
813. Horne JA. A review of the biological effects of total sleep deprivation in man. Biological Psychology. 1978;7(1–2):55-102.
814. Van den Hoofdakker RH, Bouhuys AL, Beersma DGM. The effects of sleep deprivation and sleep on depressive mood and subjective arousal. Biological Psychiatry. 1989;26(7):733-6.
815. Wilkinson RT. Sleep, arousal and performance. In: Broughton R, Ogilvie R, editors. The measurement of sleepiness. Boston: Birkhauser; 1992. p. 254-65.
816. Goeldner C, Ballard TM, Knoflach F, Wichmann J, Gatti S, Umbricht D. Cognitive impairment in major depression and the mGlu2 receptor as a therapeutic target. Neuropharmacology. 2013;64:337-46.
817. Bradshaw NJ, Porteous DJ. DISC1-binding proteins in neural development, signalling and schizophrenia. Neuropharmacology. 2012;62(3):1230-41.
818. Leucht S, Kissling W, McGrath J. Lithium for schizophrenia revisited: a systematic review and meta-analysis of randomized controlled trials. The Journal of clinical psychiatry. 2004;65(2):177-86.
819. Cross DA, Alessi DR, Cohen P, Andjelkovich M, Hemmings BA. Inhibition of glycogen synthase kinase-3 by insulin mediated by protein kinase B. Nature. 1995;378(6559):785-9.
820. Iitaka C, Miyazaki K, Akaike T, Ishida N. A role for glycogen synthase kinase-3beta in the mammalian circadian clock. J Biol Chem. 2005;280(33):29397-402.
821. Martinek S, Inonog S, Manoukian AS, Young MW. A role for the segment polarity gene shaggy/GSK-3 in the Drosophila circadian clock. Cell. 2001;105(6):769-79.
822. Yin L, Wang J, Klein PS, Lazar MA. Nuclear receptor Rev-erbalpha is a critical lithium-sensitive component of the circadian clock. Science. 2006;311(5763):1002-5.
823. Grimes CA, Jope RS. CREB DNA binding activity is inhibited by glycogen synthase kinase-3 beta and facilitated by lithium. J Neurochem. 2001;78(6):1219-32.
824. Lee B, Li A, Hansen KF, Cao R, Yoon JH, Obrietan K. CREB influences timing and entrainment of the SCN circadian clock. J Biol Rhythms. 2010;25(6):410-20.
825. Barad M, Bourtchouladze R, Winder DG, Golan H, Kandel E. Rolipram, a type IV-specific phosphodiesterase inhibitor, facilitates the establishment of long-lasting long-term potentiation and improves memory. Proc Natl Acad Sci U S A. 1998;95(25):15020-5.
826. Davis JA, Gould TJ. Rolipram attenuates MK-801-induced deficits in latent inhibition. Behav Neurosci. 2005;119(2):595-602.
827. Zhang HT, Zhao Y, Huang Y, Dorairaj NR, Chandler LJ, O'Donnell JM. Inhibition of the phosphodiesterase 4 (PDE4) enzyme reverses memory deficits produced by infusion of the MEK inhibitor U0126 into the CA1 subregion of the rat hippocampus. Neuropsychopharmacology. 2004;29(8):1432-9.
828. O'Neill JS, Reddy AB. The essential role of cAMP/Ca2+ signalling in mammalian circadian timekeeping. Biochemical Society transactions. 2012;40(1):44-50.
829. Gottlieb DJ, O'Connor GT, Wilk JB. Genome-wide association of sleep and circadian phenotypes. BMC medical genetics. 2007;8 Suppl 1:S9.
830. Duffield GE, Watson NP, Mantani A, Peirson SN, Robles-Murguia M, Loros JJ, et al. A role for Id2 in regulating photic entrainment of the mammalian circadian system. Current biology : CB. 2009;19(4):297-304.

831. Grossman MH, Emanuel BS, Budarf ML. Chromosomal mapping of the human catechol-O-methyltransferase gene to 22q11.1----q11.2. Genomics. 1992;12(4):822-5.
832. Bassett AS, Chow EW, AbdelMalik P, Gheorghiu M, Husted J, Weksberg R. The schizophrenia phenotype in 22q11 deletion syndrome. Am J Psychiatry. 2003;160(9):1580-6.
833. Quednow BB, Schmechtig A, Ettinger U, Petrovsky N, Collier DA, Vollenweider FX, et al. Sensorimotor Gating Depends on Polymorphisms of the Serotonin-2A Receptor and Catechol-O-Methyltransferase, but Not on Neuregulin-1 Arg38Gln Genotype: A Replication Study. Biological Psychiatry. 2009;66(6):614-20.
834. Papaleo F, Crawley JN, Song J, Lipska BK, Pickel J, Weinberger DR, et al. Genetic dissection of the role of catechol-O-methyltransferase in cognition and stress reactivity in mice. J Neurosci. 2008;28(35):8709-23.
835. Risbrough V, Ji B, Hauger R, Zhou X. Generation and characterization of humanized mice carrying COMT158 Met/Val alleles. Neuropsychopharmacology. 2014;39(8):1823-32.
836. Tucci V, Lassi G, Kas MJ. Current understanding of the interplay between catechol-O-methyltransferase genetic variants, sleep, brain development and cognitive performance in schizophrenia. CNS & neurological disorders drug targets. 2012;11(3):292-8.
837. Gruber R, Grizenko N, Schwartz G, Ben Amor L, Gauthier J, de Guzman R, et al. Sleep and COMT polymorphism in ADHD children: preliminary actigraphic data. Journal of the American Academy of Child and Adolescent Psychiatry. 2006;45(8):982-9.
838. Bodenmann S, Rusterholz T, Durr R, Stoll C, Bachmann V, Geissler E, et al. The functional Val158Met polymorphism of COMT predicts interindividual differences in brain alpha oscillations in young men. J Neurosci. 2009;29(35):10855-62.
839. Bodenmann S, Landolt HP. Effects of modafinil on the sleep EEG depend on Val158Met genotype of COMT. Sleep. 2010;33(8):1027-35.
840. Ebersbach G, Hahn K, Lorrain M, Storch A. Tolcapone improves sleep in patients with advanced Parkinson's disease (PD). Archives of gerontology and geriatrics. 2010;51(3):e125-8.
841. Bernstein HG, Keilhoff G, Steiner J, Dobrowolny H, Bogerts B. Nitric oxide and schizophrenia: present knowledge and emerging concepts of therapy. CNS & neurological disorders drug targets. 2011;10(7):792-807.
842. Bernstein H-G, Bogerts B, Keilhoff G. The many faces of nitric oxide in schizophrenia. A review. Schizophrenia Research. 2005;78(1):69-86.
843. Reif A, Herterich S, Strobel A, Ehlis AC, Saur D, Jacob CP, et al. A neuronal nitric oxide synthase (NOS-I) haplotype associated with schizophrenia modifies prefrontal cortex function. Mol Psychiatry. 2006;11(3):286-300.
844. Karson CN, Griffin WS, Mrak RE, Husain M, Dawson TM, Snyder SH, et al. Nitric oxide synthase (NOS) in schizophrenia: increases in cerebellar vermis. Molecular and chemical neuropathology / sponsored by the International Society for Neurochemistry and the World Federation of Neurology and research groups on neurochemistry and cerebrospinal fluid. 1996;27(3):275-84.
845. Maia-de-Oliveira JP, Trzesniak C, Oliveira IR, Kempton MJ, Rezende TM, Iego S, et al. Nitric oxide plasma/serum levels in patients with schizophrenia: a systematic review and meta-analysis. Revista brasileira de psiquiatria (Sao Paulo, Brazil : 1999). 2012;34 Suppl 2:S149-55.
846. Coyle JT. NItric oxide and symptom reduction in schizophrenia. JAMA Psychiatry. 2013;70(7):664-5.
847. Reghunandanan V, Reghunandanan R. Neurotransmitters of the suprachiasmatic nuclei. Journal of Circadian Rhythms. 2006;4:2-.
848. Caillol M, Devinoy E, Lacroix MC, Schirar A. Endothelial and neuronal nitric oxide synthases are present in the suprachiasmatic nuclei of Syrian hamsters and rats. Eur J Neurosci. 2000;12(2):649-61.
849. Starkey SJ, Grant AL, Hagan RM. A rapid and transient synthesis of nitric oxide (NO) by a constitutively expressed type II NO synthase in the guinea-pig suprachiasmatic nucleus. British journal of pharmacology. 2001;134(5):1084-92.
850. Chen D, Hurst WJ, Ding JM, Faiman LE, Mayer B, Gillette MU. Localization and characterization of nitric oxide synthase in the rat suprachiasmatic nucleus: evidence for a nitrergic plexus in the biological clock. J Neurochem. 1997;68(2):855-61.
851. Decker K, Reuss S. Nitric oxide-synthesizing neurons in the hamster suprachiasmatic nucleus: a combined NOS- and NADPH- staining and retinohypothalamic tract tracing study. Brain Res. 1994;666(2):284-8.

852. Reuss S, Decker K, Rosseler L, Layes E, Schollmayer A, Spessert R. Nitric oxide synthase in the hypothalamic suprachiasmatic nucleus of rat: evidence from histochemistry, immunohistochemistry and western blot; and colocalization with VIP. Brain Res. 1995;695(2):257-62.
853. Ding JM, Faiman LE, Hurst WJ, Kuriashkina LR, Gillette MU. Resetting the biological clock: mediation of nocturnal CREB phosphorylation via light, glutamate, and nitric oxide. J Neurosci. 1997;17(2):667-75.
854. Golombek DA, Agostino PV, Plano SA, Ferreyra GA. Signaling in the mammalian circadian clock: the NO/cGMP pathway. Neurochemistry international. 2004;45(6):929-36.
855. Ding JM, Chen D, Weber ET, Faiman LE, Rea MA, Gillette MU. Resetting the biological clock: mediation of nocturnal circadian shifts by glutamate and NO. Science. 1994;266(5191):1713-7.
856. Weber ET, Gannon RL, Michel AM, Gillette MU, Rea MA. Nitric oxide synthase inhibitor blocks light-induced phase shifts of the circadian activity rhythm, but not c-fos expression in the suprachiasmatic nucleus of the Syrian hamster. Brain Res. 1995;692(1-2):137-42.
857. Plano SA, Golombek DA, Chiesa JJ. Circadian entrainment to light-dark cycles involves extracellular nitric oxide communication within the suprachiasmatic nuclei. Eur J Neurosci. 2010;31(5):876-82.
858. Chen L, Majde JA, Krueger JM. Spontaneous sleep in mice with targeted disruptions of neuronal or inducible nitric oxide synthase genes. Brain Res. 2003;973(2):214-22.
859. Kalinchuk AV, Stenberg D, Rosenberg PA, Porkka-Heiskanen T. Inducible and neuronal nitric oxide synthases (NOS) have complementary roles in recovery sleep induction. Eur J Neurosci. 2006;24(5):1443-56.
860. Bernstein HG, Heinemann A, Krell D, Dobrowolny H, Bielau H, Keilhoff G, et al. Hypothalamic nitric oxide synthase in affective disorder: focus on the suprachiasmatic nucleus. Cell Mol Biol. 2005;51(3):279-84.
861. Boison D, Singer P, Shen HY, Feldon J, Yee BK. Adenosine hypothesis of schizophrenia--opportunities for pharmacotherapy. Neuropharmacology. 2012;62(3):1527-43.
862. Kurumaji A, Toru M. An increase in [3H] CGS21680 binding in the striatum of postmortem brains of chronic schizophrenics. Brain Res. 1998;808(2):320-3.
863. Dutra GP, Ottoni GL, Lara DR, Bogo MR. Lower frequency of the low activity adenosine deaminase allelic variant (ADA1*2) in schizophrenic patients. Revista brasileira de psiquiatria (Sao Paulo, Brazil : 1999). 2010;32(3):275-8.
864. Gotoh L, Mitsuyasu H, Kobayashi Y, Oribe N, Takata A, Ninomiya H, et al. Association analysis of adenosine A1 receptor gene (ADORA1) polymorphisms with schizophrenia in a Japanese population. Psychiatric genetics. 2009;19(6):328-35.
865. Schwab SG, Hallmayer J, Albus M, Lerer B, Hanses C, Kanyas K, et al. Further evidence for a susceptibility locus on chromosome 10p14-p11 in 72 families with schizophrenia by nonparametric linkage analysis. American journal of medical genetics. 1998;81(4):302-7.
866. Schwab SG, Hallmayer J, Lerer B, Albus M, Borrmann M, Honig S, et al. Support for a chromosome 18p locus conferring susceptibility to functional psychoses in families with schizophrenia, by association and linkage analysis. American journal of human genetics. 1998;63(4):1139-52.
867. Glatt SJ, Faraone SV, Tsuang MT. Meta-analysis identifies an association between the dopamine D2 receptor gene and schizophrenia. Mol Psychiatry. 2003;8(11):911-5.
868. Doi M, Yujnovsky I, Hirayama J, Malerba M, Tirotta E, Sassone-Corsi P, et al. Impaired light masking in dopamine D2 receptor-null mice. Nat Neurosci. 2006;9(6):732-4.
869. Gastambide F, Taylor AM, Palmer C, Svard H, Karjalainen M, Janhunen SK, et al. Alterations in spatial memory and anxiety in the MAM E17 rat model of hippocampal pathology in schizophrenia. Psychopharmacology (Berl). 2015.
870. Phillips KG, Bartsch U, McCarthy AP, Edgar DM, Tricklebank MD, Wafford KA, et al. Decoupling of sleep-dependent cortical and hippocampal interactions in a neurodevelopmental model of schizophrenia. Neuron. 2012;76(3):526-33.
871. Gil-da-Costa R, Stoner GR, Fung R, Albright TD. Nonhuman primate model of schizophrenia using a noninvasive EEG method. Proc Natl Acad Sci U S A. 2013;110(38):15425-30.
872. Simen AA, DiLeone R, Arnsten AFT. Primate models of schizophrenia: future possibilities. Progress in brain research. 2009;179:117-25.
873. Sawamura N, Ando T, Maruyama Y, Fujimuro M, Mochizuki H, Honjo K, et al. Nuclear DISC1 regulates CRE-mediated gene transcription and sleep homeostasis in the fruit fly. Mol Psychiatry. 2008;13(12):1138-48, 069.

874. Furukubo-Tokunaga K. Modeling schizophrenia in flies. Prog Brain Res. 2009;179:107-15.
875. Jagannath A, Peirson SN, Foster RG. Sleep and circadian rhythm disruption in neuropsychiatric illness. Current opinion in neurobiology. 2013;23(5):888-94.
876. Karatsoreos IN. Links between Circadian Rhythms and Psychiatric Disease. Front Behav Neurosci. 2014;8:162.
877. Lamont EW, Legault-Coutu D, Cermakian N, Boivin DB. The role of circadian clock genes in mental disorders. Dialogues Clin Neurosci. 2007;9(3):333-42.
878. Landgraf D, McCarthy MJ, Welsh DK. Circadian clock and stress interactions in the molecular biology of psychiatric disorders. Curr Psychiatry Rep. 2014;16(10):483.
879. Menet JS, Rosbash M. When brain clocks lose track of time: cause or consequence of neuropsychiatric disorders. Current opinion in neurobiology. 2011;21(6):849-57.
880. Wisor JP, Edgar DM, Yesavage J, Ryan HS, McCormick CM, Lapustea N, et al. Sleep and circadian abnormalities in a transgenic mouse model of Alzheimer's disease: a role for cholinergic transmission. Neuroscience. 2005;131(2):375-85.
881. Garcia-Garcia F, Ponce S, Brown R, Cussen V, Krueger JM. Sleep disturbances in the rotenone animal model of Parkinson disease. Brain Res. 2005;1042(2):160-8.
882. Zavalko I, Ukraintseva Y, Manolov A, Dolgikh V, Dorokhov V, Kovalzon V. Activity and sleep in a mouse model of Parkinson disease. Sleep medicine. 2013;14, Supplement 1(0):e40-e1.
883. El Yacoubi M, Bouali S, Popa D, Naudon L, Leroux-Nicollet I, Hamon M, et al. Behavioral, neurochemical, and electrophysiological characterization of a genetic mouse model of depression. Proceedings of the National Academy of Sciences of the United States of America. 2003;100(10):6227-32.
884. Popa D, El Yacoubi M, Vaugeois JM, Hamon M, Adrien J. Homeostatic regulation of sleep in a genetic model of depression in the mouse: effects of muscarinic and 5-HT1A receptor activation. Neuropsychopharmacology. 2006;31(8):1637-46.
885. Roybal K, Theobold D, Graham A, DiNieri JA, Russo SJ, Krishnan V, et al. Mania-like behavior induced by disruption of CLOCK. Proc Natl Acad Sci U S A. 2007;104(15):6406-11.
886. Morton AJ, Rudiger SR, Wood NI, Sawiak SJ, Brown GC, McLaughlan CJ, et al. Early and progressive circadian abnormalities in Huntington's disease sheep are unmasked by social environment. Hum Mol Genet. 2014;23(13):3375-83.
887. Mathes WF, Nehrenberg DL, Gordon R, Hua K, Garland T, Jr., Pomp D. Dopaminergic dysregulation in mice selectively bred for excessive exercise or obesity. Behav Brain Res. 2010;210(2):155-63.
888. Rhodes JS, Gammie SC, Garland T, Jr. Neurobiology of Mice Selected for High Voluntary Wheel-running Activity. Integrative and comparative biology. 2005;45(3):438-55.
889. van Praag H, Christie BR, Sejnowski TJ, Gage FH. Running enhances neurogenesis, learning, and long-term potentiation in mice. Proceedings of the National Academy of Sciences of the United States of America. 1999;96(23):13427-31.
890. van Praag H, Kempermann G, Gage FH. Running increases cell proliferation and neurogenesis in the adult mouse dentate gyrus. Nat Neurosci. 1999;2(3):266-70.
891. Duman CH, Schlesinger L, Russell DS, Duman RS. Voluntary Exercise Produces Antidepressant and Anxiolytic Behavioral Effects in Mice. Brain research. 2008;1199:148-58.
892. Greenwood BN, Foley TE, Day HE, Campisi J, Hammack SH, Campeau S, et al. Freewheel running prevents learned helplessness/behavioral depression: role of dorsal raphe serotonergic neurons. J Neurosci. 2003;23(7):2889-98.
893. Leise TL, Harrington ME, Molyneux PC, Song I, Queenan H, Zimmerman E, et al. Voluntary exercise can strengthen the circadian system in aged mice. Age (Dordrecht, Netherlands). 2013;35(6):2137-52.
894. Solberg LC, Horton TH, Turek FW. Circadian rhythms and depression: effects of exercise in an animal model. Am J Physiol. 1999;276(1 Pt 2):R152-61.
895. Schroeder AM, Colwell CS. How to fix a broken clock. Trends in pharmacological sciences. 2013;34(11):605-19.
896. Ramkisoensing A, Gu C, van Engeldorp Gastelaars HM, Michel S, Deboer T, Rohling JH, et al. Enhanced phase resetting in the synchronized suprachiasmatic nucleus network. J Biol Rhythms. 2014;29(1):4-15.

897. Yamanaka Y, Honma S, Honma K. Scheduled exposures to a novel environment with a running-wheel differentially accelerate re-entrainment of mice peripheral clocks to new light-dark cycles. Genes to cells : devoted to molecular & cellular mechanisms. 2008;13(5):497-507.
898. Deboer T, Tobler I. Running wheel size influences circadian rhythm period and its phase shift in mice. J Comp Physiol A. 2000;186(10):969-73.
899. Edgar DM, Dement WC. Regularly scheduled voluntary exercise synchronizes the mouse circadian clock. Am J Physiol. 1991;261(4 Pt 2):R928-33.
900. Power A, Hughes AT, Samuels RE, Piggins HD. Rhythm-promoting actions of exercise in mice with deficient neuropeptide signaling. J Biol Rhythms. 2010;25(4):235-46.